

# UC Riverside

## UC Riverside Electronic Theses and Dissertations

### Title

Isomer-Specific Biodegradation and Chemical Oxidation of Nonylphenol

### Permalink

<https://escholarship.org/uc/item/95n7h03p>

### Author

Lu, Zhijiang

### Publication Date

2014

Peer reviewed|Thesis/dissertation

UNIVERSITY OF CALIFORNIA  
RIVERSIDE

Isomer-Specific Biodegradation and Chemical Oxidation of Nonylphenol

A Dissertation submitted in partial satisfaction  
of the requirements for the degree of

Doctor of Philosophy

in

Environmental Sciences

by

Zhijiang Lu

June 2014

Dissertation Committee:

Dr. Jay Gan, Chairperson

Dr. Michael Anderson

Dr. Mark Matsumoto

Copyright by  
Zhijiang Lu  
2014

The Dissertation of Zhijiang Lu is approved:

---

---

---

Committee Chairperson

University of California, Riverside

## ACKNOWLEDGEMENTS

First of all, I would like to give my sincere appreciation and gratitude to my advisor, Dr. Jay Gan, for his continuous and invaluable guidance, assistance and support throughout these five years. I would like to thank Dr. Michael Anderson and Dr. Mark Matsumoto for serving as my dissertation committee members. I would also like to thank Dr. David Parker, Dr. Roger Atkinson and Dr. Walter Farmer for serving as my qualifying committee members. Their valuable comments and suggestions have helped the development of my research project and ultimately this dissertation. I would also like to thank Dr. Robert Graham for his advice and sharing soil samples used in one of my studies. I would like to thank Dr. Rong Ji at Nanjing University, China, for providing me with several nonylphenol isomers.

I have had the fortune to interact with many wonderful lab-mates. Dr. Weiying Jiang provided me with technical support and constructive suggestions, Dr. Fred Ernst and Dr. Ruben Reif-Lopez gave me consistent help on instrument maintenance and bioreactor setup, Dr. Xiaoqin Wu, Dr. Jeremy Conkle, Dr. Xinyi Cui, Dr. Laura Delgado-Moreno, Dr. Svetlana Bondarenko, Dr. Wei Wang, Dr. Lianjun Bao, Dr. Juying Li, Ms. Fang Jia and Ms. Laurel Dodgen all helped me in many ways over the years.

I would also like to thank *Environmental Science & Technology*, *Environmental Pollution* and *Chemical Engineering Journal* for publishing my research and permit me to use them in this dissertation. Chapter 2 is reproduced with permission from Lu, Z. J. and Gan, J. (2014), Isomer-specific biodegradation of nonylphenol in river sediments and

structure-biodegradability relationship, *Environ. Sci. Technol.* 48(2): 1008-1014. Chapter 4 is reproduced with permission from Lu, Z. and Gan, J. (2014), Isomer-specific oxidation of nonylphenol by potassium permanganate, *Chem. Eng. J.* 243(0): 43-50. Chapter 5 is reproduced with permission from Lu, Z. J. and Gan, J. (2013), Oxidation of nonylphenol and octylphenol by manganese dioxide: Kinetics and pathways, *Environ. Pollut.* 180: 214-220. Appendix is reproduced with permission from Lu, Z. J., Lin, K. D. and Gan, J. (2011), Oxidation of bisphenol F (BPF) by manganese dioxide, *Environ. Pollut.* 159(10): 2546-2551. It should also be noted that a part of Table 1-4 is adapted and reorganized with permission from Table 2 of Eganhouse, R. P., Pontolillo, J., Gaines, R. B., Frysinger, G. S., Gabriel, F. L. P., Kohler, H.-P. E., Giger, W. and Barber, L. B. (2009), Isomer-specific determination of 4-nonylphenols using comprehensive two-dimensional gas chromatography/time-of-flight mass spectrometry, *Environ. Sci. Technol.* 43(24): 9306-9313.

## ABSTRACT OF THE DISSERTATION

Isomer-Specific Biodegradation and Chemical Oxidation of Nonylphenol

by

Zhijiang Lu

Doctor of Philosophy, Graduate Program in Environmental Sciences

University of California, Riverside, June 2014

Dr. Jay Gan, Chairperson

Nonylphenol (NP), a well-known environmental estrogen with numerous isomers, is commonly treated as a single compound in the evaluation of its environmental occurrence, fate and transport, treatment removal and toxicity. Recent studies showed that NP isomers exhibited different estrogenicity and biodegradability. However, at present little systematic information is available on its isomer-specific biodegradation and chemical oxidation under natural and engineered conditions.

We comprehensively evaluated isomer selectivity in biodegradation in river sediments and during secondary wastewater treatment processes. In a well aerated river sediment, half-lives of NP isomers ranged from 0.9 to 13.2 d. The overall removal of tNP was efficient during the wastewater treatment processes simulated in a laboratory-scale conventional activated sludge bioreactor, ranging from 90 to 99%. Isomers with short

side chain and/or bulky  $\alpha$ -substituents were found to be more recalcitrant to degradation and followed the order of dimethyl  $\geq$  ethylmethyl  $>$  methylpropyl  $\geq$  *iso*-propylmethyl. Moreover, steric effect index and the degree of branching as quantified by  $I_{Dwbar}$  were identified to correlate closely with isomer biodegradability.

We also considered isomer selectivity during oxidation of NP by potassium permanganate, a promising treatment for NP-containing effluent, drinking water and ground water. The removal of NP isomers by  $KMnO_4$  was efficient during pH range 5-7. At pH 7 with 10 mg/L of  $KMnO_4$  and 50  $\mu$ g/L tNP, the half-lives of 19 isomers varied from 4.8 to 6.3 min. In general, the reactivity followed the order:  $\alpha$ -dimethyl  $>$   $\alpha$ -ethylmethyl  $\approx$   $\alpha$ -methylpropyl  $\approx$   $\alpha$ -*iso*-propylmethyl.

We further considered the role of  $MnO_2$  oxidation in the natural attenuation of NP and its structure analogues in soils. At pH 5.5 and 100 mg/L  $\delta$ - $MnO_2$ , 92, 84 and 76% of 4-*n*-NP, 4-*tert*-octylphenol and tNP were transformed in 90 min, respectively. Multiple reaction products, including hydroquinone, hydroxylated products, dimers and trimers were identified, allowing the construction of transformation pathways.

These results together suggest that isomer selectivity commonly occurs before and after the release of NP to the environment, and that knowledge of isomer-specific behavior of NP contributes to improved understanding and management of NP as an important environmental contaminant and endocrine disruptor.



## Table of Content

Chapter 1 Introduction .....	1
1.1 Nonylphenol .....	1
1.2 Naming of Nonylphenol Isomers .....	3
1.3 Analysis of Nonylphenol Isomers .....	4
1.3.1 Separation and Identification .....	4
1.3.2 Quantification .....	9
1.4 Toxicity of Nonylphenol Isomers .....	10
1.5 Occurrence of Nonylphenol Isomers .....	13
1.5.1 Composition of Technical Nonylphenol .....	13
1.5.2 Occurrence of Nonylphenol Isomers in the Environment .....	15
1.6 Biodegradation of Nonylphenol Isomers .....	18
1.6.1 Biodegradation Kinetics .....	18
1.6.2 Structure-Biodegradation Relationship .....	20
1.6.3 Biodegradation Mechanisms .....	21
1.7 Objectives .....	22
References .....	25
Tables .....	36

Chapter 2 Isomer-Specific Biodegradation of Nonylphenol in River Sediments and Structure-Biodegradability Relationship.....	46
2.1 Introduction.....	46
2.2 Materials and Methods.....	48
2.2.1 Chemicals.....	48
2.2.2 Sediment Collection and Characterization.....	49
2.2.3 Sediment Incubation Experiments.....	49
2.2.4 Sample Preparation and Analysis.....	51
2.2.5 Calculation of Molecular Descriptors.....	53
2.3 Results and Discussion.....	54
2.3.1 Degradation under Oxidic Conditions.....	54
2.3.2 Degradation under Reduced Conditions.....	56
2.3.3 Structure-Biodegradability Relationship.....	58
2.4 Environmental Implications.....	62
References.....	63
Tables.....	68
Figures.....	71
Supporting Information.....	74
Chapter 3 Isomeric-Specific Biodegradation of Nonylphenol in the Bioreactor.....	89

3.1 Introduction .....	89
3.2 Methods and Materials .....	91
3.2.1 Chemicals .....	91
3.2.2 Reactor Setup.....	92
3.2.3 Sample Preparation and Analysis .....	93
3.3 Results and Discussion.....	95
3.3.1 Isomer Selectivity in Biodegradation .....	95
3.3.2 Effects of Hydraulic Retention Time and Temperature .....	97
3.3.3 Isomer Structure-Biodegradation Relationships.....	99
3.3.4 Adsorption of Nonylphenol Isomers .....	101
3.4 Environmental Implications .....	102
References .....	104
Figures.....	109
Chapter 4 Isomer-Specific Oxidation of Nonylphenol by Potassium Permanganate .....	113
4.1 Introduction .....	113
4.2 Materials and Methods .....	115
4.2.1 Chemicals .....	115
4.2.2 Reaction Setup with Reagent Water .....	116
4.2.3 Experiments with Reclaimed Water .....	117

4.2.4 Chemical Analysis .....	117
4.2.5 Data Analysis.....	118
4.3 Results and Discussion.....	118
4.3.1 Separation and Identification of Nonylphenol Isomers .....	118
4.3.2 Reaction Kinetics of NP Isomers.....	119
4.3.3 Effect of Side Chain Length and Types of $\alpha$ -Substituents .....	122
4.3.4 Effect of $\text{KMnO}_4$ Concentration, pH and Matrix .....	125
4.4 Conclusions .....	127
References .....	129
Tables .....	134
Figures .....	138
Supporting Information.....	142
Chapter 5 Oxidation of Nonylphenol and Octylphenol by Manganese Dioxide: Kinetics and Pathways.....	144
5.1 Introduction .....	144
5.2 materials and methods.....	146
5.2.1 Chemicals and Soil. ....	146
5.2.2 Reaction setup.....	147
5.2.3 Chemical analysis. ....	149

5.3 Results and Discussion.....	149
5.3.1 Kinetics and Influencing Factors .....	149
5.3.2 Reaction of low concentrations of nonylphenol with MnO <sub>2</sub> and soil.....	153
5.3.3 Reaction Products and Pathways .....	154
5.4 Conclusions .....	158
References .....	159
Tables .....	164
Figures .....	167
Supporting Information .....	170
Chapter 6 General Conclusions and Future Work .....	229
6.1 Isomer-Specific Biodegradation in River Sediments and Bioreactor .....	229
6.2 Isomer-Specific Oxidation of Nonylphenol by Potassium Permanganate .....	229
6.3 Oxidation by Soil Manganese Dioxide .....	230
6.4 Environmental Implications .....	231
6.5 Future Work .....	231
Appendix Oxidation of Bisphenol F (BPF) by Manganese Dioxide .....	234
A.1 Introduction .....	234
A.2 Materials and Methods .....	236
A.2.1 Chemicals .....	236

A.2.2 Reaction Setup .....	237
A.2.3 Chemical Analysis .....	239
A.2.4 Molecular Modeling .....	239
A.3 Results and Discussion .....	240
A.3.1 Removal Efficiency and Orders of Reaction .....	240
A.3.2 Effect of pH .....	241
A.3.3 Effect of Cosolutes .....	242
A.3.4 Reactivity Relative to Analogs .....	245
A.3.5 Reaction Pathways .....	246
A.4 Conclusions .....	247
References .....	248
Figures .....	255
Supporting Information .....	260

## List of Tables

<b>Table 1-1</b> Names, structure, side chain length and $\alpha$ and $\beta$ substituents of representative 4-nonylphenols .....	36
<b>Table 1-2</b> Analysis of nonylphenol isomers by gas chromatography .....	38
<b>Table 1-3</b> Relative estrogenic activities of synthetic 4- $\alpha$ -quaternary nonylphenol isomers .....	39
<b>Table 1-4</b> Isomeric composition (%) of different technical nonylphenol products .....	41
<b>Table 1-5</b> Occurrences of nonylphenol isomers in environment .....	43
<b>Table 1-6</b> Isomeric biodegradation of nonylphenol .....	45
<b>Table 2-1</b> Textural and chemical properties of sediments used in this study and pH and redox potentials (Eh) during aerobic and anaerobic incubations.....	68
<b>Table 2-2</b> Estimated first-order half-lives of nonylphenol isomers in an upper river sediment under reduced conditions .....	69
<b>Table 2-3</b> Predicted half-lives (T <sub>1/2</sub> , d) of nonylphenol isomers using partial least square regression.....	70
<b>Table 4-1</b> Matrices, pH, KMnO <sub>4</sub> and nonylphenol concentrations in the batch experiments.....	134
<b>Table 4-2</b> Names, structures and pseudo first-order rate constants of 19 nonylphenol isomers separated and identified.....	135
<b>Table 4-3</b> Comparison of pseudo first-order rate constants among nonylphenol isomers with 10 mg/L KMnO <sub>4</sub> at pH 7 in reagent water.....	137

<b>Table 5-1</b> Effect of cations and humic acid on the reaction rate of 1.0 mg/L technical nonylphenol (tNP), 4-n-nonylphenol (4-n-NP) or 4-tert-octylphenol (4-tert-OP) in 100 mg/L MnO <sub>2</sub> solution at pH 5.5.....	164
<b>Table 5-2</b> Retention time, possible category, collision energy and main m/z of MS2 spectra of identified products.....	165
<b>Table A-1</b> Effects of humic acid on degradation of BPF in the reaction mixture containing 4.4 μM BPF and 100 μM MnO <sub>2</sub> (n = 3) .....	252
<b>Table A-2</b> Effects of cations (n = 3) on the reaction rate of bisphenol F (BPF) by MnO <sub>2</sub> under the initial conditions of 4.4 μM BPF, 100 μM MnO <sub>2</sub> and pH 5.5 ....	253
<b>Table A-3</b> Effects of anions (n = 3) on the reaction rate of bisphenol F (BPF) and MnO <sub>2</sub> under the initial conditions of 4.4 μM BPF, 100 μM MnO <sub>2</sub> and pH 5.5 ...	254



## List of Tables in Supporting Information

<b>Table S 2–1</b> Molecular descriptors for the 18 nonylphenol isomers identified .....	74
<b>Table S 2–2</b> Proportion of variance explained by partial least square regression.....	79
<b>Table S 2–3</b> Parameters of partial least square regression .....	80
<b>Table S 2–4</b> Variable importance in the projection of partial least square regression.....	81
<b>Table S 2–5</b> Weights of variables of partial least square regression.....	82
<b>Table S 2–6</b> Loadings of variables of partial least square regression .....	83
<b>Table S 2–7</b> Predicted half lives (d) and molecular descriptors for 4-quaternary nonylphenol isomers .....	84
<b>Table S 4–1</b> Retention time and main ion fragments of nonylphenol isomers identified .....	142
<b>Table S 4–2</b> Retention time and main ion fragments of nonylphenol isomers standards .....	143
<b>Table S 5–1</b> Properties of high Mn content soil.....	177
<b>Table S 5–2</b> Concentrations of 4-n-NP, tNP and 4-tert-OP in the MnO <sub>2</sub> -free controls at pH 5.5 compare to their initial concentrations.....	178

## List of Figures

- Figure 2-1** Degradation of representative nonylphenol isomers NP38, NP110a and NP193b in an upper river sediment (sediment A) under oxic conditions and a lower river sediment (sediment B) under slightly reduced conditions ..... 71
- Figure 2-2** Isomer-specific degradation half-lives of nonylphenol isomers in an upper river sediment (sediment A) under oxic conditions and a lower river sediment (sediment B) under slightly reduced conditions ..... 72
- Figure 2-3** Relationships of measured half-lives of nonylphenol isomers in an upper river sediment under oxic conditions with (A) side-chain length, (B)  $\alpha$ -substituent type, (C) steric index and (D) mean information index for the magnitude of distance  $IDW_{bar}$ . ..... 73
- Figure 3-1** Total ion chromatography of nonylphenol in influent, dissolved phase of effluent and sludge..... 109
- Figure 3-2** Effects of hydraulic retention time and temperature on the residue of NP isomers in the effluent. (A) dissolved phase and (B) particulate phase..... 110
- Figure 3-3** Quantitative relationships between isomer structures and residues in the effluent for nonylphenol. (a) Alkyl chain length; (b)  $\alpha$ -substituent types A  $\alpha$ -dimethyl, B  $\alpha$ -ethyl-  $\alpha$ -methyl C  $\alpha$ -methyl-  $\alpha$ -*n*-propyl D  $\alpha$ -*iso*-propyl-  $\alpha$ -methyl; (c) Steric index, and (d)  $I_{DWbar}$  ( $n=3$ , error bar stands for the standard deviation) ..... 111
- Figure 3-4** Adsorption coefficient ( $K_d$ ) of nonylphenol isomers on sludge ( $n=3$ , error bar stands for the standard deviation) ..... 112

<b>Figure 4-1</b> Isomer specific reaction rates in 10 mg L <sup>-1</sup> KMnO <sub>4</sub> at pH 7 with reagent water. (a) Removal of NP194 and NP119; and (b) Pseudo first-order rate constants of nonylphenol isomers.....	138
<b>Figure 4-2</b> Pseudo first-order rate constants of nonylphenol isomers and their ratios in 10 and 2 mg/L KMnO <sub>4</sub> at pH 7 with reagent water .....	139
<b>Figure 4-3</b> Pseudo first-order rate constants of nonylphenol isomers and their ratios in 10 mg/L KMnO <sub>4</sub> at pH 5 and pH 7 with reagent water .....	140
<b>Figure 4-4</b> Pseudo first-order rate constants of nonylphenol isomers and their ratios in reagent water and reclaimed water with 10 mg/L KMnO <sub>4</sub> at pH 7 .....	141
<b>Figure 5-1</b> Reaction kinetics of technical nonylphenol (tNP), 4-n-nonylphenol (4-n-NP) or 4-tert-octylphenol (4-tert-OP) at different MnO <sub>2</sub> concentrations and with different pH.....	167
<b>Figure 5-2</b> Possible radical coupling reactions in the formation of dimers during the reaction of 4-n-nonylphenol (4-n-NP) or 4-tert-octylphenol (4-tert-OP) with MnO <sub>2</sub> .....	168
<b>Figure 5-3</b> Tentative pathways in the oxidation of 4-n-nonylphenol (4-n-NP) or 4-tert-octylphenol (4-tert-OP) by MnO <sub>2</sub> .....	169
<b>Figure A-1</b> Chemical structures of bisphenol A (BPA), bisphenol F (BPF) and bis(2-hydroxyphenyl) methane .....	255
<b>Figure A-2</b> Removal efficiency of bisphenol F (BPF) at different initial MnO <sub>2</sub> concentrations .....	256
<b>Figure A-3</b> Removal efficiency of bisphenol F (BPF) under different pH conditions ..	257

**Figure A-4** Speciation of bisphenol F (BPF) and MnO<sub>2</sub> surface hydroxyl groups and the pseudo first order rate constants at different pH..... 258

**Figure A-5** A possible reaction pathway describing the oxidation of bisphenol F (BPF) by MnO<sub>2</sub>..... 259

## List of Figures in Supporting Information

<b>Figure S 5–1</b> X-ray diffractogram of MnO <sub>2</sub> .....	179
<b>Figure S 5–2</b> Removal of 1.0 mg/L 4-n-NP with different initial MnO <sub>2</sub> loadings (100 mg/L, 50 mg/L, 25 mg/L and 12.5 mg/L) at pH 5.5.....	180
<b>Figure S 5–3</b> Removal of 1.0 mg/L OP with different initial MnO <sub>2</sub> loadings (100 mg/L, 50 mg/L, 25 mg/L and 12.5 mg/L) at pH 5.5 .....	181
<b>Figure S 5–4</b> Removal of 1.0 mg/L 4-n-NP by 100 mg/L MnO <sub>2</sub> at different pH.....	182
<b>Figure S 5–5</b> Removal of 1.0 mg/L OP by 100 mg/L MnO <sub>2</sub> at different pH .....	183
<b>Figure S 5–6</b> GC-MS-MS spectra of NP-1-1-A at retention time 48.46 min, a dimer of nonylphenol .....	184
<b>Figure S 5–7</b> GC-MS-MS spectra of NP-1-1-B at retention time 49.67 min, a dimer of nonylphenol .....	185
<b>Figure S 5–8</b> GC-MS-MS spectra of NP-1-1-C at retention time 50.30, a dimer of nonylphenol. ....	186
<b>Figure S 5–9</b> Possible ion fragment assignments of products NP-1-1-A, B, C, dimmers of nonylphenol .....	187
<b>Figure S 5–10</b> GC-MS-MS spectra of NP-2-1 at retention time 13.1 min, hydroquinone silylated.....	188
<b>Figure S 5–11</b> Possible ion fragment assignments of products NP-2-1, hydroquinone silylated.....	189
<b>Figure S 5–12</b> GC-MS-MS spectra of NP-2-2 at retention time 30.3 min, hydroxylated nonylphenol, silylated.....	190

<b>Figure S 5–13</b>	Possible ion fragment assignments of products NP-2-2.....	191
<b>Figure S 5–14</b>	GC-MS-MS spectra of NP-2-3A at retention time 46.7 min, dimer of nonylphenol, silylated.....	192
<b>Figure S 5–15</b>	GC-MS-MS spectra of NP-2-3B at retention time 47.3 min, dimer of nonylphenol, silylated.....	193
<b>Figure S 5–16</b>	Possible ion fragment assignments of products NP-2-3A/B .....	194
<b>Figure S 5–17</b>	Another Possible ion fragment assignments of products NP-2-3A/B ....	195
<b>Figure S 5–18</b>	GC-MS-MS spectra of NP-2-4A at retention time 47.6 min, dimer of nonylphenol, silylated.....	196
<b>Figure S 5–19</b>	GC-MS-MS spectra of NP-2-4B at retention time 48.1 min, dimer of nonylphenol, silylated.....	197
<b>Figure S 5–20</b>	Possible ion fragment assignments of products NP-2-4A/B .....	198
<b>Figure S 5–21</b>	Another Possible ion fragment assignments of products NP-2-4A/B ....	199
<b>Figure S 5–22</b>	UPLC-MS-MS spectra of NP-3-1 at retention time 6.67 min, hydroxylated nonylphenol .....	200
<b>Figure S 5–23</b>	UPLC-MS-MS spectra of NP-3-2 at retention time 8.94 min, dimer of nonylphenol .....	201
<b>Figure S 5–24</b>	UPLC-MS-MS spectra of NP-3-3 at retention time 8.91 min, trimer of nonylphenol .....	202
<b>Figure S 5–25</b>	GC-MS-MS spectra of OP-1-1A at retention time 58.3 min, trimer of octylphenol .....	203

<b>Figure S 5–26</b> GC-MS-MS spectra of OP-1-1B at retention time 59.4 min, trimer of octylphenol .....	204
<b>Figure S 5–27</b> One possible ion fragmentation of Product OP-1-1A/B .....	205
<b>Figure S 5–28</b> GC-MS-MS spectra of OP-2-1 at retention time 24.5 min, hydroxylated octylphenol, silylated.....	206
<b>Figure S 5–29</b> Possible ion fragmentation of Product OP-2-1.....	207
<b>Figure S 5–30</b> GC-MS-MS spectra of OP-2-2A at retention time 39.9 min, dimer of octylphenol, silylated.....	208
<b>Figure S 5–31</b> GC-MS-MS spectra of OP-2-2B at retention time 40.4 min, dimer of octylphenol, silylated.....	209
<b>Figure S 5–32</b> Possible ion fragmentation of Product OP-2-2A/B .....	210
<b>Figure S 5–33</b> Another possible ion fragmentation of Product OP-2-2A/B .....	211
<b>Figure S 5–34</b> GC-MS-MS spectra of OP-2-3A at retention time 54.5 min, trimer of octylphenol, silylated.....	212
<b>Figure S 5–35</b> GC-MS-MS spectra of OP-2-3B at retention time 57.4 min, trimer of octylphenol, silylated.....	213
<b>Figure S 5–36</b> Figure S36. Possible ion fragmentation of Product OP-2-3A/B .....	214
<b>Figure S 5–37</b> GC-MS-MS spectra of OP-2-4A at retention time 51.5 min, trimer of octylphenol, silylated.....	215
<b>Figure S 5–38</b> GC-MS-MS spectra of OP-2-4B at retention time 52.4 min, trimer of octylphenol, silylated.....	216
<b>Figure S 5–39</b> Possible ion fragmentation of Product OP-2-4A/B .....	217

<b>Figure S 5–40</b> UPLC-MS-MS spectra of OP-3-1A at retention time 8.71 min, trimmer of octylphenol .....	218
<b>Figure S 5–41</b> UPLC-MS-MS spectra of OP-3-1B at retention time 9.59 min, trimmer of octylphenol .....	219
<b>Figure S 5–42</b> UPLC-MS-MS spectra of OP-3-1C at retention time 10.65 min, trimmer of octylphenol .....	220
<b>Figure S 5–43</b> UPLC-MS-MS spectra of OP-3-2A at retention time 9.69 min, dimmer of octylphenol. ....	221
<b>Figure S 5–44</b> UPLC-MS-MS spectra of OP-3-2B at retention time 9.79 min, dimmer of octylphenol .....	222
<b>Figure S 5–45</b> UPLC-MS-MS spectra of OP-3-2A at retention time 10.32 min, dimmer of octylphenol .....	223
<b>Figure S 5–46</b> GC-MS-MS spectra of the hydroquinone standard.....	224
<b>Figure S 5–47</b> GC-MS-MS spectra of 4-n-NP.....	225
<b>Figure S 5–48</b> GC-MS-MS spectra of 4-n-NP silylated .....	226
<b>Figure S 5–49</b> GC-MS-MS spectra of 4-tert-OP .....	227
<b>Figure S 5–50</b> GC-MS-MS spectra of 4-tert-OP silylated.....	228
<b>Figure S A–1</b> X-ray diffractogram of MnO <sub>2</sub> .....	262
<b>Figure S A–2</b> Mass spectrums and possible ion fragment assignments of 4,4'-(ethane-1,2-diyl)diphenol.....	263
<b>Figure S A–3</b> Mass spectrums and possible ion fragment assignments of 2,2'-bisphenol .....	264



<b>Figure S A-4</b> Mass spectrums and possible ion fragment assignments of 4-hydroxybenzyl alcohol.....	265
<b>Figure S A-5</b> Mass spectrums and possible ion fragment assignments of hydroquinone .....	266
<b>Figure S A-6</b> Mass spectrums and possible ion fragment assignments of 4-hydroxybenzaldehyde .....	267
<b>Figure S A-7</b> Mass spectrums and possible ion fragment assignments of authentic standards bisphenol F .....	268
<b>Figure S A-8</b> Mass spectrums of authentic standards bisphenol A.....	269
<b>Figure S A-9</b> Mass spectrums of authentic standards hydroquinone .....	269
<b>Figure S A-10</b> Mass spectrums of authentic standards 2,2'-bisphenol .....	269
<b>Figure S A-11</b> Mass spectrums of authentic standards 4-hydroxybenzyl alcohol .....	269
<b>Figure S A-12</b> Mass spectrums of authentic standards 4-hydroxybenzaldehyde.....	269

## Chapter 1 Introduction

### 1.1 Nonylphenol

Nonylphenol (NP) is a high production volume chemical and its primary use is as the raw material for the production of nonylphenol ethoxylates (NPEOs), the most widely used non-ionic surfactant (Ying et al., 2002). Nonylphenol ethoxylates are used as detergents, emulsifiers, wetting and dispersing agents, antistatic agents, demulsifiers and solubilisers in domestic, agricultural and industrial products (Soares et al., 2008; Ying et al., 2002). According to the Toxic Substances Control Act under Inventory Update Rule, the production of technical nonylphenol (tNP, CASRN: 84852-15-3) in the United States was about 100 - 500 million lbs (45.4 - 227 thousand tons) in 2006 (USEPA, 2006).

Nonylphenol has a water solubility of 4.9 mg/L,  $\log K_{ow}$  of 4.48, vapor pressure of  $2.07 \times 10^{-2}$  Pa (at 25 °C) and  $pK_a$  of 10.28 (Soares et al., 2008). Nonylphenol is well known as an endocrine disruptive compound (EDC), as it may mimic 17 $\beta$ -estradiol, with a mean potency (relative to 17 $\beta$ -estradiol) of 0.023 in *in vivo* bioassays (Soares et al., 2008). Bechi et al. (2010) reported that NP can affect cytokine secretion in human placenta at environmental levels (0.022 ng/L to 220 ng/L).

Nonylphenol has been frequently detected in water, sediment, sludge and soil (Soares et al., 2008; Ying et al., 2002). According to a national reconnaissance investigating 139 streams across 30 states during 1999 and 2000, the median and maximum concentrations of NP were 0.8 and 40  $\mu$ g/L, respectively, with a detection frequency of 50.6% (Kolpin et

al., 2002). In a recent study, NP was found in 55 out of 62 drinking water samples from 31 major cities across China with median and maximum concentrations of 27 and 558 ng/L, respectively, and in all 62 source water samples with median and maximum concentration of 123 and 918 ng/L, respectively (Fan et al., 2013). According to USEPA's 2001 national sewage sludge survey, the concentration of NP in sludge was  $534 \pm 192$  mg/kg with 100% detection frequency (Venkatesan and Halden, 2013). The mean annual loading of NP to sewage sludge was 2066-5510 tonnes, of which 1033 to 3306 tonnes was used for land application (Venkatesan and Halden, 2013). The USEPA guideline on NP for ambient water quality stipulates limits of 6.6 µg/L and 1.7 µg/L in freshwater and saltwater, respectively (Soares et al., 2008). In European Union, the maximum limit of NP in the sludge for land use is set at 50 mg/kg (European Commission, 2002).

Nonylphenol is commonly treated as a single compound in the evaluation of its environmental occurrence, fate and transport, treatment removal and toxicity (Jiang et al., 2012; Soares et al., 2008; Ying et al., 2002). However, technical nonylphenol is in fact a mixture of more than 100 isomers and congeners due to variations in the length and branching of side chains and substitution position on the benzene ring (Eganhouse et al., 2009; Ieda et al., 2005). A few recent studies showed that NP isomers have different estrogenicity and biodegradability in the environment (Eganhouse et al., 2009; Gabriel et al., 2008; Kim et al., 2005b; Shan et al., 2011). Therefore, a systematic investigation into the fate of NP at the isomeric level is of great scientific significance.

## 1.2 Naming of Nonylphenol Isomers

About 90% of tNP is made up by 4-NP and theoretically there are 211 constitutional isomers in 4-NP. Moreover, if stereoisomerism is considered, this number increases to 550 (Guenther et al., 2006). Similar to the Ballschmiter numbers used for polychlorinated biphenyls (PCBs) and polybrominated diphenyl ethers (PBDEs), a simple and easy-to-use numbering system is needed for NP, especially for 4-NP. [Table 1-1](#) lists names, structures, side chain lengths and  $\alpha$  and  $\beta$  substituents of representative 4-NP isomers. In general, there are three numbering systems - the International Union of Pure and Applied Chemistry (IUPAC) abbreviation, the Juelich nomenclature (Guenther et al., 2006), and the line-coding system (Zenkevich et al., 2009). The IUPAC abbreviation uses the first few numbers to denote the substitution positions of alkyl chains. Letter E is used to distinguish ethyl group from methyl group. The last number is used to identify the phenol substitution position on the alkyl chain. The structures of NP isomers are easily drawn from their IUPAC names or abbreviations; however, it is difficult to identify the side chain length and substituents on the  $\alpha$  (the carbon connected to benzene ring) and  $\beta$  (the carbon connected to the  $\alpha$  carbon) positions. Juelich nomenclature counts the side chain from the  $\alpha$  carbon and uses a numbering system by giving priorities to longer main chains or greater number of side chains (Guenther et al., 2006). The names given by Juelich nomenclature directly show the side chain length and substituents on the  $\alpha$  and  $\beta$  positions and the Juelich number can also roughly indicate the side chain length and branchness; however, just like the numbering system for PCB, the Juelich number does not directly reflect the isomer structure. The line-coding system uses the first number to

indicate the length of the side chain and the second number to denote the positions of branching. The number in the parentheses indicates the number of carbon atoms in the sub-chains (Zenkevich et al., 2009). This coding system directly reflects the structure but the name for each isomer is very long. In this project, the Juelich numbering is used due to its simplicity and the prefix number 4 - indicating the substitution at *para* position of benzene ring, is usually omitted (Table 1-1).

### 1.3 Analysis of Nonylphenol Isomers

#### 1.3.1 Separation and Identification

Separation and identification of NP isomers from tNP and environmental matrices is challenging. Several high performance liquid chromatography (HPLC) and gas chromatography (GC) methods have been developed to separate NP isomers (Table 1-2). However, HPLC methods were usually used to fractionate tNP for further studies, for example, estrogenic activity assays (Kim et al., 2005b; Kim et al., 2004). Therefore, these HPLC methods are not discussed here. Although the NP isomers have phenolic hydroxyl group, derivatization was not necessary before GC analysis (ISO, 2009; Moeder et al., 2006a; Thiele et al., 2004; Wheeler et al., 1997) and Eganhouse et al. (2009) reported that alkylation of NP isomers did not provide any advantage in GC separation. Mass spectrometer detector (MSD) was the most commonly used detector for identifying the structures of NP isomers (Horii et al., 2004; Moeder et al., 2006a; Moeder et al., 2006b; Thiele et al., 2004; Wheeler et al., 1997). Fourier transform infrared (FTIR) was also used to confirm the substitution at *para* position (Wheeler et al., 1997). Synthesized NP

isomers with structures confirmed by  $^1\text{H}$  and  $^{13}\text{C}$  nuclear magnetic resonance (NMR) spectroscopy were also used to compare the mass fragmentation and retention time with isomers separated from tNP (Boehme et al., 2010; Russ et al., 2005; Thiele et al., 2004; Uchiyama et al., 2008; Yu et al., 2008).

Using high resolution capillary GC columns may resolve around 20 peaks (Horii et al., 2004; ISO, 2009; Kim et al., 2005b; Thiele et al., 2004; Wheeler et al., 1997). For instance, using a 100 m Petrocol DH column, Wheeler et al. (1997) successfully observed 22 peaks from tNP. Based on the mass fragmentation patterns, the authors divided these isomers into 5 groups. Thiele et al. (2004) used the same column to analyze a different tNP sample. Interestingly, the number of resolved peaks, the elution sequence and mass spectra of each isomer were exactly the same. According to Wheeler et al. (1997), Group 1 isomers had highly characteristic mass spectra: a base peak of  $m/z$  135 and no other major peaks. The base peak of  $m/z$  135 indicated that these isomers have dimethyl substituents at  $\alpha$  position and the lack of other major peaks indicated that the  $\beta$  carbon was not quaternary. Group 2 isomers had a base peak of  $m/z$  135 and a major fragment of  $m/z$  191. This group of isomers had one methyl and one ethyl substituent at  $\alpha$  position and also no substituent at  $\beta$  position. The structures of group 1 and group 2 isomers have been confirmed by later studies using a two dimensional GC (GC $\times$ GC) method (Eganhouse et al., 2009), a GC tandem mass spectrometry method (Moeder et al., 2006a) and synthetic NP isomers (Gabriel et al., 2008; Katase et al., 2008; Russ et al., 2005; Shioji et al., 2006; Thiele et al., 2004). Group 3 isomers had a base peak of  $m/z$  149 and no major peaks of  $m/z$  163, 177 and 191. Wheeler et al. (1997) suggested that the lack of  $m/z$  191 indicated

no ethyl substitution at  $\alpha$  position and they proposed  $\alpha$ -methyl- $\beta$ -methyl structures for these isomers. Thiele et al. (2004) analyzed two synthetic isomers with this structure, i.e., 4-(1,2,5-trimethylhexyl)phenol and 4-(1-methyl-2-ethylhexyl)phenol, and found that this structure would only produce base peak of  $m/z$  121. Katase et al. synthesized NP<sub>110a/b</sub> (a and b are used to denote diastereomers) and found that the mass spectra and retention time matched with these group 3 isomers (Katase et al., 2008; Makino et al., 2008). Thus, group 3 isomers have  $\alpha$ -methyl,  $\alpha$ -ethyl and  $\beta$ -methyl substituents. Group 4 isomers had a base peak of  $m/z$  163 and a major peak of  $m/z$  121. Wheeler et al. (1997) suggested an  $\alpha$ -butyl configuration for the formation of  $m/z$  163 and suggested  $\alpha$ -methyl and  $\beta$ -ethyl structures. Thiele et al. (2004) suggested that  $m/z$  121 could not be explained by this structure. Katase et al. (Katase et al., 2008; Makino et al., 2008) synthesized NP<sub>193a/b</sub> and finally determined that the substituents were  $\alpha$ -methyl,  $\alpha$ -n-propyl, and  $\beta$ -methyl. Group 5 isomers had an intense peak of  $m/z$  121 and major peaks of  $m/z$  163 and  $m/z$  177. Wheeler et al. (1997) suggested  $\alpha$ -methyl and  $\alpha$ -propyl structures. After analyzing synthetic isomers NP<sub>194</sub>, NP<sub>143</sub> and NP<sub>152</sub>, Thiele et al. (2004) splitted this group into two sub-groups, group 5 isomers with  $\alpha$ -methyl and  $\alpha$ -n-propyl substituents and group 6 isomers with  $\alpha$ -methyl and  $\alpha$ -*iso*-propyl substituents. Since group 6 isomers had lower abundance of  $m/z$  163, indicating that cleavage of the *iso*-propyl group was preferred over the butyl group. Therefore, well characterized synthetic NP isomers are essential for further understanding the mass fragmentation mechanisms and identification of NP isomers in the technical mixtures.

Co-elution is one of the most critical problems in the analysis NP isomers by GC-MS. For example, according to Gabriel et al. (2008), the method used by ISO and many others (Guruge et al., 2011; Horii et al., 2004; Horii et al., 2010; ISO, 2009) had the co-elution of NP<sub>112</sub>/NP<sub>128</sub>, NP<sub>119</sub>/NP<sub>152</sub> and NP<sub>110a</sub>/NP<sub>143</sub>. To solve this issue, some GC×GC methods with much higher separation capacity have been proposed (Table 1-2). Ieda et al. (2005) was the first to develop a GC×GC method for the separation of NP isomers in tNP and in environmental samples. Using a 30-m non-polar DB-5 column and 1-m polar DB-WAX column as the primary and secondary columns, respectively, separation of 102 peaks was achieved. Moeder et al. (2006b) used another set of columns and were able to observe 40 peaks. Guenther et al. (2006) separated about 80 NP isomers. To date, Eganhouse et al. (2009) have carried out the most comprehensive study on the isomeric compositions in different tNPs. Under optimal chromatographic conditions, 153-204 alkylphenol peaks were detected, among which, 59-66 peaks were identified to be 4-NPs, comprising 86-94% of tNP and 53-83 peaks were 2-NPs, comprising 2.5-9% of tNP. Moreover, in Eganhouse et al. (2009), the authors found a minor peak with a base mass fragment of  $m/z$  121 and a secondary fragment of  $m/z$  135 and attributed this peak to have  $\alpha$ -H- $\alpha$ -methyl structure by comparing to the spectra of two synthetic isomers (4-(1,2,5-trimethylhexyl)phenol and 4-(1-methyl-2-ethylhexyl)phenol) from Thiele et al. (2004). Vallejo et al. (2011) used a combination of MSD and flame ionization detection (FID) in the GC×GC system, and detected 79 peaks in the FID and confirmed 38 of these peaks in the MSD. The GC×GC systems have advantages over the conventional GC when co-



eluting components do not produce abundant, specific ions for quantitation, or when only one of the two components has an abundant, specific ion (Eganhouse et al., 2009).

Other techniques have also been tested for separating and identifying NP isomers. Moeder et al. (2006a) successfully separated 35 peaks and proposed structures for 18 NP isomers by gas chromatography-tandem mass spectrometry (GC-MS/MS) combined with cluster analysis. More importantly, the authors proposed structures for 13 4- $\alpha$ -tertiary-NP isomers before the elution of major 4- $\alpha$ -quaternary-NP isomers. Gabriel et al. (2012) identified 7  $\alpha$ -H- $\alpha$ -methyl isomers by analyzing their metabolites 2-nonyl-*p*-benzoquinones from *Sphingobium xenophagum* Bayram and they also tentatively identified 5 of these isomers among the early eluting tNP isomers using GC-MS. Wu et al. (2010) applied the heuristic evolving latent projection (HELP) chemometric resolution method to GC-MS analysis of NP isomers. The chemometric resolution method successfully corrected the incorrect identification of one isomer by extracting ion chromatogram data. Zenkevich et al. (2009) predicted the GC retention indices with a mean deviation of  $\pm 11$  index units for all of the 211 NP isomers based on experimentally determined index values of reference 4-NP isomers and also retention indices of 75 isodecanes. With this index, the co-elution of NP isomers may be tentatively predicted.

Chiral separation of three NP isomers NP<sub>35</sub>, NP<sub>111</sub> and NP<sub>112</sub> have been achieved by Zhang et al. by using GC-MS and HPLC (Zhang et al., 2009a; Zhang et al., 2007). In the GC-MS method, Hydrodex- $\beta$ -6TBDM column (25 m  $\times$  0.25 mm, 0.25  $\mu$ m) and DB5-MS column (30 m  $\times$  0.25 mm, 0.25  $\mu$ m) were used for the methylated derivatives, and HP-

FFAP column (30 m × 0.25 mm, 0.25 μm) and Hydrodex-β-6TBDM column (25 m × 0.25 mm, 0.25 μm) were used for silylated derivatives. Nucleodex-β-PM column (5 μm, 200 × 4 mm) was used to separate NP<sub>35</sub> and NP<sub>112</sub> in the HPLC method (Zhang et al., 2007).

### 1.3.2 Quantification

Both MSD and FID responses of NP isomers have been used to quantify the isomer concentrations in tNP and environmental matrices (Eganhouse et al., 2009; ISO, 2009; Katase et al., 2008; Thiele et al., 2004; Wheeler et al., 1997). Since MSD response varied significantly among isomers, the quantification of NP isomers relied on the inclusion of synthetic pure standards (Katase et al., 2008; Russ et al., 2005). In comparison, FID produces more linear response for isomers (Jorgensen et al., 1990); therefore, FID was frequently used in the quantification of NP isomers (Guenther et al., 2006; Guruge et al., 2011; ISO, 2009; Wheeler et al., 1997). However, two issues still remain: the linear response of NP isomers by FID should be confirmed, and the separation of NP isomers should be complete (Katase et al., 2008). Both of these two issues could contribute to inaccurate quantification of NP isomers and may further lead to inaccurate assessment of risks of NP. For example, the total calculated estrogenicity was 2.7-3.0 times greater than that actually measured in seawater (Kim et al., 2005b). The two-dimensional GC separation would help resolving the incomplete separation.

#### 1.4 Toxicity of Nonylphenol Isomers

The isomeric estrogenic activity of NP has been well demonstrated with fractions of tNP (Kim et al., 2005b; Kim et al., 2004) and also synthetic NP isomers by various methods (Gabriel et al., 2008; Katase et al., 2008; Makino et al., 2008; Preuss et al., 2006; Puy-Azurmendi et al., 2014; Saito et al., 2007; Shioji et al., 2006; Uchiyama et al., 2008; Ying et al., 2012) (Table 1-3). Kim et al. (2004) separated tNP into 7 fractions and tested their estrogenicity by yeast estrogen screen assay (YES) and found that NP<sub>37</sub> was highly estrogenic; the estrogenicity of NP<sub>37</sub> was several orders of magnitude higher than tNP and other NP isomers. The authors further separated the tNP into 14 fractions with preparative GC and tested the estrogenic activity again using the same method (Kim et al., 2005b). However, the authors found that NP<sub>119</sub> was most estrogenic and its relative potency (RP) was only a few times higher than the other isomers including NP<sub>37</sub>. Moreover, the calculated total estrogenic activity of seawater samples were 2.7 to 3.0 times greater than the measured values (Kim et al., 2005b). As mentioned above, this may be attributed to inaccurate quantification of NP isomers due to incomplete peak separation. Another possibility may be inaccurate measurement of estrogenic activities of NP fractions due to co-elution on HPLC and preparative GC.

Table 1-3 lists the relative potencies of synthetic 4- $\alpha$ -quaternary-NP isomers by yeast estrogen screen assay (YES), yeast two-hybrid assay, MVLN cell assay and E-screen assay. The RP values were calculated from the minimal effective concentration (MEC), half maximal effective concentration (EC50), and 20% maximal effective concentration

(EC20). Large differences were observed for the same NP isomers among different studies or even in the same study when using different calculation methods. For example, the RP values for NP<sub>112</sub> and NP<sub>9</sub> ranged from 0.16 to 1.87 and from 0.023 to 0.95, respectively (Table 1-3). Overall, most of synthesized 4- $\alpha$ -quaternary-NP isomers showed relatively lower estrogenic activity than tNP, with just a few exceptions (e.g., NP<sub>128</sub> and NP<sub>119</sub>). Therefore, it is likely that some unidentified isomers have higher estrogenic activities. It is also possible that some minor components, for example,  $\alpha$ -tertiary isomers, may contribute estrogenic activity higher than that indicated by their content in the tNP. Shioji et al. (2006) tested 11 4- $\alpha$ -tertiary-NP isomers and found 2 isomers, NP<sub>176</sub> and NP<sub>210</sub>, have higher RP values (153 and 4.8, respectively). Gabriel et al. (2008) reported the RP values of 3 4- $\alpha$ -tertiary-NP isomers and the highest one was 1.68 (NP<sub>70</sub>).

Given the large number of NP isomers, it is infeasible to synthesize all the isomers and test their estrogenicity. Thus, understanding the structure–estrogenicity relationship is imperative. After investigating various NP isomers and congeners, Shioji et al. (2006) concluded that: 1) suitable alkyl chain length was necessary for high estrogenicity; 2) bulkiness at  $\beta$  and  $\gamma$  carbons increased the estrogenicity; 3) branching at  $\alpha$  carbon was weakly related to estrogenicity; and 4) isomers having only  $\alpha$  substituents had low estrogenicity. Preuss et al. (2006) suggested that the substituents at  $\alpha$  carbon was also important since  $\alpha$ -ethyl- $\alpha$ -methyl isomers showed higher estrogenicity than  $\alpha$ -dimethyl isomers. Gabriel et al. (2008) agreed with all the conclusions made by Shioji et al. and further pointed out that isomers with 4-6 carbon side chain length had the highest

estrogenicity. Rabinowitz and Little (2011) used a computational approach by calculating the binding affinities of NP isomers to the estrogen receptor. They found that 13 of the 15 strongest binding isomers were  $\alpha$ -secondary isomers (no substitution adjacent to the phenyl ring) and that substitution at  $\alpha$  position may reduce the estrogenicity. Therefore, minor components 4- $\alpha$ -tertiary-NP may in fact contribute significantly to the overall estrogenicity of tNP.

Ying et al. (2012) reported that NP isomers may inhibit the release of testosterone in Leydig cells and the order of inhibition followed  $NP_{112} > NP_{65} > NP_{38} > NP_{111} > tNP > 4$ -n-NP ( $NP_1$ ). This order was different from that for estrogenicity, indicating another mechanism may be present on the steroidogenesis of NP isomers. Preuss et al. (2010) suggested that the isomeric estrogenicity difference of NP isomers may be caused by differences in receptor affinity, receptor activation, or activation/deactivation of non-receptor mediated side paths of reporter gene translation. The authors classified  $NP_{111}$ ,  $NP_{112}$ ,  $NP_{65}$ ,  $NP_{37}$  and tNP as partially estrogenic in the MVLN cell assay because they showed estrogenicity but did not reach 100% efficacy, and  $NP_{38}$ ,  $NP_9$  and  $NP_1$  as antiestrogenic since they had the same binding affinity but did not show estrogenic activity. Cormio et al. (2011) reported that all of the 4 isomers,  $NP_{112}$ ,  $NP_{111}$ ,  $NP_{65}$  and  $NP_1$ , showed no response in the yeast androgenic screen (YAS) assay while all responded in the androgenic competition assay (anti-YAS) and followed the same order in the YES assay, i.e.,  $NP_{111} > NP_1 > NP_{65} > NP_{112}$ .

Since some NP isomers have one or more chiral carbons, it is important to consider the difference between enantiomers and diastereomers (Makino et al., 2008; Saito et al., 2007) (Table 1-3). Interestingly, diastereomers NP<sub>110a/b</sub>, NP<sub>111a/b</sub> and NP<sub>193a/b</sub> showed significant differences while enantiomers *S*-NP<sub>119</sub>, *R*-NP<sub>119</sub> and *S*-NP<sub>194</sub>, *R*-NP<sub>194</sub> showed no difference (Makino et al., 2008) (Table 1-3). Isomers having the  $\beta$ -methyl group over the benzene ring exhibited 2-4 times estrogenic activity than their diastereomers (Makino et al., 2008). In another study by Saito et al. (2007), the RP values for *S*- and *R*-NP<sub>119</sub> were both 4.5 while the values for *S*- and *R*-NP<sub>194</sub> were 0.79 and 0.45 respectively. The difference in isomeric estrogenic activity supported that it is inaccurate to only evaluate the risk of tNP as a whole; rather, careful consideration of constitutional isomers and even stereoisomers is necessary.

## 1.5 Occurrence of Nonylphenol Isomers

### 1.5.1 Composition of Technical Nonylphenol

The composition of tNP has been extensively characterized (Eganhouse et al., 2009; Guenther et al., 2006; Horii et al., 2010; ISO, 2009; Katase et al., 2008; Russ et al., 2005; Vallejo et al., 2011; Wheeler et al., 1997). Eganhouse et al. (2009) investigated the composition of 7 tNP products and found that approximately, tNP products consisted of 0.04-0.3% of C<sub>3</sub>-C<sub>7</sub> phenols, 0.01-2.2% of octylphenol (OP), 2.5-8.9% of 2-NP, 85.6-93.7% of 4-NP and 2.2-4.6% of decylphenol (DP). These results were in good agreement with Wheeler et al. (1997) who reported the fractions as 3-6% 2-NP, 90-93% 4-NP, and 2-5% DP. Eganhouse et al. (2009) also observed that all of the 21 major components of

tNP were 4- $\alpha$ -quaternary isomers, of which 18 had elucidated structures. One of the six significant minor components was believed to have  $\alpha$ -H- $\alpha$ -methyl substitution. The percentages of major 4- $\alpha$ -quaternary NP are listed in [Table 1-4](#). The ISO standard (2009) also lists compositions of 7 different tNP products and the results are the same as Horii et al. (2010); however, the suppliers of tNP were not given, and therefore, the results are not included in [Table 1-4](#). Vallejo et al. (2011) reported the concentrations of NP<sub>9</sub> and NP<sub>112</sub> in Aldrich and Fluka tNP, and the respective concentrations for NP<sub>9</sub> were  $1.98 \pm 0.09\%$  and  $2.28 \pm 0.15\%$  (NP<sub>9</sub>) and the respective concentrations for NP<sub>112</sub> were  $7.71 \pm 0.82\%$ , and  $11.70 \pm 0.61\%$ . For the tNP from the same supplier, usually Horii et al. (2010) gave the highest value for each isomer, especially for NP<sub>112</sub> and NP<sub>119</sub>. For example, for NP<sub>112</sub> in Aldrich tNP, the values given by Horii et al. (2010) were 18 and 19% for two samples, whereas values given by all other studies were between 8% and 10%. There are two possible causes for the difference: incomplete separation as pointed out by Gabriel et al. (2008) and inaccurate quantification by FID. There were also some small differences among tNP products from different suppliers; however the differences were not consistent among different studies. For example, in Eganhouse et al. (2009) study, the fraction of NP<sub>36</sub> was found to be higher in Acros tNP than in Fluka tNP, while in Russ et al. (2005), the results were opposite. This may be due to the difference in the quantification methods or composition variations among different lots. For example, tNP produced before 1980s had a smaller content of 4- $\alpha$ -quaternary-NP (Eganhouse et al., 2009) ([Table 1-4](#)).

### 1.5.2 Occurrence of Nonylphenol Isomers in the Environment

The widespread occurrence of NP in the environment has been well demonstrated by numerous studies (Fan et al., 2013; Sharma et al., 2009; Soares et al., 2008; Venkatesan and Halden, 2013; Ying et al., 2002); However, only a limited number of studies have evaluated NP occurrence at the isomeric level (Eganhouse et al., 2009; Guruge et al., 2011; Horii et al., 2004; Isobe et al., 2001; Jin et al., 2004; Kim et al., 2005a; Kim et al., 2005b). Among the reported studies, most provided only qualitative descriptions; only a few studies gave quantitative concentration of NP isomers and all these studies focused on water (Table 1-5). Horii et al. (2004) investigated NP isomeric concentrations in water samples from Arakawa River and Hanamigawa River around Tokyo Bay, Japan. The concentrations of NP isomers ranged from a few ng/L to hundreds ng/L. Among the 9 sites investigated, a few showed no significant change on isomer compositions as compared to that of tNP. At some other sites, isomer compositions showed significant shifts from that of tNP. For example, NP<sub>36</sub> showed much higher concentrations than NP<sub>194</sub> in tNP, and sites 4 and 8, while at sites 3 and 5, their concentrations of these two isomers were similar (Table 1-5). This phenomenon suggested that isomer selective degradation occurred at some sites. Kim et al. (2005b) investigated NP isomeric concentrations at 3 sites (near the rivermouth, 7 km offshore, and 12 km offshore) in the Ariake Sea, Japan. As expected, the overall NP concentrations decreased as the distance from the rivermouth increased. Interestingly, selective degradation was observed (Table 1-5). For example, the concentration of NP<sub>36</sub> decreased substantially from the rivermouth to 7 km offshore while the concentration of NP<sub>194</sub> stayed the same. Guruge et al. (2011)



investigated the occurrence of NP isomers in surface water of Sri Lanka. The isomer concentrations ranged from 1 to about 200 ng/L. The composition of Negombo Lagoon showed significant differences from tNP, indicating selective degradation (Table 1-5). In the ISO method (2009), isomeric concentrations of two river water samples and two waste water samples were also reported (Table 1-5); however, no sampling sites were given. It should be noted that the quantification of NP isomers in these studies were based on the response on FID and also due to incomplete separation on a 30-m GC column, the concentrations of each isomer may be inaccurate. Eganhouse et al. (2009) used 8 synthetic isomers as standards and determined the isomeric concentrations of NP in wastewater treatment plant effluent from the Los Angeles Joint Water Pollution Control Plant. The concentrations of NP isomers ranged from 1010 to 3970 ng/L (Table 1-5). Ieda et al. (2005) reported the concentrations of NP<sub>37</sub> and NP<sub>119</sub> in 3 rivers in Japan. The concentrations ranged from 2.6 to 13.3 ng/L and from 0.8 to 11.9 ng/L, respectively.

Kim et al. (2005a) analyzed NP isomers in the dissolved phase and suspended solids of a water sample from the New York-New Jersey Harbor. They found that the compositions were different than that in the tNP, again indicating isomeric degradation; moreover, NP<sub>119</sub> had high adsorption affinity on the suspended solids than other isomers, suggesting some isomer differences in adsorption. However, Isobe et al. (2001) reported that profiles of 10 isomers were consistent in the primary/secondary effluent, river water and sediment, indicating an absence of isomer selective degradation or adsorption. Jin et al. (2004) investigated the isomer concentrations in the Haihe River, China and for the 11

isomers separated, the median concentrations ranged from 4.2 to 40.6 ng/L. However, the authors did not identify the structures of these isomers.

Since some NP isomers are chiral and enantiomers may have different estrogenicity, it is further necessary to determine the concentrations of enantiomers. The only data available are on NP<sub>35</sub> and NP<sub>112</sub> in the influent and effluent water samples reported by Zhang et al. (2007). In the influent, the enantiomer ratio (ER) ranged from 0.93 to 1.70 and from 1.03 to 1.70 for NP<sub>35</sub> and NP<sub>112</sub>, respectively; while in the effluent, the values changed to from 1.02 to 1.07 and from 1.02 to 1.10, respectively.

Based on the concentration and estrogenic activity of individual isomers, the estrogen equivalent concentration (EEC) may be calculated. These values may be further used to identify the most environmentally important isomers, thus allowing a focused research effort on those isomers posing the greatest environmental risks. According to the EEC values reported, NP<sub>112</sub> had the highest environmental risk (Guruge et al., 2011; Kim et al., 2005b). However, as mentioned above, the calculated estrogenicity in seawater samples were 2.7 to 3 times higher than that actually measured (Kim et al., 2005b). Since Guruge et al. (2011) used the same approach as Kim et al. (2005b), the same issue could also exist in that study. The causes may include inaccurate estrogenicity data and inaccurate quantification of NP isomers, as discussed above. More comprehensive research at the isomer scale is clearly needed for both tNP and different environmental compartments.

## 1.6 Biodegradation of Nonylphenol Isomers

### 1.6.1 Biodegradation Kinetics

In addition to the indirect evidence of isomer selective biodegradation observed through changes in isomer profiles in occurrence (Horii et al., 2004; Kim et al., 2005b), direct observations of selective biodegradation was reported in cultures, soils, sediments, wastewater and biosolids (Das and Xia, 2008; Eganhouse et al., 2009; Gabriel et al., 2005a; Gabriel et al., 2008; Hao et al., 2009; Shan et al., 2011; Toyama et al., 2011). Gabriel et al. (2005a) investigated the degradation kinetics and pathways of 5 NP isomers with *Sphingomonas xenophaga* Bayram, a bacterial strain isolated from activated sludge, and found that the biodegradability of NP isomers followed the order:  $NP_{93} > NP_{112} > NP_9 > NP_2 > NP_1$  for the mixture and  $NP_{112} > NP_{93} > NP_9 >> NP_1 > NP_2$  for individual isomers. They also observed that only  $\alpha$ -quaternary NP isomers served as the carbon source. These findings suggested that there may be intrinsic differences among NP isomers in their susceptibility to biodegradation. Gabriel et al. (2008) subsequently explored the relationship between degradation rates and structures of NP isomers. After 9 d of incubation, most isomers (12 out of 18 isomers) were removed by 80% (Gabriel et al., 2008) (Table 1-6); however, some isomers were recalcitrant to degradation. For example, only about 30% of  $NP_{193}$  was degraded. However, due to the presence of numerous microorganisms in the natural environment, biodegradation selectivity may be less straightforward than in a pure culture. Shan et al. (2011) compared degradation of 5 synthetic NP isomers in a rice paddy soil under oxic conditions and the half lives

followed the order: NP<sub>111</sub> (10.3 d) > NP<sub>112</sub> (8.4 d) > NP<sub>65</sub> (5.8 d) > NP<sub>38</sub> (2.1 d) > NP<sub>1</sub> (1.4 d) (Table 1-6). The study findings suggested that if only NP1 is used as the surrogate for NP, overestimation of NP biodegradability or underestimation of risks would occur. Hao et al. (2009) reported that biodegradation of NP was isomer selective in the wastewater treatment process simulated in a sequencing batch reactor. Biodegradation rate of 4 identified isomers followed the order: NP<sub>36</sub> (75.4%) > NP<sub>111</sub> (42.9%) > NP<sub>170</sub> (40.7%) > NP<sub>194</sub> (36.2%) (Table 1-6). These biodegradation rates were smaller than those reported by USEPA. After examining 26 municipal wastewater treatment plants with full-scale activated sludge treatment, the range of NP removal was from 57% to 100% with an average of 90% (USEPA, 2010).

A few additional studies also considered isomeric biodegradation; however, no identification of NP isomers or quantification of biodegradation rates was carried out (Das and Xia, 2008; Eganhouse et al., 2009; Toyama et al., 2011). Eganhouse et al. (2009) analyzed the bacterial biodegradation samples from Gabriel et al. (2008) using GC×GC. The authors confirmed the findings by Gabriel et al. (2008): some isomers such as NP<sub>36</sub>, NP<sub>37</sub> and NP<sub>38</sub> were largely removed while some other isomers such as NP<sub>194</sub>, NP<sub>193</sub> and NP<sub>152</sub> were relatively enriched. Moreover, the authors showed that some minor and trace components were persistent and these isomers may contribute significantly to the overall estrogenicity. Ikunaga et al. (2004) examined the biodegradation of tNP by two bacterial strains *Sphingobium amiense* and *Sphingomonas cloacae*. Biodegradation of tNP by *Sphingobium amiense* showed isomer selectivity. For example, isomers with  $\alpha$ -dimethyl and  $\alpha$ -ethyl- $\alpha$ -methyl substituents had higher degradation rates (0.356 h<sup>-1</sup> and 0.554 h<sup>-1</sup>,

respectively). Isomers with  $\alpha$ -methyl- $\alpha$ -propyl substituents had a lower degradation rate ( $0.036 \text{ h}^{-1}$ ). Meanwhile, biodegradation by *Sphingomonas cloacae* was not isomer selective ( $0.996 \text{ h}^{-1}$ ). Das and Xia (2008) explored the degradation of NP isomers during biosolid composting. They separated the NP isomers into 8 groups. Under optimal conditions, the half live of tNP was  $1.3 \pm 0.2 \text{ d}$  while half-lives for group 1 isomers ( $\alpha$ -methyl- $\alpha$ -propyl) and group 2 isomers ( $\alpha$ -dimethyl) were  $12.6 \pm 0.3 \text{ d}$  and  $0.8 \pm 0.1 \text{ d}$ , respectively. Toyama et al. (2011) observed that in the rhizosphere sediment, peaks of many NP isomers decreased after 42 d while the peaks of a few isomers remained unchanged. Unfortunately, the authors did not structurally identify these persistent isomers. In the soil amended with biosolid, the biodegradation rates for 8 NP peaks were found to be different; plant *Triticum aestivum L* increased the overall NP degradation rates but did not change the residue profile (Brown et al., 2009). Zhang et al. (2009b) did not observe chiral selective biodegradation in two German agricultural soils.

### 1.6.2 Structure-Biodegradation Relationship

Given the large number of NP isomers, it is intuitive to explore the structure-biodegradation relationship to screen out the most recalcitrant isomers. Gabriel et al. (2005a) concluded that highly branched isomers had higher biodegradation rates after investigating the degradation of NP<sub>112</sub>, NP<sub>93</sub>, NP<sub>9</sub>, NP<sub>2</sub> and NP<sub>1</sub> by *Sphingomonas xenophaga* Bayram. However, after testing additional isomers with the same bacterial strain, the authors concluded that degradation was more efficient when  $\alpha$ -substituents were less bulky and followed the order:  $\alpha$ -dimethyl >  $\alpha$ -ethyl- $\alpha$ -methyl >  $\alpha$ -ethyl- $\alpha$ -

methyl- $\beta$ -methyl >  $\alpha$ -methyl- $\alpha$ -*n*-propyl >  $\alpha$ -*iso*-propyl- $\alpha$ -methyl >  $\alpha$ -methyl- $\alpha$ - *sec*-butyl. On the other hand, the authors maintained that their former conclusion held as a general principle except when the  $\alpha$ -substituents were too bulky (Gabriel et al., 2008). Other studies also found that isomers with  $\alpha$ -dimethyl and  $\alpha$ -ethyl- $\alpha$ -methyl had higher biodegradability (Das and Xia, 2008; Ikunaga et al., 2004). Hao et al. (2009) evaluated the relationship between NP isomer biodegradation rates and their molecular connectivity indexes  ${}^2\chi^v$  and  ${}^4\chi_{pc}^v$ , and showed that a bulkier structure and short nonyl moiety would result in lower degradability. However, in their study, only 4 isomers were considered, and the derived empirical model thus lacks the necessary robustness.

### 1.6.3 Biodegradation Mechanisms

The different biodegradation kinetics of NP isomers may result from their different biodegradation mechanisms. The biodegradation mechanisms of NP isomers by bacterial strains *Sphingomonas xenophaga* Bayram (Gabriel et al., 2007; Gabriel et al., 2005a; Gabriel et al., 2005b; Gabriel et al., 2012) and *Sphingomonas sp.* strain TTNP3 (Corvini et al., 2005; Corvini et al., 2007; Corvini et al., 2004a; Corvini et al., 2006; Corvini et al., 2004b; Corvini et al., 2004c) have been well evaluated and further summarized by Gabriel et al. (2008) and Corvini et al. (Corvini et al., 2006; Gabriel et al., 2008; Kolvenbach and Corvini, 2012). The initial step was *ipso*-hydroxylation at the *para* position. According to Gabriel et al. (2008), the bulk  $\alpha$ -substituents may affect the biodegradation kinetics in two ways: electronic effects and steric effects. The bulky substituent may increase the electron density at the *para*-position and thus facilitate the

electrophilic addition of oxygen species and finally increase the biodegradation rate. On the other hand, the bulky substituent may increase the steric hindrance and thus decrease the biodegradation rate. The NP isomers with bulky  $\alpha$ -substituents showed lower biodegradation rates, suggesting that the steric effect was dominant. Nitrification of NP isomers at *ortho* position was also an important pathway and it may count for up to 40% of NP applied to soil/sludge system (Telscher et al., 2005). However, the nitrification rate of different NP isomers are unknown. Alkyl-chain oxidation products of NP isomers were also found in the laboratory-scale membrane bioreactor (Cirja et al., 2006). Moreover, biodegradation of NP by fungi may involve  $\omega$ - and then  $\beta$ -oxidation of the nonyl chain (Corvini et al., 2006). Therefore, the importance of alkyl chain oxidation in the isomeric selectivity of NP biodegradation merits investigation.

### 1.7 Objectives

The ultimate goal of this project is to obtain a systematic understanding of biodegradation and chemical oxidation of individual NP isomers to better characterize NP's environmental attenuation mechanisms, identify potential advanced treatment options, and improve risk assessment. The specific objectives are:

Objective 1: Investigate the isomer specific biodegradation kinetics of NP in river sediments under controlled conditions and establish the structure-biodegradability relationship.

Hypothesis 1: Previous research has shown that the biodegradation of NP is important for NP attenuation in various environmental compartments. Biodegradation studies of NP in culture also showed isomer-specific characteristics. Thus, it may be anticipated that biodegradation of NP in river sediments may also be isomer selective. Many different methods have been used for describing the quantitative structure-biodegradability relationships of other environmental contaminants. It may be further assumed that simple molecular descriptors may be chosen to adequately describe the biodegradability of NP isomers.

Objective 2: Evaluate isomer specific biodegradation kinetics of NP during wastewater treatment in a laboratory simulated conventional activated sludge (CAS) bioreactor.

Hypothesis 2: Previous studies have shown that biodegradation of NP was isomer selective by bacterial strains isolated from activated sludge. It may be hypothesized that biodegradation of NP in activated sludge treatment processes with various microorganisms should also be isomer selective.

Objective 3: Characterize the isomer specific chemical oxidation kinetics of NP by  $\text{KMnO}_4$ .

Hypothesis 3: Nonylphenol has been frequently detected in aquatic environments, including source drinking water. Chemical oxidation processes were effective at removing NP in water. However, no isomer specific reaction information has been reported to date. It may be hypothesized that the oxidation kinetics of individual isomers



may be different because of different reactivity among the isomers. The relative reactivity by oxidation may further differ from that of biodegradation due to different reaction mechanisms.

Objective 4: Explore the chemical oxidation kinetics of NP and octylphenol by soil manganese dioxides ( $\text{MnO}_2$ ) and establish the reaction pathways.

Hypothesis 4: Nonylphenol is introduced into soil when NP-containing sludge is applied to fields. It is known that manganese dioxides play a key role in the abiotic degradation of phenolic compounds in soil. It may be hypothesized that oxidation by  $\text{MnO}_2$  may also be an important pathway for the natural attenuation of NP in soil.

## References

- Bechi, N., Ietta, F., Romagnoli, R., Jantra, S., Cencini, M., Galassi, G., Serchi, T., Corsi, I., Focardi, S. and Paulesu, L. (2010). Environmental levels of *para*-nonylphenol are able to affect cytokine secretion in human placenta. *Environ. Health Perspect.* **118**(3): 427-431.
- Boehme, R. M., Andries, T., Dotz, K. H., Thiele, B. and Guenther, K. (2010). Synthesis of defined endocrine-disrupting nonylphenol isomers for biological and environmental studies. *Chemosphere* **80**(7): 813-821.
- Brown, S., Devin-Clarke, D., Doubrava, M. and O'Connor, G. (2009). Fate of 4-nonylphenol in a biosolids amended soil. *Chemosphere* **75**(4): 549-554.
- Cirja, M., Zuehlke, S., Ivashechkin, P., Schaeffer, A. and Corvini, P. F. X. (2006). Fate of a C-14-labeled nonylphenol isomer in a laboratory-scale membrane bioreactor. *Environ. Sci. Technol.* **40**(19): 6131-6136.
- Cormio, P. G., Christmann, M., Rastall, A., Grund, S., Hollert, H., Schuphan, I. and Schmidt, B. (2011). Chlorinated isomers of nonylphenol differ in estrogenic and androgenic activity. *Journal of Environmental Science and Health Part a-Toxic/Hazardous Substances & Environmental Engineering* **46**(4): 329-336.
- Corvini, P. F. X., Elend, M., Hollender, J., Ji, R., Preiss, A., Vinken, R. and Schaffer, A. (2005). Metabolism of a nonylphenol isomer by *Sphingomonas sp* strain TTNP3. *Environ. Chem. Lett.* **2**(4): 185-189.
- Corvini, P. F. X., Meesters, R., Mundt, M., Schaffer, A., Schmidt, B., Schroder, H. F., Verstraete, W., Vinken, R. and Hollender, J. (2007). Contribution to the detection

- and identification of oxidation metabolites of nonylphenol in *Sphingomonas sp* Strain TTNP3. *Biodegradation* **18**(2): 233-245.
- Corvini, P. F. X., Meesters, R. J. W., Schaffer, A., Schroder, H. F., Vinken, R. and Hollender, J. (2004a). Degradation of a nonylphenol single isomer by *Sphingomonas sp* strain TTNP3 leads to a hydroxylation-induced migration product. *Appl. Environ. Microbiol.* **70**(11): 6897-6900.
- Corvini, P. F. X., Schaffer, A. and Schlosser, D. (2006). Microbial degradation of nonylphenol and other alkylphenols -- our evolving view. *Appl. Microbiol. Biotechnol.* **72**(2): 223-243.
- Corvini, P. F. X., Vinken, R., Hommes, G., Mundt, M., Hollender, J., Meesters, R., Schroder, H. F. and Schmidt, B. (2004b). Microbial degradation of a single branched isomer of nonylphenol by *Sphingomonas* TTNP3. *Water Sci. Technol.* **50**(5): 189-194.
- Corvini, P. F. X., Vinken, R., Hommes, G., Schmidt, B. and Dohmann, M. (2004c). Degradation of the radioactive and non-labelled branched 4(3',5'-dimethyl-3'-heptyl)-phenol nonylphenol isomer by *Sphingomonas* TTNP3. *Biodegradation* **15**(1): 9-18.
- Das, K. C. and Xia, K. (2008). Transformation of 4-nonylphenol isomers during biosolids composting. *Chemosphere* **70**(5): 761-768.
- Eganhouse, R. P., Pontolillo, J., Gaines, R. B., Frysinger, G. S., Gabriel, F. L. P., Kohler, H.-P. E., Giger, W. and Barber, L. B. (2009). Isomer-specific determination of 4-

- nonylphenols using comprehensive two-dimensional gas chromatography/time-of-flight mass spectrometry. *Environ. Sci. Technol.* **43**(24): 9306-9313.
- European Commission (2002). Risk assessment report: 4-Nonylphenol (branched) and nonylphenol [http://esis.jrc.ec.europa.eu/doc/risk\\_assessment/REPORT/4-nonylphenol\\_nonylphenolreport017.pdf](http://esis.jrc.ec.europa.eu/doc/risk_assessment/REPORT/4-nonylphenol_nonylphenolreport017.pdf).
- Fan, Z., Hu, J., An, W. and Yang, M. (2013). Detection and occurrence of chlorinated byproducts of bisphenol A, nonylphenol, and estrogens in drinking water of China: Comparison to the parent compounds. *Environ. Sci. Technol.*
- Gabriel, F. L. P., Cyris, M., Jonkers, N., Giger, W., Guenther, K. and Kohler, H. P. E. (2007). Elucidation of the *ipso*-substitution mechanism for side-chain cleavage of  $\alpha$ -quaternary 4-nonylphenols and 4-*t*-butoxyphenol in *Sphingobium xenophagum* Bayram. *Appl. Environ. Microbiol.* **73**(10): 3320-3326.
- Gabriel, F. L. P., Giger, W., Guenther, K. and Kohler, H. P. E. (2005a). Differential degradation of nonylphenol isomers by *Sphingomonas xenophaga* bayram. *Appl. Environ. Microbiol.* **71**(3): 1123-1129.
- Gabriel, F. L. P., Heidelberger, A., Rentsch, D., Giger, W., Guenther, K. and Kohler, H. P. E. (2005b). A novel metabolic pathway for degradation of 4-nonylphenol environmental contaminants by *Sphingomonas xenophaga* Bayram: *ipso*-Hydroxylation and intramolecular rearrangement. *J. Biol. Chem.* **280**(16): 15526-15533.
- Gabriel, F. L. P., Mora, M. A., Kolvenbach, B. A., Corvini, P. F. X. and Kohler, H. P. E. (2012). Formation of toxic 2-nonyl-*p*-benzoquinones from  $\alpha$ -tertiary 4-

- nonylphenol isomers during microbial metabolism of technical nonylphenol. *Environ. Sci. Technol.* **46**(11): 5979-5987.
- Gabriel, F. L. P., Routledge, E. J., Heidelberger, A., Rentsch, D., Guenther, K., Giger, W., Sumpter, J. P. and Kohler, H. P. E. (2008). Isomer-specific degradation and endocrine disrupting activity of nonylphenols. *Environ. Sci. Technol.* **42**(17): 6399-6408.
- Guenther, K., Kleist, E. and Thiele, B. (2006). Estrogen-active nonylphenols from an isomer-specific viewpoint: A systematic numbering system and future trends. *Anal. Bioanal. Chem.* **384**(2): 542-546.
- Guruge, K. S., Horii, Y. and Yamashita, N. (2011). Profiles of nonylphenol isomers in surface waters from Sri Lanka. *Mar. Pollut. Bull.* **62**(4): 870-873.
- Hao, R. X., Li, J. B., Zhou, Y. W., Cheng, S. Y. and Zhang, Y. (2009). Structure-biodegradability relationship of nonylphenol isomers during biological wastewater treatment process. *Chemosphere* **75**(8): 987-994.
- Horii, Y., Katase, T., Kim, Y. S. and Yamashita, N. (2004). Determination of individual nonylphenol isomers in water samples by using relative response factor method. *Bunseki Kagaku* **53**(10): 1139-1147.
- Horii, Y., Taniyasu, S., Tsuchiya, Y., Nakagawa, J., Takasuga, T., Yamashita, N. and Miyazaki, A. (2010). Interlaboratory trial on the analysis of individual isomers of nonylphenol in water samples according to ISO 24293: 2009. *Bunseki Kagaku* **59**(4): 319-327.

- Ieda, T., Horii, Y., Petrick, G., Yamashita, N., Ochiai, N. and Kannan, K. (2005). Analysis of nonylphenol isomers in a technical mixture and in water by comprehensive two-dimensional gas chromatography-mass spectrometry. *Environ. Sci. Technol.* **39**(18): 7202-7207.
- Ikunaga, Y., Miyakawa, S. I., Hasegawa, M., Kasahara, Y., Kodama, O. and Ohta, H. (2004). Degradation profiles of branched nonylphenol isomers by *Sphingobium amiense* and *Sphingomonas cloacae*. *Soil Sci. Plant Nutr.* **50**(6): 871-875.
- ISO (2009). Water quality--Determine the individual isomers of nonylphenol. Method using solid phase extraction (SPE) and gas chromatography/mass spectrometry (GC/MS). **ISO 24293 2009 (E)**.
- Isobe, T., Nishiyama, H., Nakashima, A. and Takada, H. (2001). Distribution and behavior of nonylphenol, octylphenol, and nonylphenol monoethoxylate in Tokyo metropolitan area: Their association with aquatic particles and sedimentary distributions. *Environ. Sci. Technol.* **35**(6): 1041-1049.
- Jiang, J., Pang, S. Y., Ma, J. and Liu, H. L. (2012). Oxidation of phenolic endocrine disrupting chemicals by potassium permanganate in synthetic and real waters. *Environ. Sci. Technol.* **46**(3): 1774-1781.
- Jin, X., Huang, G., Jiang, G., Zhou, Q. and Liu, J. (2004). Distribution of 4-nonylphenol isomers in surface water of the Haihe River, People's Republic of China. *Bull. Environ. Contam. Toxicol.* **73**(6): 1109-1116.

- Jorgensen, A. D., Picel, K. C. and Stamoudis, V. C. (1990). Prediction of gas chromatography flame ionization detector response factors from molecular structures. *Anal. Chem.* **62**(7): 683-689.
- Katase, T., Okuda, K., Kim, Y. S., Eun, H., Takada, H., Uchiyama, T., Salto, H., Makino, M. and Fujimoto, Y. (2008). Estrogen equivalent concentration of 13 branched para-nonylphenols in three technical mixtures by isomer-specific determination using their synthetic standards in SIM mode with GC-MS and two new diastereomeric isomers. *Chemosphere* **70**(11): 1961-1972.
- Kim, Y.-S., Katase, T., Makino, M., Uchiyama, T., Fujimoto, Y., Inoue, T. and Yamashita, N. (2005a). Separation, structural elucidation and estrogenic activity studies of the structural isomers of nonylphenol by GC-PFC coupled with MS and NMR. *Australas. J. Ecotoxicol.* **11**: 137-148.
- Kim, Y. S., Katase, T., Horii, Y., Yamashita, N., Makino, M., Uchiyama, T., Fujimoto, Y. and Inoue, T. (2005b). Estrogen equivalent concentration of individual isomer-specific 4-nonylphenol in Ariake sea water, Japan. *Mar. Pollut. Bull.* **51**(8-12): 850-856.
- Kim, Y. S., Katase, T., Sekine, S., Inoue, T., Makino, M., Uchiyama, T., Fujimoto, Y. and Yamashita, N. (2004). Variation in estrogenic activity among fractions of a commercial nonylphenol by high performance liquid chromatography. *Chemosphere* **54**(8): 1127-1134.
- Kolpin, D. W., Furlong, E. T., Meyer, M. T., Thurman, E. M., Zaugg, S. D., Barber, L. B. and Buxton, H. T. (2002). Pharmaceuticals, hormones, and other organic

- wastewater contaminants in US streams, 1999-2000: A national reconnaissance. Environ. Sci. Technol. **36**(6): 1202-1211.
- Kolvenbach, B. A. and Corvini, P. F. X. (2012). The degradation of alkylphenols by *Sphingomonas sp* strain TTNP3-a review on seven years of research. New Biotechnol. **30**(1): 88-95.
- Makino, M., Uchiyama, T., Saito, H., Ogawa, S., Iida, T., Katase, T. and Fujimoto, Y. (2008). Separation, synthesis and estrogenic activity of 4-nonylphenols: Two sets of new diastereomeric isomers in a commercial mixture. Chemosphere **73**(8): 1188-1193.
- Moeder, M., Martin, C., Harynuk, J., Gorecki, T., Vinken, R. and Corvini, P. F. X. (2006a). Identification of isomeric 4-nonylphenol structures by gas chromatography-tandem mass spectrometry combined with cluster analysis. J. Chromatogr. A **1102**(1-2): 245-255.
- Moeder, M., Martin, C., Schlosser, D., Harynuk, J. and Gorecki, T. (2006b). Separation of technical 4-nonylphenols and their biodegradation products by comprehensive two-dimensional gas chromatography coupled to time-of-flight mass spectrometry. J. Chromatogr. A **1107**(1-2): 233-239.
- Preuss, T. G., Gehrhardt, J., Schirmer, K., Coors, A., Rubach, M., Russ, A., Jones, P. D., Giesy, J. P. and Ratte, H. T. (2006). Nonylphenol isomers differ in estrogenic activity. Environ. Sci. Technol. **40**(16): 5147-5153.



- Preuss, T. G., Gurer-Orhan, H., Meerman, J. and Ratte, H. T. (2010). Some nonylphenol isomers show antiestrogenic potency in the MVLN cell assay. *Toxicol. in Vitro* **24**(1): 129-134.
- Puy-Azurmendi, E., Olivares, A., Vallejo, A., Ortiz-Zarragoitia, M., Pina, B., Zuloaga, O. and Cajaraville, M. P. (2014). Estrogenic effects of nonylphenol and octylphenol isomers *in vitro* by recombinant yeast assay (RYA) and *in vivo* with early life stages of zebrafish. *The Science of the total environment* **466-467**: 1-10.
- Rabinowitz, J. R. and Little, S. B. (2011). Computational docking of the isomers of nonylphenol to the ligand binding domain of the estrogen receptor. Annual Meeting of the Society of Toxicology, Washington, DC.
- Russ, A. S., Vinken, R., Schuphan, I. and Schmidt, B. (2005). Synthesis of branched *para*-nonylphenol isomers: Occurrence and quantification in two commercial mixtures. *Chemosphere* **60**(11): 1624-1635.
- Saito, H., Uchiyama, T., Makino, M., Katase, T., Fujimoto, Y. and Hashizume, D. (2007). Optical resolution and absolute configuration of branched 4-nonylphenol isomers and their estrogenic activities. *J. Health Sci.* **53**(2): 177-184.
- Shan, J., Jiang, B. Q., Yu, B., Li, C. L., Sun, Y. Y., Guo, H. Y., Wu, J. C., Klumpp, E., Schaffer, A. and Ji, R. (2011). Isomer-specific degradation of branched and linear 4-nonylphenol isomers in an oxic soil. *Environ. Sci. Technol.* **45**(19): 8283-8289.
- Sharma, V. K., Anquandah, G. A. K., Yngard, R. A., Kim, H., Fekete, J., Bouzek, K., Ray, A. K. and Golovko, D. (2009). Nonylphenol, octylphenol, and bisphenol-A in the aquatic environment: A review on occurrence, fate, and treatment. *Journal*

- of Environmental Science and Health Part a-Toxic/Hazardous Substances & Environmental Engineering **44**(5): 423-442.
- Shioji, H., Tsunoi, S., Kobayashi, Y., Shigemori, T., Ike, M., Fujita, M., Miyaji, Y. and Tanaka, M. (2006). Estrogenic activity of branched 4-nonylphenol isomers examined by yeast two-hybrid assay. *J. Health Sci.* **52**(2): 132-141.
- Soares, A., Guieysse, B., Jefferson, B., Cartmell, E. and Lester, J. N. (2008). Nonylphenol in the environment: A critical review on occurrence, fate, toxicity and treatment in wastewaters. *Environ. Int.* **34**(7): 1033-1049.
- Telscher, M. J. H., Schuller, U., Schmidt, B. and Schäffer, A. (2005). Occurrence of a nitro metabolite of a defined nonylphenolisomer in soil/sewage sludge mixtures. *Environ. Sci. Technol.* **39**(20): 7896-7900.
- Thiele, B., Heinke, V., Kleist, E. and Guenther, K. (2004). Contribution to the structural elucidation of 10 isomers of technical *p*-nonylphenol. *Environ. Sci. Technol.* **38**(12): 3405-3411.
- Toyama, T., Murashita, M., Kobayashi, K., Kikuchi, S., Sei, K., Tanaka, Y., Ike, M. and Mori, K. (2011). Acceleration of nonylphenol and 4-tert-octylphenol degradation in sediment by *Phragmites australis* and associated rhizosphere bacteria. *Environ. Sci. Technol.* **45**(15): 6524-6530.
- Uchiyama, T., Makino, M., Saito, H., Katase, T. and Fujimoto, Y. (2008). Syntheses and estrogenic activity of 4-nonylphenol isomers. *Chemosphere* **73**(1): S60-S65.
- USEPA. (2006). "Non-confidential 2006 IUR company/chemical records." Retrieved March 1, 2014, from <http://cfpub.epa.gov/iursearch/index.cfm>.

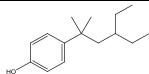
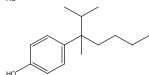
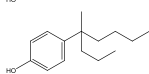
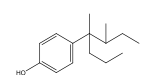
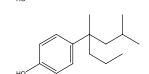
- USEPA (2010). Treating contaminants of emerging concern: A literature review database. Washington, DC.
- Vallejo, A., Olivares, M., Fernandez, L. A., Etxebarria, N., Arrasate, S., Anakabe, E., Usobiaga, A. and Zuloaga, O. (2011). Optimization of comprehensive two dimensional gas chromatography-flame ionization detection-quadrupole mass spectrometry for the separation of octyl- and nonylphenol isomers. *J. Chromatogr. A* **1218**(20): 3064-3069.
- Venkatesan, A. K. and Halden, R. U. (2013). National inventory of alkylphenol ethoxylate compounds in U.S. sewage sludges and chemical fate in outdoor soil mesocosms. *Environ. Pollut.* **174**(0): 189-193.
- Wheeler, T. F., Heim, J. R., LaTorre, M. R. and Janes, A. B. (1997). Mass spectral characterization of p-nonylphenol isomers using high-resolution capillary GC-MS. *J. Chromatogr. Sci.* **35**(1): 19-30.
- Wu, Z. Y., Zeng, Z. D. and Marriott, P. J. (2010). Comparative qualitative analysis of nonylphenol isomers by gas chromatography-mass spectrometry combined with chemometric resolution. *J. Chromatogr. A* **1217**(49): 7759-7766.
- Ying, F., Ding, C., Ge, R., Wang, X., Li, F., Zhang, Y., Zeng, Q., Yu, B., Ji, R. and Han, X. (2012). Comparative evaluation of nonylphenol isomers on steroidogenesis of rat Leydig Cells. *Toxicol. in Vitro* **26**(7): 1114-1121.
- Ying, G. G., Williams, B. and Kookana, R. (2002). Environmental fate of alkylphenols and alkylphenol ethoxylates - a review. *Environ. Int.* **28**(3): 215-226.

- Yu, B., Bian, X.-s. and Ji, R. (2008). Synthesis and characterization of four *para*-nonylphenol isomers containing a quaternary alpha-carbon. *Asian Journal of Ecotoxicology* **3**(1): 98-104.
- Zenkevich, I. G., Makarov, A. A., Schrader, S. and Moeder, M. (2009). A new version of an additive scheme for the prediction of gas chromatographic retention indices of the 211 structural isomers of 4-nonylphenol. *J. Chromatogr. A* **1216**(18): 4097-4106.
- Zhang, H., Oppel, I. M., Spiteller, M., Guenther, K., Boehmler, G. and Zuehlke, S. (2009a). Enantiomers of a nonylphenol isomer: Absolute configurations and estrogenic potencies. *Chirality* **21**(2): 271-275.
- Zhang, H., Spiteller, M., Guenther, K., Boehmler, G. and Zuehlke, S. (2009b). Degradation of a chiral nonylphenol isomer in two agricultural soils. *Environ. Pollut.* **157**(6): 1904-1910.
- Zhang, H., Zuehlke, S., Guenther, K. and Spiteller, M. (2007). Enantioselective separation and determination of single nonylphenol isomers. *Chemosphere* **66**(4): 594-602.

## Tables

**Table 1-1** Names, structure, side chain length and  $\alpha$  and  $\beta$  substituents of representative 4-nonylphenols

Juelich number.	Structure	Juelich nomenclature name	IUPAC name	IUPAC abbrev.	line-coding system	Side chain length	$\alpha$ Substit.	$\beta$ Substit
NP <sub>9</sub>		4-[1,1-dimethylheptyl]phenol	4-(2-methyloctan-2-yl)phenol	22NP	7-1,1(1)	7	Me, Me	None
NP <sub>35</sub>		4-[1,1,2-trimethylhexyl]phenol	4-(2,3-dimethylheptan-2-yl)phenol	232NP	6-1,1,2(1)	6	Me, Me	Me
NP <sub>36</sub>		4-[1,1,3-trimethylhexyl]phenol	4-(2,4-dimethylheptan-2-yl)phenol	242NP	6-1,1,3(1)	6	Me, Me	None
NP <sub>37</sub>		4-[1,1,4-trimethylhexyl]phenol	4-(2,5-dimethylheptan-2-yl)phenol	252NP	6-1,1,4(1)	6	Me, Me	None
NP <sub>38</sub>		4-[1,1,5-trimethylhexyl]phenol	4-(2,6-dimethylheptan-2-yl)phenol	262NP	6-1,1,5(1)	6	Me, Me	None
NP <sub>65</sub>		4-[1-ethyl-1-methylhexyl]phenol	4-(3-methyloctan-3-yl)phenol	33NP	6-1(2),1(1)	6	Me, Et	Me
NP <sub>96</sub>		4-[1,1,4,4-tetramethylpentyl]phenol	4-(2,5,5-trimethylhexan-2-yl)phenol	2552NP	5-1,1,4,4(1)	5	Me, Me	None
NP <sub>110</sub>		4-[1-ethyl-1,2-dimethylpentyl]phenol	4-(3,4-dimethylheptan-3-yl)phenol	343NP	5-1(2),1,2(1)	5	Me, Et	Me, Me
NP <sub>111</sub>		4-[1-ethyl-1,3-dimethylpentyl]phenol	4-(3,5-dimethylheptan-3-yl)phenol	353NP	5-1(2),1,3(1)	5	Me, Et	Me
NP <sub>112</sub>		4-[1-ethyl-1,4-dimethylpentyl]phenol	4-(3,6-dimethylheptan-3-yl)phenol	363NP	5-1(2),1,4(1)	5	Me, Et	Me
NP <sub>119</sub>		4-[2-ethyl-1,1-dimethylpentyl]phenol	4-(3-ethyl-2-methylhexan-2-yl)phenol	3E22NP		5	Me, Me	Et

NP <sub>128</sub>		4-[3-ethyl-1,1-dimethylpentyl]phenol	4-(4-ethyl-2-methylhexan-2-yl)phenol	4E22NP	5	Me, Me	None
NP <sub>143</sub>		4-[1-isopropyl-1-methylpentyl]phenol	4-(2,3-dimethylheptan-3-yl)phenol	233NP	5	Me, <i>i</i> -Pr	Me, Me
NP <sub>152</sub>		4-[1-methyl-1-n-propylpentyl]phenol	4-(4-methyloctan-4-yl)phenol	44NP	5	Me, Pr	Et
NP <sub>193</sub>		4-[1,2-dimethyl-1-n-propylbutyl]phenol	4-(3,4-dimethylheptan-4-yl)phenol	344NP	4	Me, Pr	Me, Et
NP <sub>194</sub>		4-[1,3-dimethyl-1-n-propylbutyl]phenol	4-(2,4-dimethylheptan-4-yl)phenol	244NP	4	Me, Pr	Et

**Table 1-2** Analysis of nonylphenol isomers by gas chromatography

Instrument	Detectors	Column	Isomers identified /separated	References
GC×GC	MSD FID	Primary :HP-5 MS (30m×0.25mm, 0.25 μm) Secondary:DB-17MS (5m×0.25mm, 0.25 μm)	unknown/79	(Vallejo et al., 2011)
GC	MSD	BPX5(30m×0.25mm, 0.25 μm)	15	(Wu et al., 2010)
GC×GC	ToFMSD	Primary: DB-5 MS (30 m×0.25 mm, 1.0 μm ) Secondary: Supelcowax 10 (2.0m× 0.1mm, 0.1 μm)	18/153-204	(Eganhouse et al., 2009)
GC	MSD	HP-5 (30 m×0.25 mm, 0.25 μm )	15	(Katase et al., 2008)
GC	MSD FID	DB-5 (30 m×0.25 mm, 0.25 μm )	13	(Horii et al., 2004; ISO 2009)
GC	MSD	DB-17(30 m×0.25 mm, 0.25 μm)	18/40	(Gabriel et al., 2008)
GC×GC	ToFMSD	Primary: VF-5MS (30 m×0.25 mm, 0.25 μm ) Secondary VF-23MS (1.6 m×0.1mm, 0.1 μm )	13/40	(Moeder et al., 2006b)
GC	MS-MS	HP-5 MS (30m×0.25mm, 0.25 μm)	18/35	(Moeder et al., 2006a)
GC	MS	DB-5 (30m×0.25mm, 0.25 μm)	11/14	(Kim et al., 2005)
GC×GC	MS	Primary: DB-5(30 m×0.25 mm, 1 μm ); secondary: DB-WAX (1 m×0.1 mm, 0.1 μm )	13/102	(Ieda et al., 2005)
GC	MS	Petrocol DH (100 m ×0.25 mm i.d. ×0.5 μm)	10/21	
GC	MS	Petrocol DH (100 m ×0.25 mm i.d. ×0.5 μm)	unkown/22	(Wheeler et al., 1997)

**Table 1-3** Relative estrogenic activities of synthetic 4- $\alpha$ -quaternary nonylphenol isomers

Chemicals	Puy-Azurmendi et al., 2014		Cormio et al., 2011	Gabriel et al., 2008	Uchiyama et al., 2008	Makino et al., 2008
tNP source	Fluka		None	Fluka	TKK <sup>1</sup>	TCI
Assay	YES		YES	YES	YES	YES
Concentration used for calculation	EC <sub>50</sub>	MEC	EC <sub>50</sub>	Concentration showing EC <sub>50</sub> of E2	MEC	EC <sub>50</sub>
E2				3168	964	1389
tNP	1	1		1	1	1
NP <sub>1</sub>			1			
NP <sub>9</sub>	0.95	0.54		0.023		0.46
NP <sub>35</sub>					0.65	0.78
NP <sub>36</sub>						0.54
NP <sub>37</sub>					0.67	0.67
NP <sub>38</sub>						0.44
NP <sub>65</sub>	0.18	0.26	1.28	0.25	0.44	0.36
NP <sub>93</sub>				1.87 <sup>2</sup>		
NP <sub>94</sub>						
NP <sub>96</sub>						1.00
NP <sub>110a/b</sub>						0.90/2.03
NP <sub>111a/b</sub>			5.97	0.78	0.53	0.53/0.75
NP <sub>112</sub>	1.87	0.45	0.23	0.60	0.57	0.47
NP <sub>119</sub>					3.18	4.68/4.68 <sup>3</sup>
NP <sub>128</sub>					1.57	1.55
NP <sub>152</sub>				0.70	0.71	0.64
NP <sub>170</sub>				0.56		
NP <sub>193a/b</sub>						0.28/1.22
NP <sub>194</sub>				0.49 <sup>4</sup>		0.60/0.32 <sup>3</sup>



**Table 1–3** Relative estrogenic activities of synthetic 4- $\alpha$ -quaternary nonylphenol isomers (continued)

Chemicals	Katase et al., 2008	Saito et al., 2007	Shioji et al., 2006	Preuss et al., 2006	
tNP source	TCI	n.a.	Kishida	Acros	
Assay	YES	YES	Yeast two-hybrid	MVLN	E-screen
Concentration used for calculation	MEC	EC <sub>50</sub>	Concentration showing EC <sub>10</sub> of E2	EC <sub>20</sub>	EC <sub>50</sub>
E2	444	1515	538	74074	24630
tNP	1	1	1	1	1
NP <sub>1</sub>					
NP <sub>9</sub>	0.29		0.07		
NP <sub>35</sub>	0.20		0.12		
NP <sub>36</sub>	0.17	0.64	0.16		
NP <sub>37</sub>	0.14		0.15	0.15	
NP <sub>38</sub>	0.28		0.04		0.07
NP <sub>65</sub>	0.06		0.11	0.45	
NP <sub>93</sub>					
NP <sub>94</sub>			3.0		
NP <sub>96</sub>			0.58		
NP <sub>110a/b</sub>					
NP <sub>111a/b</sub>	0.16			0.70	0.18
NP <sub>112</sub>	0.11			0.51	0.16
NP <sub>119</sub>	1.12	4.5/4.5 <sup>3</sup>			
NP <sub>128</sub>	0.34		0.9		
NP <sub>152</sub>	0.12		0.08		
NP <sub>170</sub>			0.76		
NP <sub>193a/b</sub>					
NP <sub>194</sub>	0.16	0.79/0.45			

<sup>1</sup>Tokyo Kasei Kogyo Co

<sup>2</sup>Contains 17% NP<sub>95</sub>

<sup>3</sup>For *S*- and *R*-enantiomers

<sup>4</sup>Contains 14% NP<sub>36</sub>

**Table 1-4** Isomeric composition (%) of different technical nonylphenol products

isomer	Eganhouse et al., 2009						
	Acros	Aldrich	Chem Service	Fluka <sub>WG</sub> <sup>1</sup>	Fluka	Schen <sup>2</sup>	Schen. HP <sup>3</sup>
NP <sub>9</sub>	1.2 ± 0.						1.2 ± 0.
NP <sub>35</sub>	1	1.0 ± 0.1	1.3 ± 0.1	1.1 ± 0.1	1.5 ± 0.1	1.3 ± 0.2	1
NP <sub>36</sub>	14.9 ± 0	11.3 ± 0.			10.9 ± 0.	11.2 ± 0.	9.6 ± 0.
NP <sub>37</sub>	.7	6	11.2 ± 0.5	8.0 ± 0.3	6	4	6
NP <sub>38</sub>							
NP <sub>65</sub>	2.1,2.0	1.8,1.7	2.2,2.4	2.0,2.1	2.8,2.8	2.3,2.3	2.2,2.4
NP <sub>96</sub>							
NP <sub>110a</sub>							
NP <sub>110b</sub>							
NP <sub>111a</sub>	6.1 ± 0.						5.8 ± 0.
	6	6.0 ± 0.6	5.5 ± 0.4	5.0 ± 0.2	5.6 ± 0.5	5.4 ± 0.2	9
NP <sub>111b</sub>	7.0 ± 0.						7.0 ± 0.
	6	7.2 ± 0.4	6.4 ± 0.5	5.9 ± 0.5	6.6 ± 0.5	7.0 ± 0.6	7
NP <sub>112</sub>	9.1 ± 1.				10.6 ± 1.		9.0 ± 0.
NP <sub>119</sub>	0	8.4 ± 0.7	9.2 ± 0.8	7.3 ± 0.6	0	9.4 ± 0.9	9
NP <sub>128</sub>							
NP <sub>152</sub>	2.3 ± 0.						2.4 ± 0.
NP <sub>193a</sub>	1	2.1 ± 0.2	2.4 ± 0.2	2.2 ± 0.2	2.9 ± 0.2	2.4 ± 0.2	2
NP <sub>193b</sub>							
NP <sub>194</sub>	3.5 ± 0.			2.9 ± 0.0		4.1 ± 0.0	4.4 ± 0.
	02	4.2 ± 0.1	3.8 ± 0.1	1	4.1 ± 0.1	2	2

Part of this table is adapted and reorganized from Eganhouse, et al. 2009 (Table 2) with permission of American Chemical Society.

<sup>1</sup>Obtained before 1980.

<sup>2</sup>Schenectady International Inc. technical product.

<sup>3</sup>Schenectady International Inc. high purity product.

<sup>4</sup>Percentage of each isomer were based on the response on flame ionization detector. According to Gabriel et al., 2008, assigned peak for NP<sub>112</sub> contained NP<sub>128</sub>, peak for NP<sub>119</sub> contained NP<sub>152</sub>, and peak for NP<sub>110a</sub> contained NP<sub>143</sub>.

**Table 1–4** Isomeric composition (%) of different technical nonylphenol products (continued)

isomer	Russ, et al., 2005		Katase, et al., 2008				Horii et al., 2010 <sup>4</sup>			
	Acros	Fluka	TCI	Aldrich	Fluka	TCI	Aldrich	Kanto Chemical	Wako Pure Chemical	Kisida
NP <sub>9</sub>	1	2	3	3.4	2.9					
NP <sub>35</sub>			9.2	6.4	7.4	13	12	12, 15	14	13
NP <sub>36</sub>	12	14	9.4	7	7.9	12	12	12, 16	11	13
NP <sub>37</sub>	3	7	7.7	7.2	7.1	7.2	7.5, 7.9	7.5, 9.3	5.8	6.1
NP <sub>38</sub>	2	5	3.9	4.4	4.4					
NP <sub>65</sub>	2	4	5.9	5.2	5	3	4, 4.4	5.4, 3.8	2.7	2.9
NP <sub>96</sub>	<<1	<<1								
NP <sub>110</sub> <sup>a</sup>						8.3	7.6, 6.7	7.8, 5.5	9.2	9.3
NP <sub>110</sub> <sup>b</sup>						6.2	5.7, 5.5	3.8, 3.5	7.2	6.5
NP <sub>111</sub> <sup>a</sup>	10	10	8.8	7.4	7.4	6.9	6.5, 6.6	6.6, 6.8	6.9	7
NP <sub>111</sub> <sup>b</sup>	10	10	7.3	6	6.1	6.8	6.6, 6.5	6.9	6.8	6.9
NP <sub>112</sub>	9	13	1	9.9	10.1	16	18, 19	18, 19	14	14
NP <sub>119</sub>			5.4	4.4	4.3	6.7	6.8, 7.3	6.7, 5.8	7.2	6.5
NP <sub>128</sub>	3	6	8.2	5.9	7.3					
NP <sub>152</sub>			3.2	3.6	3.3					
NP <sub>193</sub> <sup>a</sup>						4	3.4, 3.1	3.6, 2.1	4.7	4.5
NP <sub>193</sub> <sup>b</sup>						4.4	3.9, 3.7	4, 3	5.2	4.8
NP <sub>194</sub>			6.1	3.8	3.8	5.6	4.8, 5.1	5.5, 3.9	6.2	5.3

**Table 1-5 Occurrences of nonylphenol isomers in environment**

isomer	Eganhouse et al.,	Horii et al., 2004 <sup>1</sup>										Kim et al., 2005 <sup>1</sup>		
	2009	Hanamigawa River		Atakawa River								Sea water		
	WWTP effluent	2	3	4	5	6	7	8	9	10	River mouth	7 km offshore	12 km offshore	
NP <sub>9</sub>	1120													
NP <sub>35</sub>		450	10	100	14	11	19	57	2.7	18	4.3	2.2	1.3	
NP <sub>36</sub>	3970	380	13	74	11	13	15	45	6.9	18	6.4	2.6	1.1	
NP <sub>37</sub>		170	3.9	46	3.8	4.4	5.5	21	1.7	7.6	1.7	1.2	0.7	
NP <sub>65</sub>	1100	100	3.6	16	3	2.6	2.9	7.5	0.63	2.8	3.1	0.7	0.4	
NP <sub>110a</sub>		780	24	60	23	23	22	40	8	21	3.9	2.7	0.9	
NP <sub>110b</sub>		570	18	62	16	15	17	34	5	16	2.7	1.8	0.8	
NP <sub>111a</sub>	2100	430	13	48	13	15	14	22	5.5	15	3.2	2	1	
NP <sub>111b</sub>	2400	580	18	74	17	21	18	37	8	21	3.7	2.3	1.2	
NP <sub>112</sub>	3670	470	13	87	12	15	15	45	6.9	18	8	3	1.6	
NP <sub>119</sub>		440	9.3	44	11	10	12	23	4.9	12	2.4	1.3	0.5	
NP <sub>152</sub>	1460													
NP <sub>193a</sub>		350	17	31	17	13	15	22	6.3	13	5.7	2.5	1.1	
NP <sub>193b</sub>		450	26	50	27	22	23	34	10	21	2.8	2.6	0.2	
NP <sub>194</sub>	1400	270	11	27	13	10	12	11	5.4	10	1.6	1.6	0.6	

<sup>1</sup>These studies based on the similar method. Concentrations of each isomer were based on the response on flame ionization detector. According to Gabriel et al., 2008, assigned peak for NP<sub>112</sub> contained NP<sub>128</sub>, peak for NP<sub>119</sub> contained NP<sub>152</sub>, and peak for NP<sub>110a</sub> contained NP<sub>143</sub>.

**Table 1–5** Occurrence of nonylphenol isomers in environment (continued)

isomer	ISO 2009 <sup>1</sup>				Guruge et al., 2011				
	Riverwater		Waste water		Negombo Lagoon	Kirillapone Canal	Bire Lake	Kelani River	Kandy Lake
	low	high	low	high					
NP <sub>9</sub>									
NP <sub>35</sub>	81.6	355	340.6	1455	9	47	178	9	51
NP <sub>36</sub>	79.2	344	392.9	1358	10	58	195	11	58
NP <sub>37</sub>	35	159	136.3	617	7.0	30	87	7.4	31
NP <sub>65</sub>	17.2	69	117.9	322	12	9	44	2.9	24
NP <sub>110a</sub>	55.6	244	210.7	834	17	29	167	7.0	30
NP <sub>110b</sub>	36.9	183	259.5	924	8.2	10	88	3.9	21
NP <sub>111a</sub>	44.2	196	158	706	10	28	120	6.7	33
NP <sub>111b</sub>	45.7	196	165.8	686	13	40	170	9	43
NP <sub>112</sub>	93.4	414	358	1619	13	53	227	14	74
NP <sub>119</sub>	36.7	175	155.9	755	9	22	135	4.1	20
NP <sub>152</sub>									
NP <sub>193a</sub>	26.2	122	951	442	13	13	141	5.2	20
NP <sub>193b</sub>	30.3	139	120.5	537	16	20	167	5.3	21
NP <sub>194</sub>	32.8	124	126.8	581	10	12	117	4.3	19

**Table 1-6** Isomeric biodegradation of nonylphenol

Isomers	Shan et al., 2011	Hao et al., 2009	Gabriel et al., 2008
Sources	synthetic isomers	tNP (Tokyo Kasei Kogyo)	tNP(Fluka)
Matrix	soil	sequencing batch reactor	Minimal Medium with <i>Sphingobium xenophagum</i> Bayram
Conditions	oxic	oxic	oxic
Parameters	Half life (d)	Removal rate (%)	9 Day removal rate (%)
NP <sub>1</sub>	1.4		
NP <sub>9</sub>			96.1
NP <sub>35</sub>			97.6
NP <sub>36</sub>		75.4	98.8
NP <sub>37</sub>			96.6
NP <sub>38</sub>	2.1		99.3
NP <sub>65</sub>	5.8		81.0
NP <sub>110a</sub>			77.5
NP <sub>110b</sub>			76.3
NP <sub>111a</sub>	10.3 <sup>1</sup>	42.9 <sup>2</sup>	94.0
NP <sub>111b</sub>	10.3 <sup>1</sup>	42.9 <sup>2</sup>	90.4
NP <sub>112</sub>	8.4		98.2
NP <sub>119</sub>			99.7
NP <sub>128</sub>			99.7
NP <sub>143</sub>			52.2
NP <sub>152</sub>			56.2
NP <sub>170</sub>		40.7	
NP <sub>193a</sub>			31.3
NP <sub>193b</sub>			30.5
NP <sub>194</sub>		36.2	61.8

<sup>1</sup> Mixture of NP<sub>111a</sub> and NP<sub>111b</sub>

<sup>2</sup> Not specified if it was NP<sub>111a</sub> or NP<sub>111b</sub>.

## **Chapter 2 Isomer-Specific Biodegradation of Nonylphenol in River Sediments and Structure-Biodegradability Relationship**

### 2.1 Introduction

Nonylphenol (NP) is a high production volume chemical for manufacturing nonylphenol ethoxylates (NPEOs) - the most widely used nonionic surfactants (Soares et al., 2008; Ying et al., 2002). Nonylphenol ethoxylates may degrade to NP through nonylphenol monoethoxylate and nonylphenoxyethoxy acetic acid (Giger et al., 2009). The consumption and production capacities of NP in 2006 in the United States were 163 thousand tones and 194 thousand tones, respectively (Anonymous, 2007). It was estimated that approximately 60% of NP was released into the aquatic environment via discharge of wastewater treatment plant (WWTP) effluents (Ying et al., 2002). Because of its high octanol-water partition coefficient (average  $\log K_{ow}$  4.48) and organic carbon partition coefficient ( $\log K_{oc}$   $5.22 \pm 0.38$ ) (Ying et al., 2002), the bed sediment of surface aquatic systems is the primary environmental sink of NP (Mao et al., 2012; Soares et al., 2008; Writer et al., 2011; Ying et al., 2002). For example, Writer et al. (2012) reported that the NP concentration was 140  $\mu\text{g}/\text{kg}$  in the sediment of Redwood River, Minnesota, downstream of a WWTP. Rice et al. (2003) reported NP concentrations ranging from 75 to 340  $\mu\text{g}/\text{kg}$  in sediments from Cuyahoga River, Ohio. Nonylphenol is known as an environmental estrogen (Soares et al., 2008) and even at extreme low levels (0.022 to 220  $\text{ng}/\text{L}$ ), NP may increase cytokine secretion in human placenta which may result in implantation failure, pregnancy loss, or other complications (Bechi et al., 2010).

Nonylphenol biodegradation in sediments has attracted considerable attention, as it affects the potential for NP secondary pollution and food chain accumulation (Chang et al., 2004; De Weert et al., 2010; De Weert et al., 2011; Lalah et al., 2003; Sarmah and Northcott, 2008; Writer et al., 2011; Yuan et al., 2004). For example, Yuan et al. (2004) reported that the half-lives of NP in four river sediments under oxic conditions varied from 13 to 99 d. However, a few other studies showed that NP was highly persistent in sediments, especially under anoxic or reduced conditions (De Weert et al., 2010; De Weert et al., 2011; Shang et al., 1999). Shang et al. detected NP in marine sediment cores near a Canadian coast which may date back to 1960s, with the estimated half-life longer than 60 years (Shang et al., 1999).

Technical nonylphenol is a complicated mixture of alkylphenols and about 86-94% is comprised by 4-NP. Up to 66 4-NP isomers have been identified, of which 21 major components are all  $\alpha$ -quaternary isomers and one of the 6 significant minors is identified as  $\alpha$ -tertiary isomer (Eganhouse et al., 2009). A few recent studies started to further indicate that there exists isomer specificity in the estrogenicity and biodegradability of the numerous isomers contained in the technical NP mixtures. The estrogenicity of some NP isomers was found to differ as much as 85 times (Gabriel et al., 2008). Gabriel et al. (2008) evaluated the degradation of  $\alpha$ -quaternary NP isomers by *Sphingobium xenophagum* Bayram, a bacterial strain isolated from activated sludge. After incubation for 9 d, 99.7% of NP<sub>128</sub> and NP<sub>119</sub> was removed, while only 30.5% of NP<sub>193b</sub> dissipated. In an oxic rice paddy soil, the half-lives of 4  $\alpha$ -quaternary isomers followed the order of NP<sub>111</sub> (10.3 d) > NP<sub>112</sub> (8.4 d) > NP<sub>65</sub> (5.8 d) > NP<sub>38</sub> (2.1 d) (Shan et al., 2011). However,



to date, isomer specificity during biodegradation of NP in sediments has yet to be characterized. The negligence of isomer specificity is also evident from the use of 4-*n*-NP as the surrogate for NP, even though 4-*n*-NP tends to have much greater biodegradability and lower estrogenicity (De Weert et al., 2011; Sarmah and Northcott, 2008). Therefore, systematic information about isomer-specific biodegradation of NP in sediments is imperative for improving our ability to better predict the fate and risks of NP in the environment.

The objectives of this study were to compare biodegradation kinetics of a large suite of NP isomers in river sediments under oxic or anoxic conditions and to explore the structure-biodegradability relationships using simple molecular descriptors.

## 2.2 Materials and Methods

### 2.2.1 Chemicals

Technical NP (tNP), a mixture of NP isomers with branched side chains (CAS No. 84852-15-3) was purchased from TCI America (Portland, OR). Isomers NP<sub>36</sub>, NP<sub>37</sub>, NP<sub>119</sub>, NP<sub>128</sub> and NP<sub>194</sub> (10 mg/g in hexane; >95% purity) were obtained from ChemCollect GmbH (Reimscheid, Germany). Isomers NP<sub>38</sub> (48.2 mg/g), NP<sub>65</sub> (59.5 mg/g), NP<sub>111</sub> (49.5 mg/g) and NP<sub>112</sub> (48.52 mg/g) in methanol were kindly provided by Prof. Rong Ji at Nanjing University, China. 4-*n*-Nonylphenol (>98%, CAS No. 104-40-5) was from Alfa Aesar (Ward Hill, MA). 4-*tert*-Octylphenol-3,5-*d*<sub>2</sub> solution (CAS No. 1173021-20-9) in acetone (1 µg/mL) was from Sigma-Aldrich (St. Louis, MO). Gas

chromatography (GC) grade hexane, acetone and methylene chloride, calcium chloride dihydrate (99-105%) and Ottawa sand were from Fisher Scientific (Fair Lawn, NJ). Sodium azide (99.7%) was from Mallinckrodt Baker (Phillipsburg, NJ). Reagent water (18.3 M.cm resistivity) was prepared using a Barnstead Nanopure water system (Barnstead, Dubuque, IA).

### 2.2.2 Sediment Collection and Characterization

Two surface sediments (0-5cm) were grab-sampled from Santa Ana River in Southern California. Sediment A was from a location in the upper river located in the San Bernardino National Forest (Latitude, Longitude: 34.165228, -117.015170). Sediment B was from a middle segment of the river located about 200 m below the outlet channel of Prado Dam in Corona, California (Latitude, Longitude: 33.883195, -117.646555). Sediments were collected manually using a shovel, and transported to the laboratory within 4 h of collection. The sediment samples were drained of free water, wet sieved (< 2 mm) and stored at 4 °C before use. Sediment properties including texture, carbon content (loss on ignition) and cation exchange capacity were analyzed using standard methods ([Table 2-1](#)). There was no detachable NP residue in both sediments.

### 2.2.3 Sediment Incubation Experiments

For aerobic incubation, 10 g (dry weight equivalent) sediment and 5 mL of 0.01 mol/L CaCl<sub>2</sub> solution were added into 125-mL amber glass jars. These samples were acclimated for 3 d and then 50 µL of 1000 mg/L tNP in acetone was added. The spiked samples were

gently vortexed for 1 min, and loosely covered with aluminum foil. The water loss from each sample vial was checked every other day by weighing and deionized water was added when significant water loss occurred. The sample containers were gently vortexed periodically to ensure adequate aeration during the incubation.

For anaerobic incubation, the setup was similar to that in Lin et al. (Lin et al., 2008) Amber glass vials (40 mL) were filled with 10 g sediment (dry weight equivalent) and 5 mL of 0.01 mol/L CaCl<sub>2</sub> solution and then the uncovered vials were placed in a plastic glove chamber (Cole Parmer, Vernon Hills, IL), flushed with nitrogen by alternately inflating and deflating the glove chamber for several times. After equilibration in the inflated glove chamber for 1 d, vials were tightly closed with screw caps with Teflon-lined butyl rubber septa in the glove chamber and these samples were further acclimated for 12 d to ensure anoxic conditions. The sample vials were taken out of the glove chamber and then 50 µL of 1000 mg/L tNP in acetone was spiked using a micro-syringe. The spiked samples were gently vortexed for 1 min and then returned to the nitrogen-filled glove chamber. The glove chamber was checked daily and filled with more nitrogen if noticeable deflation occurred.

The sterilized control treatments were prepared by steam autoclaving at 121 °C for 45 min each day and for 3 consequent days. The sterilized sediment samples were also amended with 200 mg/L sodium azide, and then included in both the aerobic and anaerobic incubation experiments using sediment A. All the samples were incubated at the room temperature (21±0.8 °C). At selected time intervals (0, 1, 3, 7, 14, 21, 35, 56

and 84 d), 3 replicate samples from each treatment were randomly removed and were immediately transferred to a -70 °C freezer to stop the degradation. Additional samples of sediments A and B under both oxic and anoxic conditions were sacrificed for measurement of redox potential and pH at the same time intervals (Table 1). Redox potentials were measured by inserting a Thermo Orion 9197B Triode ORP electrode vertically into the sediment sample through the sediment-water interface and reading (in mV) was recorded after the reading was stabilized. The electrode was calibrated with Thermo Orion ORP standards and connected to a Thermo Orion 250 A plus portable meter (Fisher Scientific, Fair Lawn, NJ). For the anaerobic samples, the redox potentials and pH were measured in the glove chamber under anoxic conditions.

#### 2.2.4 Sample Preparation and Analysis

The frozen sediment samples were freeze-dried for 3 d and then stored at 4 °C before extraction on a Dionex accelerated solvent extraction system (Dionex ASE 350, Sunnyvale, CA). Aliquots of the freeze-dried sediment samples (2 g) were packed into 11-mL stainless steel extraction cells along with Ottawa sand and the packed cells were preheated for 5 min followed by 5 min static extraction (50 °C and 1500 psi). Two extraction cycles were used with 60% rinse volume and acetone-hexane (1:1; v/v) as solvents. Finally, the extraction cells were purged with nitrogen for 100 s. The extract was concentrated to about 1 mL under a gentle nitrogen stream and cleaned up with Thermo Scientific HyperSep Florisil SPE columns (Fisher Scientific, Fair Lawn, NJ) with 5 g sorption bed. The cartridges were preconditioned with 25 mL hexane before

sample loading. The retained NP was eluted with 35 mL methylene chloride. The extract was concentrated under nitrogen to about 1 mL and added with 5 mL hexane, followed by concentration to about 1 mL. The final extract was transferred to 2-mL autosampler vials. The samples were stored at -20 °C before analysis. A surrogate (50 µL 10 mg/L 4-n-NP in acetone) was spiked before the ASE extraction and an internal standard (25 µL 1 mg/L 4-tert-octylphenol-3,5-d<sub>2</sub> in hexane ) was added before the gas chromatography-mass spectrometry analysis.

The separation and identification of NP isomers were carried out on an Agilent 6890 gas chromatography coupled with 5973 mass spectrometer (Agilent, Santa Clara, CA). Briefly, samples (2 µL) were introduced into the inlet at 250 °C and the separation was achieved on a DB-5MS Ultra Inert capillary column (60 m × 0.25 mm × 0.25 µm, Agilent, Santa Clara, CA). The carrier gas was helium (99.999%) and the flow rate was set at 1.0 mL/min. The column temperature was programmed initially at 80 °C for 0 min, then ramped to 160 °C at 10 °C/min and held for 42 min, and further ramped to 300 °C at 30 °C/min and held for 3 min. The mass spectrometer was operated in the electron ionization-selective ion monitoring (SIM) mode at 70 eV. The ions with m/z 137 and 107 were used for the quantification of the internal standard and recovery surrogate, respectively. Ions with m/z 121, 135, 149, 163, 177 and 191 were used for the quantification of different NP isomers. For the identification of NP isomers, both a full scan mode (m/z 40 to m/z 800) and the SIM mode (m/z 107, 121, 135, 149, 163, 177, 191 and 220) were employed. A total of 19 α-quaternary isomers (Table 2-2), including 6 diastereomers (denoted as a and b), were separated and identified by comparing the

retention time, total ion chromatogram peak intensity and fragmentation patterns against the available authentic NP isomer standards and/or chromatographic and mass spectrometric characteristics of NP isomers in the published studies.(Thiele et al., 2004; Wheeler et al., 1997; Zenkevich et al., 2009) The recovery for the recovery surrogate 4-n-NP was  $102 \pm 6$  % and the recoveries of the various NP isomers were  $87 \pm 3$  %. There was no significant difference among NP isomers in the method recovery.

### 2.2.5 Calculation of Molecular Descriptors

The topological steric index was calculated according to Cao et al.(Cao and Liu, 2004) Common topological indices, such as the molecular connectivity chi indices, kappa shape indices and information indices were calculated by Molconn-Z (version 4.12S, eduSoft, La Jolla, CA). The detailed list and definitions can be found in the software user's guide(Lowell H. Hall et al., 2008) and the definitions can also be found in Todeschini et al.(Todeschini et al., 2009) To obtain information-rich descriptors, all the descriptors were checked to ensure that there was a variation in the values and then pairwise correlations were used to further check the colinearity of the remaining descriptors. For each pair that had correlation greater than 0.995, only one descriptor was kept. Values of all 57 descriptors are given in the Supporting Information (SI, [Table S 2-1](#)). In total, 18 isomers (NP<sub>X</sub> was not included since the structure was not fully identified, see below) were randomly split into training set (12 isomers) and validation set. Since the number of descriptors was much larger than the number of isomers and also the colinearity among the descriptors, partial least square (PLS) regression was carried out using SPSS Statistics

21.0 with the PLS extension module (IBM, New York, NY) to establish the relation between the half-lives and molecular descriptors. The PLS analysis has features from both principal component analysis and multiple linear regression. The dependent variable (Y) and independent variables (X) are all used to extract the latent factors which may explain the maximum covariance between Y and X followed by a regression step that predicts Y values using the latent factors (Wold et al., 2001). The PLS results including the proportion of variance explained, parameter and importance in the projection of each molecular descriptor can be found in [SI Table S 2-2-6](#). All other statistics including t-test, linear regression and linear correlation were also carried out using SPSS Statistics.

## 2.3 Results and Discussion

### 2.3.1 Degradation under Oxidic Conditions

Biodegradation of NP isomers in sediment A under oxidic conditions was found to be generally efficient and clearly isomer-specific ([Figures 2-1A and 2-2](#)). In the sterilized control group, there was no significant change in NP concentrations, indicating that biodegradation was responsible for the observed NP disappearance. Nonylphenol isomers underwent an initial phase (14-21 d) of fast degradation, with half-lives ranging from 0.9-13.2 d, which was followed by a slower second phase. For example, NP<sub>38</sub> exhibited first-order decay with a half-life of 2.9 d for the initial 14 d but did not dissipate noticeably thereafter ([Figures 2-1A](#)). The degradation of NP<sub>110a</sub> and NP<sub>193b</sub> was slower than the other isomers during the initial phase, with half-lives of 9.8 and 12.6 d, respectively.

Yuan et al. (2004) studied the aerobic biodegradation of tNP in the sediments of Erren River in Taiwan and the half-lives measured in the four different sediments were 13.6 (upper river sample), 77.0 (mid-section), 99.0 and 63.9 d (lower river), respectively. The half-life in the upper river sediment was comparable to the values in sediment A while half lives in the other sediments in their study were much longer than those observed in this study. When cultivated with bacterial strain *Sphingobium xenophagum* Bayram in a minimal medium under oxic conditions, biodegradation of 1 mg/mL tNP was shown to be isomer-specific and generally the half-lives were shorter than those found in this study. For example, 77.5% of NP<sub>110a</sub> was degraded after 9 d while in this study, the half-life of the same isomer was 11.6 d (Gabriel et al., 2008). More interestingly, the general pattern in the biodegradability of NP isomers by *Sphingobium xenophagum* Bayram was similar to that in sediment A, i.e., if a NP isomer was recalcitrant to transformations by *Sphingobium xenophagum* Bayram, it was also more persistent in sediment A, and vice versa. For example, after 9 d of incubation, the degradation percentages of NP<sub>9</sub>, NP<sub>143</sub> and NP<sub>193b</sub> were 96.1, 52.6 and 30.5%, respectively, while the corresponding half-lives in sediment A were 0.9, 11.6 and 12.6 d, respectively. In an oxic soil, the half-lives of four NP isomers followed the order of NP<sub>111</sub> (10.3 d) > NP<sub>112</sub> (8.4 d) > NP<sub>65</sub> (5.8 d) > NP<sub>38</sub> (2.1 d) (Shan et al., 2011), which was also consistent with the order found in this study for the same isomers, 9.8 and 9.1 d for NP<sub>111a/b</sub>, respectively, 6.3 d for NP<sub>112</sub>, 3.2 d for NP<sub>65</sub>, and 2.9 d for NP<sub>38</sub>. In a sequencing batch reactor with about 80 µg/L tNP in simulated wastewater, the degradation percentages for NP<sub>194</sub>, NP<sub>111</sub> and NP<sub>36</sub> were 36.2, 42.9 and 75.4%, respectively (Hao et al., 2009), a trend again mirroring that in the



present study for these isomers. Therefore, observations from this and other studies suggest that there may be intrinsic, structurally based properties influencing the degradability of NP isomers. Thus, it is valuable to explore a possible structure-biodegradability relationship to better describe degradation of NP isomers.

### 2.3.2 Degradation under Reduced Conditions

When sediment B was incubated under the “oxic” conditions, the actual redox potential was measured to be about 255 mV (Table 2-1), as compared to 413 mV in sediment A under the same conditions. The redox potential in sediment B was reflective of nitrate reducing conditions (DeLaune and Reddy, 2005) and may be in fact referred as “anoxic”(Chang et al., 2004; De Weert et al., 2011) or “facultative” (DeLaune and Reddy, 2005). Given that both sediments A and B were exposed to the same conditions, the lower redox potential in sediment B was likely due to its properties such as its higher organic carbon content and lower sand content (Table 2-1). In sediment B, the NP isomers underwent stagnant degradation during the first 7-14 d, which was followed by a faster degradation phase with half-lives varying from 15.1 to 20.1 d (Figure 2-1B and 2-2). The overall half-lives of NP isomers in sediment B were much longer than those in sediment A under the same conditions. For example, the half-lives of NP<sub>38</sub> in sediments A and B were 2.9 and 16.3 d, respectively. Moreover, NP biodegradation in sediment B appeared to be less isomer-specific as compared to that in sediment A (Figure 2-2). In addition, compared to sediment A from the upper reach of the Santa Ana River, sediment B was likely well acclimated to NP contamination, as the river receives effluent

discharged from multiple WWTPs. This site-specific biodegradation may be attributed to different indigenous microbial communities and activities dictated by environmental conditions such as redox potential (Corvini et al., 2006). A precise characterization of nonylphenol-degrading microorganism communities, activities or specific enzymes in sediments A and B is beyond the scope of this study. Chang et al. (2004) reported that the biodegradation half-life of tNP under nitrate reducing conditions in a NP-acclimated river sediment was 20.4 d, which was similar to the results in this study. In the nitrate reducing soil, less than 1% of NP<sub>111</sub> was mineralized while up to 30% of radioactivity was recovered as metabolites after 75 d incubation (Liu et al., 2008). However, Der Weert et al. observed no degradation of tNP during 703-d incubation of a nitrate reducing river sediment (De Weert et al., 2011). These different observations may be again attributed to different indigenous microbial populations.

Biodegradation of NP isomers was extremely slow in both sediments exposed to nitrogen (Table 2-2). The redox potentials of sediment A and B incubated under nitrogen were -92 and -122 mV respectively (Table 2-1), indicating sulfate reducing conditions (DeLaune and Reddy, 2005). In sediment A, the estimated first-order half-lives of all NP isomers were greater than 200 d (Table 2-2), while in sediment B, no detectable degradation occurred for any of the isomers after 84 d. Therefore, NP isomers were extremely persistent under anoxic conditions in this study. De Weert et al. observed a lack of biodegradation of tNP under sulfur reducing and methanogenesis conditions in a river sediment (De Weert et al., 2011). Marine sediment core samples taken from the Strait of Georgia, British Columbia, Canada, suggested that if NP were incorporated into marine

sediments, it would remain intact in the sediment for decades.(Shang et al., 1999) Therefore, observations from this and earlier studies consistently suggested prolonged persistence of NPs in sediments under reduced conditions, or that significant attenuation may occur only in well oxidized sediments.

In this study, only  $\alpha$ -quaternary isomers were quantified and the half-lives were also only obtained for these isomers. Gabriel et al. found that  $\alpha$ -tertiary isomers which are minor components of technical NP had distinctive biodegradation pathways and metabolites (Gabriel et al., 2005). The identification and quantification of the  $\alpha$ -tertiary NP isomers are difficult, especially in the complex sediment matrix. Future research should also include  $\alpha$ -tertiary NP isomers.

### 2.3.3 Structure-Biodegradability Relationship

In sediment A under oxic conditions, the biodegradability of NP isomers depended closely on their structures (Figure 2-3). The half-lives of NP isomers in sediment A under oxic conditions were used to explore the structure-biodegradability relationship. The side chain length and  $\alpha$ -substituent were the first factors examined. Apparently, NP isomers with longer side chain appeared to be more susceptible to biodegradation and generally had shorter half-lives (Figure 2-3A). For example, the half-lives for NP isomers with 6-carbon side chain were 3.5 d (NP<sub>35</sub>), 4.4 d (NP<sub>36</sub>), 3.3 d (NP<sub>37</sub>), 2.9 d (NP<sub>38</sub>) and 3.2 d (NP<sub>65</sub>) while the values for those with 4-carbon side chain were 13.2 d (NP<sub>193a</sub>), 12.6 d (NP<sub>193b</sub>) and 11.5 d (NP<sub>194</sub>). Since the numbering of NP isomers followed the priority of side chain length (Guenther et al., 2006), i.e., a smaller number means a longer side chain,

the numbering of NP isomers may be used to roughly estimate their biodegradability. The  $\alpha$ -substitution also affected the biodegradability (Figure 2-3B). Generally, NP isomers with less bulky  $\alpha$ -substituents exhibited faster degradation, following the order of dimethyl  $\approx$  ethylmethyl  $>$  methylpropyl  $\approx$  *iso*-propylmethyl. However, large variations existed among the isomers with the same  $\alpha$ -substituent, especially for NP isomers with dimethyl and ethylmethyl substituents. Therefore, the  $\alpha$ -substitution alone cannot be used as a good indicator for the recalcitrance of NP isomers. The side chain length and  $\alpha$ -substituent were also found to influence the biodegradability of NP isomers by *Sphingobium xenophagum* Bayram (Gabriel et al., 2005; Gabriel et al., 2008). Less bulky  $\alpha$ -substituents also resulted in faster biodegradation by *Sphingobium xenophagum* Bayram (Gabriel et al., 2008). A few other studies also reported the biodegradability of NP isomers (Hao et al., 2009; Shan et al., 2011); however, as only a few isomers were considered in those studies, analysis of trends was infeasible.

The side chain length is a discontinuous variable and  $\alpha$ -substitution type is a categorical variable, and therefore both are not optimal for inclusion in a quantitative structure-biodegradability relationship. In the biodegradation study with *Sphingobium xenophagum* Bayram, it was proposed that the isomer-specificity may be related to the *ipso*-hydroxylation rate at the *para*-position, i.e., where the side chain is attached to the benzene ring and further governed by the steric hindrance of the side chain (Gabriel et al., 2008). Therefore, a simple topological steric index describing this steric hindrance may explain the isomer-specificity (Cao and Liu, 2004). Moreover, numerous commonly used topological indices containing information on the size, branching, unsaturation, electron

characteristics and polarity, among others, were also considered in this study. In general, NP isomers with smaller steric index values had shorter half-lives (Figure 2-3C; linear regression,  $R^2=0.70$ ); therefore, the steric hindrance likely contributed significantly to different *ipso*-hydroxylation rates which in turn resulted in isomer-specific biodegradation rates.

It is evident, however, that the steric hindrance index and half-life regression was still fairly variable, with relatively wide 95% confidence intervals (Figure 2-3C). To identify better molecular descriptors, 56 other topological indices were individually calculated and regression with the measured half-lives was performed. The screening showed that the mean information index for the magnitude of distance ( $I_{Dwbar}$ ) gave the best regression fit ( $R^2=0.88$ ; Figure 2-3D). This index is considered an appropriate measurement of branching degree, especially for isomers, with larger values indicating a higher degree of branching (Bonchev and Trinajstić, 1977). As shown in Figure 2-3D, the NP isomers with larger values of  $I_{Dwbar}$  consistently displayed longer half-lives or lower biodegradability. Compared to the steric hindrance index,  $I_{Dwbar}$  was a better descriptor for estimating the half-lives of NP isomers, as evident from the fact that the data points were less scattered and the 95% prediction band was narrower (Figure 2-3C and D). Hao et al. used molecular connectivity indices (chi indices)  ${}^2\chi^v$  and  ${}^4\chi^v_{pc}$  to establish the structure and biodegradability of 4 NP isomers (Hao et al., 2009); however, in this study, regressions using these indices were found to be less satisfactory.

To further improve the performance of structure-biodegradability relationships, a combination of multiple molecular descriptors were used in the regression analysis. In this study, the partial least squares (PLS) approach was used to establish the relationships of half-lives of NP isomers and 57 molecular descriptors (Table 2-3 and SI Table S 2-2-7). With 4 latent factors, the PLS model explained 91.6% X variance and 93.0% Y variance (i.e.,  $R^2=0.93$ ). The model gave reasonable estimates of half-lives of NP isomers: for 12 isomers in the training set, the residue was from 0.3 to 2.0 d, while for 6 isomers in the validation set, the residue was from 0.0 to 2.3 d (Table 2-3), suggesting the possibility to use this model for more accurately predicting the half-lives of the other NP isomers. Since  $\alpha$ -quaternary 4-NP isomers are dominant in tNP (Eganhouse et al., 2009) and also only these isomers were used to establish the model, the molecular descriptors and half-lives were calculated only for  $\alpha$ -quaternary NP isomers (SI Table S 2-7). The results showed that some isomers were even more recalcitrant than those tested in this study. For example, the estimated half-lives for NP<sub>211</sub> and NP<sub>202</sub> were 16.4 and 14.9 d, respectively, while the longest half-life of the 19 isomers in this study was only 13.2 d (NP<sub>193b</sub>). Hence, this or a similar model may be effectively used to provide guidance to test the most recalcitrant NP isomers.

Results from this study showed that NP biodegradation in bed sediments was isomer-specific, site-specific and affected greatly by the redox potential. While most NP isomers were resistant to degradation in reduced sediments, under true oxic conditions, the half-lives of NP isomers ranged from 0.9 to 13.2 d. The biodegradability under oxic conditions was closely dependent on the structures of NP isomers. Isomers with short

side chain and bulky  $\alpha$ -substituents generally were more persistent. The degree of branching as quantified by  $I_{Dwbar}$  further improved the structure-biodegradability relationship and should be further evaluated in its predictability of NP isomers under different conditions.

## 2.4 Environmental Implications

Surface aquatic systems are often the primary sink of NP contamination due to the often-practiced discharge of NP-containing WWTP effluents. This study provided direct evidence to show isomer-specific biodegradation of NP in sediments, especially under well aerated conditions. The isomer selectivity appears to be predictable using regressions with single or multiple molecular descriptors. The isomer-specificity in NP attenuation may result in selective accumulation of recalcitrant NP isomers in the bed sediment and other environmental matrices such as the overlaying water due to sediment resuspension and desorption of NP. The preferential attenuation of NP isomers in the environment may further translate into selective exposure and bioaccumulation in aquatic organisms. Therefore, consideration of isomer selectivity in biodegradation and ecotoxicity may significantly improve the assessment of fate and risks of NP. The molecular descriptor-based structure-biodegradability relationships may be used to identify the most recalcitrant isomers, thus allowing a focused research effort on those isomers posing the greatest environmental risks.

## References

- Anonymous (2007). Overview of the US nonylphenol sector. Focus on Surfactants **2007**(8): 4.
- Bechi, N., Ietta, F., Romagnoli, R., Jantra, S., Cencini, M., Galassi, G., Serchi, T., Corsi, I., Focardi, S. and Paulesu, L. (2010). Environmental levels of *para*-nonylphenol are able to affect cytokine secretion in human placenta. Environ. Health Perspect. **118**(3): 427-431.
- Bonchev, D. and Trinajstić, N. (1977). Information theory, distance matrix, and molecular branching. J. Chem. Phys. **67**(10): 4517-4533.
- Cao, C. Z. and Liu, L. (2004). Topological steric effect index and its application. J. Chem. Inf. Comput. Sci. **44**(2): 678-687.
- Chang, B. V., Yu, C. H. and Yuan, S. Y. (2004). Degradation of nonylphenol by anaerobic microorganisms from river sediment. Chemosphere **55**(4): 493-500.
- Corvini, P. F. X., Schaffer, A. and Schlosser, D. (2006). Microbial degradation of nonylphenol and other alkylphenols -- our evolving view. Appl. Microbiol. Biotechnol. **72**(2): 223-243.
- De Weert, J., Stremínska, M., Hua, D., Grotenhuis, T., Langenhoff, A. and Rijnaarts, H. (2010). Nonylphenol mass transfer from field-aged sediments and subsequent biodegradation in reactors mimicking different river conditions. J. Soils Sediments **10**(1): 77-88.



- De Weert, J. P. A., Vinas, M., Grotenhuis, T., Rijnaarts, H. H. M. and Langenhoff, A. A. M. (2011). Degradation of 4-n-nonylphenol under nitrate reducing conditions. *Biodegradation* **22**(1): 175-187.
- DeLaune, R. D. and Reddy, K. R. (2005). Redox potential. *Encyclopedia of soils in the environment*. H. Editor-in-Chief: Daniel. Oxford, Elsevier: 366-371.
- Eganhouse, R. P., Pontolillo, J., Gaines, R. B., Frysiner, G. S., Gabriel, F. L. P., Kohler, H. P. E., Giger, W. and Barber, L. B. (2009). Isomer-specific determination of 4-nonylphenols using comprehensive two-dimensional gas chromatography/time-of-flight mass spectrometry. *Environ. Sci. Technol.* **43**(24): 9306-9313.
- Gabriel, F. L. P., Giger, W., Guenther, K. and Kohler, H. P. E. (2005). Differential degradation of nonylphenol isomers by *Sphingomonas xenophaga* bayram. *Appl. Environ. Microbiol.* **71**(3): 1123-1129.
- Gabriel, F. L. P., Routledge, E. J., Heidlberger, A., Rentsch, D., Guenther, K., Giger, W., Sumpter, J. P. and Kohler, H. P. E. (2008). Isomer-specific degradation and endocrine disrupting activity of nonylphenols. *Environ. Sci. Technol.* **42**(17): 6399-6408.
- Giger, W., Gabriel, F. L. P., Jonkers, N., Wettstein, F. E. and Kohler, H. P. E. (2009). Environmental fate of phenolic endocrine disruptors: field and laboratory studies. *Philos T R Soc A* **367**(1904): 3941-3963.
- Guenther, K., Kleist, E. and Thiele, B. (2006). Estrogen-active nonylphenols from an isomer-specific viewpoint: A systematic numbering system and future trends. *Anal. Bioanal. Chem.* **384**(2): 542-546.

- Hao, R. X., Li, J. B., Zhou, Y. W., Cheng, S. Y. and Zhang, Y. (2009). Structure-biodegradability relationship of nonylphenol isomers during biological wastewater treatment process. *Chemosphere* **75**(8): 987-994.
- Lalah, J. O., Schramm, K. W., Henkelmann, B., Lenoir, D., Behechti, A., Günther, K. and Kettrup, A. (2003). The dissipation, distribution and fate of a branched 14C-nonylphenol isomer in lake water/sediment systems. *Environ. Pollut.* **122**(2): 195-203.
- Lin, K., Haver, D., Oki, L. and Gan, J. (2008). Transformation and sorption of fipronil in urban stream sediments. *J. Agric. Food Chem.* **56**(18): 8594-8600.
- Liu, Q., Ji, R., Hommes, G., Schaffer, A. and Corvini, P. F. X. (2008). Fate of a branched nonylphenol isomer in submerged paddy soils amended with nitrate. *Water Res.* **42**(19): 4802-4808.
- Lowell H. Hall, Glen E. Kellogg and Haney, D. N. (2008). Software package for molecular topology analysis user's guide.
- Mao, Z., Zheng, X. F., Zhang, Y. Q., Tao, X. X., Li, Y. and Wang, W. (2012). Occurrence and biodegradation of nonylphenol in the environment. *Int. J. Mol. Sci.* **13**(1): 491-505.
- Rice, C. P., Schmitz-Afonso, I., Loyo-Rosales, J. E., Link, E., Thoma, R., Fay, L., Altfater, D. and Camp, M. J. (2003). Alkylphenol and alkylphenol-ethoxylates in carp, water, and sediment from the Cuyahoga River, Ohio. *Environ. Sci. Technol.* **37**(17): 3747-3754.

- Sarmah, A. K. and Northcott, G. L. (2008). Laboratory degradation studies of four endocrine disruptors in two environmental media. *Environ. Toxicol. Chem.* **27**(4): 819-827.
- Shan, J., Jiang, B. Q., Yu, B., Li, C. L., Sun, Y. Y., Guo, H. Y., Wu, J. C., Klumpp, E., Schaffer, A. and Ji, R. (2011). Isomer-specific degradation of branched and linear 4-nonylphenol isomers in an oxic soil. *Environ. Sci. Technol.* **45**(19): 8283-8289.
- Shang, D. Y., Macdonald, R. W. and Ikononou, M. G. (1999). Persistence of nonylphenol ethoxylate surfactants and their primary degradation products in sediments from near a municipal outfall in the strait of Georgia, British Columbia, Canada. *Environ. Sci. Technol.* **33**(9): 1366-1372.
- Soares, A., Guieysse, B., Jefferson, B., Cartmell, E. and Lester, J. N. (2008). Nonylphenol in the environment: A critical review on occurrence, fate, toxicity and treatment in wastewaters. *Environ. Int.* **34**(7): 1033-1049.
- Thiele, B., Heinke, V., Kleist, E. and Guenther, K. (2004). Contribution to the structural elucidation of 10 isomers of technical *p*-nonylphenol. *Environ. Sci. Technol.* **38**(12): 3405-3411.
- Todeschini, R., Consonni, V., Mannhold, R., Kubinyi, H. and Folkers, G. (2009). *Molecular Descriptors for Chemoinformatics*, Wiley.
- Wheeler, T. F., Heim, J. R., LaTorre, M. R. and Janes, A. B. (1997). Mass spectral characterization of *p*-nonylphenol isomers using high-resolution capillary GC-MS. *J. Chromatogr. Sci.* **35**(1): 19-30.

- Wold, S., Sjöström, M. and Eriksson, L. (2001). PLS-regression: a basic tool of chemometrics. *Chemom. Intell. Lab. Syst.* **58**(2): 109-130.
- Writer, J. H., Barber, L. B., Ryan, J. N. and Bradley, P. M. (2011). Biodegradation and attenuation of steroidal hormones and alkylphenols by stream biofilms and sediments. *Environ. Sci. Technol.* **45**(10): 4370-4376.
- Writer, J. H., Ryan, J. N., Keefe, S. H. and Barber, L. B. (2012). Fate of 4-nonylphenol and 17 beta-estradiol in the Redwood River of Minnesota. *Environ. Sci. Technol.* **46**(2): 860-868.
- Ying, G. G., Williams, B. and Kookana, R. (2002). Environmental fate of alkylphenols and alkylphenol ethoxylates - a review. *Environ. Int.* **28**(3): 215-226.
- Yuan, S. Y., Yu, C. H. and Chang, B. V. (2004). Biodegradation of nonylphenol in river sediment. *Environ. Pollut.* **127**(3): 425-430.
- Zenkevich, I. G., Makarov, A. A., Schrader, S. and Moeder, M. (2009). A new version of an additive scheme for the prediction of gas chromatographic retention indices of the 211 structural isomers of 4-nonylphenol. *J. Chromatogr. A* **1216**(18): 4097-4106.

Tables

**Table 2-1** Textural and chemical properties of sediments used in this study and pH and redox potentials (Eh) during aerobic and anaerobic incubations

Sediment	N (%)	OC (%)	CEC <sup>a</sup>	Texture (%)			Eh (mV)		pH	
				Sand	Silt	Clay	Aerobic	Anaerobic	Aerobic	Anaerobic
A	0.021	0.24	4.8	90	8	2	413	-92	7.0	6.8
B	0.21	1.87	21.0	52	27	21	255 <sup>b</sup>	-122	7.1	6.7

<sup>a</sup>Unit for CEC is meq/100g; <sup>b</sup>The measured Eh is indicative of nitrate reducing state.

**Table 2-2** Estimated first-order half-lives of nonylphenol isomers in an upper river sediment under reduced conditions

Isomer	IUPAC name	Half-life (d)
9	4-[1,1-dimethylheptyl]-phenol	514±160
35	4-[1,1,2-trimethylhexyl]-phenol	420±115
36 <sup>1</sup>	4-[1,1,3-trimethylhexyl]-phenol	420±98
37 <sup>1</sup>	4-[1,1,4-trimethylhexyl]-phenol	458±151
38 <sup>1</sup>	4-[1,1,5-trimethylhexyl]-phenol	497±209
65 <sup>1</sup>	4-[1-ethyl-1-methylhexyl]phenol	467±134
110a	4-[1-ethyl-1,2-dimethylpentyl]phenol	423±99
110b	4-[1-ethyl-1,2-dimethylpentyl]phenol	521±131
111a <sup>1</sup>	4-[1-ethyl-1,3-dimethylpentyl]phenol	475±172
111b <sup>1</sup>	4-[1-ethyl-1,3-dimethylpentyl]phenol	475±169
112 <sup>1</sup>	4-[1-ethyl-1,4-dimethylpentyl]phenol	348±82
119 <sup>1</sup>	4-[2-ethyl-1,1-dimethylpentyl]phenol	488±151
128 <sup>1</sup>	4-[3-ethyl-1,1-dimethylpentyl]phenol	367±94
143	4-[1-isopropyl-1-methylpentyl]phenol	349±72
152	4-[1-methyl-1-n-propylpentyl]phenol	385±87
193a	4-[1,2-dimethyl-1-n-propylbutyl]phenol	343±67
193b	4-[1,2-dimethyl-1-n-propylbutyl]phenol	373±84
194 <sup>1</sup>	4-[1,3-dimethyl-1-n-propylbutyl]phenol	514±160
X <sup>2</sup>		271±54

<sup>1</sup>Isomers confirmed with authentic standards.

<sup>2</sup>The structure of this nonylphenol isomer was not fully identified; it may be NP<sub>92</sub>, NP<sub>93</sub> or NP<sub>95</sub> and the systematic name may be 4-[1,1,2,3-tetramethylpentyl]phenol, 4-[1,1,2,4-tetramethylpentyl]phenol or 4-[1,1,3,4-tetramethylpentyl]phenol.

**Table 2-3** Predicted half-lives (T<sub>1/2</sub>, d) of nonylphenol isomers using partial least square regression

Sample sets	NP isomer	Measured T <sub>1/2</sub> (d)	Predicted T <sub>1/2</sub> (d)	Residue (d)
Training Set	9	0.9	1.1	-0.3
	36	4.4	4.1	0.3
	38	2.9	1.9	1.1
	65	3.2	4.5	-1.3
	110a	11.6	9.6	2.0
	110b	8.2	9.6	-1.4
	111b	9.1	9.8	-0.6
	119	9.6	10.4	-0.8
	128	8.9	9.3	-0.4
	152	12.0	10.6	1.5
	193a	13.2	12.5	0.6
194	11.5	12.1	-0.6	
Validation Set	35	3.5	4.9	-1.4
	37	3.3	3.5	-0.2
	111a	9.8	9.8	0.0
	112	6.3	8.5	-2.3
	143	11.6	10.2	1.5
	193b	12.6	12.5	0.1

Figures

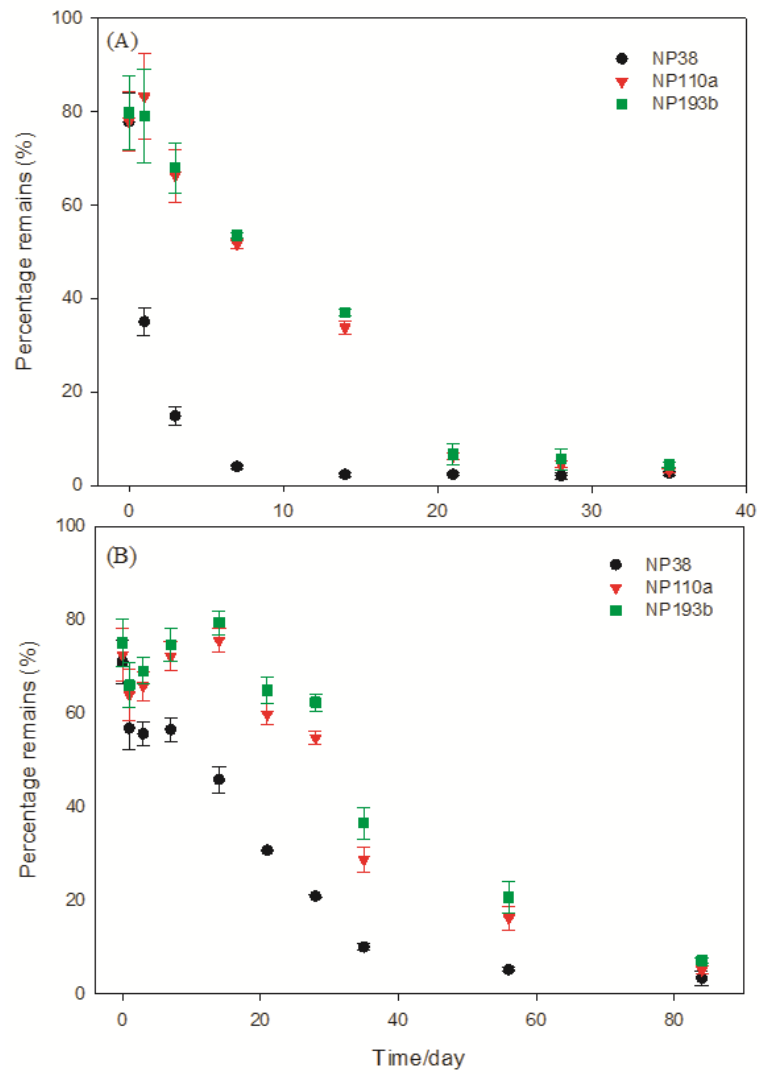


**Figure 2-1** Degradation of representative nonylphenol isomers NP38, NP110a and NP193b in an upper river sediment (sediment A) under oxic conditions and a lower river sediment (sediment B) under slightly reduced conditions



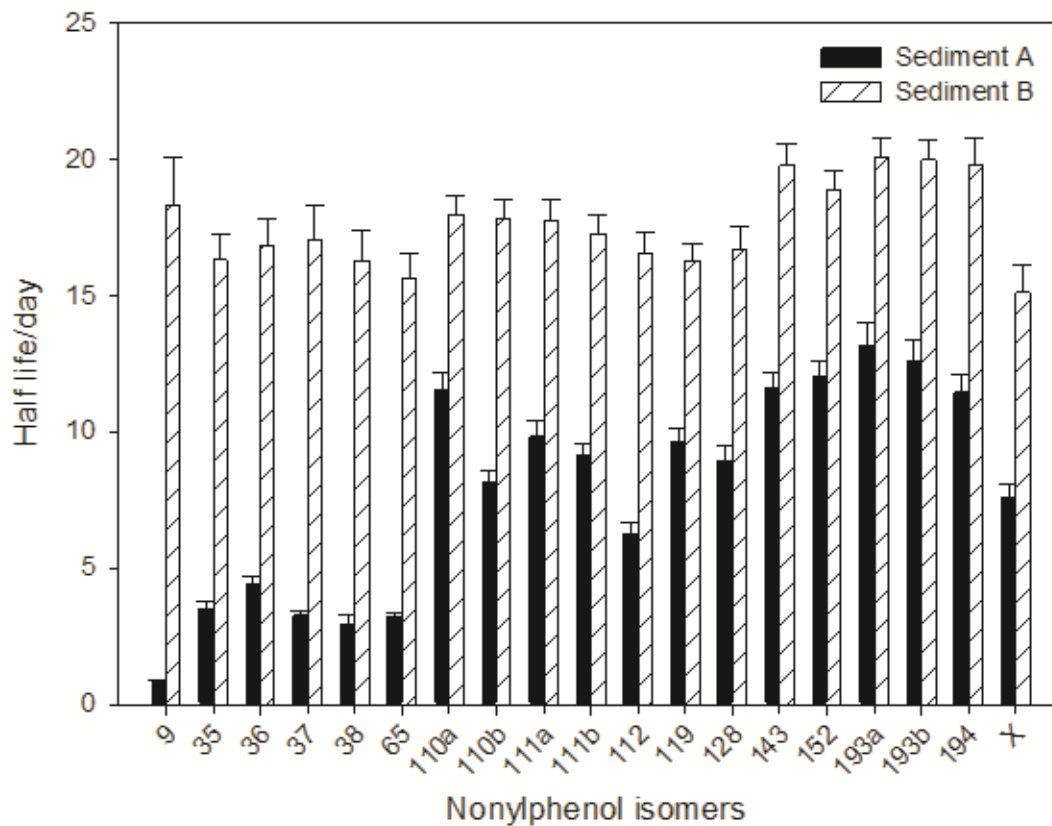


**Figure 2-2** Isomer-specific degradation half-lives of nonylphenol isomers in an upper river sediment (sediment A) under oxic conditions and a lower river sediment (sediment B) under slightly reduced conditions

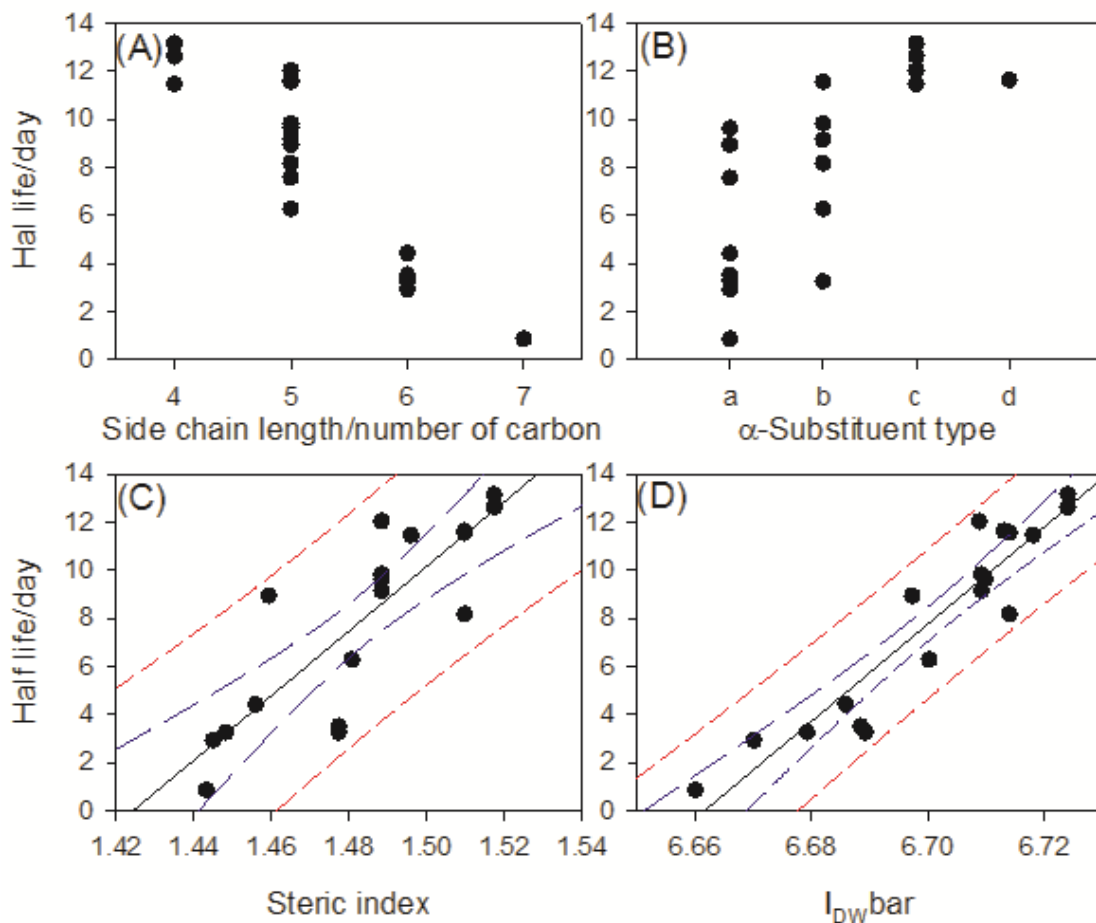


**Figure 2-3** Relationships of measured half-lives of nonylphenol isomers in an upper river sediment under oxic conditions with (A) side-chain length, (B)  $\alpha$ -substituent type, (C) steric index and (D) mean information index for the magnitude of distance IDWbar.

Each black dot represents a nonylphenol isomer; the black solid line is the regression line; the blue long-dash curve is the 95% confidence limit and the red short-dash line is the 95% prediction limit.  $\alpha$ -Substituent types: a, dimethyl; b, ethylmethyl; c, methylpropyl; d, isopropylmethyl.

## Supporting Information

**Table S 2–1** Molecular descriptors for the 18 nonylphenol isomers identified

isomers	steric	nclass	nX2	nXp3	nXp4	nXp5	nXp6	nXp7	nXp8	nXp9	nXp10
9	1.443	13	21	23	24	27	26	19	12	10	8
35	1.477	13	22	26	26	29	27	20	12	8	6
36	1.456	13	22	24	27	28	27	18	14	10	6
37	1.448	13	22	24	24	29	27	18	12	12	8
38	1.445	12	22	23	24	27	28	18	12	10	10
65	1.477	14	21	25	26	29	28	21	12	8	6
110	1.510	14	22	28	29	30	27	22	12	6	2
110	1.510	14	22	28	29	30	27	22	12	6	2
111	1.488	14	22	26	28	31	27	20	14	8	2
111	1.488	14	22	26	28	31	27	20	14	8	2
112	1.481	13	22	25	26	31	28	20	12	10	4
119	1.488	13	22	27	29	30	26	20	14	8	2
128	1.459	11	22	25	27	30	26	18	14	12	4
143	1.510	13	22	27	28	31	28	22	12	6	2
152	1.488	14	21	25	28	31	28	21	14	8	2
193	1.517	14	22	28	30	31	27	22	14	4	0
193	1.517	14	22	28	30	31	27	22	14	4	0
194	1.496	13	22	25	30	31	28	20	16	6	0

**Table S 2-1** Molecular descriptors for the 18 nonylphenol isomers identified (continued)

isomers	X1	X2	Xp3	Xp4	Xp5	Xp6	Xp7	Xp8	Xp9	Xp10	nXpc4
9	7.560	6.756	4.796	3.253	2.347	1.624	0.799	0.307	0.181	0.101	16.000
35	7.480	6.821	5.329	3.289	2.421	1.577	0.686	0.257	0.116	0.075	23.000
36	7.454	7.043	4.777	3.701	2.239	1.636	0.600	0.325	0.150	0.075	18.000
37	7.454	6.997	5.099	3.068	2.471	1.651	0.642	0.265	0.198	0.099	18.000
38	7.416	7.231	4.724	3.212	2.227	1.815	0.652	0.294	0.156	0.133	17.000
65	7.620	6.421	5.161	3.405	2.451	1.716	0.866	0.315	0.142	0.092	19.000
110	7.541	6.506	5.558	3.722	2.439	1.485	0.803	0.271	0.106	0.024	26.000
110	7.541	6.506	5.558	3.722	2.439	1.485	0.803	0.271	0.106	0.024	26.000
111	7.514	6.682	5.321	3.497	2.605	1.544	0.718	0.339	0.140	0.024	21.000
111	7.514	6.682	5.321	3.497	2.605	1.544	0.718	0.339	0.140	0.024	21.000
112	7.476	6.897	5.102	3.245	2.650	1.661	0.759	0.279	0.188	0.048	20.000
119	7.518	6.672	5.250	3.788	2.546	1.438	0.647	0.314	0.140	0.024	24.000
128	7.492	6.832	5.091	3.530	2.569	1.491	0.605	0.295	0.212	0.048	19.000
143	7.503	6.721	5.336	3.441	2.608	1.626	0.822	0.297	0.130	0.029	25.000
152	7.620	6.464	4.924	3.642	2.677	1.671	0.818	0.385	0.172	0.029	19.000
193	7.541	6.522	5.475	3.777	2.549	1.512	0.764	0.382	0.076	0.000	26.000
193	7.541	6.522	5.475	3.777	2.549	1.512	0.764	0.382	0.076	0.000	26.000
194	7.476	6.959	4.697	3.934	2.528	1.672	0.679	0.450	0.110	0.000	20.000

**Table S 2-1** Molecular descriptors for the 18 nonylphenol isomers identified (continued)

isomers	Xc3	Xc4	Xpc4	knotp	knotpv	sumdell	tets1	htets1	htets2	diam	muldiam	rad	mulrad
9	1.483	0.204	2.527	-0.927	-0.875	5.593	47.484	37.269	9.704	11	2	6	2
35	1.548	0.167	3.596	-1.007	-0.955	6.075	45.614	38.650	10.163	10	2	5	1
36	1.772	0.204	2.777	-1.255	-1.196	6.072	46.204	38.246	10.012	10	2	5	1
37	1.772	0.204	3.020	-1.012	-0.960	6.037	46.507	37.913	9.906	10	2	5	1
38	1.892	0.204	2.816	-1.047	-0.995	5.967	46.586	37.600	9.811	10	3	5	1
65	1.236	0.144	2.764	-0.837	-0.748	5.778	48.782	38.741	10.116	10	2	5	1
110	1.330	0.118	3.604	-0.992	-0.904	6.254	46.968	39.984	10.549	9	2	5	2
110	1.330	0.118	3.604	-0.992	-0.904	6.254	46.968	39.984	10.549	9	2	5	2
111	1.524	0.144	3.119	-1.059	-0.964	6.221	47.489	39.520	10.375	9	2	5	2
111	1.524	0.144	3.119	-1.059	-0.964	6.221	47.489	39.520	10.375	9	2	5	2
112	1.644	0.144	3.053	-0.957	-0.868	6.147	47.686	39.126	10.244	9	3	5	2
119	1.488	0.167	3.362	-1.147	-1.077	6.164	46.291	39.303	10.363	9	2	5	2
128	1.688	0.204	2.939	-1.128	-1.069	6.098	46.555	38.560	10.106	9	3	5	2
143	1.414	0.118	3.642	-1.004	-0.921	6.184	47.021	40.031	10.530	9	2	5	2
152	1.236	0.144	2.589	-1.012	-0.910	5.856	49.189	39.440	10.298	9	2	5	2
193	1.330	0.118	3.510	-1.086	-0.986	6.287	47.296	40.428	10.660	8	3	4	1
193	1.330	0.118	3.510	-1.086	-0.986	6.287	47.296	40.428	10.660	8	3	4	1
194	1.644	0.144	2.715	-1.294	-1.186	6.214	47.718	39.905	10.462	8	4	4	1

**Table S 2-1** Molecular descriptors for the 18 nonylphenol isomers identified (continued)

isomers	W	Tg3	IDC	IDWbar	Si	SHBa	SwHBa	Hmin	Gmin	SHCsats	SsssCH	SaasC
9	497	0	376.985	6.660	72.207	9.268	9.309	0.348	0.224	3.753	0.000	1.674
35	457	2	356.344	6.688	73.893	9.302	9.303	0.361	0.183	3.887	0.664	1.662
36	464	0	359.100	6.686	73.347	9.289	9.292	0.363	0.197	3.858	0.758	1.662
37	473	1	363.407	6.679	73.005	9.279	9.286	0.368	0.205	3.832	0.802	1.662
38	484	0	368.607	6.670	72.645	9.271	9.282	0.377	0.211	3.801	0.788	1.663
65	465	1	358.713	6.689	73.252	9.309	9.418	0.358	0.267	3.832	0.000	1.708
110	432	2	338.821	6.714	74.881	9.337	9.402	0.378	0.226	3.960	0.673	1.694
110	432	2	338.821	6.714	74.881	9.337	9.402	0.378	0.226	3.960	0.673	1.694
111	441	2	343.468	6.709	74.235	9.323	9.390	0.383	0.239	3.922	0.749	1.693
111	441	2	343.468	6.709	74.235	9.323	9.390	0.383	0.239	3.922	0.749	1.693
112	452	1	349.554	6.700	73.752	9.313	9.384	0.393	0.248	3.884	0.753	1.694
119	437	0	342.123	6.710	74.552	9.322	9.348	0.380	0.193	3.944	0.710	1.675
128	453	0	351.230	6.697	73.686	9.297	9.308	0.387	0.199	3.889	0.795	1.666
143	436	2	340.226	6.713	74.576	9.337	9.402	0.374	0.226	3.938	0.614	1.694
152	449	0	346.043	6.709	73.666	9.328	9.463	0.374	0.276	3.867	0.000	1.721
193	425	2	331.365	6.724	75.071	9.348	9.430	0.399	0.233	3.976	0.664	1.702
193	425	2	331.365	6.724	75.071	9.348	9.430	0.399	0.233	3.976	0.664	1.702
194	436	0	336.547	6.718	74.284	9.334	9.418	0.398	0.247	3.926	0.699	1.702

**Table S 2-1** Molecular descriptors for the 18 nonylphenol isomers identified (continued)

isomers	minSHaa CH	minSsC H3	minSssC H2	minSsssC H	minSaas C	maxSHCs ats	maxSsC H3	maxSssC H2	maxSaaC H	maxSsO H
9	1.211	2.241	1.220	0.000	0.352	0.572	2.283	1.339	2.037	9.268
35	1.217	2.236	1.260	0.664	0.348	0.616	2.322	1.294	2.040	9.302
36	1.214	2.240	1.200	0.758	0.348	0.589	2.325	1.293	2.036	9.289
37	1.213	2.248	1.201	0.802	0.349	0.579	2.312	1.268	2.034	9.279
38	1.212	2.271	1.204	0.788	0.349	0.574	2.278	1.293	2.032	9.271
65	1.217	2.240	1.154	0.000	0.357	0.579	2.328	1.313	2.060	9.309
110	1.222	2.240	1.138	0.673	0.352	0.621	2.333	1.255	2.061	9.337
110	1.222	2.240	1.138	0.673	0.352	0.621	2.333	1.255	2.061	9.337
111	1.219	2.245	1.141	0.749	0.353	0.593	2.325	1.230	2.057	9.323
111	1.219	2.245	1.141	0.749	0.353	0.593	2.325	1.230	2.057	9.323
112	1.218	2.243	1.143	0.753	0.353	0.583	2.321	1.255	2.055	9.313
119	1.219	2.246	1.210	0.710	0.350	0.631	2.309	1.268	2.049	9.322
128	1.215	2.265	1.213	0.795	0.349	0.593	2.289	1.248	2.039	9.297
143	1.222	2.234	1.214	0.614	0.352	0.600	2.333	1.260	2.061	9.337
152	1.219	2.239	1.209	0.000	0.359	0.579	2.346	1.275	2.070	9.328
193	1.223	2.237	1.192	0.664	0.354	0.616	2.344	1.201	2.067	9.348
193	1.223	2.237	1.192	0.664	0.354	0.616	2.344	1.201	2.067	9.348
194	1.221	2.235	1.199	0.699	0.354	0.589	2.336	1.204	2.063	9.334

**Table S 2–2** Proportion of variance explained by partial least square regression

Latent Factors	Statistics				
	X Variance	Cumulative X Variance	Y Variance	Cumulative Y Variance (R-square)	Adjusted R-square
1	.512	.512	.816	.816	.797
2	.175	.688	.073	.889	.865
3	.135	.823	.029	.919	.888
4	.093	.916	.011	.930	.890



**Table S 2–3** Parameters of partial least square regression

Independent Variables	Dependent Variables half_life	Independent Variables	Dependent Variables half_life	Independent Variables	Dependent Variables half_life
(Constant)	-366.385	Xp9	5.326	Si	.131
steric	3.635	Xp10	-5.055	SHBa	5.296
nclass	-.141	nXpc4	.019	SwHBa	2.116
nX2	.049	Xc3	-.226	Hmin	18.555
nXp3	.046	Xc4	-.430	Gmin	1.511
nXp4	.066	Xpc4	.075	SHCsats	1.892
nXp5	.179	knotp	-.737	SsssCH	.098
nXp6	-.035	knotpv	-.636	SaasC	5.692
nXp7	.019	sumdelI	.402	minSHaaCH	31.339
nXp8	.120	tets1	.075	minSsCH3	18.505
nXp9	.022	htets1	.141	minSssCH2	8.680
nXp10	-.061	htets2	.430	minSsssCH	.098
X1	.785	diam	-.303	minSaasC	32.222
X2	-.231	muldiam	.096	maxSHCsats	2.586
Xp3	.063	rad	-.104	maxSsCH3	1.885
Xp4	.416	mulrad	.649	maxSssCH2	-4.791
Xp5	2.556	W	-.007	maxSaaCH	10.034
Xp6	-1.057	Tg3	-.121	maxSsOH	5.304
Xp7	-.818	IDC	-.014		
Xp8	1.685	IDWbar	10.062		

**Table S 2–4** Variable importance in the projection of partial least square regression

Variables	Latent Factors				Variables	Latent Factors			
	1	2	3	4		1	2	3	4
steric	.168	-.055	-.021	.022	htets1	.184	.011	.017	.023
nclass	.060	-.247	-.144	-.172	htets2	.182	.000	-.008	.030
nX2	.079	.044	-.205	.036	diam	-.192	-.178	-.124	-.101
nXp3	.149	-.077	-.044	.114	muldiam	.056	.176	-.027	-.177
nXp4	.186	.061	-.012	-.059	rad	-.141	-.072	.106	.200
nXp5	.190	.162	.205	.067	mulrad	.041	.155	.421	.570
nXp6	.013	-.042	-.014	-.073	W	-.187	-.050	-.014	-.047
nXp7	.117	-.153	-.002	.050	Tg3	.075	-.244	-.214	-.043
nXp8	.117	.263	.076	-.240	IDC	-.192	-.075	-.047	-.062
nXp9	-.128	.151	.166	.142	IDWbar	.193	.083	.072	.057
nXp10	-.191	-.102	-.088	.025	Si	.175	-.003	-.043	.057
X1	.031	-.080	.198	.011	SHBa	.181	.005	.037	.017
X2	-.083	.110	-.122	-.055	SwHBa	.138	-.010	.142	-.011
Xp3	.099	-.150	-.062	.140	Hmin	.167	.215	.122	.187
Xp4	.162	.069	-.061	-.140	Gmin	.044	-.034	.155	-.094
Xp5	.155	.240	.400	.185	SHCsats	.176	.025	-.042	.057
Xp6	-.109	-.027	-.028	-.128	SsssCH	.065	.068	-.183	.054
Xp7	.004	-.214	.037	-.007	SaasC	.111	-.016	.165	-.028
Xp8	.093	.166	.070	-.287	minSHaaCH	.179	-.013	.003	.016
Xp9	-.096	.238	.374	.300	minSsCH3	-.067	.200	.239	.494
Xp10	-.190	-.121	-.103	-.025	minSssCH2	-.034	.324	.360	.322
nXpc4	.141	-.091	-.077	.142	minSsssCH	.065	.068	-.183	.054
Xc3	-.075	.122	-.125	-.049	minSaasC	.058	.000	.239	-.009
Xc4	-.139	.133	.057	.049	maxSHCsats	.122	-.057	-.107	.099
Xpc4	.106	-.118	-.131	.191	maxSsCH3	.138	-.057	-.020	-.102
knotp	-.074	-.214	.059	.118	maxSssCH2	-.176	-.152	-.036	-.026
knotpv	-.049	-.213	.063	.090	maxSaaCH	.150	-.010	.121	-.006
sumdelI	.148	.033	-.130	.045	maxSsOH	.181	.005	.037	.017
tets1	.024	.005	.230	-.066	half_life	.169	.099	.069	.053

**Table S 2–5** Weights of variables of partial least square regression

Variables	Latent Factors				Variables	Latent Factors				Variables	Latent Factors			
	1	2	3	4		1	2	3	4		1	2	3	4
steric	.168	-.055	-.021	.022	Xp10	-.190	-.121	-.103	-.025	Si	.175	-.003	-.043	.057
nclass	.060	-.247	-.144	-.172	nXpc4	.141	-.091	-.077	.142	SHBa	.181	.005	.037	.017
nX2	.079	.044	-.205	.036	Xc3	-.075	.122	-.125	-.049	SwHBa	.138	-.010	.142	-.011
nXp3	.149	-.077	-.044	.114	Xc4	-.139	.133	.057	.049	Hmin	.167	.215	.122	.187
nXp4	.186	.061	-.012	-.059	Xpc4	.106	-.118	-.131	.191	Gmin	.044	-.034	.155	-.094
nXp5	.190	.162	.205	.067	knotp	-.074	-.214	.059	.118	SHCsats	.176	.025	-.042	.057
nXp6	.013	-.042	-.014	-.073	knotpv	-.049	-.213	.063	.090	SsssCH	.065	.068	-.183	.054
nXp7	.117	-.153	-.002	.050	sumdelI	.148	.033	-.130	.045	SaasC	.111	-.016	.165	-.028
nXp8	.117	.263	.076	-.240	tets1	.024	.005	.230	-.066	minSHaaCH	.179	-.013	.003	.016
nXp9	-.128	.151	.166	.142	htets1	.184	.011	.017	.023	minSsCH3	-.067	.200	.239	.494
nXp10	-.191	-.102	-.088	.025	htets2	.182	.000	-.008	.030	minSssCH2	-.034	.324	.360	.322
X1	.031	-.080	.198	.011	diam	-.192	-.178	-.124	-.101	minSsssCH	.065	.068	-.183	.054
X2	-.083	.110	-.122	-.055	muldiam	.056	.176	-.027	-.177	minSaasC	.058	.000	.239	-.009
Xp3	.099	-.150	-.062	.140	rad	-.141	-.072	.106	.200	maxSHCsats	.122	-.057	-.107	.099
Xp4	.162	.069	-.061	-.140	mulrad	.041	.155	.421	.570	maxSsCH3	.138	-.057	-.020	-.102
Xp5	.155	.240	.400	.185	W	-.187	-.050	-.014	-.047	maxSssCH2	-.176	-.152	-.036	-.026
Xp6	-.109	-.027	-.028	-.128	Tg3	.075	-.244	-.214	-.043	maxSaaCH	.150	-.010	.121	-.006
Xp7	.004	-.214	.037	-.007	IDC	-.192	-.075	-.047	-.062	maxSsOH	.181	.005	.037	.017
Xp8	.093	.166	.070	-.287	IDWbar	.193	.083	.072	.057	half_life	.169	.099	.069	.053
Xp9	-.096	.238	.374	.300										

**Table S 2–6** Loadings of variables of partial least square regression

Variables	Latent Factors				Variables	Latent Factors			
	1	2	3	4		1	2	3	4
steric	.181	-.087	-.006	-.002	htets1	.186	-.023	.003	-.011
nclass	.100	-.254	.047	-.153	htets2	.186	-.024	-.025	.020
nX2	.074	.164	-.300	.123	diam	-.169	-.135	-.003	.018
nXp3	.165	-.100	-.068	.163	muldiam	.030	.241	-.045	-.170
nXp4	.181	.059	-.020	-.017	rad	-.133	-.135	.073	.205
nXp5	.170	.068	.130	.022	mulrad	.018	-.042	.152	.380
nXp6	.020	-.050	.043	-.340	W	-.183	-.029	.034	-.060
nXp7	.143	-.219	.059	-.015	Tg3	.114	-.213	-.107	.079
nXp8	.079	.287	.066	-.164	IDC	-.185	-.044	.016	-.026
nXp9	-.155	.126	.050	.146	IDWbar	.185	.039	.015	.017
nXp10	-.179	-.056	-.064	.000	Si	.179	-.006	-.081	.094
X1	.044	-.224	.288	-.002	SHBa	.185	-.043	.036	-.018
X2	-.102	.229	-.188	-.092	SwHBa	.143	-.116	.190	-.137
Xp3	.124	-.179	-.062	.249	Hmin	.137	.191	-.065	.023
Xp4	.155	.102	-.046	-.079	Gmin	.050	-.141	.262	-.246
Xp5	.122	.066	.271	.098	SHCsats	.176	.030	-.096	.103
Xp6	-.107	-.002	.044	-.321	SsssCH	.056	.185	-.296	.132
Xp7	.037	-.307	.173	-.071	SaasC	.116	-.133	.230	-.175
Xp8	.070	.166	.137	-.345	minSHaaCH	.185	-.046	.003	-.004
Xp9	-.135	.116	.181	.165	minSsCH3	-.099	.139	-.064	.236
Xp10	-.176	-.073	-.047	-.025	minSssCH2	-.084	.229	.104	-.039
nXpc4	.159	-.098	-.116	.154	minSsssCH	.056	.185	-.296	.132
Xc3	-.095	.245	-.202	-.018	minSaasC	.060	-.147	.305	-.188
Xc4	-.163	.165	-.029	.048	maxSHCsats	.134	-.033	-.151	.228
Xpc4	.127	-.099	-.192	.238	maxSsCH3	.150	-.086	.059	-.200
knotp	-.043	-.306	.136	.108	maxSssCH2	-.157	-.154	.055	.016
knotpv	-.018	-.311	.156	.077	maxSaaCH	.155	-.106	.160	-.115
sumdelI	.146	.096	-.205	.089	maxSsOH	.185	-.043	.036	-.018
tets1	.024	-.129	.318	-.215	half_life	1.000	1.000	1.000	1.000

**Table S 2–7** Predicted half lives (d) and molecular descriptors for 4-quaternary nonylphenol isomers

isomers	Predicted half life (d)	steric	nclass	nX2	nXp3	nXp4	nXp5	nXp6	nXp7	nXp8	nXp9	nXp10	X1
91	7.2	1.51	12	24	29	28	29	26	22	12	6	2	7.31
94	7.3	1.47	12	24	25	28	29	26	18	16	10	2	7.27
96	7.0	1.45	11	24	23	24	31	26	18	12	14	6	7.21
137	11.4	1.51	12	21	27	29	31	28	22	12	6	2	7.68
165	3.7	1.52	11	25	31	28	28	26	22	14	4	0	7.19
166	4.6	1.50	11	25	28	29	28	26	20	16	6	0	7.15
168	9.6	1.54	13	24	31	30	29	26	24	12	2	0	7.37
169	11.6	1.52	13	23	29	30	30	26	22	14	4	0	7.41
170	10.7	1.50	12	24	25	30	31	26	20	16	6	0	7.27
173	9.5	1.52	11	24	31	29	28	26	22	14	4	0	7.37
174	11.3	1.50	12	23	28	31	28	26	20	16	6	0	7.39
178	14.1	1.54	12	22	30	32	30	26	24	12	2	0	7.60
179	14.8	1.52	11	22	27	31	32	26	22	14	4	0	7.54
180	13.1	1.52	12	22	29	31	30	26	22	14	4	0	7.58
185	12.1	1.54	13	23	30	31	30	26	24	12	2	0	7.42
186	13.2	1.52	12	23	27	30	32	26	22	14	4	0	7.36
198	10.5	1.54	12	24	29	30	31	26	24	12	2	0	7.31
201	14.1	1.54	13	22	29	32	31	26	24	12	2	0	7.56
202	14.9	1.52	11	21	27	31	32	27	22	14	4	0	7.68
208	14.5	1.56	10	24	31	33	28	26	26	10	0	0	7.37
209	8.4	1.56	11	25	31	32	28	26	26	10	0	0	7.19
211	16.4	1.56	10	23	31	34	28	26	26	10	0	0	7.45
92	7.1	1.49	12	24	29	28	29	26	22	12	6	2	7.31
93	8.5	1.48	13	23	28	28	29	26	20	14	8	2	7.39
95	7.3	1.46	12	24	25	28	29	26	18	16	10	2	7.27

**Table S 2–7** Predicted half lives (d) and molecular descriptors for 4-quaternary nonylphenol isomers (continued)

isomers	X2	Xp3	Xp4	Xp5	Xp6	Xp7	Xp8	Xp9	Xp10	nXpc4	Xc3	Xc4	Xpc4	knotp	knotpv
91	7.31	5.66	3.48	2.25	1.36	0.707	0.226	0.092	0.021	34	2.22	0.321	5.30	-1.28	-1.25
94	7.64	5.01	3.54	2.29	1.46	0.558	0.343	0.151	0.021	22	2.69	0.454	3.65	-1.51	-1.45
96	8.01	4.64	2.94	2.68	1.48	0.626	0.238	0.234	0.063	19	3.04	0.558	3.28	-1.24	-1.19
137	6.13	5.32	3.79	2.67	1.67	0.882	0.319	0.130	0.029	22	1.04	0.102	2.79	-0.77	-0.65
165	7.55	6.14	3.25	2.04	1.34	0.671	0.272	0.048	0.000	40	2.38	0.289	6.44	-1.26	-1.22
166	7.87	5.48	3.47	2.05	1.38	0.606	0.319	0.072	0.000	31	2.85	0.455	4.90	-1.48	-1.42
168	6.97	6.08	3.62	2.25	1.32	0.829	0.272	0.029	0.000	37	2.02	0.279	5.28	-1.19	-1.12
169	6.85	5.75	3.66	2.38	1.36	0.762	0.324	0.056	0.000	29	1.63	0.118	4.14	-1.14	-1.04
170	7.70	4.74	3.73	2.54	1.42	0.680	0.390	0.088	0.000	22	2.80	0.498	3.17	-1.49	-1.39
173	6.95	6.15	3.64	2.07	1.37	0.670	0.302	0.059	0.000	37	1.99	0.269	5.43	-1.18	-1.13
174	7.04	5.27	4.16	2.10	1.42	0.605	0.368	0.090	0.000	27	1.79	0.167	3.72	-1.44	-1.36
178	6.21	5.74	4.17	2.50	1.33	0.917	0.316	0.034	0.000	29	1.16	0.083	3.51	-0.94	-0.82
179	6.62	5.10	3.97	2.81	1.39	0.831	0.384	0.068	0.000	23	1.45	0.102	2.93	-1.03	-0.91
180	6.33	5.63	4.05	2.46	1.39	0.760	0.359	0.068	0.000	27	1.27	0.118	3.47	-1.03	-0.93
185	6.79	5.81	3.76	2.40	1.34	0.857	0.295	0.034	0.000	32	1.52	0.096	4.39	-1.17	-1.09
186	7.22	5.12	3.67	2.66	1.40	0.771	0.363	0.068	0.000	26	1.82	0.118	3.78	-1.28	-1.19
198	7.37	5.40	3.61	2.54	1.36	0.836	0.309	0.042	0.000	34	2.31	0.352	4.89	-1.31	-1.25
201	6.45	5.35	4.14	2.70	1.35	0.921	0.339	0.042	0.000	28	1.25	0.083	3.47	-1.03	-0.92
202	6.17	5.08	4.04	2.88	1.55	0.829	0.427	0.083	0.000	22	1.04	0.102	2.65	-0.91	-0.77
208	7.07	5.55	4.31	2.18	1.28	0.989	0.243	0.000	0.000	37	2.16	0.322	4.61	-1.37	-1.29
209	7.64	5.68	3.81	2.13	1.28	0.928	0.221	0.000	0.000	40	2.51	0.333	5.59	-1.52	-1.48
211	6.73	5.54	4.51	2.20	1.28	1.013	0.251	0.000	0.000	34	1.46	0.068	4.11	-1.27	-1.17
92	7.31	5.66	3.48	2.25	1.36	0.707	0.226	0.092	0.021	34	2.22	0.321	5.30	-1.28	-1.25
93	6.95	5.74	3.46	2.25	1.40	0.637	0.277	0.114	0.020	27	1.75	0.167	4.15	-1.18	-1.12
95	7.64	5.01	3.54	2.29	1.46	0.558	0.343	0.151	0.021	22	2.69	0.454	3.65	-1.51	-1.45

**Table S 2–7** Predicted half lives (d) and molecular descriptors for 4-quaternary nonylphenol isomers (continued)

isomers	sumdell	tets1	htets1	htets2	diam	muldiam	rad	mulrad	W	Tg3	IDC	IDWbar	Si	SHBa
91	6.45	41.14	41.8	11.3	9	2	5	2	424	4	337	6.71	75.7	9.33
94	6.41	43.26	41.6	11.3	9	2	5	2	440	2	345	6.70	74.5	9.30
96	6.28	44.09	41.0	11.1	9	4	5	2	460	0	355	6.69	73.6	9.28
137	5.90	50.08	40.0	10.5	9	2	5	2	438	0	340	6.72	74.3	9.34
165	6.65	38.59	42.3	11.5	8	3	4	1	411	8	328	6.72	76.6	9.33
166	6.60	40.21	42.4	11.6	8	4	4	1	420	5	333	6.71	75.9	9.32
168	6.59	42.65	42.6	11.5	8	2	4	1	408	5	323	6.73	76.5	9.36
169	6.50	45.21	40.5	10.7	8	3	4	1	419	4	330	6.72	75.6	9.34
170	6.46	44.38	42.0	11.4	8	4	4	1	428	1	335	6.72	75.0	9.33
173	6.54	41.78	42.3	11.5	8	3	4	1	413	4	328	6.72	76.3	9.34
174	6.43	44.45	39.8	10.5	8	4	4	1	424	0	333	6.72	75.3	9.33
178	6.35	48.24	41.0	10.9	8	2	4	1	414	1	324	6.73	75.7	9.36
179	6.27	48.64	40.5	10.7	8	3	4	1	425	0	331	6.73	74.9	9.35
180	6.30	47.46	40.4	10.7	8	3	4	1	421	1	330	6.73	75.3	9.35
185	6.55	44.87	41.0	10.9	8	2	4	1	412	4	324	6.73	76.0	9.36
186	6.49	45.40	40.5	10.7	8	3	4	1	423	2	331	6.72	75.2	9.34
198	6.50	42.57	42.2	11.4	8	2	4	1	412	3	325	6.73	76.1	9.36
201	6.31	48.26	41.1	10.9	8	2	4	1	416	0	325	6.73	75.5	9.36
202	5.94	50.38	40.5	10.6	8	3	4	1	429	0	332	6.73	74.6	9.35
208	6.59	43.64	42.8	11.6	7	6	4	3	401	0	315	6.74	76.8	9.37
209	6.71	39.57	42.8	11.7	7	6	4	3	399	5	315	6.74	77.1	9.36
211	6.59	45.90	41.7	11.1	7	6	4	3	403	0	315	6.74	76.5	9.37
92	6.45	41.14	41.8	11.3	9	2	5	2	424	4	337	6.71	75.7	9.33
93	6.41	43.94	39.5	10.4	9	2	5	2	433	4	341	6.71	75.0	9.32
95	6.41	43.26	41.6	11.3	9	2	5	2	440	2	345	6.70	74.5	9.30

**Table S 2–7** Predicted half lives (d) and molecular descriptors for 4-quaternary nonylphenol isomers (continued)

isomers	SwHBa	Hmin	Gmin	SHCsats	SsssCH	SaasC	minSHaaCH	minSsCH3	minSssCH2	minSsssCH
91	9.26	0.382	0.122	3.38	0.00	1.64	1.22	2.23	1.20	0.000
94	9.25	0.391	0.160	3.39	0.00	1.64	1.22	2.24	1.15	0.000
96	9.24	0.411	0.182	3.37	0.00	1.64	1.21	2.27	1.17	0.000
137	9.52	0.374	0.309	3.91	0.00	1.74	1.22	2.24	1.17	0.000
165	9.21	0.431	0.092	3.44	0.61	1.62	1.22	2.27	0.00	0.608
166	9.21	0.441	0.117	3.48	0.56	1.62	1.22	2.27	0.00	0.560
168	9.34	0.414	0.162	3.43	0.00	1.66	1.23	2.24	1.11	0.000
169	9.36	0.424	0.196	4.03	1.29	1.67	1.22	2.24	1.12	0.627
170	9.33	0.434	0.200	3.43	0.00	1.67	1.22	2.23	1.12	0.000
173	9.29	0.417	0.129	3.41	0.00	1.64	1.22	2.26	1.16	0.000
174	9.30	0.412	0.163	4.01	1.34	1.66	1.22	2.26	1.19	0.664
178	9.48	0.408	0.266	4.02	0.67	1.72	1.23	2.26	1.16	0.673
179	9.47	0.417	0.280	3.97	0.70	1.72	1.22	2.26	1.16	0.703
180	9.43	0.410	0.233	4.00	0.71	1.70	1.22	2.26	1.14	0.710
185	9.37	0.408	0.183	4.05	1.23	1.67	1.23	2.24	1.18	0.590
186	9.36	0.417	0.196	4.00	1.28	1.67	1.22	2.26	1.18	0.597
198	9.34	0.401	0.162	3.42	0.00	1.66	1.23	2.23	1.17	0.000
201	9.48	0.401	0.266	4.01	0.63	1.72	1.23	2.24	1.16	0.627
202	9.54	0.399	0.317	3.93	0.00	1.75	1.22	2.25	1.18	0.000
208	9.39	0.446	0.195	3.46	0.00	1.68	1.23	2.25	1.12	0.000
209	9.28	0.461	0.112	3.49	0.55	1.64	1.23	2.26	0.00	0.553
211	9.42	0.446	0.216	4.08	1.20	1.69	1.23	2.26	1.13	0.599
92	9.26	0.382	0.122	3.38	0.00	1.64	1.22	2.23	1.20	0.000
93	9.28	0.387	0.156	3.99	1.34	1.65	1.22	2.24	1.21	0.627
95	9.25	0.391	0.160	3.39	0.00	1.64	1.22	2.24	1.15	0.000



**Table S 2–7** Predicted half lives (d) and molecular descriptors for 4-quaternary nonylphenol isomers (continued)

isomers	minSaasC	maxSHCsats	maxSsCH3	maxSssCH2	maxSaaCH	maxSsOH
91	0.341	0.531	2.32	1.21	2.03	9.33
94	0.342	0.603	2.31	1.19	2.03	9.30
96	0.343	0.583	2.28	1.21	2.03	9.28
137	0.361	0.583	2.27	1.28	2.08	9.34
165	0.335	0.559	2.31	0.00	2.03	9.33
166	0.336	0.640	2.30	0.00	2.03	9.32
168	0.344	0.569	2.32	1.15	2.05	9.36
169	0.347	0.631	2.32	1.12	2.05	9.34
170	0.345	0.603	2.31	1.15	2.05	9.33
173	0.342	0.527	2.35	1.16	2.04	9.34
174	0.345	0.640	2.30	1.19	2.04	9.33
178	0.356	0.621	2.33	1.20	2.08	9.36
179	0.356	0.593	2.28	1.21	2.07	9.35
180	0.354	0.631	2.34	1.21	2.07	9.35
185	0.346	0.621	2.33	1.18	2.06	9.36
186	0.347	0.602	2.32	1.18	2.05	9.34
198	0.344	0.583	2.32	1.18	2.05	9.36
201	0.356	0.607	2.30	1.21	2.08	9.36
202	0.363	0.579	2.28	1.24	2.09	9.35
208	0.346	0.574	2.30	1.12	2.06	9.37
209	0.337	0.611	2.31	0.00	2.04	9.36
211	0.348	0.611	2.29	1.13	2.07	9.37
92	0.341	0.531	2.32	1.21	2.03	9.33
93	0.343	0.631	2.32	1.21	2.04	9.32
95	0.342	0.603	2.31	1.19	2.03	9.30

## Chapter 3 Isomeric-Specific Biodegradation of Nonylphenol in the Bioreactor

### 3.1 Introduction

Nonylphenol (NP) is a well known environmental estrogen of emerging concern (Soares et al., 2008; Ying et al., 2002). It is a high production volume chemical and its annual production in the United States was 100 - 500 million lbs (45.4 - 227 thousand tons) in 2006 (USEPA, 2006). Nonylphenol is used as the raw material for the production of nonylphenol ethoxylates (NPEOs), which are the most widely used non-ionic surfactants (Ying et al., 2002). Incomplete biodegradation of NPEOs in the wastewater treatment plants (WWTP) is the most important source for NP release into the environment. Therefore, high concentrations of NP have been frequently detected in WWTP effluent impacted surface water, sediment and aquatic organisms (Maruya et al., 2012; Soares et al., 2008; Venkatesan and Halden, 2013; Vidal-Dorsch et al., 2012; Ying et al., 2002). For example, the median concentration in municipal wastewater effluents in Southern California was 1.42  $\mu\text{g/L}$  ( $n=16$ , 94% detection) and the maximum concentration in sea water receiving these effluents was 0.23  $\mu\text{g/L}$  ( $n=20$ , 35% detection) (Vidal-Dorsch et al., 2012). In the same area, the median concentrations of NP in sediments and livers of flatfish hornyhead turbot (*Pleuronichthys verticalis*) were 30 and 83  $\mu\text{g/kg}$ , respectively (Maruya et al., 2012). According to USEPA's 2001 national sewage sludge survey, the concentration of NP in sludge was  $534 \pm 192$  mg/kg with 100% detection frequency and the estimated mean annual loading of NP into sewage sludge was 2066-5510 tons, of which 1033 to 3306 tons was used for land application (Venkatesan and Halden, 2013).

Hence, control of NP release from WWTPs is crucial to reducing its environmental exposure.

Technical nonylphenol (tNP) is in fact a mixture of more than 100 isomers and congeners due to variations in the length and branching of side chains and substitution position on the benzene ring (Eganhouse et al., 2009; Ieda et al., 2005). Recent studies showed that biodegradation of NP was isomer-specific (Gabriel et al., 2008; Hao et al., 2009; Ikunaga et al., 2004; Lu and Gan, 2014; Shan et al., 2011). However, it is still inconclusive whether or not biodegradation during wastewater treatment process is isomer-specific. After 9 d of incubation with *Sphingomonas xenophaga* Bayram, a bacterial strain isolated from activated sludge, 12 out of 18 NP isomers were removed by 80% while some isomers were recalcitrant. For example, only about 30% of NP<sub>193</sub> was degraded (Gabriel et al., 2008). Since the microorganism community at a WWTP, especially in activated sludge, is extremely diverse, isomer selective biodegradation observed with isolated strains may not suggest similar selectivity at WWTPs. Hao et al. (2009) measured the removal of 4 NP isomers in a lab-scale sequencing batch reactor (SBR), and observed the following order: NP<sub>36</sub> (75.4%) > NP<sub>111</sub> (42.9%) > NP<sub>170</sub> (40.7%) > NP<sub>194</sub> (36.2%). On the other hand, Isobe et al. (2001) showed that the profiles of 10 isomer peaks varied only slightly in primary and secondary effluents. Ikunaga et al. (2004) reported that biodegradation of NP by *Sphingomonas cloacae*, which was also enriched from WWTP sludge, was not isomer selective and the initial degradation rates for all peaks were estimated at  $0.996 \pm 0.18 \text{ h}^{-1}$ . A more comprehensive investigation into the fate of NP isomers during wastewater treatment processes is clearly necessary and will add to a

better understanding the loadings and profiles of NP isomers discharged into the environment, leading to improved risk assessments.

The objectives of this study were to evaluate the fate of NP isomers during simulated wastewater treatment processes and to explore the structure-biodegradability relationships at the isomer scale. To achieve these objectives, we constructed a laboratory-scale continuous flow conventional activated sludge (CAS) bioreactor and measured removal percentages and adsorption coefficients of 19 isomers under various operational conditions.

## 3.2 Methods and Materials

### 3.2.1 Chemicals

Technical NP was purchased from TCI America (Portland, OR). Standards of NP<sub>36</sub>, NP<sub>37</sub>, NP<sub>119</sub>, NP<sub>128</sub> and NP<sub>194</sub> (>95% purity) were obtained from ChemCollect GmbH (Remscheid, Germany). Standards of NP<sub>38</sub>, NP<sub>65</sub>, NP<sub>111</sub> and NP<sub>112</sub> in methanol were kindly provided by Prof. Rong Ji at Nanjing University, China. In this study, the Juelich number was used to name the NP isomers due to its simplicity (Guenther et al., 2006). The prefix number 4 - indicating the substitution at *para* position of benzene ring, is usually omitted. 4-*n*-Nonylphenol (NP<sub>1</sub>, >98%) was purchased from Alfa Aesar (Ward Hill, MA) and 4-*tert*-octylphenol (>97%) was from Sigma-Aldrich (St. Louis, MO).

Gas chromatography (GC) grade hexane and methylene chloride and HPLC grade acetone and methanol were purchased from Fisher Scientific (Fair Lawn, NJ). Potassium

phosphate, monobasic (99%) was purchased from J. T. Baker Chemical (Philipsburg, NJ). Sodium bicarbonate (100.3%), sodium phosphate, dibasic, anhydrous (reagent ACS), ammonium chloride (99.9%), sodium acetate trihydrate (100.3%), zinc sulfate (U.S.P 99.0 to 108.7%) and cupric sulfate pentahydrate (U.S.P) were purchased from Fisher. Potassium iodide (U.S.P) and boric acid (analytical reagent) were purchased from Mallinckrodt (Darmstadt, Germany). Manganese (II) chloride (98%) and zinc sulfate (U.S.P, 99.0 to 108.7%) were from Sigma-Aldrich.

### 3.2.2 Reactor Setup

The CAS bioreactor consisted of an aeration tank (32 cm height, 18 cm diameter; 5.2 L working volume) and a clarifier (33 cm height, 10 cm diameter, 2.2 L working volume). The bioreactor was inoculated with activated sludge from a local WWTP (Moreno Valley Regional Water Reclamation Facility, Moreno Valley, CA) and fed with diluted synthetic influent made with 1 part concentrated synthetic wastewater and 5 parts tap water. The diluted synthetic influent contained 100 µg/L tNP, CH<sub>3</sub>COONa (500 mg/L chemical oxygen demand COD), NH<sub>4</sub>Cl (40 mg/L NH<sub>3</sub>-N), Na<sub>2</sub>HPO<sub>4</sub> (24.3 mg/L), KH<sub>2</sub>PO<sub>4</sub> (11.8 mg/L) (total P 8 mg/L), NaHCO<sub>3</sub> (200 mg/L) and trace minerals. The composition of trace minerals was as follows: FeCl<sub>3</sub>·6H<sub>2</sub>O (1.5 mg/L), H<sub>3</sub>BO<sub>3</sub> (0.15 mg/L), CuSO<sub>4</sub>·5H<sub>2</sub>O (0.03 mg/L), KI (0.03 mg/L), ZnSO<sub>4</sub>·7H<sub>2</sub>O (0.12 mg/L), CoCl<sub>2</sub>·6H<sub>2</sub>O (0.15 mg/L), MnCl<sub>2</sub>·4H<sub>2</sub>O (0.12 mg/L). The concentrated synthetic wastewater was adjusted to pH 7, kept at 4 °C in a mini refrigerator and renewed weekly before use. The hydraulic retention time (HRT) was adjusted to 12 hr or 24 hr by the influent flow rate controlled

by two peristaltic pumps. Aeration tank temperature was controlled at 20, 30 or 15 °C within 0.1 °C accuracy by a jacketed water bath connected to a Neslab RTE-101 refrigerated water bath (Newington, NH). The dissolved oxygen (DO) level was maintained above 3 mg/L to ensure the nitrifying process. Temperature and flow rates were checked daily; COD, NH<sub>3</sub>-N and P contents in the influent and effluent were measured weekly. Dissolved oxygen, total suspended solid (TSS) and volatile suspended solid (VSS) in the aeration tank and effluent were also measured weekly.

In total, four different operational schemes were considered: 1) 20 °C with 24 h HRT; 2) 20 °C with 12 h HRT; 3) 30 °C with 12 h HRT; and 4) 15 °C with 12 h HRT. Each scheme was kept at least for 3 wks and influent (200 mL), effluent (200 mL) and sludge (0.5 g, dry weight) samples were taken weekly for analysis of NP isomers.

### 3.2.3 Sample Preparation and Analysis

Effluent samples were filtered through a Whatman GF/F 0.5 µm glass fiber filter and 50 mL influent or filtered effluent sample was extracted by shaking with 15 mL hexane for 30 min. The extraction was repeated for two consecutive times. Sludge samples were freeze-dried and 0.1 g of the dried sludge was sonicated in 20 mL hexane/acetone (9:1, V:V) for 20 min using a Fisher Scientific FS110H ultrasonic water bath (Fair Lawn, NJ). The extraction was repeated for two consecutive times. The cleanup procedure is similar to that in a previous study (Lu and Gan, 2014). Briefly, the extract was concentrated to about 1 mL and passed through a HyperSep Florisil SPE column (Thermo Scientific, Pittsburgh, PA) with a 5-g sorbent bed. The cartridges were preconditioned with 25 mL

hexane and eluted with 35 mL methylene chloride. The extracts of influent and effluent, and elutes of sludge samples were condensed with a gentle nitrogen stream to about 1 mL (influent and sludge samples) or 0.1 mL (effluent samples). A surrogate (10 mg/L 4-n-NP in acetone, 100  $\mu$ L for influent and sludge samples, and 10  $\mu$ L for effluent samples) was spiked before extraction and the same amount of internal standard (10 mg/L 4-tert-octylphenol in hexane) was added before instrument analysis. Triplicates were used for all influent, effluent and sludge samples.

The methods for separation and identification of NP isomers may be found in a previous study (Lu and Gan, 2014). Briefly, an Agilent 6890 GC coupled with an Agilent 5973 mass spectrometer (Agilent, Santa Clara, CA) and an Agilent DB-5MS Ultra Inert capillary column (60 m  $\times$  0.25 mm  $\times$  0.25  $\mu$ m) was used for the analysis. The column temperature was programmed initially at 80  $^{\circ}$ C for 0 min, then ramped to 160  $^{\circ}$ C at 10  $^{\circ}$ C/min and held for 42 min, and further ramped to 300  $^{\circ}$ C at 30  $^{\circ}$ C/min and held for another 3 min. The mass fragments m/z 135 and 107 were used for quantification of the internal standard and recovery surrogate, respectively. Ions with m/z 121, 135, 149, 163, 177 and 191 were used for quantification of different NP isomers. A total of 19  $\alpha$ -quaternary isomers, including 6 diastereomers (denoted as a and b), were resolved and identified. One isomer NP<sub>x</sub> had  $\alpha$ -dimethyl substituents, but its structure was not fully elucidated due to the lack of authentic standard.

### 3.3 Results and Discussion

#### 3.3.1 Isomer Selectivity in Biodegradation

The bioreactor consistently removed COD and NH<sub>3</sub>-N efficiently during the period of operation. During the experiments, COD removal ranged from 94 to 98% and removal of NH<sub>3</sub>-N was greater than 99%. [Figure 3-1](#) shows the total ion chromatography of NP in the influent, the dissolved phase of effluent and sludge. The profile of NP isomers in the effluent or sludge clearly deviated from that in the influent. For example, NP<sub>194</sub> was relatively enriched in the dissolved phase of effluent and also in sludge while NP<sub>36</sub> and NP<sub>9</sub> were essentially eliminated. Moreover, the profile of NP isomers in the dissolved phase of effluent was similar to that in the sludge, i.e., the enriched NP isomers found in the effluent also appeared in the sludge, and vice versa. The shift in isomer composition was also observed in previous studies (Gabriel et al., 2008; Hao et al., 2009). However, in Isobe et al. (2001), only small differences were observed between the primary and secondary effluents. It is possible that changes in isomer profiles may be masked by two sources of variations, i.e., co-elution of some NP isomers and seasonal and site-to-site variations. Gabriel et al. (2008) validated that when a 30-m DB-5 column was used to resolve 13 NP peaks, co-elution of major components including pairs of NP<sub>112</sub>/NP<sub>128</sub>, NP<sub>119</sub>/NP<sub>152</sub>, and NP<sub>110a</sub>/NP<sub>143</sub> happened. Therefore, co-elution of two or more isomers could be very possible in Isobe et al. (2001) since only 10 peaks were resolved. In addition, in Isobe et al. (2001), five WWTPs were sampled seasonally. The site-to-site and seasonal variations may have also contributed to large deviations in the



concentrations of individual isomers, which could further mask the isomeric differences. For example, although the average concentrations of peak 9 showed a large difference between the primary and secondary effluents, the huge standard deviations made the difference statistically insignificant (Isobe et al., 2001).

In this study, the overall removal of tNP was efficient, ranging from 90 to 99%, depending on the operational conditions and isomer structures. These removal values were consistent with those cited by U.S. EPA (2010), which ranged from 57 to 100% with an average of 90%. Gori et al. (2010) reported a value of  $76 \pm 7.5\%$  in Spain and Isobe et al. (2001) reported an averaged removal of 93% (79-99%) during secondary treatment in Japan. It should be noted that the removal rates of NP in WWTPs were likely underestimated due to the continuous formation of NP from biodegradation of NPEO. The removal of NP isomers in this study may be attributed to biodegradation, accumulation on the sludge, volatilization and weekly sludge withdrawal for chemical analysis. Due to the relatively long operation duration, a steady-state was almost reached. Thus, accumulation on the sludge only counted for about 0.3-2% of NP removal according to the changes in NP concentrations on sludge and changes of TSS levels in the aeration tank. Volatilization of NP may be minimal because of the low vapor pressure of tNP ( $2.07 \times 10^{-2}$  Pa at 25 °C) (Soares et al., 2008). According to Cirja et al. (2006), volatilization accounted for less than 1% in a bioreactor. The weekly sludge withdrawal for chemical analysis only contributed to 0.1-1.2% of the weekly NP loading. Therefore, biodegradation may be considered as the predominant pathway for NP removal, and the primary cause for shifts in NP isomer profiles in the effluent and sludge.

### 3.3.2 Effects of Hydraulic Retention Time and Temperature

Figure 3-2 shows residues of NP isomers in the particulate phase and dissolved phase of effluent under different operational schemes. It should be noted that, due to its extremely low residue in the effluent, NP<sub>9</sub> was not quantitatively evaluated (Figure 3-1). Changes in operational conditions induced variations in NP isomer profiles in the effluent. When HRT was decreased from 24 h to 12 h, the remaining levels of NP isomers in the dissolved phase of effluent increased. For example, the residue of NP<sub>35</sub> increased from 0.84% to 1.51%. In the particulate phase, although the concentration increased, the residue in fact decreased due to the decrease of TSS in the effluent (Figure 3-2).

Decreasing aeration tank temperature from 20 °C to 15 °C significantly increased NP residues in the dissolved phase of the effluent. However, this increase appeared to be isomer selective. While residues after the temperature change were similar for the readily degradable isomers, larger increases were observed for the recalcitrant isomers. For example, residues of NP<sub>35</sub> and NP<sub>37</sub> in the dissolved phase were  $1.51 \pm 0.05\%$  and  $1.41 \pm 0.04\%$ , respectively, at 20 °C, and  $1.8 \pm 0.1\%$  and  $1.0 \pm 0.1\%$ , respectively, at 15 °C. In comparison, the corresponding values were  $2.28 \pm 0.07\%$  and  $4.1 \pm 0.1\%$  for NP<sub>194</sub> and NP<sub>143</sub> at 20 °C, and  $4.9 \pm 0.4\%$  and  $7.4 \pm 0.1\%$  at 15 °C. It should be noticed that at 15 °C, NP<sub>119</sub> was also enriched in the effluent (Figure 3-2); NP<sub>119</sub> was to be the most estrogenic 4- $\alpha$ -quaternary NP isomer (Makino et al., 2008; Uchiyama et al., 2008). Therefore, decreasing temperature to 15 °C would enrich more recalcitrant and estrogenic NP isomers. A similar trend was found for NP profiles in the particulate phase. Tanghe et al.

(1998) reported that when temperature decreased from 28 °C to 10-15 °C, removal of tNP decreased from near total removal to 13-86% in laboratory-scale activated sludge units. Koh et al. (2009) investigated removal of NP in a nitrifying/denitrifying activated sludge plant, and found that the removal rates to be 30% and -12%, respectively, in the summer of 2004 (sewage temperature 18 °C) and winter of 2006 (sewage temperature 12 °C). Soares et al. (2006) reported that in a packed-bed bioreactor, removal rates of tNP at 15, 10 and 5.5 °C were 94.0-100%, 95.8-100%, and 84.0-99.0%, respectively, and concluded that the optimal temperature was 10 °C. However, it may be argued that even though the removal of tNP was slightly higher at 10 °C as compared to that at 15 °C, the decrease of removal rate was much more pronounced when temperature was decreased to 5 °C. Therefore, results from this and other studies together show that a decrease of temperature would decrease the removal rate of NP, while findings from this study further suggested that temperature changes may also lead to changes in isomer profiles.

When the temperature was increased to 30 °C from 20 °C, residues of NP in the dissolved phase did not change appreciably. Moreover, residues in the particulate phase displayed a significant increase, likely due to the increase of effluent suspended solids (Figure 3-2). This finding was in contrast with a previous study where an increase of temperature to 30 °C resulted in increased NP removal (Chang et al., 2005). Chang et al. (2005) observed that the half lives of tNP in the sludge were 7.5, 4.7, 2.8 and 1.8 d, respectively, at 20, 30, 40 and 50 °C. The possible cause for the unexpected increase in the current study was that temperature increase changed sludge settleability, leading to increased suspended solid levels in the effluent (Morgan-Sagasturne and Allen, 2004). Elevated

effluent suspended solid levels directly increased NP residues in the particulate phase and it also shortened the sludge retention time, which may result in higher residues of NP in the dissolved phase.. Therefore, it is critical to reduce effluent suspended solid levels to minimize NP discharge into the environment.

### 3.3.3 Isomer Structure-Biodegradation Relationships

Due to the large number of isomers in tNP and challenges in the analysis of NP isomers, a quantitative understanding of the relationships between isomer structures and their biodegradability offers advantages over experimentation and may also provide guidance to isomers for which analysis is not yet possible. [Figure 3-3](#) shows the relationships of some key structure parameters with residues of NP isomers in the effluent including both dissolved phase and particulate phase. With an increase in alkyl chain length, residues of NP isomers generally decreased, although significant variations were evident for different isomers ([Figure 3-3a](#)). The  $\alpha$ -substituent types showed a better monotonous trend:  $\alpha$ -dimethyl >  $\alpha$ -ethyl- $\alpha$ -methyl >  $\alpha$ -methyl- $\alpha$ -*n*-propyl >  $\alpha$ -*iso*-propyl- $\alpha$ -methyl ([Figure 3-3b](#)). This trend was consistent with the biodegradability of NP isomer with *Sphingomonas xenophaga* Bayram, a bacteria strain isolated from activated sludge (Gabriel et al., 2008). However, in Gabriel et al. (2008), the isomer selectivity was much more pronounced than that in the current study. For example, only 30.5% of NP<sub>193a</sub> was removed, while this value was 98.8% for NP<sub>36</sub>. Ikunaga et al. (2004) showed that *Sphingobium amiense*, another bacteria strain isolated from activated sludge, also preferentially degraded  $\alpha$ -dimethyl and  $\alpha$ -ethyl- $\alpha$ -methyl isomers (Ikunaga et al., 2004).

However, in the current study, the largest difference was between NP<sub>193a</sub> and NP<sub>38</sub> at 15 °C and the corresponding residues were 11.1% and 0.97%, respectively. The more limited isomer selectivity observed in this study may be attributed to the much more complex and diverse microbial communities in the bioreactor than a single bacteria strain. Hao et al. (2009) considered the biodegradation of a few NP isomers in a sequencing batch reactor and observed that biodegradability followed a trend of NP<sub>36</sub> (75.4%) > NP<sub>111</sub> (42.9%) > NP<sub>170</sub> (40.7%) > NP<sub>194</sub> (36.2%), which was in agreement with this study. In oxic river sediments, alkyl chain length and  $\alpha$ -substituent types also greatly influenced the biodegradation of NP isomers (Lu and Gan, 2014). However, in river sediments, the effect of  $\alpha$ -substituent types appeared to be less monotonous than that in the bioreactor, while an opposite effect was found for the alkyl chain length.

In incubated river sediments, steric effect index and  $I_{Dw}$  (the mean information index for the magnitude of distance) were identified to be the two best molecular descriptors for describing isomer-specific biodegradability. In this study, these two descriptors were also found to provide good predictions for NP residues in the effluent (Figure 3-3c/d), as evident from  $R^2$  values (0.76 and 0.68, respectively). The steric effect index describes the steric hindrance of alkyl chain at the *ipso* position, where the alkyl chain is attached to the benzene ring. Isomers with a larger steric hindrance at the *ipso* position had higher residues in the effluent or lower biodegradability. This finding indicated that the *ipso* position was an important site for NP biodegradation and reactions at this site were likely one of the rate limiting steps. Previous studies suggested that there were three biodegradation pathways for NP isomers: *ipso*-hydroxylation (Corvini et al., 2006;

Gabriel et al., 2008; Kolvenbach and Corvini, 2012), nitrication at *ortho* position of benzene ring (Telscher et al., 2005) and alkyl-chain oxidation (Cirja et al., 2006; Corvini et al., 2006). Bulky  $\alpha$ -substituents may directly hamper the *ipso*-hydroxylation, but have only a limited effect on the nitrication on the benzene ring or alkyl-chain oxidation. Therefore, the strong inhibitive effect of steric hindrance may indicate that *ipso*-hydroxylation was the dominant pathway for NP degradation in the bioreactor. The trend that isomers with higher steric effect index had higher residues further implied that other isomers with even higher steric effect index values, for example, NP<sub>211</sub> (4-[1,1-diethyl-2,2-dimethylpropyl]phenol) and NP<sub>209</sub> (4-[1-ethyl-1-isopropyl-2-methylpropyl]phenol), could be more recalcitrant to biodegradation and should be targeted for evaluation in the future. Hao et al. (2009) evaluated the relationship between biodegradation rates of 4 NP isomers and their molecular connectivity indexes  ${}^2\chi^v$  and  ${}^4\chi^v_{pc}$ ; however, regressions using these indices were less satisfactory in this study.

#### 3.3.4 Adsorption of Nonylphenol Isomers

The separate analysis of NP isomers in the dissolved and solid phases allowed the estimation of adsorption coefficients  $K_d$  for the target isomers. Figure 3-4 shows the derived  $K_d$  values of NP isomers on the sludge under various conditions. In general, NP<sub>38</sub> and NP<sub>65</sub> had the highest  $K_d$  values at  $(1.6 \pm 0.2) \times 10^4$  and  $(1.6 \pm 0.1) \times 10^4$  L/kg, respectively (20 °C), while NP<sub>193a</sub> and NP<sub>193b</sub> had the lowest values at  $(0.95 \pm 0.06) \times 10^4$  and  $(0.98 \pm 0.06) \times 10^4$  L/kg, respectively. The corresponding organic carbon partition coefficient values ( $\log K_{OC}$ ) were  $4.24 \pm 0.04$ ,  $4.23 \pm 0.02$ ,  $4.03 \pm 0.02$  and  $4.02 \pm 0.02$ ,

respectively. Therefore, there were detectable differences in the sorption capacity among some of the NP isomers (one-way ANOVA,  $P < 0.0001$ ). Statistical analysis using all pairwise multiple comparison procedures (Holm-Sidak method) showed that 61 and 23 out of the 153 pairs exhibited statistically significant differences ( $p < 0.05$ ) at 20 °C and 15 °C, respectively. Therefore, for the majority of NP isomers, no difference was observed between isomers in sorption to the solids. This observation was consistent with (Isobe et al., 2001), where the profiles of 10 NP peaks were found to be identical between the dissolved and particulate phases for the primary/secondary effluents and river water. Gundersen et al. (2001) calculated the log  $K_{ow}$  values for several NP isomers using the Broto's method with ChemDraw Pro (Version 4.5, Cambridge Software, Cambridge, MA) and the values ranged from 4.78 to 5.72. However, the calculation method gave a standard error of 0.4 log unit (Consonni and Todeschini, 2000), which would prevent its use for discerning isomer specific differences.

### 3.4 Environmental Implications

Results from this study showed that wastewater treatment processes simulated in the laboratory-scale CAS bioreactor led to significant changes in the profile of NP isomers in the effluent and sludge. Isomers with less bulky  $\alpha$ -substituents were more effectively removed while isomers with bulky  $\alpha$ -substituents were more recalcitrant to biodegradation in the bioreactor and became relatively enriched in both dissolved and particulate phases of effluent. Regression analysis validated that steric effect index may be used to predict the relative biodegradability of NP isomers. Low temperatures would

further enhance the enrichment of recalcitrant isomers that are also of greater estrogenicity. Given that wastewater treatment plants are the primary source for NP entering the environment, the isomer preferential enrichment implies that some NP isomers are introduced into the environment at levels higher than that indicated by non-discriminatory analysis of NP. Therefore, isomeric selectivity should be taken into consideration to better predict the occurrence, fate, and ecological risks of NP.



## References

- Chang, B. V., Chiang, F. and Yuan, S. Y. (2005). Biodegradation of nonylphenol in sewage sludge. *Chemosphere* **60**(11): 1652-1659.
- Cirja, M., Zuehlke, S., Ivashechkin, P., Schaeffer, A. and Corvini, P. F. X. (2006). Fate of a C-14-labeled nonylphenol isomer in a laboratory-scale membrane bioreactor. *Environ. Sci. Technol.* **40**(19): 6131-6136.
- Consonni, V. and Todeschini, R. (2000). *Handbook of molecular descriptors*. Weinheim ; New York, Wiley-VCH.
- Corvini, P. F. X., Schaffer, A. and Schlosser, D. (2006). Microbial degradation of nonylphenol and other alkylphenols -- our evolving view. *Appl. Microbiol. Biotechnol.* **72**(2): 223-243.
- Eganhouse, R. P., Pontolillo, J., Gaines, R. B., Frysinger, G. S., Gabriel, F. L. P., Kohler, H.-P. E., Giger, W. and Barber, L. B. (2009). Isomer-specific determination of 4-nonylphenols using comprehensive two-dimensional gas chromatography/time-of-flight mass spectrometry. *Environ. Sci. Technol.* **43**(24): 9306-9313.
- Gabriel, F. L. P., Routledge, E. J., Heidlberger, A., Rentsch, D., Guenther, K., Giger, W., Sumpter, J. P. and Kohler, H. P. E. (2008). Isomer-specific degradation and endocrine disrupting activity of nonylphenols. *Environ. Sci. Technol.* **42**(17): 6399-6408.
- Gori, R., Cammilli, L., Petrovic, M., Gonzalez, S., Barcelo, D., Lubello, C. and Malpei, F. (2010). Fate of surfactants in membrane bioreactors and conventional activated sludge plants. *Environ. Sci. Technol.* **44**(21): 8223-8229.

- Guenther, K., Kleist, E. and Thiele, B. (2006). Estrogen-active nonylphenols from an isomer-specific viewpoint: A systematic numbering system and future trends. *Anal. Bioanal. Chem.* **384**(2): 542-546.
- Gundersen, J. L. (2001). Separation of isomers of nonylphenol and select nonylphenol polyethoxylates by high-performance liquid chromatography on a graphitic carbon column. *J. Chromatogr. A* **914**(1-2): 161-166.
- Hao, R. X., Li, J. B., Zhou, Y. W., Cheng, S. Y. and Zhang, Y. (2009). Structure-biodegradability relationship of nonylphenol isomers during biological wastewater treatment process. *Chemosphere* **75**(8): 987-994.
- Ieda, T., Horii, Y., Petrick, G., Yamashita, N., Ochiai, N. and Kannan, K. (2005). Analysis of nonylphenol isomers in a technical mixture and in water by comprehensive two-dimensional gas chromatography-mass spectrometry. *Environ. Sci. Technol.* **39**(18): 7202-7207.
- Ikunaga, Y., Miyakawa, S. I., Hasegawa, M., Kasahara, Y., Kodama, O. and Ohta, H. (2004). Degradation profiles of branched nonylphenol isomers by *Sphingobium amiense* and *Sphingomonas cloacae*. *Soil Sci. Plant Nutr.* **50**(6): 871-875.
- Isobe, T., Nishiyama, H., Nakashima, A. and Takada, H. (2001). Distribution and behavior of nonylphenol, octylphenol, and nonylphenol monoethoxylate in Tokyo metropolitan area: Their association with aquatic particles and sedimentary distributions. *Environ. Sci. Technol.* **35**(6): 1041-1049.
- Koh, Y. K. K., Chiu, T. Y., Boobis, A. R., Scrimshaw, M. D., Bagnall, J. P., Soares, A., Pollard, S., Cartmell, E. and Lester, J. N. (2009). Influence of operating

- parameters on the biodegradation of steroid estrogens and nonylphenolic compounds during biological wastewater treatment processes. *Environ. Sci. Technol.* **43**(17): 6646-6654.
- Kolvenbach, B. A. and Corvini, P. F. X. (2012). The degradation of alkylphenols by *Sphingomonas sp* strain TTNP3-a review on seven years of research. *New Biotechnol.* **30**(1): 88-95.
- Lu, Z. J. and Gan, J. (2014). Isomer-specific biodegradation of nonylphenol in river sediments and structure-biodegradability relationship. *Environ. Sci. Technol.* **48**(2): 1008-1014.
- Makino, M., Uchiyama, T., Saito, H., Ogawa, S., Iida, T., Katase, T. and Fujimoto, Y. (2008). Separation, synthesis and estrogenic activity of 4-nonylphenols: Two sets of new diastereomeric isomers in a commercial mixture. *Chemosphere* **73**(8): 1188-1193.
- Maruya, K. A., Vidal-Dorsch, D. E., Bay, S. M., Kwon, J. W., Xia, K. and Armbrust, K. L. (2012). Organic contaminants of emerging concern in sediments and flatfish collected near outfalls discharging treated wastewater effluent to the Southern California Bight. *Environ. Toxicol. Chem.* **31**(12): 2683-2688.
- Morgan-Sagasturne, F. and Allen, D. G. (2004). The assessment of different operating strategies for minimising activated sludge deflocculation under temperature transient conditions. *Water Sci. Technol.* **50**(3): 67-77.

- Shan, J., Jiang, B. Q., Yu, B., Li, C. L., Sun, Y. Y., Guo, H. Y., Wu, J. C., Klumpp, E., Schaffer, A. and Ji, R. (2011). Isomer-specific degradation of branched and linear 4-nonylphenol isomers in an oxic soil. *Environ. Sci. Technol.* **45**(19): 8283-8289.
- Soares, A., Guieysse, B., Jefferson, B., Cartmell, E. and Lester, J. N. (2008). Nonylphenol in the environment: A critical review on occurrence, fate, toxicity and treatment in wastewaters. *Environ. Int.* **34**(7): 1033-1049.
- Soares, A., Murto, M., Guieysse, B. and Mattiasson, B. (2006). Biodegradation of nonylphenol in a continuous bioreactor at low temperatures and effects on the microbial population. *Appl. Microbiol. Biotechnol.* **69**(5): 597-606.
- Tanghe, T., Devriese, G. and Verstraete, W. (1998). Nonylphenol degradation in lab scale activated sludge units is temperature dependent. *Water Res.* **32**(10): 2889-2896.
- Telscher, M. J. H., Schuller, U., Schmidt, B. and Schäffer, A. (2005). Occurrence of a nitro metabolite of a defined nonylphenolisomer in soil/sewage sludge mixtures. *Environ. Sci. Technol.* **39**(20): 7896-7900.
- Uchiyama, T., Makino, M., Saito, H., Katase, T. and Fujimoto, Y. (2008). Syntheses and estrogenic activity of 4-nonylphenol isomers. *Chemosphere* **73**(1): S60-S65.
- USEPA. (2006). "Non-confidential 2006 IUR company/chemical records." Retrieved March 1, 2014, from <http://cfpub.epa.gov/iursearch/index.cfm>.
- Venkatesan, A. K. and Halden, R. U. (2013). National inventory of alkylphenol ethoxylate compounds in U.S. sewage sludges and chemical fate in outdoor soil mesocosms. *Environ. Pollut.* **174**(0): 189-193.

Vidal-Dorsch, D. E., Bay, S. M., Maruya, K., Snyder, S. A., Trenholm, R. A. and Vanderford, B. J. (2012). Contaminants of emerging concern in municipal wastewater effluents and marine receiving water. *Environ. Toxicol. Chem.* **31**(12): 2674-2682.

Ying, G. G., Williams, B. and Kookana, R. (2002). Environmental fate of alkylphenols and alkylphenol ethoxylates - a review. *Environ. Int.* **28**(3): 215-226.

## Figures

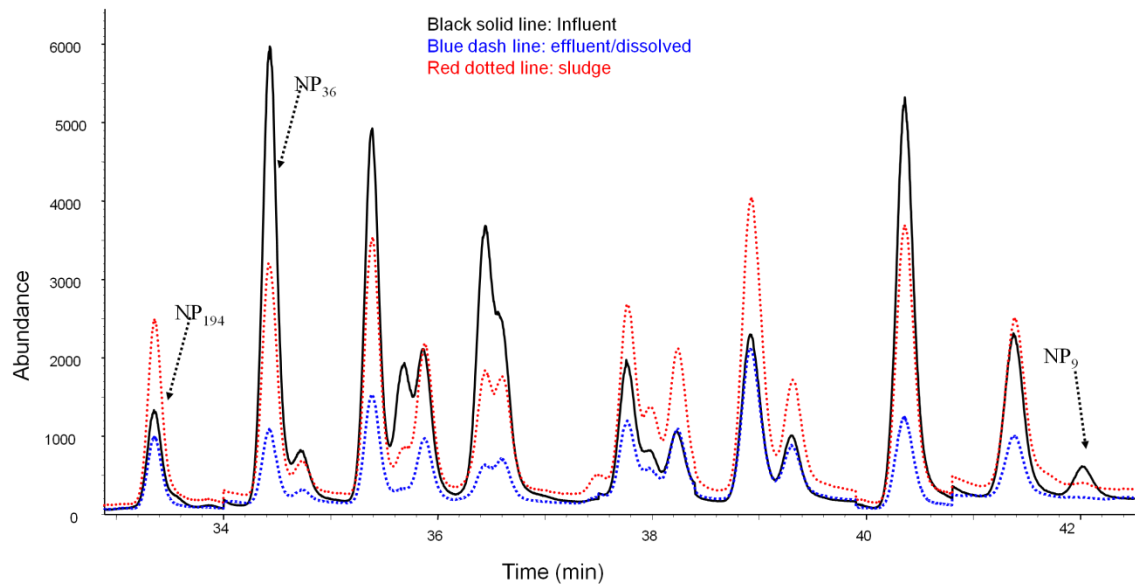


**Figure 3-1** Total ion chromatography of nonylphenol in influent, dissolved phase of effluent and sludge

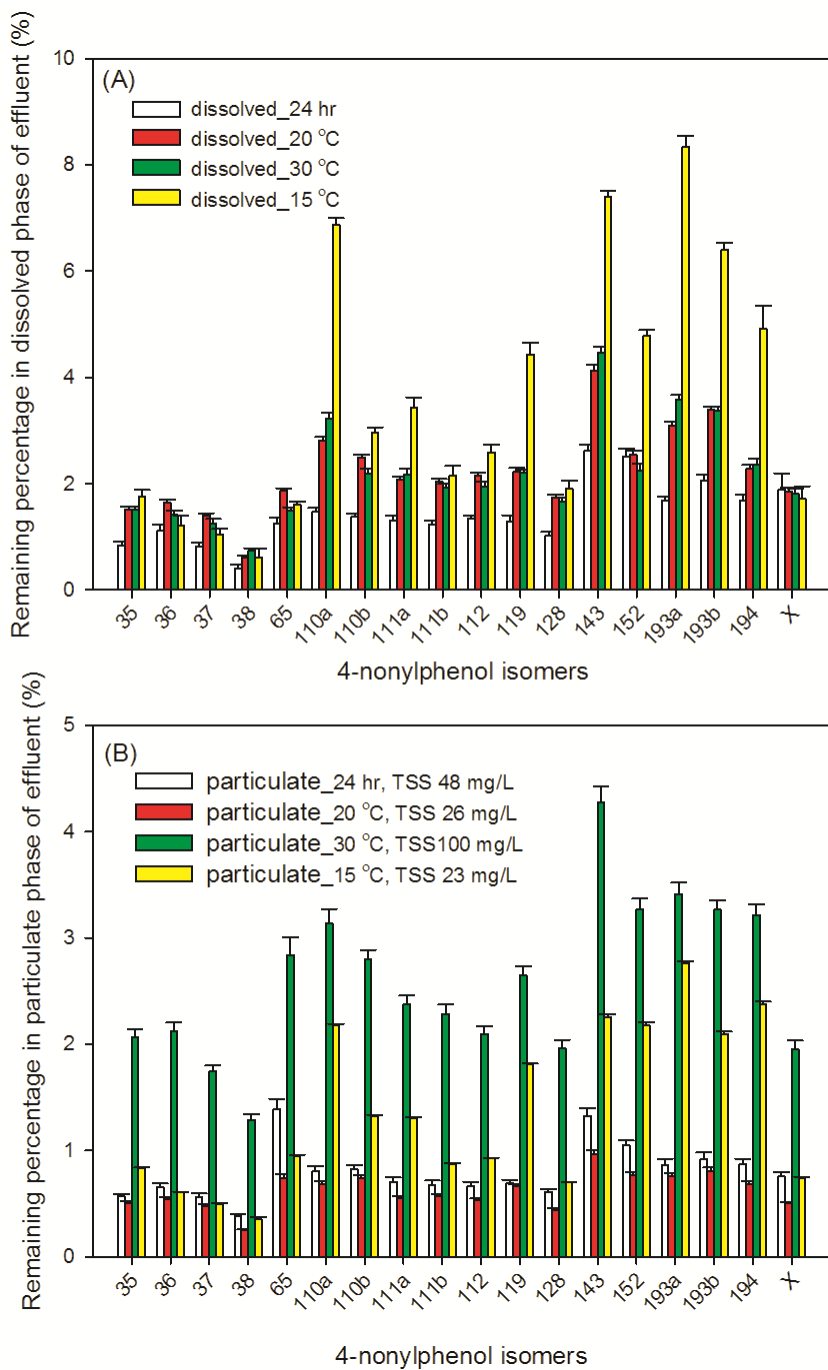


**Figure 3-2** Effects of hydraulic retention time and temperature on the residue of NP isomers in the effluent. (A) dissolved phase and (B) particulate phase.

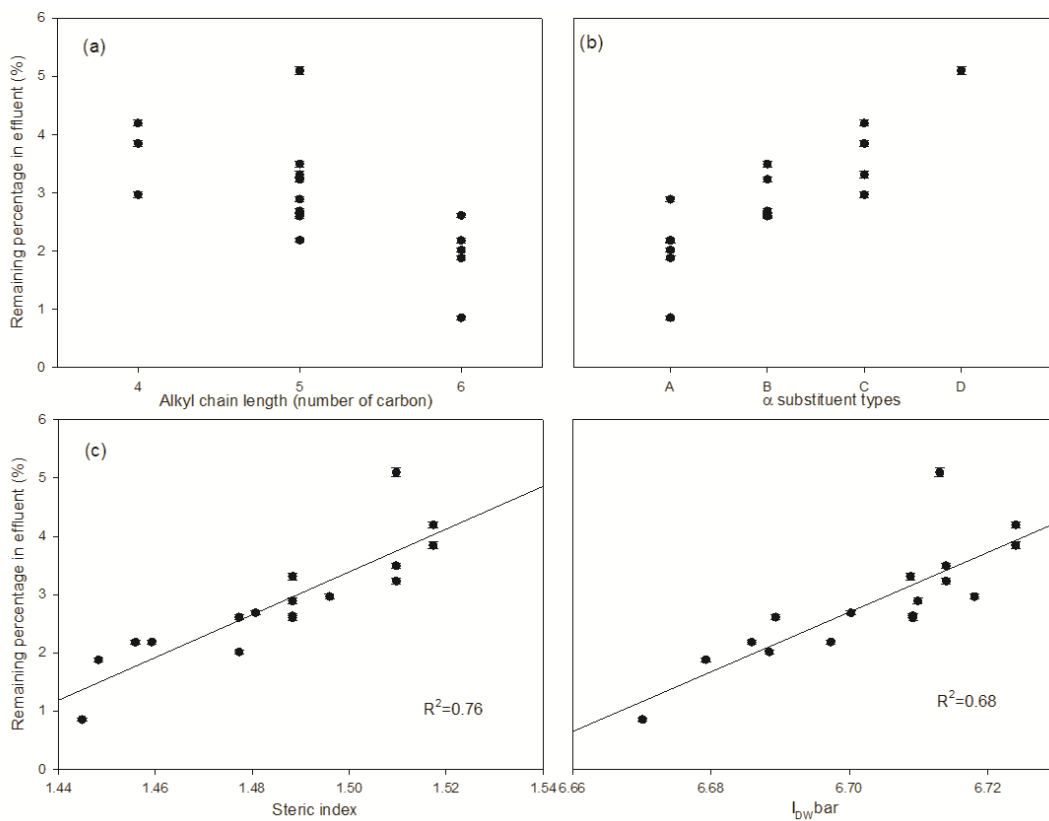


**Figure 3-3** Quantitative relationships between isomer structures and residues in the effluent for nonylphenol. (a) Alkyl chain length; (b)  $\alpha$ -substituent types A  $\alpha$ -dimethyl, B  $\alpha$ -ethyl-  $\alpha$ -methyl C  $\alpha$ -methyl-  $\alpha$ -*n*-propyl D  $\alpha$ -*iso*-propyl-  $\alpha$ -methyl; (c) Steric index, and (d)  $I_{DWbar}$  ( $n=3$ , error bar stands for the standard deviation)



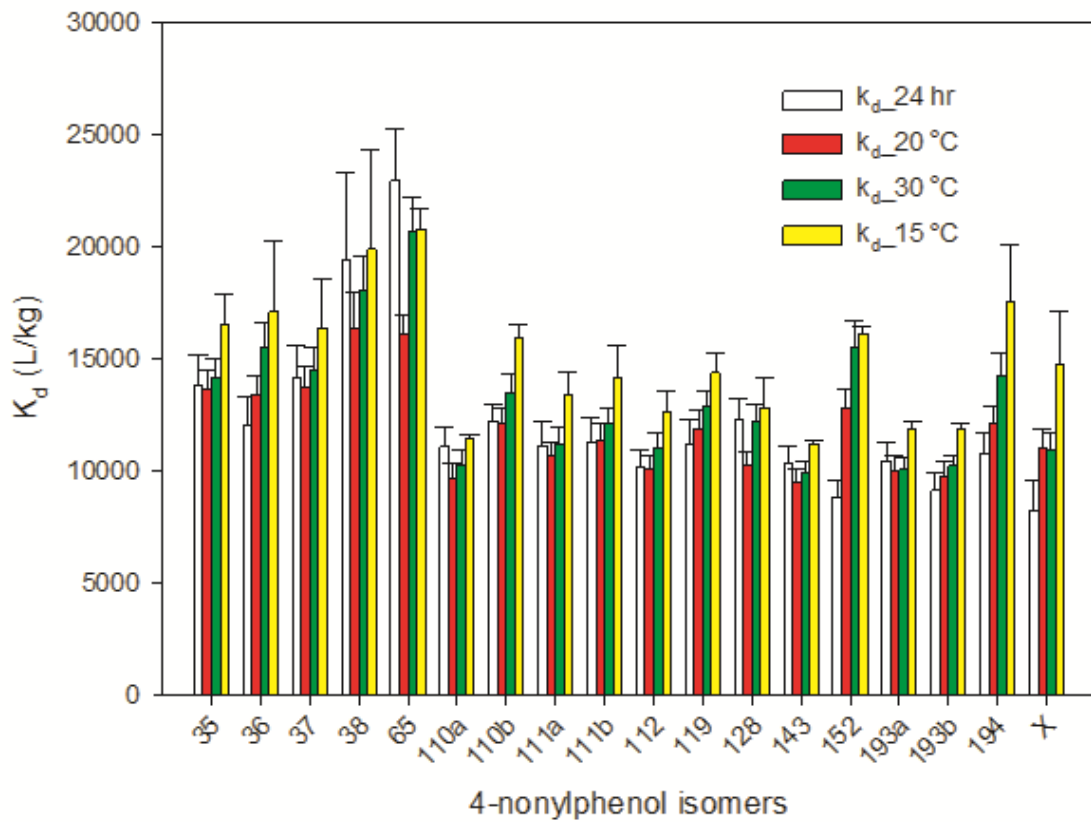


**Figure 3-4** Adsorption coefficient ( $K_d$ ) of nonylphenol isomers on sludge (n=3, error bar stands for the standard deviation)

## Chapter 4 Isomer-Specific Oxidation of Nonylphenol by Potassium Permanganate

### 4.1 Introduction

Nonylphenol (NP) is the metabolite of the heavily used nonylphenol ethoxylate surfactants (Soares et al., 2008; Ying et al., 2002). Due to the wide use of nonylphenol ethoxylates in agricultural, industrial and domestic products, NP is frequently detected in surface water, effluents of wastewater treatment plants and even in drinking water (Fan et al., 2013; Ying et al., 2002). For example, levels up to 48  $\mu\text{g/L}$  have been reported in water from Hudson River Estuary, New York (Dachs et al., 1999). In a recent study, NP was found in 55 out of 62 drinking water samples from 31 major cities across China with a median concentration of 27 ng/L, whereas and in all 62 source water samples with a median concentration of 123 ng/L (Fan et al., 2013). Nonylphenol is known as a potent endocrine disruptor and the potency of NP relative to 17 $\beta$ -estradiol ranges from 0.001 to 0.05 with arithmetic mean of 0.023 in *in vivo* bioassays (Soares et al., 2008).

Nonylphenol is commonly treated as a single compound in the evaluation of its environmental occurrence, fate and transport, treatment removal and toxicity (Jiang et al., 2012; Soares et al., 2008; Ying et al., 2002). However, technical nonylphenol (tNP) is in fact a mixture of more than 100 isomers (Eganhouse et al., 2009; Ieda et al., 2005). A few recent studies showed that NP isomers have different estrogenicity or biodegradability in the environment (Eganhouse et al., 2009; Gabriel et al., 2008; Kim et al., 2005; Shan et al., 2011). For example, Gabriel et al. (Gabriel et al., 2008) reported that if the average estrogenicity of tNP in the yeast estrogen assays was set to be 1, the value for NP<sub>93</sub> was

1.87 while the value for NP<sub>112</sub> was only 0.60. Biodegradation of NP by *Sphingobium xenophagum* Bayram was also isomer specific, with 99.7% of NP<sub>128</sub> degraded after 9 d while only 31% of NP<sub>193</sub> dissipated under the same conditions (Gabriel et al., 2008). The isomer-specific biodegradation was expected to result in the selective enrichment of recalcitrant and possibly highly estrogenic NP isomers in the environment (Gabriel et al., 2008). This prediction was corroborated by the profile of NP isomers found in river water and sea water (Horii et al., 2004; Kim et al., 2005). Such isomer selectivity arises from differences in physicochemical properties due to changes in spatial hindrance and electron distribution among the isomers (Gabriel et al., 2008), and is thus an intrinsic property of NP that has not been adequately understood.

Advanced oxidation with potassium permanganate is a promising process for removing NP (Abe et al., 2001; Jiang et al., 2012) and also other micropollutants (Guan et al., 2010). A recent study showed that KMnO<sub>4</sub> was more effective at removing endocrine disrupting chemicals, including 4-n-NP (i.e., NP<sub>1</sub>), than ozone, ferrate or chlorine in wastewater (Jiang et al., 2012). At pH 7, 80% of NP (1.0 mg/L) was degraded in 120 min by 3.2 mg/L KMnO<sub>4</sub> (Abe et al., 2001). When KMnO<sub>4</sub> concentration was increased to 16 or 32 mg/L, 100% NP removal was achieved in 100 min. In another study, with 9.48 mg/L of KMnO<sub>4</sub> at pH 7, the half-life of 4-n-NP (33 µg/L) was only 3.0 min (Jiang et al., 2012). However, to date no study has considered the isomer specificity in the chemical oxidation of NP with permanganate or any other oxidants (Bertanza et al., 2011; Zhang et al., 2008).

The objectives of this study were to investigate the oxidation of tNP by  $\text{KMnO}_4$ , to obtain isomer-specific oxidation rates and to understand the influence of side chain length and  $\alpha$ -substituents. The oxidation kinetics of each isomer was measured under different  $\text{KMnO}_4$  concentrations and pH conditions. Statistics were used to analyze the relationship between the reaction rate and structural properties including the side chain length and types of  $\alpha$ -substituents.

## 4.2 Materials and Methods

### 4.2.1 Chemicals

Technical NP (tNP), a mixture of NP isomers with branched side chains (CAS No. 84852-15-3) was purchased from TCI America (Portland, OR). Isomers  $\text{NP}_{36}$ ,  $\text{NP}_{37}$ ,  $\text{NP}_{119}$ ,  $\text{NP}_{128}$  and  $\text{NP}_{194}$  (10 mg/g in hexane; >95% purity) were obtained from ChemCollect GmbH (Reimscheid, Germany). Isomers  $\text{NP}_{38}$  (48.2 mg/g),  $\text{NP}_{65}$  (59.5 mg/g),  $\text{NP}_{111}$  (49.5 mg/g) and  $\text{NP}_{112}$  (48.52 mg/g) in methanol were kindly provided by Prof. Rong Ji at Nanjing University, China. Potassium permanganate ( $\text{KMnO}_4$ , 99+%), 4-*tert*-octylphenol (>97%), sodium phosphate dibasic ( $\text{Na}_2\text{HPO}_4$ , 99+%), sodium tetraborate decahydrate ( $\text{Na}_2\text{B}_4\text{O}_7 \cdot 10\text{H}_2\text{O}$ , > 99.5%) and L-ascorbic acid (>99.0%) were from Sigma-Aldrich (St. Louis, MO). Sodium acetate trihydrate (99.0 -101.0%) and gas chromatography (GC) grade hexane were from Fisher Scientific (Fair Lawn, NJ). Reagent water (18.3 M $\Omega$ -cm resistivity) was prepared using a Barnstead Nanopure water system (Barnstead, Dubuque, IA). The stock solution of 100 mg/L tNP in methanol was stored at -20 °C before use. The stock solution of 1000 mg/L  $\text{KMnO}_4$  was prepared with

boiled reagent water and stored at 4 °C. The  $\text{KMnO}_4$  stock solution was used within a month after preparation and before each use, its concentration was determined on a UV-Vis spectrometer at 525 nm after dilution to 20 mg/L. The results showed there was no change in  $\text{KMnO}_4$  under these conditions.

#### 4.2.2 Reaction Setup with Reagent Water

Batch experiments were conducted in 125-mL wide-mouth amber borosilicate glass bottles with Teflon-faced caps at room temperature ( $22 \pm 0.5$  °C). Reaction solutions prepared with reagent water were maintained at the desired pH using 0.01 mol/L of the following pH buffers: pH 5, sodium acetate; pH 7, sodium phosphate dibasic; pH 9, sodium tetraborate decahydrate. The reaction solution (50 mL) with 50  $\mu\text{g/L}$  tNP was constantly stirred at 480 rpm. The reaction was initiated by adding  $\text{KMnO}_4$  to arrive at the initial concentration of 1, 2 or 10 mg/L. At selected time intervals (0, 2, 4, 6, 8, 10, 15, 20, 30, 40 min), 0.5 mL of 200 g/L L-ascorbic acid was added to quench the reaction. A control group was included with 50  $\mu\text{g/L}$  tNP at pH 7 but without  $\text{KMnO}_4$ . All reactions were carried out in 4 replicates. Additional groups at pH 5, 7 and 9 with 50  $\mu\text{g/L}$  tNP and 10 mg/L or 1 mg/L  $\text{KMnO}_4$  were used to monitor the change in temperature, pH or  $\text{KMnO}_4$  concentration during the reaction. During the 40 min of reaction, there was no detectable change in pH or  $\text{KMnO}_4$  concentration, while the temperature increased by 2.0 °C, likely due to the constant stirring.

#### 4.2.3 Experiments with Reclaimed Water

Reclaimed water (COD 21 mg/L,  $\text{NO}_3^-$ -N 3 mg/L,  $\text{NH}_3$ -N 0.062 mg/L, o-phosphate-P 0.06 mg/L) was collected from Michelson Water Reclamation Plant, Irvine, CA and filtered with 0.7  $\mu\text{m}$  glass fiber membranes. The reaction was initiated by adding 0.5 mL of 1000 mg/L  $\text{KMnO}_4$  to 50 mL filtered reclaimed water containing 50  $\mu\text{g/L}$  tNP maintained at pH 7 using 0.01 mol/L of phosphate buffer. The other conditions were the same as above. The detailed reaction conditions of the batch experiments with reagent and reclaimed water are listed in [Table 4-1](#).

#### 4.2.4 Chemical Analysis

The quenched reaction solutions were extracted twice with hexane (15 and 10 mL, respectively) by liquid-liquid extraction. The combined extracts were condensed to about 1 mL under a gentle nitrogen stream and then 10  $\mu\text{L}$  of 100 mg/L 4-*tert* octylphenol was added as the internal standard. The samples were analyzed on an Agilent 6890 GC coupled with 5973 mass spectrometer (Agilent Technologies, Santa Clara, CA). Samples (2  $\mu\text{L}$ ) were introduced into the inlet at 250  $^\circ\text{C}$  and the separation was achieved on a DB-5MS Ultra Inert capillary column (60 m  $\times$  0.25 mm  $\times$  0.25  $\mu\text{m}$ , Agilent, Wilmington, DE). The carrier gas was helium (99.999%) and the flow rate was set at 1.0 mL/min. The column temperature was programmed initially at 80  $^\circ\text{C}$  for 0 min, then ramped to 160  $^\circ\text{C}$  at 10  $^\circ\text{C}/\text{min}$  and held for 42 min, and further ramped to 300  $^\circ\text{C}$  at 30  $^\circ\text{C}/\text{min}$  and held for 3 min. The mass spectrometer was operated in the electron ionization – selective ion monitoring (SIM) mode at 70 eV. The ion with  $m/z$  135 was used for the quantification

of the internal standard and ions with  $m/z$  121, 135, 149, 163, 177 and 191 were used for the quantification of different NP isomers. For the identification of NP isomers, both a full scan mode ( $m/z$  40 to  $m/z$  800) and the SIM mode ( $m/z$  107, 121, 135, 149, 163, 177, 191 and 220) were applied. The recovery of NP isomers was  $97 \pm 3\%$ .

#### 4.2.5 Data Analysis

All statistical analyses, including linear regression, one-way ANOVA and two-way ANOVA, were carried out using SigmaPlot 11 (San Jose, CA) at the significant level of 0.05. The Holm-Sidak method was used in the pairwise multiple comparison procedure in the one-way and two-way ANOVA.

### 4.3 Results and Discussion

#### 4.3.1 Separation and Identification of Nonylphenol Isomers

A total of 19 isomers, including 6 diastereoisomers (Table 4-2, Table S 4-1), were separated and identified under the used analytical conditions by comparing the retention time, peak intensity and fragmentation patterns against the available authentic NP isomer standards and/or chromatographic and mass spectrometric characteristics of NP isomers in published studies (Gabriel et al., 2008; Thiele et al., 2004). All identifications agreed with the NP isomer fragmentation mechanism in Thiele et al. (Thiele et al., 2004). In Table 4-1 and Table S 4-1, an NP isomer labeled as NP<sub>x</sub> was not fully identified. This isomer had the dominant fragment at  $m/z$  135 and also a few minor fragments at  $m/z$  107 (9%), 121 (5%) and 220 (3%) but an absence of fragments at  $m/z$  149, 163, 177 and 191.

According to the fragmentation mechanism (Thiele et al., 2004), this isomer should have two methyl groups at the  $\alpha$  position and no dimethyl group at the other positions or ethyl group or propyl group. Therefore, the isomer NP<sub>x</sub> may be NP<sub>92</sub>, NP<sub>93</sub> or NP<sub>95</sub> and its systematic name may be 4-[1,1,2,3-tetramethylpentyl]phenol, 4-[1,1,2,4-tetramethylpentyl]phenol or 4-[1,1,3,4-tetramethylpentyl]phenol.

According to their  $\alpha$  substituents, the 19 identified isomers are grouped in 4 groups: Group 1 with two methyl substituents; Group 2 with one methyl and one ethyl substituents; Group 3 with one methyl and one propyl substituents; and Group 4 with one methyl and one *iso*-propyl substituent. A similar number of NP isomers were separated in Gabriel et al. (2008); however, more authentic NP isomer standards were used in this study to confirm the identification. With more sophisticated instruments, for example, two dimensional GC, a better separation may be achieved (Vallejo et al., 2011).

#### 4.3.2 Reaction Kinetics of NP Isomers

The oxidation of NP isomers by KMnO<sub>4</sub> was consistently rapid (Table 2-2 and Figure 4-1). For example, at pH 7 with 10 mg/L KMnO<sub>4</sub>, about 90% of 50  $\mu$ g/L tNP was removed (Figure 4-1) while there was no change in the KMnO<sub>4</sub>-free control. The oxidation reaction was pseudo-first order as shown in Figure 4-1a for NP<sub>119</sub> and NP<sub>194</sub> at pH 7 with 10 mg/L KMnO<sub>4</sub>, with the first-order rate constants of  $0.1098 \pm 0.0016$  and  $0.1478 \pm 0.0026$  min<sup>-1</sup>, or half-lives of 4.8 and 6.3 min, respectively. The high efficiency and pseudo-first order behavior agreed with previous studies (Abe et al., 2001; Jiang et al., 2012). For example, Jiang et al. (2012) showed that the oxidation of 0.15  $\mu$ mol/L 4-n-NP (i.e., 33



$\mu\text{g/L NP}_1$ ) with  $\text{KMnO}_4$  was pseudo-first order at pH 7; the second-order rate constant was estimated to be  $63.9 \text{ L mol}^{-1}\text{s}^{-1}$ . Using the reported rate constants, the half-life of 4-n-NP in  $60 \mu\text{mol/L KMnO}_4$  solution (or  $9.48 \text{ mg/L}$ ) should be about 3 min, which agrees well with that observed in this study (Table 4-2).

The oxidation reaction was obviously isomer specific (Table 4-2 and Figure 4-1). With higher  $\text{KMnO}_4$  concentrations or at higher pH, the isomeric difference was much more significant, probably due to larger pseudo first order rate constants. To clearly identify the difference among isomers, a one-way ANOVA with Holm-Sidak pairwise multiple comparisons was carried out to determine if the differences were statistically significant (Table 4-3). For example, at pH 7 with  $10 \text{ mg/L KMnO}_4$ , the rate constant of  $\text{NP}_{119}$  ( $0.1478 \pm 0.0029 \text{ min}^{-1}$ ) was significantly different from that of  $\text{NP}_{194}$  ( $0.1098 \pm 0.0016 \text{ min}^{-1}$ ). The rate constant of  $\text{NP}_{38}$  ( $0.1232 \pm 0.0017 \text{ min}^{-1}$ ) was also significantly different from that of  $\text{NP}_{152}$  ( $0.1130 \pm 0.0015 \text{ min}^{-1}$ ) (Table 4-3). However, the isomeric differences in this study were generally smaller than those observed in biodegradation (Gabriel et al., 2008; Shan et al., 2011). For instance, in an oxic soil, the biodegradation half-life was 10.3 d for  $\text{NP}_{111}$ , 8.4 d for  $\text{NP}_{112}$ , 5.8 d for  $\text{NP}_{65}$  and 2.1 d for  $\text{NP}_{38}$  (Shan et al., 2011). In Gabriel et al. (2008), isomeric biodegradation was measured only by the percentages degraded after 9 d of incubation with *Sphingobium xenophagum* Bayram. Over 90% removal was achieved for more than half of the NP isomers while only about 30% degradation was found for  $\text{NP}_{193\text{a/b}}$ . The relative differences in isomer selectivity are likely due to the fact that biotransformation catalyzed by specific enzymes affords more selectivity than chemical reactions. The biodegradation of NP isomers was initiated by

*ipso*-hydroxylation process in which a hydroxyl group was attached at the *para* position (Gabriel et al., 2007; Kolvenbach and Corvini, 2012). The corresponding enzyme NP *ipso*-hydroxylase was a member of the flavin monooxygenase enzyme family (Porter and Hay, 2007). The bulky  $\alpha$ -substituents could hinder the *ipso*-hydroxylation sterically and thus resulted in isomeric biodegradation of NP (Gabriel et al., 2008).

Some NP isomers have two chiral carbon centers, and these isomers may have four stereoisomers. After the non-chiral selective GC separation, these four stereoisomers appeared as two peaks in diastereomers, e.g., NP<sub>111a/b</sub> and NP<sub>193a/b</sub>. In this study, two diastereomers are noted by alphabets a and b according their retention times. Unlike the enantiomers, diastereomers are not mirror images of each other; therefore, they may have different physical properties and chemical reactivity. However, in this study, the diastereomers did not show any difference in their oxidation by KMnO<sub>4</sub> in most cases. For example, at pH 7 with 10 mg/L of KMnO<sub>4</sub>, the rate constants for NP<sub>110a</sub> and NP<sub>110b</sub> were  $0.1174 \pm 0.0014$  and  $0.1182 \pm 0.0013$  min<sup>-1</sup>, respectively. The only exception was the diastereomers NP<sub>193a</sub> and NP<sub>193b</sub> at pH 7 with 10 mg/L of KMnO<sub>4</sub>, where the rate constants were  $0.1177 \pm 0.0016$  and  $0.1224 \pm 0.0016$  min<sup>-1</sup>, respectively. Limited differences between diastereomers were also observed for biodegradation (Gabriel et al., 2008). For instance, after 9 d of incubation with *Sphingobium xenophagum* Bayram, the removal rates for NP<sub>111a</sub> and NP<sub>111b</sub> were 94.0 and 90.4%, respectively (Gabriel et al., 2008).

#### 4.3.3 Effect of Side Chain Length and Types of $\alpha$ -Substituents

Gabriel et al. (2008) reported that  $\alpha$ -substitution was the most important factor controlling the biodegradation rate of NP isomers with *Sphingobium xenophagum* Bayram. This was also confirmed by the study on the degradation of four NP isomers in an oxic soil (Shan et al., 2011). Gabriel et al. (2008) also showed that a suitable main chain length (4-6 carbon atoms) was important for estrogenicity of NP isomers. Moreover, in previous studies, the types of substituents were found to greatly affect the oxidation rates of other substituted phenols. For instance, the oxidation of mono-substituted phenols with singlet oxygen followed the order of 4-(*tert*-butyl) phenol > 4-methylphenol > phenol (Tratnyek and Holgne, 1991) and the oxidation with manganese dioxides followed the order 4-methyl phenol > 4-ethylphenol > phenol (Stone, 1987). Stone concluded that electron donating substituents enhanced the reaction of substituted phenols with manganese dioxides while the electron withdrawing groups were inhibitory (Stone, 1987). Therefore, we hypothesized that  $\alpha$ -substitution and side chain length were two most important factors in determining the oxidation rate of NP isomers.

To test this hypothesis, two-way ANOVA was performed using  $\alpha$ -substitution type and side chain length as two factors (Table 4-2). The results showed that the side chain length did not have a significant influence on the reaction kinetics ( $p = 0.68$ ). However, the effect of  $\alpha$ -substituents was found to be statistically significant ( $p = 0.005$ ). The pairwise multiple comparisons also showed that Group 1 isomers (with dimethyl substitution) were significantly different from Group 2 (with methylethyl substitution) or Group 3

(with methylpropyl substitution), while there was no significant difference among the other groups.

As the variation within a group may mask the variation between groups, comparisons were further made for isomers within the same group and between groups (Table 4-3). For Group 1 isomers, there were large variations within the group and in many cases the isomers in Group 1 differed significantly from each other. In addition, all Group 1 isomers showed significant difference from isomers in Group 2, 3 or 4 with a few exceptions, i.e., NP<sub>38</sub>, NP<sub>X</sub> and NP<sub>9</sub> had no significant difference from NP<sub>193b</sub>. Therefore, Group 1 isomers generally displayed significant differences from all other groups, although the two-way ANOVA showed no significant difference between Group 1 and Group 4 isomers due to large variations within Group 1. Group 2 isomers had some variations within the group and in some cases they had no significant differences from isomers in Group 3 or 4. Group 3 isomers also had some variations within the group and some isomers had significant differences from the isomers in Group 4. Therefore, the overall conclusion was that Group 1 isomers consistently showed differences from isomers in the other groups and the differences of isomers among the other groups were less consistent. That is, with respect to  $\alpha$ -substitution, the reactivity of NP isomers toward KMnO<sub>4</sub> followed the order of  $\alpha$ -dimethyl >  $\alpha$ -ethylmethyl  $\approx$   $\alpha$ -methylpropyl  $\approx$   $\alpha$ -isopropylmethyl (Figure 4-1).

The substituent effects in this study may originate from inductive effects and /or steric hindrance. Previous studies showed that oxidation rates of phenols were greatly affected

by the inductive capacity of substituents and the effect may be described by the Hammett equation (Hansch et al., 1991; Khansole et al., 2010; Stone, 1987) depicting that electron donating groups increase the reaction while the electron withdrawing groups decrease the reaction. Therefore, the electron donating capacities of alky substituents may have influenced the oxidation rate of NP. The well recognized Hammett's constants for *para*-methyl, ethyl, *iso*-propyl, *n*-propyl are -0.17, -0.15, -0.15 and -0.13, respectively (Hansch et al., 1991). Therefore, the *para*-methyl substitution may increase the reaction as compared to the other substitutions. However, in this study, the differences of substituents were at the  $\alpha$  position instead of the *para* position and the inductive effects decreased with increasing distance. For example, the Hammett's constants for *tert*-butyl ( $C(CH_3)_3$ ) and triethylmethyl ( $C(C_2H_5)_3$ ) are both -0.20 (Hansch et al., 1991). However, the NP isomers with  $\alpha$ -dimethyl substituent had the highest reactivity, indicating that its inductive effect was still greater than the others. The steric hindrance in this study might be negligible since the phenoxy oxygen was bound with manganese (VII) atom in the complex and the substituents were far away (Khansole et al., 2010). In comparison, during biodegradation, the *ipso*-hydroxylation happened at the *para* position, and thus the steric hindrance was likely more important (Gabriel et al., 2008). The oxidation rate of phenols by permanganate under both acidic and alkaline conditions was found to be limited by the electron transfer from the phenol/phenolate anion to phenoxy radical (Copolovici and Baldea, 2007; Lee and Sebastian, 1981). Therefore, another parameter to describe the reactivity of organics could be the oxidation/ionization potential (Evans, 2008). However, the measured values for oxidation and ionization potentials of NP

isomers are not available in the literature, preventing a further elucidation of the potential significance of this mechanism.

#### 4.3.4 Effect of $\text{KMnO}_4$ Concentration, pH and Matrix

The reaction rate consistently increased with increasing concentrations of  $\text{KMnO}_4$  (Table 4-2 and Figure 4-2). For example, the increase in  $\text{KMnO}_4$  concentration from 2 to 10 mg/L at pH 7 resulted in an increase in the first-order rate constant of NP<sub>119</sub> from  $0.0614 \pm 0.0024$  to  $0.1478 \pm 0.0029 \text{ min}^{-1}$ . When the  $\text{KMnO}_4$  concentration was increased 5 fold, the reaction rate constant generally increased by a factor of 2.1-2.6 (mean value 2.23) (Figure 4-2). If the reaction order with respect to  $\text{KMnO}_4$  is 0.5, the ratio should be 2.236. No significant differences were found between the measured value for each NP isomer and 2.236 after t-test (the smallest p value was 0.11) (Figure 4-2), indicating that the reaction order with respect to  $\text{KMnO}_4$  was 0.5 and that there was a general absence of isomer selectivity. Since the order with respect to  $\text{KMnO}_4$  was not 1, in this study, pseudo first-order rate constants instead of second-order rate constants were used. The order with respect to  $\text{KMnO}_4$  was found to be 1 in other studies (Hu et al., 2009; Jiang et al., 2010; Jiang et al., 2012). The inconsistency may indicate that another oxidative species, for example, Mn (III), also reacted with NP. Mn (III) was found to form during  $\text{KMnO}_4$  treatment and to oxidize bisphenol A that contained two phenol moieties (Jiang et al., 2010). Further investigations are needed to better understand the cause for the deviation from the second-order reaction kinetics.

When the solution pH was increased, the reaction between NP isomers and  $\text{KMnO}_4$  increased drastically (Table 4-2 and Figure 4-3). For example, when pH increased from pH 5 to pH 7 in the 10 mg/L  $\text{KMnO}_4$  solution, the reaction rate constant for NP<sub>119</sub> increased from  $0.0561 \pm 0.0014$  to  $0.1478 \pm 0.0029 \text{ min}^{-1}$ . When pH further increased to pH 9, although the concentration of  $\text{KMnO}_4$  was only  $1 \text{ mg L}^{-1}$ , the rate constant increased to  $0.2135 \pm 0.0067 \text{ min}^{-1}$  (Table 4-2). Similar strong pH dependence was found in the oxidation of other phenolic compounds, including bisphenol A,  $17\beta$ -estradiol and dichlorophenol (Jiang et al., 2012). Deprotonation of phenolic compounds was believed to be the cause for the pH dependence (Jiang et al., 2012) since deprotonated phenols showed a higher reactivity than protonated phenols (Tratnyek and Holgne, 1991). For example, when reacting with singlet oxygen, the second-order rate constants for deprotonated and protonated 4-(*tert*-butyl) phenol were  $1.2 \pm 1.3 \times 10^7$  and  $3.55 \pm 0.23 \times 10^8 \text{ mol}^{-1} \text{ s}^{-1}$ , respectively (Tratnyek and Holgne, 1991). Therefore, this pH dependence would be monotonic in pH range 5-9 due to the monotonic deprotonation, even though the reaction kinetics was measured only at pH 5, 7 and 9. Moreover, NP isomers with different capacities for deprotonation may have different dependence on pH. Figure 4-3 shows the ratio of rate constants at pH 5 and pH 7 in the 10 mg/L  $\text{KMnO}_4$  solution. Although large variations existed within Group 1 isomers, it is clear that pH exhibited a greater influence on the oxidation of Group 1 isomers than isomers in the other groups. A similar trend was also observed when pH was varied from pH 7 to pH 9 (Table 4-2). Since electron donating substituents decrease the acidity of substituted phenols,  $\alpha$ -dimethyl substituent should have a larger electron donating effect than the other

substituents in this study. Therefore, Group 1 isomers were more deprotonated and have relatively higher reactivity at high pH than the other isomers and thus exhibit higher pH dependence.

Nonylphenol isomers generally showed a higher reactivity in the reclaimed water (Figure 4-4 and Table 4-2), and the reaction rates increased by 1.40 to 2.07 times (average 1.76) as compared to those in the reagent water. The increase was not isomer selective. The enhancement of  $\text{KMnO}_4$  catalyzed oxidation of phenolic compounds in real water (i.e., waste water, surface water, et al.) over synthetic water was also observed in other studies (Jiang et al., 2012). Various hypotheses have been proposed, such as unknown ligands existing in real water helping to stabilize reactive Mn(III) species, phenoxy radicals formed from organic matter, and also formation of Mn(V) and Mn(VI) species during reaction (Jiang et al., 2012). Except for NP<sub>9</sub>, Group 1 isomers still displayed a higher reactivity than isomers from the other groups. This further confirmed that intrinsic properties, for example,  $\alpha$ -substitution, contributed to the isomer specificity.

#### 4.4 Conclusions

Nonylphenol, the commonly occurring metabolite from nonylphenol ethoxylate surfactants, encompasses a large number of isomers, and yet its isomer-specific behaviors are relatively unknown. Results from this study showed that some isomeric selectivity was apparent in the oxidation of NP by  $\text{KMnO}_4$ , although the selectivity appeared to be more limited as compared to that in biodegradation. In general, NP isomers with dimethyl substitution at the  $\alpha$  position were more reactive toward  $\text{KMnO}_4$  than isomers with



ethylmethyl, methylpropyl or *iso*-propylmethyl substitution. Oxidation by  $\text{KMnO}_4$  increased with increasing pH, and the influence of pH was more pronounced for NP isomers with  $\alpha$ -dimethyl substitution than those with other substituents. Isomeric specificity in other oxidation systems, such as ozonation, merits further investigation. Isomer-dependent reactivity or removal of NP during wastewater treatment should be considered when predicting the discharge of NP into the open environment, as isomeric selectivity in both occurrence and toxicological effects may affect the overall environmental risk of NP. Moreover, the isomeric selectivity during drinking water treatment may have a direct implication on human exposure and health.

## References

- Abe, Y., Umemura, T. and Tsunoda, K. (2001). Decomposition of phenolic endocrine disrupting chemicals by potassium permanganate. *Nippon Kagaku Kaishi*(4): 239-242.
- Bertanza, G., Pedrazzani, R., Dal Grande, M., Papa, M., Zambarda, V., Montani, C., Steimberg, N., Mazzoleni, G. and Di Lorenzo, D. (2011). Effect of biological and chemical oxidation on the removal of estrogenic compounds (NP and BPA) from wastewater: An integrated assessment procedure. *Water Res.* **45**(8): 2473-2484.
- Copolovici, L. and Baldea, I. (2007). Kinetics of the phenol oxidation by permanganate in acidic media. *Rev. Roum. Chim.* **52**(11): 1045-1050.
- Dachs, J., Van Ry, D. A. and Eisenreich, S. J. (1999). Occurrence of estrogenic nonylphenols in the urban and coastal atmosphere of the lower Hudson River estuary. *Environ. Sci. Technol.* **33**(15): 2676-2679.
- Eganhouse, R. P., Pontolillo, J., Gaines, R. B., Frysjinger, G. S., Gabriel, F. L. P., Kohler, H. P. E., Giger, W. and Barber, L. B. (2009). Isomer-specific determination of 4-nonylphenols using comprehensive two-dimensional gas chromatography/time-of-flight mass spectrometry. *Environ. Sci. Technol.* **43**(24): 9306-9313.
- Evans, D. H. (2008). One-electron and two-electron transfers in electrochemistry and homogeneous solution reactions. *Chem. Rev.* **108**(7): 2113-2144.
- Fan, Z., Hu, J., An, W. and Yang, M. (2013). Detection and occurrence of chlorinated byproducts of bisphenol A, nonylphenol, and estrogens in drinking water of China: Comparison to the parent compounds. *Environ. Sci. Technol.*

- Gabriel, F. L. P., Cyris, M., Jonkers, N., Giger, W., Guenther, K. and Kohler, H. P. E. (2007). Elucidation of the *ipso*-substitution mechanism for side-chain cleavage of  $\alpha$ -quaternary 4-nonylphenols and 4-t-butoxyphenol in *Sphingobium xenophagum* Bayram. *Appl. Environ. Microbiol.* **73**(10): 3320-3326.
- Gabriel, F. L. P., Routledge, E. J., Heidlberger, A., Rentsch, D., Guenther, K., Giger, W., Sumpter, J. P. and Kohler, H. P. E. (2008). Isomer-specific degradation and endocrine disrupting activity of nonylphenols. *Environ. Sci. Technol.* **42**(17): 6399-6408.
- Guan, X. H., He, D., Ma, J. and Chen, G. H. (2010). Application of permanganate in the oxidation of micropollutants: a mini review. *Front Environ Sci En* **4**(4): 405-413.
- Hansch, C., Leo, A. and Taft, R. W. (1991). A survey of Hammett substituent constants and resonance and field parameters. *Chem. Rev.* **91**(2): 165-195.
- Horii, Y., Katase, T., Kim, Y. S. and Yamashita, N. (2004). Determination of individual nonylphenol isomers in water samples by using relative response factor method. *Bunseki Kagaku* **53**(10): 1139-1147.
- Hu, L., Martin, H. M., Arcs-Bulted, O., Sugihara, M. N., Keatlng, K. A. and Strathmann, T. J. (2009). Oxidation of carbamazepine by Mn(VII) and Fe(VI): Reaction kinetics and mechanism. *Environ. Sci. Technol.* **43**(2): 509-515.
- Ieda, T., Horii, Y., Petrick, G., Yamashita, N., Ochiai, N. and Kannan, K. (2005). Analysis of nonylphenol isomers in a technical mixture and in water by comprehensive two-dimensional gas chromatography-mass spectrometry. *Environ. Sci. Technol.* **39**(18): 7202-7207.

- Jiang, J., Pang, S. Y. and Ma, J. (2010). Role of ligands in permanganate oxidation of organics. *Environ. Sci. Technol.* **44**(11): 4270-4275.
- Jiang, J., Pang, S. Y., Ma, J. and Liu, H. L. (2012). Oxidation of phenolic endocrine disrupting chemicals by potassium permanganate in synthetic and real waters. *Environ. Sci. Technol.* **46**(3): 1774-1781.
- Khansole, S. V., Gaikwad, D. D., Gaikwad, S. D. and Kankariya, R. D. (2010). Kinetics and mechanism of acid catalyzed oxidation of phenol and substituted phenols by isoquinolinium bromochromate. *Russ. J. Phys. Chem. A* **84**(13): 2233-2237.
- Kim, Y. S., Katase, T., Horii, Y., Yamashita, N., Makino, M., Uchiyama, T., Fujimoto, Y. and Inoue, T. (2005). Estrogen equivalent concentration of individual isomer-specific 4-nonylphenol in Ariake sea water, Japan. *Mar. Pollut. Bull.* **51**(8-12): 850-856.
- Kolvenbach, B. A. and Corvini, P. F. X. (2012). The degradation of alkylphenols by *Sphingomonas* sp. strain TTNP3 – a review on seven years of research. *New Biotechnol.* **30**(1): 88-95.
- Lee, D. G. and Sebastian, C. F. (1981). The oxidation of phenol and chlorophenols by alkaline permanganate. *Canadian Journal of Chemistry-Revue Canadienne De Chimie* **59**(18): 2776-2779.
- Porter, A. W. and Hay, A. G. (2007). Identification of *opdA*, a gene involved in biodegradation of the endocrine disrupter octylphenol. *Appl. Environ. Microbiol.* **73**(22): 7373-7379.

- Shan, J., Jiang, B. Q., Yu, B., Li, C. L., Sun, Y. Y., Guo, H. Y., Wu, J. C., Klumpp, E., Schaffer, A. and Ji, R. (2011). Isomer-specific degradation of branched and linear 4-nonylphenol isomers in an oxic soil. *Environ. Sci. Technol.* **45**(19): 8283-8289.
- Soares, A., Guieysse, B., Jefferson, B., Cartmell, E. and Lester, J. N. (2008). Nonylphenol in the environment: A critical review on occurrence, fate, toxicity and treatment in wastewaters. *Environ. Int.* **34**(7): 1033-1049.
- Stone, A. T. (1987). Reductive dissolution of manganese(III/IV) oxides by substituted phenols. *Environ. Sci. Technol.* **21**(10): 979-988.
- Thiele, B., Heinke, V., Kleist, E. and Guenther, K. (2004). Contribution to the structural elucidation of 10 isomers of technical *p*-nonylphenol. *Environ. Sci. Technol.* **38**(12): 3405-3411.
- Tratnyek, P. G. and Holgne, J. (1991). Oxidation of substituted phenols in the environment: A QSAR analysis of rate constants for reaction with singlet oxygen. *Environ. Sci. Technol.* **25**(9): 1596-1604.
- Vallejo, A., Olivares, M., Fernandez, L. A., Etxebarria, N., Arrasate, S., Anakabe, E., Usobiaga, A. and Zuloaga, O. (2011). Optimization of comprehensive two dimensional gas chromatography-flame ionization detection-quadrupole mass spectrometry for the separation of octyl- and nonylphenol isomers. *J. Chromatogr. A* **1218**(20): 3064-3069.
- Ying, G. G., Williams, B. and Kookana, R. (2002). Environmental fate of alkylphenols and alkylphenol ethoxylates - a review. *Environ. Int.* **28**(3): 215-226.

Zhang, Y. P., Zhou, X., Lin, Y. X. and Zhang, X. (2008). Ozonation of nonylphenol and octylphenol in water. *Fresenius Environ. Bull.* **17**(6): 760-766.

Tables

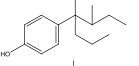
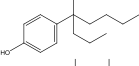
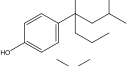
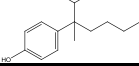
**Table 4-1** Matrices, pH, KMnO<sub>4</sub> and nonylphenol concentrations in the batch experiments

Reaction conditions	A	B	C	D	E
Matrix	Reagent water	Reagent water	Reagent water	Reagent water	Reclaimed water
pH	5	7	7	9	7
KMnO <sub>4</sub> concentration (mg/L)	10	10	2	1	10
tNP concentration (µg/L)	50	50	50	50	50

**Table 4-2** Names, structures and pseudo first-order rate constants of 19 nonylphenol isomers separated and identified

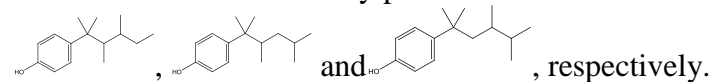
Isomer	Structure	Side chain length	$\alpha$ Substituents	Group	Rate constant ( $\text{min}^{-1}$ )				
					A	B	C	D	E
36 <sup>1</sup>		6	Me, Me	1	0.0564 ± 0.0016	0.1319 ± 0.0024	0.0556 ± 0.0024	0.2120 ± 0.0082	0.258 ± 0.016
X <sup>2</sup>		5	Me, Me	1	0.0489 ± 0.0015	0.1261 ± 0.0022	0.0566 ± 0.0022	0.2242 ± 0.0081	0.261 ± 0.016
128 <sup>1</sup>		5	Me, Me	1	0.0552 ± 0.0017	0.1382 ± 0.0024	0.0628 ± 0.0024	0.2285 ± 0.0087	0.277 ± 0.016
38 <sup>1</sup>		6	Me, Me	1	0.0552 ± 0.0016	0.1232 ± 0.0017	0.0543 ± 0.0022	0.1860 ± 0.0069	0.241 ± 0.014
37 <sup>1</sup>		6	Me, Me	1	0.0543 ± 0.0016	0.1300 ± 0.0018	0.0589 ± 0.0023	0.2025 ± 0.0074	0.248 ± 0.013
119 <sup>1</sup>		5	Me, Me	1	0.0561 ± 0.0014	0.1478 ± 0.0029	0.0614 ± 0.0024	0.2135 ± 0.0067	0.280 ± 0.015
35		6	Me, Me	1	0.0579 ± 0.0017	0.1443 ± 0.0023	0.0617 ± 0.0027	0.2134 ± 0.0080	0.258 ± 0.017
9		7	Me, Me	1	0.0576 ± 0.0015	0.1268 ± 0.0025	0.0480 ± 0.0025	0.1648 ± 0.0089	0.177 ± 0.008
65 <sup>1</sup>		6	Me, Et	2	0.0586 ± 0.0014	0.1184 ± 0.0018	0.0521 ± 0.0024	0.1400 ± 0.0083	0.185 ± 0.014
112 <sup>1</sup>		5	Me, Et	2	0.0525 ± 0.0015	0.1114 ± 0.0014	0.0529 ± 0.0021	0.1557 ± 0.0059	0.203 ± 0.010
111a <sup>1</sup>		5	Me, Et	2	0.0572 ± 0.0014	0.1146 ± 0.0014	0.0553 ± 0.0023	0.1648 ± 0.0062	0.212 ± 0.010
111b <sup>1</sup>		5	Me, Et	2	0.0601 ± 0.0014	0.1172 ± 0.0014	0.0572 ± 0.0024	0.1695 ± 0.0067	0.212 ± 0.012
110a		5	Me, Et	2	0.0582 ± 0.0013	0.1174 ± 0.0014	0.0554 ± 0.0025	0.1535 ± 0.0049	0.175 ± 0.009
110b		5	Me, Et	2	0.0585 ± 0.0014	0.1182 ± 0.0013	0.0549 ± 0.0025	0.1526 ± 0.0052	0.203 ± 0.011
193a		4	Me, Pr	3	0.0581 ± 0.0012	0.1177 ± 0.0016	0.0544 ± 0.0024	0.1488 ± 0.0053	0.185 ± 0.009



193b		4	Me, Pr	3	0.0598±0.00130.1224±0.00160.0560±0.00260.1551±0.0055*
152		5	Me, Pr	3	0.0555±0.00130.1130±0.00150.0505±0.00220.1289±0.00890.188±0.012
194 <sup>1</sup>		4	Me, Pr	3	0.0577±0.00130.1098±0.00160.0492±0.00180.1536±0.00520.189±0.010
143		5	Me, <i>i</i> -Pr	4	0.0582±0.00130.1159±0.00140.0557±0.00240.1419±0.00670.191±0.010

<sup>1</sup>Isomers confirmed with authentic standards.

<sup>2</sup>The structure of this nonylphenol isomer is not fully identified; it may be NP<sub>92</sub>, NP<sub>93</sub> or NP<sub>95</sub> and the structure may be



\* Measurement was not possible due to interference.

**Table 4-3** Comparison of pseudo first-order rate constants among nonylphenol isomers with 10 mg/L KMnO<sub>4</sub> at pH 7 in reagent water

Isomers	X	128	38	37	119	35	9	65	112	111a	111b	110A	110B	193A	193B	152	194	143
36	Y	Y	Y	N	Y	Y	Y	Y	Y	Y	Y	Y	Y	Y	Y	Y	Y	Y
X		Y	N	N	Y	Y	N	Y	Y	Y	Y	Y	Y	Y	N	Y	Y	Y
128			Y	Y	Y	Y	Y	Y	Y	Y	Y	Y	Y	Y	Y	Y	Y	Y
38				Y	Y	Y	N	Y	Y	Y	Y	Y	Y	Y	N	Y	Y	Y
37					Y	Y	N	Y	Y	Y	Y	Y	Y	Y	Y	Y	Y	Y
119						N	Y	Y	Y	Y	Y	Y	Y	Y	Y	Y	Y	Y
35							Y	Y	Y	Y	Y	Y	Y	Y	Y	Y	Y	Y
9								Y	Y	Y	Y	Y	Y	Y	N	Y	Y	Y
65									Y	N	N	N	N	N	N	Y	Y	N
112										N	Y	Y	Y	Y	Y	N	N	Y
111a											N	N	N	N	Y	N	Y	N
111b												N	N	N	Y	N	Y	N
110a													N	N	Y	N	Y	N
110b														N	N	Y	Y	N
193a															Y	Y	Y	N
193b																Y	Y	Y
152																	N	N
194																	Y	Y

Y: significant difference between two NP isomers.

N: no significant difference between two NP isomers.

Figures

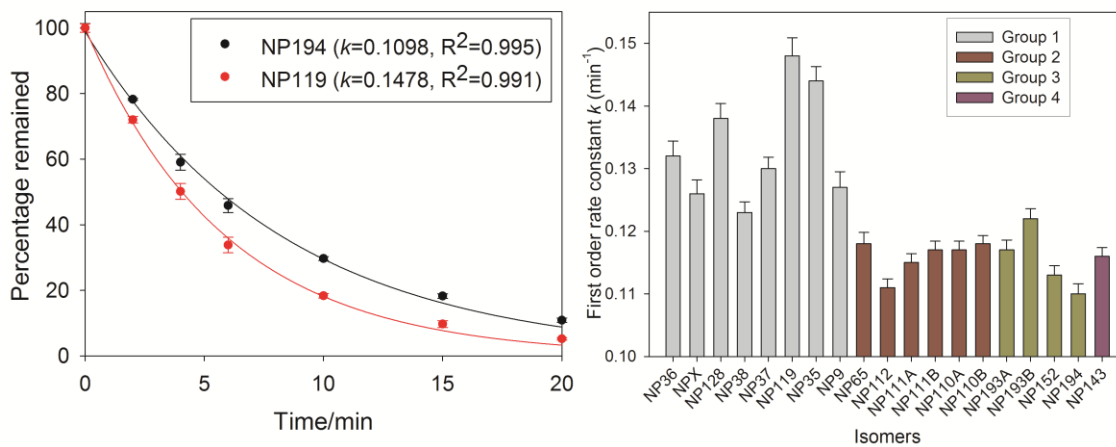


**Figure 4-1** Isomer specific reaction rates in 10 mg L<sup>-1</sup> KMnO<sub>4</sub> at pH 7 with reagent water. (a) Removal of NP194 and NP119; and (b) Pseudo first-order rate constants of nonylphenol isomers

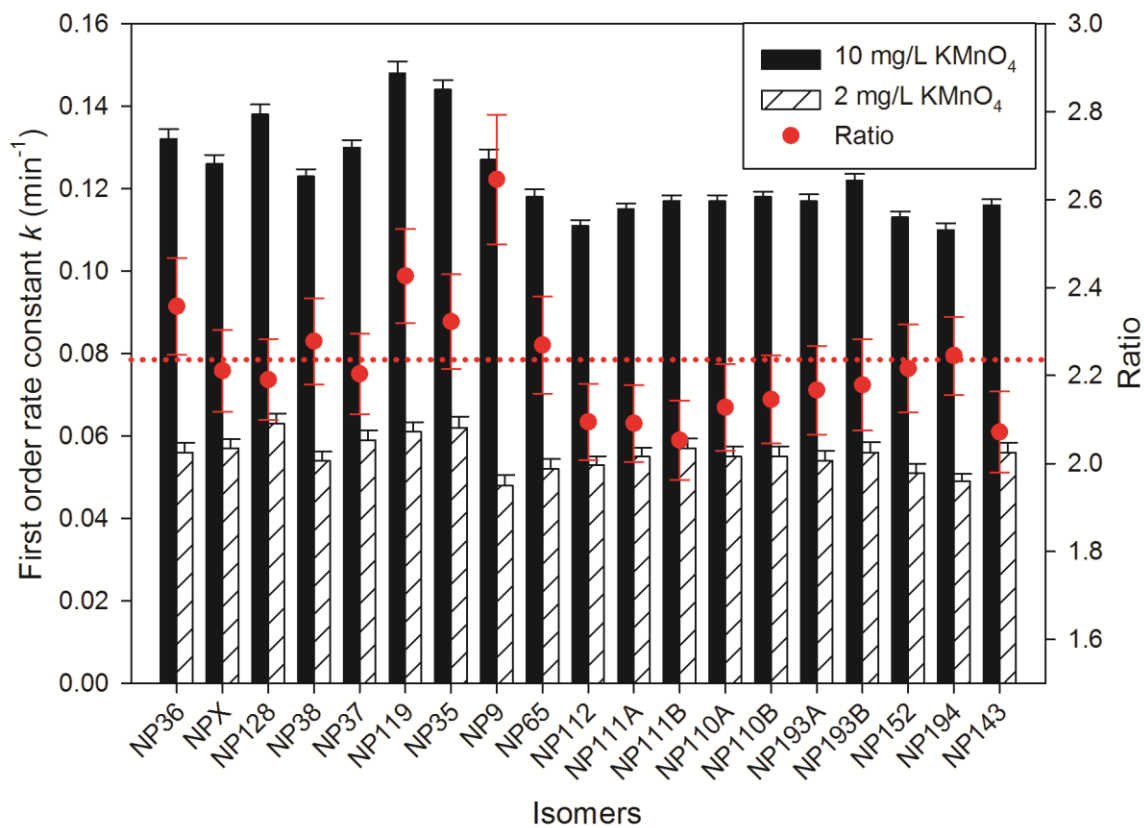


**Figure 4-2** Pseudo first-order rate constants of nonylphenol isomers and their ratios in 10 and 2 mg/L  $\text{KMnO}_4$  at pH 7 with reagent water

The red dotted reference line is 0.236.

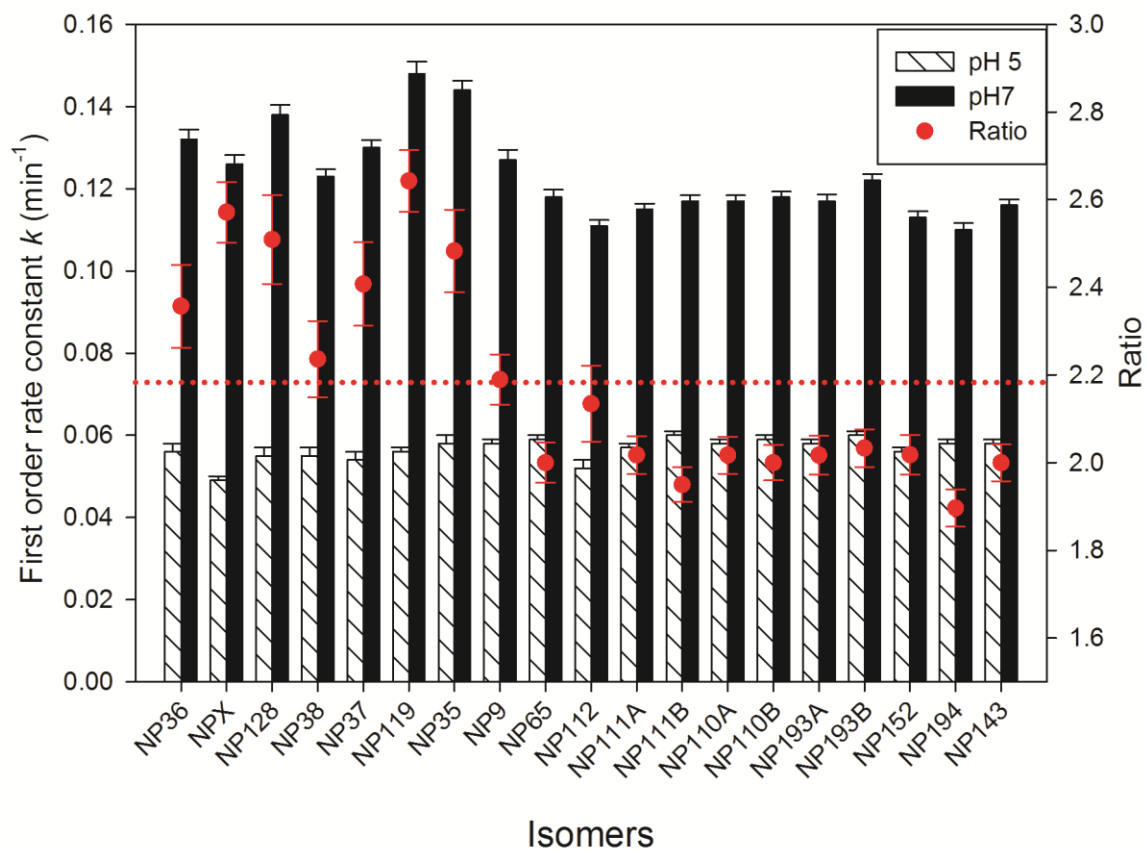


**Figure 4-3** Pseudo first-order rate constants of nonylphenol isomers and their ratios in 10 mg/L KMnO<sub>4</sub> at pH 5 and pH 7 with reagent water

The red dotted reference line shows the ratio 2.18.

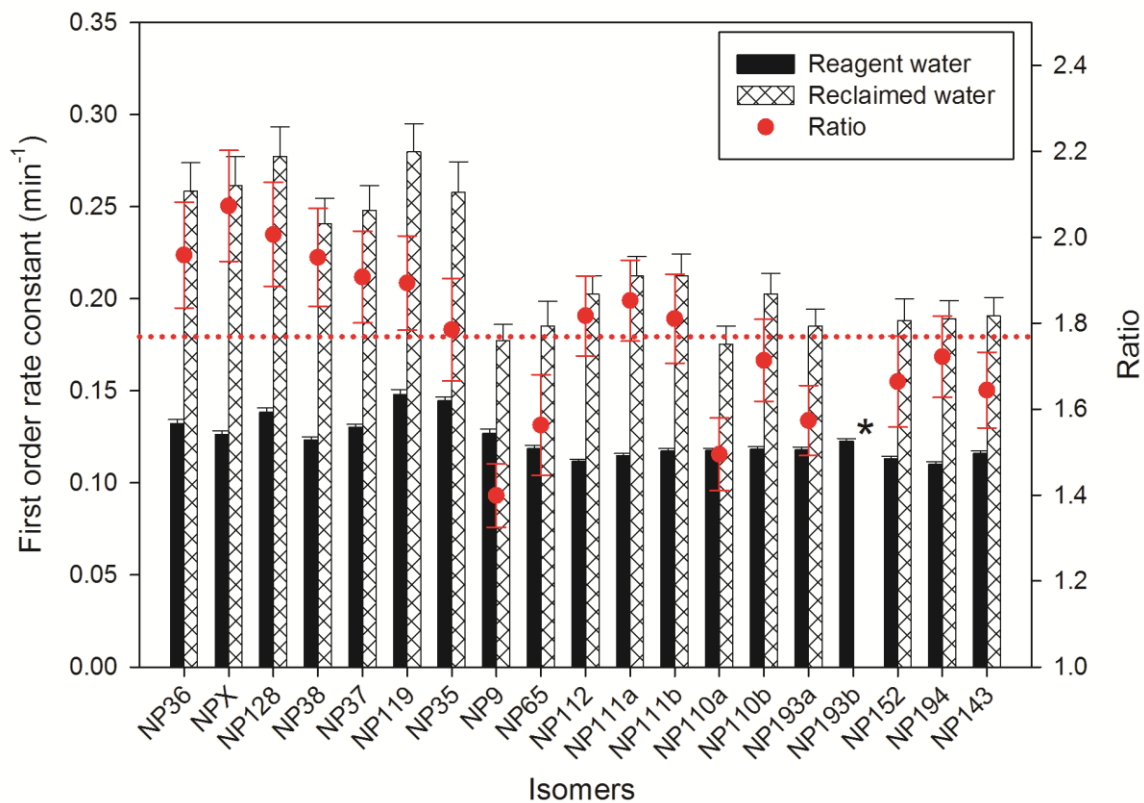


**Figure 4-4** Pseudo first-order rate constants of nonylphenol isomers and their ratios in reagent water and reclaimed water with 10 mg/L KMnO<sub>4</sub> at pH 7

The red dotted reference line shows the ratio 1.77. \* Measurement was not possible due to interference.

Supporting Information

**Table S 4–1** Retention time and main ion fragments of nonylphenol isomers identified

NP isomer	Retention time (min)	107	121	135	149	163	177	191	220
194	35.07	45	100	4	1	44	18	0	5
36	36.226	11	6	100	0	0	0	0	3
X	36.546	9	5	100	0	0	0	0	3
128	37.243	72	49	100	96	0	0	28	10
112	37.272	71	52	83	100	0	0	31	11
38	37.585	12	4	100	0	0	0	0	4
111a	37.765	49	76	15	100	0	0	16	7
37	38.382	15	10	100	5	0	0	1	5
111b	38.539	49	81	21	100	0	0	17	7
119	39.761	10	1	100	0	0	0	0	1
152	40.009	100	97	21	1	67	50	0	10
193a	40.254	78	63	4	1	100	2	0	3
110a	40.984	19	0	0	100	0	0	0	1
143	41.051	67	46	6	100	2	33	0	3
193b	41.403	80	88	35	1	100	2	0	3
35	42.528	13	3	100	3	0	0	0	2
110a/65*	53.539-43.599	46	16	4	100	0	2	6	3
9	44.282	13	3	100	0	0	0	0	4

\* NP<sub>110</sub> and NP<sub>65</sub> cannot be fully separated; however, they can still be quantify use the m/z 149 and 191

**Table S 4–2** Retention time and main ion fragments of nonylphenol isomers standards

Isomer	Retention								
	time (min)	107	121	135	149	163	177	191	220
194	35.086	47	100	4	1	40	16	0	4
36	36.236	11	5	100	0	0	0	0	3
128	37.231	11	5	100	0	0	0	0	3
112	37.277	68	52	9	100	0	0	28	7
38	37.598	14	5	100	0	0	0	0	4
111a	37.767	50	79	9	100	0	0	15	6
37	38.379	12	5	100	0	0	0	0	4
111b	38.548	51	81	9	100	0	0	16	6
119	39.772	12	1	100	0	0	0	0	1
65	43.539	80	50	6	100	0	0	33	8



## **Chapter 5 Oxidation of Nonylphenol and Octylphenol by Manganese Dioxide: Kinetics and Pathways**

### 5.1 Introduction

Nonylphenol (NP) and octylphenol (OP) are raw materials and also hydrolytic metabolites of NP ethoxylates (NPEOs) and OP ethoxylates (OPEOs) which are non-ionic surfactants widely used in agricultural, industrial and domestic products (Soares et al., 2008; Ying et al., 2002). Nonylphenol is one of the high production volume chemicals and the production of the technical nonylphenol (tNP, mixture of ring and chain isomers) in the United States was 45-227 thousand tons in 2006 (USEPA, 2006) and the estimated annual release to soil by sewage sludge disposal and application was about 1.03 to 3.31 thousand tons (Venkatesan and Halden, 2013). Due to the widespread use of NPEOs and OPEOs, NP and OP are frequently found in soil, water and sediment (Mao et al., 2012). For example, Writer et al. (2012) investigated the fate of NP in Redwood River of Minnesota and found that the mean concentrations of NP in water and sediment downstream from a wastewater treatment plant were 620 ng/L and 140 µg/kg, respectively. Nonylphenol and OP are known as environmental estrogens and many studies have shown that NP and OP may have developmental toxicity and other effects on aquatic and terrestrial species or potentially human health (Domene et al., 2009; Soares et al., 2008). In different *in vivo* and *in vitro* studies, the potency of NP relative to 17β-estradiol ranges from  $7.2 \times 10^{-7}$  to 0.05, with an arithmetic mean potency of 0.003 from *in vitro* studies and 0.023 from *in vivo* studies (Soares et al., 2008).

To assess the potential health and ecological risks of NP and OP, a thorough understanding of their fate and transport processes is essential. Photolysis, biodegradation, and chemical oxidation may all contribute to the attenuation of NP and OP in water, soil and sediment. So far, however, the importance of abiotic oxidation has been largely ignored in the elucidation of environmental fate of NP and OP. Manganese oxides/hydroxides are important components of most soils, sediments and water ecosystems. Their characteristic properties, such as low point of zero charge, dynamic redox behavior and large surface areas make them chemically active in oxidizing organic and inorganic compounds (Negra et al., 2005). Previous studies showed that manganese oxides/hydroxides were effective at oxidizing sulfamethazine, lincosamide, acid azo dyes, bisphenol A, tetrachlorophenols and trichlorophenols (Chen et al., 2010; Clarke et al., 2010; Gao et al., 2012; Lin et al., 2009a; Xu et al., 2008; Zhang et al., 2008; Zhao et al., 2009). It may thus be hypothesized that MnO<sub>2</sub> facilitated oxidation is potentially important for NP and OP in the environment. However, the substituted phenols commonly studied in the literature so far are either chlorinated or short alky substituted. Nonylphenol and octylphenol have numerous isomers and much longer alky substitutions (9 and 8 carbons respectively). The long alky substitutions are expected to affect sorption onto MnO<sub>2</sub> surfaces, and reactivity with radicals, potentially leading to differences in reaction kinetics and pathways. The objective of this study was to investigate the kinetics, influencing factors and pathways of the oxidation of tNP, 4-*n*-NP and 4-*tert*-OP by MnO<sub>2</sub>. The oxidation kinetics were measured under different conditions, including different initial MnO<sub>2</sub> concentrations or pH, and presence of cosolutes such as Mn<sup>2+</sup>, Ca<sup>2+</sup> and

humic acids. The role of MnO<sub>2</sub> dioxide-catalyzed oxidation in the natural attenuation of NP was further validated in soil.

## 5.2 materials and methods

### 5.2.1 Chemicals and Soil.

Technical NP (tNP), a mixture of NP isomers with branched side chains (CAS: 84852-15-3) was purchased from TCI America (Portland, OR); 4-*n*-NP (>98%, CAS: 104-40-5) was from Alfa Aesar (Ward Hill, MA); and 4-*tert*-OP (>97%, CAS: 140-66-9) and hydroxylamine hydrochloride (99+%) were from Sigma-Aldrich (St. Louis, MO). Information on other chemicals is given in Supporting Information (SI).

Manganese dioxide ( $\delta$ -MnO<sub>2</sub>) was synthesized according to Murray's method (Murray, 1974). Briefly, 6.56 L of reagent water was constantly sparged with nitrogen and then mixed with 320 mL of 0.1 M NaMnO<sub>4</sub> and 640 mL of 0.1 M NaOH. The constantly stirred solution was added drop-wise with 80 mL of 0.1 M MnCl<sub>2</sub>. The newly formed MnO<sub>2</sub> particles were allowed to settle, and the supernatant was decanted and replaced with fresh reagent water several times until the conductivity of the supernatant was below 2  $\mu$ S/cm. The MnO<sub>2</sub> suspensions were stored at 4 °C and were diluted to appropriate concentrations prior to use. The surface area of MnO<sub>2</sub> was measured to be 269.1 m<sup>2</sup>/g (Micromeritics 2100, Micromeritics, Norcross, GA). Powder X-ray diffraction (XRD) analysis (Bruker D8 Advance Diffractometer, Bruker AXS, WI) with Cu K $\alpha$  radiation showed that the synthetic MnO<sub>2</sub> was poorly crystallized (Figure S 5-1). The XRD pattern

showed that the synthesized  $\text{MnO}_2$  was turbostratic birnessite ( $\text{Na}^+$  and  $\text{H}_2\text{O}$ ) having hexagonal layer symmetry, which is commonly found in soils (Drits et al., 2007). A well characterized fine, septic, mesic Typic Kandihumult soil with high Mn content was taken at the 700 m elevation in the Klamath Mountains, CA. The soil was sieved through a 2 mm mesh and air dried. The Mn and Fe contents were 4.2 and 438 g/kg as determined by the standard citrate-bicarbonate-dithionite method and other selected properties of the soil are given in [Table S 5-1](#). The soil was further ground to pass a 60 mesh (0.25 mm) sieve, and a subsample was selectively removed the indigenous Mn oxides with hydroxylamine hydrochloride to produce Mn-removed soil (Neaman et al., 2004).

#### 5.2.2 Reaction setup.

Batch experiments were conducted in 125-mL wide mouth amber borosilicate glass bottles with Teflon-faced caps at room temperature. The reaction solution temperature was  $25.2 \pm 0.5$  °C (mean  $\pm$  standard deviation). Reaction solutions (methanol: water, 40:60, v/v) were maintained at the desired pH using 0.01 mol/L of the following pH buffers: pH 4.5 and pH 5.5, acetic acid/sodium acetate; pH 6.5 and pH 7.5, 4-morpholinepropanesulfonic acid (MOPS) and its sodium salt; pH 8.6 and pH 9.6, 2-(cyclohexylamino) ethanesulfonic acid (CHES) and its sodium salt. Sodium perchlorate was added to maintain the ionic strength at 0.01 mol/L. The addition of methanol was necessary to increase the solubility of NP and OP. The effects of methanol on the recoveries and reaction rates of NP and OP are given in SI. The  $\text{MnO}_2$  solution (50 mL) was first stirred at 480 rpm for 1 h and the reaction was initiated by adding 50  $\mu\text{L}$  of 1000

mg/L tNP, 4-*n*-NP or 4-*tert*-OP stock solution. At different time intervals from the onset of reaction, 1.0 mL of the reaction solution was withdrawn with a pipette and transferred to 2-mL HPLC vials containing 10  $\mu$ L L-ascorbic acid solution (50 mg/mL) and immediately vortexed for 10 s for quenching. All samples were stored at 4  $^{\circ}$ C and analyzed by HPLC within 24 h. Preliminary experiments showed that there was no change in the concentration during the short storage.

The effect of pH was evaluated in solutions maintained at different pH values under the fixed conditions of 100 mg/L MnO<sub>2</sub>, 1 mg/L NP or OP, and 0.01 mol/L ionic strength. The cosolute effects of cations were investigated by fortifying 0.01 mol/L of CaCl<sub>2</sub> or MgCl<sub>2</sub>, or  $1 \times 10^{-5}$  mol/L MnCl<sub>2</sub> at pH 5.5. The effect of humic acid was determined at pH 5.5 by amending the reaction solution with Sigma-Aldrich humic acid (CAS: 68131-04-4, Sigma-Aldrich, St. Louis, MO) at 0.1 or 10 mg/L under the fixed conditions of 100 mg/L MnO<sub>2</sub>, 1 mg/L NP or OP, and 0.01 mol/L ionic strength.

To validate the role of MnO<sub>2</sub>-catalyzed oxidation in soil, tNP (50  $\mu$ g/L) was reacted with 100 mg/L synthetic MnO<sub>2</sub>, or suspension of 0.6 g Mn-containing soil in 40 mL water, or 0.6 g Mn-removed soil in 40-mL water. No pH buffers were used in this experiment and the measured pH values were both 6.30. Before the reaction, the soils were autoclaved at 121  $^{\circ}$ C for 45 min over three consecutive days and sodium azide was added at 200 mg/L to the soil suspension to suppress microbial transformation. At selected time intervals (0, 2, 4, 6, 10, 20, 30 min for synthetic MnO<sub>2</sub>; 0, 4, 12, 24, 36 and 48 h for Mn-containing

soil; and 0, 12, 24, 48, 96 and 168 h for Mn-removed soil), 0.5 mL of 50 mg/mL L-ascorbic acid solution was added to quench the reaction.

### 5.2.3 Chemical analysis.

Analysis of tNP, 4-*n*-NP and 4-*tert*-OP was carried out on an Agilent 1100 HPLC (Agilent Technologies, Wilmington, DE) coupled with a fluorescence detector. Samples containing low concentrations of tNP were extracted by 15 mL hexane twice and analyzed on an Agilent 6890 GC with 5973 MSD. Both GC-MS/MS (with or without silylation) and UPLC-MS/MS were used in this study for the identification of reaction products. For silylation derivatization, 150  $\mu$ L of *N,O*-bis-(trimethylsilyl)-trifluoroacetamide (BSTFA) with 1% trimethylsilyl chloride (TMCS) was added, and the mixture kept at room temperature for 2 h. More detailed information is given in SI. All data analysis was done using SPSS 16.0 (IBM, Armonk, NY).

## 5.3 Results and Discussion

### 5.3.1 Kinetics and Influencing Factors

In general, oxidation of tNP, 4-*n*-NP and 4-*tert*-OP by MnO<sub>2</sub> was fast and efficient, with the rate of oxidation following the order of 4-*n*-NP > 4-*tert*-OP > tNP (Figure 5-1A). For example, with 1.0 mg/L tNP, 4-*n*-NP or 4-*tert*-OP and 100 mg/L MnO<sub>2</sub> at pH 5.5, after 90 min, 76.3 $\pm$ 0.2, 92 $\pm$ 2 and 83.7 $\pm$ 0.5% of the initial chemical disappeared from the solution, respectively, and the corresponding half-lives were about 45, 23 and 35 min (Figure 5-1A). In contrast, the levels of these chemicals remained unchanged in the

MnO<sub>2</sub>-free controls (Table S 5-2). The details on the derivation of kinetic expressions are given in Text S 5-3 of SI.

With increasing initial MnO<sub>2</sub> concentrations, the removal of tNP, 4-*n*-NP or 4-*tert*-OP increased. For example, at pH 5.5, the removal after 90 min for 1.0 mg/L tNP with initially 100, 50, 25 and 12.5 mg/L MnO<sub>2</sub> were 76.3±0.2, 48.8±0.9, 34.1±0.6 and 21±2%, respectively (Figure 5-1B). The removal of 4-*n*-NP and 4-*tert*-OP also showed a similar trend (Figures S 5-2 and S 5-3). According to Equation S5-6, when plotting log<sub>10</sub> *k*<sub>observ</sub> against log<sub>10</sub> [MnO<sub>2</sub>], the slope of the regression line was the order with respect to MnO<sub>2</sub> (Figure 5-1C). When reacting with tNP, 4-*n*-NP and 4-*tert*-OP, the orders of MnO<sub>2</sub> were determined to be 0.94±0.05, 0.6±0.1 and 1.01±0.09, respectively. In previous studies, the orders of MnO<sub>2</sub> were 0.8 and 1.25, respectively, when reacting with tetrabromobisphenol A (TBBPA) and bisphenol F (Lin et al., 2009b; Lu et al., 2011). Zhao et al. (2009) showed that the order of MnO<sub>2</sub> ranged from 0.45 to 1.64 when reacting with three tetrachlorophenols and three trichlorophenols. Therefore, the order of MnO<sub>2</sub> was highly dependent on the substrates. In this study, the orders of MnO<sub>2</sub> were similar between tNP and 4-*tert*-OP, but were smaller for 4-*n*-NP. This may be attributed to the structural differences among these three substrates. It is known that tNP is a mixture of branched nonyl-substituted phenols, mostly with a quaternary α carbon, e.g., 4-[1,1,2-trimethylhexyl]phenol (Thiele et al., 2004); while the nonyl substitution in 4-*n*-NP is linear. 4-*tert*-Octylphenol also has the quaternary α carbon with two methyl substitutions. Thus, structurally, tNP is more similar to 4-*tert*-OP than to 4-*n*-NP. This phenomenon

indicates that the side chain properties such as the length and bulkiness may significantly affect the chemical reactivity of NP isomers.

The oxidation of tNP, 4-*n*-NP and 4-*tert*-OP by MnO<sub>2</sub> was significantly influenced by pH, with the reaction rate consistently decreasing with increasing pH (Figures 5-1D, 1E and S 5-4 and S 5-5). For example, after 90 min, the removal for 1.0 mg/L tNP with 100 mg/L MnO<sub>2</sub> at pH 4.5, 5.5, 6.5, 7.5 and 8.6 were 94.3±0.4, 76.3±0.2, 24±2, 21±2, and 13±2%, respectively; while at pH 9.6 there was no appreciable dissipation of tNP (data not shown). According to Equation S5-7, plotting log<sub>10</sub> *k*<sub>observ</sub> against pH would yield a slope representing the reaction order with respect to H<sup>+</sup> (Figure 5-1E). When reacting with tNP, 4-*n*-NP and 4-*tert*-OP, the orders of H<sup>+</sup> were 0.35±0.06, 0.36±0.08 and 0.37±0.03, respectively (Figure 5-1E). Thus, the effect of pH was generally similar among tNP, 4-*n*-NP and 4-*tert*-OP and the order of H<sup>+</sup> between pH 4.5 to 8.6 was about 0.36. The deprotonated phenols have higher reactivity than the undeprotonated phenols (Stone, 1987); however, the pK<sub>a</sub> of tNP is 10.28 (Soares et al., 2008), thus during pH 4.5 and 8.6, tNP is mainly undeprotonated. Therefore, the pH dependence in the reaction of NP and OP with MnO<sub>2</sub> was dominated by the reduction potential of MnO<sub>2</sub>, which decreases monotonically with increasing pH according to Nernst equation.

The oxidation of tNP, 4-*n*-NP and 4-*tert*-OP by MnO<sub>2</sub> was inhibited by metal ions, such as Ca<sup>2+</sup>, Mg<sup>2+</sup> and Mn<sup>2+</sup> (Table 5-1). For example, the observed pseudo-first order rate constants of 1.0 mg/L tNP with no metal ion, 0.01 mol/L Ca<sup>2+</sup> or Mg<sup>2+</sup> and 1.0×10<sup>-5</sup> mol/L Mn<sup>2+</sup> were 1.54 (±0.05) ×10<sup>-2</sup>, 9.43 (±0.07) ×10<sup>-3</sup>, 1.21 (±0.01) ×10<sup>-2</sup> and 2.38



( $\pm 0.03$ )  $\times 10^{-3}$   $\text{min}^{-1}$ , respectively. This pattern was consistent with the observation in previous studies (Lin et al., 2009a; Lu et al., 2011; Zhang et al., 2008). The strong inhibition of  $\text{Mn}^{2+}$  may be attributed to its strong adsorption on the  $\text{MnO}_2$  surface (Gao et al., 2012).

The effect of humic acid on the reaction rate was also quantified. At pH 5.5 with 100 mg/L  $\text{MnO}_2$  and 1.0 mg/L tNP, 4-*n*-NP or 4-*tert*-OP, the reaction rate increased slightly after amendment of humic acid at 0.1 mg/L. The increase was more pronounced with the addition of 10 mg/L humic acid, where the degree of enhancement followed the order: 4-*n*-NP > tNP  $\gg$  4-*tert*-OP (Table 5-1). This enhancement effect was consistent with that observed for the oxidation of 17 $\beta$ -estradiol by  $\delta$ - $\text{MnO}_2$  with addition of humic acid from an unknown source (Xu et al., 2008). Bialk et al. (2005) also observed that some surrogate humic constituents, such as syringic acid, protocatechuic acid and catechol enhanced the reaction of sulfonamide antimicrobials and acid birnessite. However, this observation was in disagreement with the oxidation of bisphenol A, bisphenol F and substituted anilines in previous studies where  $\delta$ - $\text{MnO}_2$  and Aldrich humic acid were evaluated (Klausen et al., 1997; Lin et al., 2009a; Lu et al., 2011). It should be noted that the enhancement effect of humic acid was much smaller for 4-*tert*-OP than for tNP or 4-*n*-NP. Humic acid is known to have extremely complex structures containing phenolic moiety and has both electron donating and electron accepting capacities. For instance, the electron donating capacity is  $535 \pm 10$  mmol<sub>e</sub>/g for Aldrich humic acid at 0.61 V and pH 7, and the electron accepting capacity is  $923 \pm 60$  mmol<sub>e</sub>/g at -0.49 V and pH 7 (Aeschbacher et al., 2012). Humic acid may be adsorbed onto the  $\text{MnO}_2$  surface, thus competing with

the organic substrate for binding sites and inhibiting the reaction (Klausen et al., 1997). Humic acid may even react with  $\text{MnO}_2$  to form low molecular weight products, such as pyruvate and acetaldehyde (Tebo et al., 2004). Meanwhile, humic acid may also bind  $\text{Mn}^{2+}$  and thus enhance the reaction (Xu et al., 2008). Moreover, humic acid may react with some target compounds (e.g., sulfonamide antimicrobials) and incorporate them in to its structure (Bialk et al., 2005). Therefore, the effect of humic acid on the reaction rate may depend on the combination of all these effects. More carefully-controlled investigations are needed to further elucidate the effects of humic acids on  $\text{MnO}_2$  related reactions.

### 5.3.2 Reaction of low concentrations of nonylphenol with $\text{MnO}_2$ and soil

The reaction of a low concentration (50  $\mu\text{g/L}$ ) of tNP with synthetic  $\text{MnO}_2$  also followed the pseudo-first order kinetics ( $R^2=0.88$ ) with a half-life of  $10.1 \pm 0.5$  min, which was shorter than the reaction when the starting tNP concentration was 1 mg/L. In the Mn-containing soil and Mn-removed soil, the half-lives of tNP were measured to be  $39 \pm 3$  h and  $104 \pm 5$  h, respectively. Therefore, with the same Mn loading, the reactivity of synthetic  $\text{MnO}_2$  was about two orders of magnitude faster than that in the soil. This may be partly attributed to the complicate matrix effects of soil, including multiple cations, other minerals and soil organic matters. It should be noted that treatments including air drying, autoclaving and sodium azide addition all cause  $\text{Mn}^{2+}$  release in soils (Bartlett and James, 1980; Skipper and Westermann, 1973), which greatly inhibited the reaction of  $\text{MnO}_2$  and NP. Other sterilization methods, such as ethylene oxide addition and gamma

irradiation also increase  $\text{Mn}^{2+}$  release (Skipper and Westermann, 1973). However, these treatments are necessary to distinguish the abiotic and biotic degradation. Therefore, the “real” reactivity of  $\text{MnO}_2$  in soils may be much higher than that indicated in this study. After  $\text{MnO}_2$  removal, the reactivity of the same soil decreased about 3 times; this difference strongly supported the hypothesis that soil  $\text{MnO}_2$  plays an important role in the natural attenuation of tNP. It may be further argued that with a more complete removal of  $\text{MnO}_2$ , and elimination of the influence by iron oxides and/or other factors, even a more pronounced role by  $\text{MnO}_2$  may be found in the attenuation of tNP in soil.

Previous studies reported isomer-specific biodegradation of NP (Gabriel et al., 2008). In this study, there was no noticeable isomer-specific reactivity in the oxidation of tNP by  $\text{MnO}_2$  or in soils when 19 individual peaks from tNP after GC elution were separately analyzed.

### 5.3.3 Reaction Products and Pathways

According to the general mechanistic understanding of the oxidation of phenolic and aniline-like compounds by  $\text{MnO}_2$ , the organic substrate forms a surface complex with  $\text{MnO}_2$  and then a single electron is transferred from the substrate to  $\text{MnO}_2$  to form substrate radicals. The radicals may be coupled to radicals to form dimers and even trimers, or the radicals may also be further oxidized (Gao et al., 2012; Lin et al., 2009a; Lu et al., 2011; Stone, 1987; Zhao et al., 2009). In this study, we used mass spectra obtained by both GC-MS/MS with or without silylation and LC-MS/MS to elucidate the reaction products and pathways. A summary of retention times, molecular weights,

collision energies and main  $m/z$  of MS<sup>2</sup> spectra are shown in Table 5-2. Detailed mass spectra of all identified products and their possible ion fragmentation mechanisms are given in Figures S5-6 to S5-45 in SI. The mass spectra of silylated hydroquinone, 4-*n*-NP, silylated 4-*n*-NP, 4-*tert*-OP and silylated 4-*tert*-OP produced by GC-MS/MS are also given in SI (Figures S5-46 to S5-50).

Both 4-*n*-NP and silylated 4-*n*-NP may characteristically lose C<sub>8</sub>H<sub>17</sub>• (presence of [M-113]<sup>+</sup> peaks, Figures S 5-47 and S 5-48), and this may be an important indicator of presence of the linear nonyl side chain attached to the benzene ring in the product. There were 3 products (NP-1-1A/B/C) with the same molecular weight and similar structures detected in their original forms by GS-MS/MS (Table 5-2). The molecular ion  $m/z$  438.6 indicates that these products may be the dimers of 4-*n*-NP. The fragments  $m/z$  325 and  $m/z$  311 indicate the loss of C<sub>8</sub>H<sub>17</sub>• and C<sub>9</sub>H<sub>19</sub>•. The dimers of 4-*n*-NP may contain 1 or 2 hydroxyl groups, and therefore, after silylation, two types of dimers with molecular weights of 510 and 582, respectively, may be found. Detection of NP-2-3A/B and NP-2-4A/B (Table 5-2) confirmed the formation of such dimers. For NP-2-3A/B,  $m/z$  73 (•Si(CH<sub>3</sub>)<sub>3</sub>) indicates that these products are silylated;  $m/z$  469 indicates the loss of C<sub>8</sub>H<sub>17</sub>• and  $m/z$  365 indicates loss of •CH<sub>3</sub> (commonly observed for silylated products). For NP-2-4A/B,  $m/z$  397 also indicates the loss of C<sub>8</sub>H<sub>17</sub>• and  $m/z$  567 indicates the loss of •CH<sub>3</sub>. The dimer was also detected by LC-MS/MS (NP-3-2, Table 5-2). According to the information above, at most 4 dimers were formed during the reaction of 4-*n*-NP and MnO<sub>2</sub>. The dimers were formed likely due to the coupling of radicals and there are 3 possible radicals due to resonance of the phenoxy radical (Figure 5-2). All the possible

coupling reactions are listed in [Figure 5-2](#). The coupling product of R1 and R1 is peroxide which is not stable due to the reactivity of the peroxy group. The intermediate from the coupling of R1 and R3 may undergo dienone-phenol rearrangement. According to Vitullo and Logue (1972), the alkyl substituent has greater priority than the alkoxy substituent during the dienone-phenol rearrangement, and thus formation of P2 may be the most possible product of R1 and R3. The intermediate of R2 and R3 may also have two possible different dienone-phenol rearrangements; however, the aromatic substituent has greater priority than the alkyl substituent (Marx et al., 1974), leading to the formation of P4. Therefore, there are only four dimers that may be formed through the coupling of the radicals, among which two dimers have one hydroxyl group and the other two have two hydroxyl groups. This analysis is consistent with the elucidation of the structures of NP-2-3A/B and NP-2-4A/B above.

The product NP-2-1 may be hydroquinone, which is commonly found in the oxidation of phenolic compounds by MnO<sub>2</sub> (Chirkst et al., 2011; Lin et al., 2009a; Lu et al., 2011). After comparing with the hydroquinone standard with reference to retention time and mass spectrum ([Figure S5-46](#)), NP-2-1 was confirmed to be hydroquinone. The product NP-3-1 has a molecular weight of 236 which is greater than 4-*n*-NP by 16, indicating that it may be a hydroxylated product of 4-*n*-NP. Product NP-2-2 has the characteristic loss of C<sub>8</sub>H<sub>17</sub>• indicating a nonyl chain attached to the benzene ring. Since NP-2-2 can be silylated, it may contain at least one hydroxyl group. The difference of a 144 mass unit between m/z 380 and m/z 236 in the NP-3-1 spectrum suggested the presence of two hydroxyl groups, as silylation of each hydroxyl group would increase the molecular

weight by 72 because of the introduction of Si(CH<sub>3</sub>)<sub>3</sub> group. The product NP-3-3 may be a trimer of 4-*n*-NP and m/z 543 indicating the loss of C<sub>8</sub>H<sub>17</sub>•, but no further information has been collected on its structure. [Figure S5-27](#) gives one possible structure of the trimer; however, other structures are also possible.

According to [Figures S5-49](#) and [S5-50](#), 4-*tert*-OP and silylated 4-*tert*-OP may characteristically lose C<sub>5</sub>H<sub>11</sub>•, and the loss may indicate the existence of the 4-(1,1,3,3-tetramethylbutyl) substituent on the benzene ring. The product OP 1-1-A/B has a molecular weight of 615, indicating that they may be the trimers of 4-*tert*-OP and that m/z 543 shows a characteristic loss of C<sub>5</sub>H<sub>11</sub>•. The m/z 431 may be formed by the loss of the whole alky chain on one benzene ring and also C<sub>5</sub>H<sub>11</sub>• on the other benzene ring. After silylation, more trimers were found (OP-2-3A/B and OP-2-4A/B) and among them, two have one hydroxyl group and two have two hydroxyl groups due to the increases in molecular weight by 72 and 144, respectively. The m/z 615.7 in OP-2-3 A/B shows a characteristic loss of C<sub>5</sub>H<sub>11</sub>• and for the same reason, m/z 503 may result in the formation of m/z 431 in OP-1-1B. Presence of OP-3-1A/B/C also confirms the formation of trimers. By the same reasoning, products like OP-2-2A/B and OP-3-2A/B/C confirm the formation of dimers. Like NP-2-1, OP-2-2 may be the hydroxylated product of 4-*tert*-OP.

Overall, 1 hydroxylated product, 4 dimers, 1 trimer and hydroquinone were identified from the reaction of 4-*n*-NP and MnO<sub>2</sub>. In comparison, 1 hydroxylated product, 3 dimers and 3 trimers were found for the reaction of 4-*tert*-OP and MnO<sub>2</sub>. It should be noted that only 3 dimers were found in the reaction with 4-*tert*-OP while 4 dimers were detected for

4-*n*-OP. This may be due to analytical inadequacy; however, it is also possible that only 3 dimers were formed for 4-*tert*-OP, since the steric hindrance in reactions involving R3 (Figure 5-2) may be much greater in 4-*tert*-OP than in 4-*n*-NP. More evidence is needed to confirm this speculation.

Based on the products identified, a tentative pathway was proposed (Figure 5-3). First, 4-*n*-NP or 4-*tert*-OP is adsorbed onto the surface of MnO<sub>2</sub>, forming a surface complex. One electron is transferred from 4-*n*-NP or 4-*tert*-OP to MnO<sub>2</sub>, yielding 4-*n*-NP or 4-*tert*-OP phenoxy radicals. These three radicals further couple to each other, forming four possible dimers. These dimers may be further attacked by the phenoxy radicals to form trimers. The phenoxy radicals may be also further oxidized to form hydroxylated products and hydroquinone.

#### 5.4 Conclusions

Results from this study suggest that naturally occurring MnO<sub>2</sub> has the capability to oxidize tNP, 4-*n*-NP and 4-*tert*-OP in soil, water and sediment. In addition, this study suggested that the oxidation was significant in a broad pH range from pH 4.5 to pH 8.6. However, as demonstrated by the reaction of tNP and soil in this study, the reaction of NP and OP in the environment may be substantially slower than with synthetic MnO<sub>2</sub> possibly due to the co-presence of metal ions, other clay minerals, etc. The main product of the reaction of NP and OP with MnO<sub>2</sub> were hydroquinone, hydroxylated products, dimers and trimers.

## References

- Aeschbacher, M., Graf, C., Schwarzenbach, R. P. and Sander, M. (2012). Antioxidant properties of humic substances. *Environ. Sci. Technol.* **46**(9): 4916-4925.
- Bartlett, R. and James, B. (1980). Studying dried, stored soil samples — some pitfalls. *Soil Sci. Soc. Am. J.* **44**(4): 721-724.
- Bialk, H. M., Simpson, A. J. and Pedersen, J. A. (2005). Cross-coupling of sulfonamide antimicrobial agents with model humic constituents. *Environ. Sci. Technol.* **39**(12): 4463-4473.
- Chen, W. R., Ding, Y. J., Johnston, C. T., Teppen, B. J., Boyd, S. A. and Li, H. (2010). Reaction of lincosamide antibiotics with manganese oxide in aqueous solution. *Environ. Sci. Technol.* **44**(12): 4486-4492.
- Chirkst, D. E., Cheremisina, O. V., Sulimova, M. A., Kuzhaeva, A. A. and Zgonnik, P. V. (2011). Kinetics of oxidation of phenol with manganese dioxide. *Russ. J. Gen. Chem.* **81**(4): 704-709.
- Clarke, C. E., Kielar, F., Talbot, H. M. and Johnson, K. L. (2010). Oxidative decolorization of acid azo dyes by a Mn oxide containing waste. *Environ. Sci. Technol.* **44**(3): 1116-1122.
- Domene, X., Ramirez, W., Sola, L., Alcaniz, J. M. and Andres, P. (2009). Soil pollution by nonylphenol and nonylphenol ethoxylates and their effects to plants and invertebrates. *J. Soils Sediments* **9**(6): 555-567.
- Drits, V. A., Lanson, B. and Gaillot, A. C. (2007). Birnessite polytype systematics and identification by powder X-ray diffraction. *Am. Mineral.* **92**(5-6): 771-788.



- Gabriel, F. L. P., Routledge, E. J., Heidlberger, A., Rentsch, D., Guenther, K., Giger, W., Sumpter, J. P. and Kohler, H. P. E. (2008). Isomer-specific degradation and endocrine disrupting activity of nonylphenols. *Environ. Sci. Technol.* **42**(17): 6399-6408.
- Gao, J., Hedman, C., Liu, C., Guo, T. and Pedersen, J. A. (2012). Transformation of sulfamethazine by manganese oxide in aqueous solution. *Environ. Sci. Technol.* **46**(5): 2642-2651.
- Klausen, J., Haderlein, S. B. and Schwarzenbach, R. P. (1997). Oxidation of substituted anilines by aqueous MnO<sub>2</sub>: Effect of co-solutes on initial and quasi-steady-state kinetics. *Environ. Sci. Technol.* **31**(9): 2642-2649.
- Lin, K., Liu, W. and Gan, J. (2009a). Oxidative removal of bisphenol A by manganese dioxide: Efficacy, products, and pathways. *Environ. Sci. Technol.* **43**(10): 3860-3864.
- Lin, K. D., Liu, W. P. and Gan, J. (2009b). Reaction of tetrabromobisphenol A (TBBPA) with manganese dioxide: Kinetics, products, and pathways. *Environ. Sci. Technol.* **43**(12): 4480-4486.
- Lu, Z. J., Lin, K. D. and Gan, J. (2011). Oxidation of bisphenol F (BPF) by manganese dioxide. *Environ. Pollut.* **159**(10): 2546-2551.
- Mao, Z., Zheng, X. F., Zhang, Y. Q., Tao, X. X., Li, Y. and Wang, W. (2012). Occurrence and biodegradation of nonylphenol in the environment. *Int. J. Mol. Sci.* **13**(1): 491-505.

- Marx, J. N., Argyle, J. C. and Norman, L. R. (1974). Migration of electronegative substituents. I. Relative migratory aptitude and migration tendency of the carboxy group in the dienone-phenol rearrangement. *J. Am. Chem. Soc.* **96**(7): 2121-2129.
- Murray, J. W. (1974). Surface chemistry of hydrous manganese dioxide. *J. Colloid Interface Sci.* **46**(3): 357-371.
- Neaman, A., Waller, B., Mouele, F., Trolard, F. and Bourrie, G. (2004). Improved methods for selective dissolution of manganese oxides from soils and rocks. *Eur. J. Soil Sci.* **55**(1): 47-54.
- Negra, C., Ross, D. S. and Lanzirrotti, A. (2005). Oxidizing behavior of soil manganese: Interactions among abundance, oxidation state, and pH. *Soil Sci. Soc. Am. J.* **69**(1): 87-95.
- Skipper, H. D. and Westermann, D. T. (1973). Comparative effects of propylene oxide, sodium azide, and autoclaving on selected soil properties. *Soil Biology and Biochemistry* **5**(4): 409-414.
- Soares, A., Guieysse, B., Jefferson, B., Cartmell, E. and Lester, J. N. (2008). Nonylphenol in the environment: A critical review on occurrence, fate, toxicity and treatment in wastewaters. *Environ. Int.* **34**(7): 1033-1049.
- Stone, A. T. (1987). Reductive dissolution of manganese(III/IV) oxides by substituted phenols. *Environ. Sci. Technol.* **21**(10): 979-988.

- Tebo, B. M., Bargar, J. R., Clement, B. G., Dick, G. J., Murray, K. J., Parker, D., Verity, R. and Webb, S. M. (2004). Biogenic manganese oxides: Properties and mechanisms of formation. *Annu. Rev. Earth Planet. Sci.* **32**: 287-328.
- Thiele, B., Heinke, V., Kleist, E. and Guenther, K. (2004). Contribution to the structural elucidation of 10 isomers of technical *p*-nonylphenol. *Environ. Sci. Technol.* **38**(12): 3405-3411.
- USEPA. (2006). "Non-confidential 2006 IUR company/chemical records." Retrieved March 1, 2014, from <http://cfpub.epa.gov/iursearch/index.cfm>.
- Venkatesan, A. K. and Halden, R. U. (2013). National inventory of alkylphenol ethoxylate compounds in U.S. sewage sludges and chemical fate in outdoor soil mesocosms. *Environ. Pollut.* **174**(0): 189-193.
- Vitullo, V. P. and Logue, E. A. (1972). Cyclohexadienyl cations. IV. Methoxy substituent effects in the dienone-phenol rearrangement. *The Journal of Organic Chemistry* **37**(21): 3339-3342.
- Writer, J. H., Ryan, J. N., Keefe, S. H. and Barber, L. B. (2012). Fate of 4-nonylphenol and 17 beta-estradiol in the Redwood River of Minnesota. *Environ. Sci. Technol.* **46**(2): 860-868.
- Xu, L., Xu, C., Zhao, M. R., Qiu, Y. P. and Sheng, G. D. (2008). Oxidative removal of aqueous steroid estrogens by manganese oxides. *Water Res.* **42**(20): 5038-5044.
- Ying, G. G., Williams, B. and Kookana, R. (2002). Environmental fate of alkylphenols and alkylphenol ethoxylates - a review. *Environ. Int.* **28**(3): 215-226.

- Zhang, H. C., Chen, W. R. and Huang, C. H. (2008). Kinetic modeling of oxidation of antibacterial agents by manganese oxide. *Environ. Sci. Technol.* **42**(15): 5548-5554.
- Zhao, L., Yu, Z. Q., Peng, P. A., Huang, W. L. and Dong, Y. H. (2009). Oxidative transformation of tetrachlorophenols and trichlorophenols by manganese dioxide. *Environ. Toxicol. Chem.* **28**(6): 1120-1129.

Tables

**Table 5-1** Effect of cations and humic acid on the reaction rate of 1.0 mg/L technical nonylphenol (tNP), 4-n-nonylphenol (4-n-NP) or 4-tert-octylphenol (4-tert-OP) in 100 mg/L MnO<sub>2</sub> solution at pH 5.5

cosolute	Concentration (mol/L)	Observed pseudo-first order reaction rate constant $k_{\text{observ}}(\text{min}^{-1})$		
		tNP	4-n-NP	OP
Control	No cation	0.0154 ± 0.0005	0.030 ± 0.002	0.0195 ± 0.0007
Ca <sup>2+</sup>	0.01	0.0094 ± 0.0001	0.0164 ± 0.0001	0.0013 ± 0.0001
Mg <sup>2+</sup>	0.01	0.0121 ± 0.0001	0.0216 ± 0.0001	0.0182 ± 0.0002
Mn <sup>2+</sup>	10 <sup>-5</sup>	0.0024 ± 0.0001	0.0039 ± 0.0008	0.0035 ± 0.0001
Humic acid	0.1	0.0169 ± 0.0002	0.0399 ± 0.0005	0.0203 ± 0.0002
Humic acid	10	0.0290 ± 0.0002	0.0618 ± 0.0005	0.0247 ± 0.0002

**Table 5-2** Retention time, possible category, collision energy and main m/z of MS<sup>2</sup> spectra of identified products

Product ID	Identification Method	Retention Time/min	Possible Category	Molecular Weight*	Collision Energy/Volt	Main m/z of MS <sup>2</sup> spectra
NP-1-1-A	GC-MS/MS	48.46	Dimer	438.6	10	438.6, 325.4, 311.3, 213.1
NP-1-1-B	GC-MS/MS	49.67	Dimer	438.6	10	438.6, 325.3, 213.2
NP-1-1-C	GC-MS/MS	50.30	Dimer	438.6	5	438.6, 325.3
NP-2-1	GC-MS/MS, silylation	13.1	Hydroquinone	254.3/110	5	254.3, 239.4, 72.9
NP-2-2	GC-MS/MS, silylation	30.3	Hydroxylated	380.3/236	5	380.2, 365.3, 267.2, 179.1
NP-2-3A	GC-MS/MS, silylation	46.7	Dimer	582.7/438	10	582.7, 567.7, 469.6, 357.4, 73.0
NP-2-3B	GC-MS/MS, silylation	47.3	Dimer	582.7/438	5	582.7, 469.6
NP-2-4A	GC-MS/MS, silylation	47.6	Dimer	510.2/438	20	510.2, 398.6, 285.2, 206.7
NP-2-4B	GC-MS/MS, silylation	48.1	Dimer	510.5/438	15	510.5, 495.6, 397.5, 285.2, 243.3, 179.4
NP-3-1	UPLC-MS/MS	6.67	Hydroxylated	236	15	235, 217, 132
NP-3-2	UPLC-MS/MS	8.94	Dimer	438	40	438, 323, 310, 268, 225, 212, 197, 121, 106
NP-3-3	UPLC-MS/MS	8.91	Trimer	657	50	656, 637, 543, 443
OP-1-1-A	GC-MS/MS	58.3	Trimer	614.6	5	614.6, 543.5, 431.1
OP-1-1-B	GC-MS/MS	59.4	Trimer	615.2	5	615.2, 600.0, 503.4, 338.6
OP-2-1	GC-MS/MS, silylation	24.5	Hydroxylated	366.3/222	10, 20	366.3, 295.3, 206.9, 179.1, 73.0
OP-2-2A	GC-MS/MS, silylation	39.9	Dimer	482.8/410	5	482.8, 411.5, 298.8, 250.1
OP-2-2B	GC-MS/MS, silylation	40.4	Dimer	482.7/410	10	482.7, 411.4

OP-2-3A	GC-MS/MS, silylation	54.5	Trimer	687.0/614	5	687.0, 615.7, 503.9, 487.0, 391.3
OP-2-3B	GC-MS/MS, silylation	57.4	Trimer	686.9/614	3	686.9, 615.8, 401.9
OP-2-4A	GC-MS/MS, silylation	51.5	Trimer	759.8/614	35	759.8, 687.8, 599.5, 484.7, 430.5
OP-2-4B	GC-MS/MS, silylation	52.4	Trimer	759/614	35	688.5, 618.5, 370.4
OP-3-1A	UPLC-MS/MS	8.71	Trimer	615	50	614, 542
OP-3-1B	UPLC-MS/MS	9.59	Trimer	615	50	614, 542
OP-3-1C	UPLC-MS/MS	10.65	Trimer	614	50	613, 542, 407
OP-3-2A	UPLC-MS/MS	9.69	Dimer	410	35	410, 338
OP-3-2B	UPLC-MS/MS	9.79	Dimer	410	35	410, 337
OP-3-2C	UPLC-MS/MS	10.32	Dimer	410	35	410, 338

\*If the products are identified by GC-MS/MS after silylation, two molecular weights are given: the former is after silylation, and the latter is possible molecular weight before silylation.

## Figures

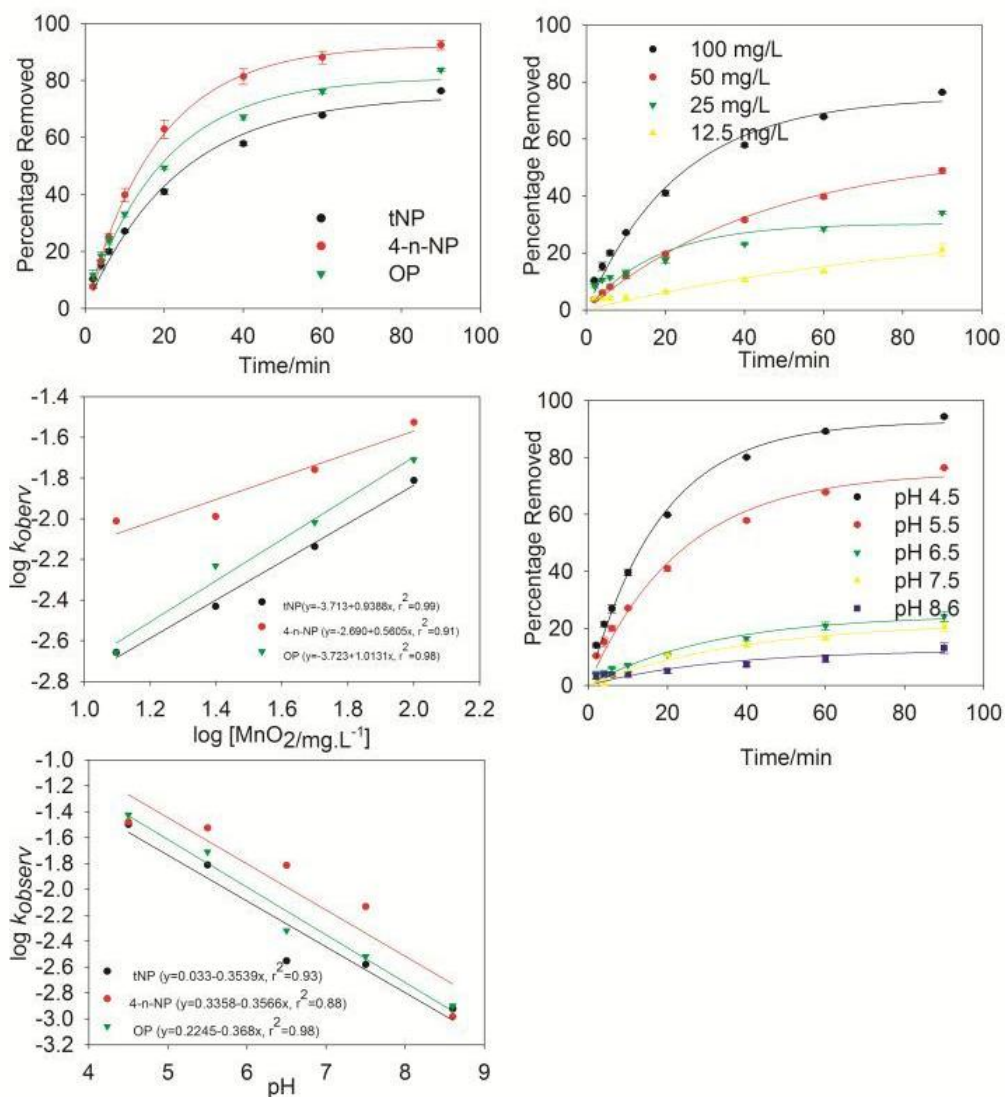


**Figure 5-1** Reaction kinetics of technical nonylphenol (tNP), 4-n-nonylphenol (4-n-NP) or 4-tert-octylphenol (4-tert-OP) at different MnO<sub>2</sub> concentrations and with different pH

(A) Removal of 1.0 mg/L tNP, 4-n-NP or OP in 100-mg/L MnO<sub>2</sub> solution at pH 5.5; (B) Removal of 1.0 mg/L tNP with different initial MnO<sub>2</sub> concentrations at pH 5.5; (C) Correlation of observed rate constant  $k_{\text{observ}}$  and MnO<sub>2</sub> concentration, with the slope indicating the reaction order with respect to MnO<sub>2</sub>; (D) Removal of 1.0 mg/L tNP by 100 mg/L MnO<sub>2</sub> at different pH; (E) Correlation of the observed reaction rate constant  $k_{\text{observ}}$  and solution pH, with the slope indicating the reaction order with respect to H<sup>+</sup>. Data points are given as mean  $\pm$  standard deviation ( $n = 3$ ).



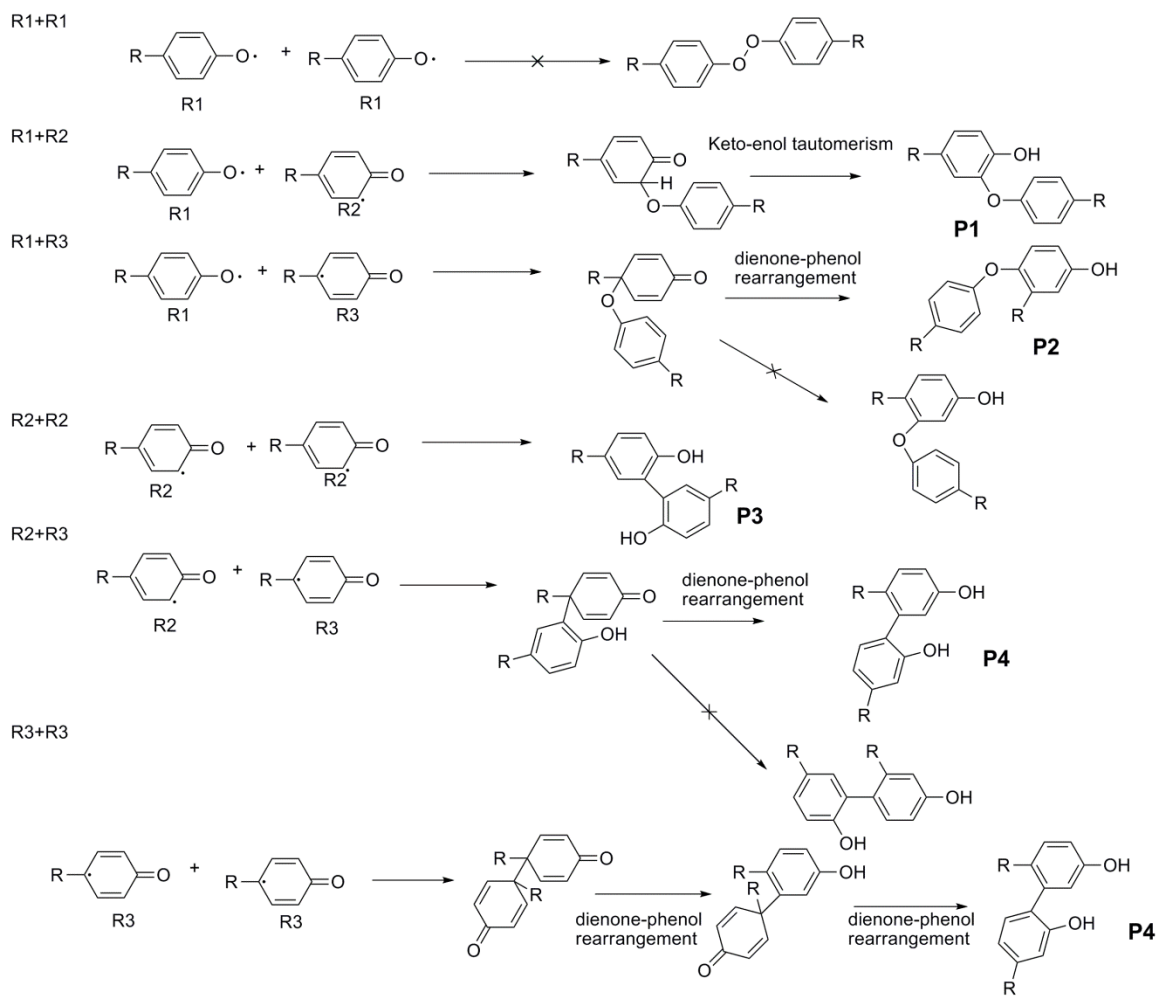


**Figure 5-2** Possible radical coupling reactions in the formation of dimers during the reaction of 4-n-nonylphenol (4-n-NP) or 4-tert-octylphenol (4-tert-OP) with  $\text{MnO}_2$

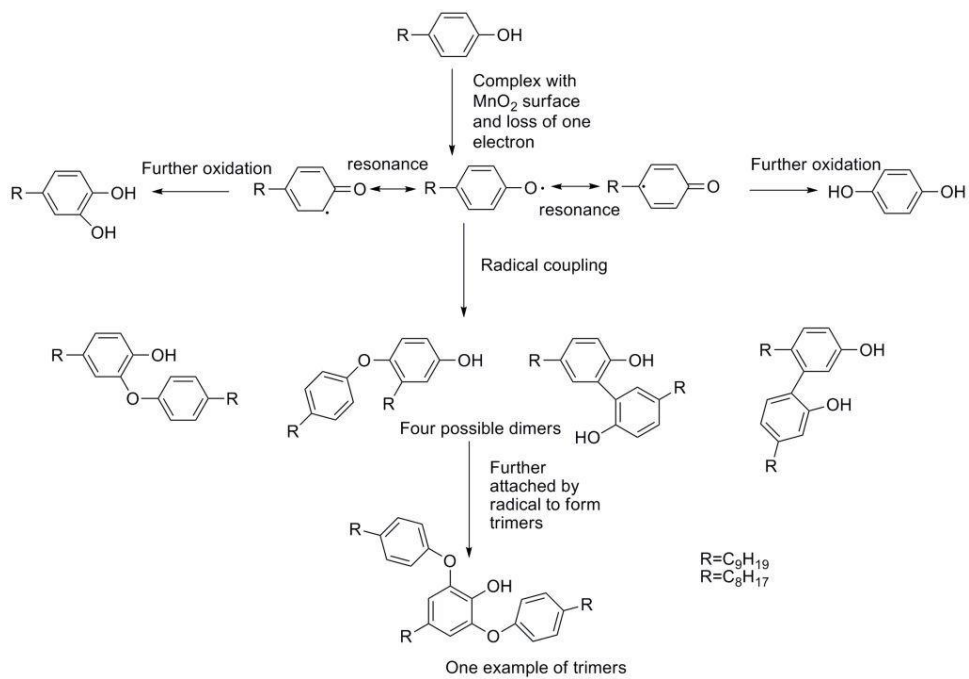


**Figure 5-3** Tentative pathways in the oxidation of 4-n-nonylphenol (4-n-NP) or 4-tert-octylphenol (4-tert-OP) by  $\text{MnO}_2$

## Supporting Information

### Text S 5-1. Chemicals Used:

Hydroquinone (99%), and analytical grade chemicals of manganese chloride (>98%), sodium permanganate (>97%), humic acid (sodium saturated), 4-morpholinepropanesulfonic acid (MOPS), 2-(cyclohexylamino) ethanesulfonic acid (CHES), L-ascorbic acid, sodium perchlorate (99+ %), perchloric acid (70% solution in water) and 4-*tert*-Octylphenol-3,5- $d_2$  solution ( $1 \mu\text{g}\cdot\text{mL}^{-1}$  in acetone) were purchased from Sigma-Aldrich (St. Louis, MO). Silylation reagent *N,O*-bis-(trimethylsilyl)-trifluoroacetamide with trimethylchlorosilane (BSTFA+TMCS, 99:1) was purchased from Supelco (Bellefonte, PA). Sodium acetate trihydrate and HPLC grade methanol and acetonitrile were all purchased from Fisher Scientific (Fair Lawn, NJ). Reagent water (18.3 M.cm resistivity) was prepared using a Barnstead Nanopure water system (Barnstead/Thermolyne, Dubuque, IA). Stock solutions of 1000 mg/L tNP, 4-*n*-NP and 4-*tert*-OP were prepared in methanol and stored at 4 °C prior to use.

### Text S2. Effect of Methanol on Recoveries and Reaction Rates

The addition of methanol greatly increased the recoveries of tNP, 4-*n*-NP and 4-*tert*-OP. With 0, 10%, 20%, 30%, 40%, 60%, 80% addition of methanol, the recoveries of tNP, 4-*n*-NP and 4-*tert*-OP were:  $55 \pm 5\%$ ,  $78 \pm 2\%$ ,  $95 \pm 1\%$ ,  $98 \pm 1\%$ ,  $98 \pm 1\%$ ,  $98 \pm 1\%$  and  $101 \pm 1\%$ ;  $43 \pm 3\%$ ,  $52 \pm 2\%$ ,  $77 \pm 1\%$ ,  $92 \pm 1\%$ ,  $96 \pm 1\%$ ,  $97 \pm 1\%$  and  $99 \pm 1\%$ ; and  $77 \pm 2\%$ ,  $92 \pm 1\%$ ,  $96 \pm 1\%$ ,  $98 \pm 1\%$ ,  $99 \pm 1\%$ ,  $101 \pm 1\%$  and  $100 \pm 1\%$ , respectively. Therefore, we select 40%

methanol addition as the reaction solvent to make sure at least 95% recovery for all the three chemicals.

The addition of methanol also inhibited the reaction. The addition of 60% and 80% methanol in the reaction with tNP, 4-*n*-NP and 4-*tert*-OP may decrease the reaction rates to  $26 \pm 2\%$ ,  $4 \pm 2\%$ ;  $17 \pm 1\%$ ,  $6 \pm 1\%$ ; and  $30 \pm 1\%$ ,  $11 \pm 1\%$  of that at the addition of 40% methanol, respectively.

### Text S5-3 Chemical Analysis

#### Analysis of NP and OP disappearance in the Reaction Solutions

Analysis of tNP, 4-*n*-NP and 4-*tert*-OP was carried out on an Agilent 1100 HPLC (Agilent Technologies, Wilmington, DE) coupled with a fluorescence detector and a Dionex Acclaim<sup>®</sup> 120 C18 column (4.6 × 250 mm, 5 μm). Isocratic mobile phase was made of acetonitrile (90%) and water (10%) at 1.0 mL/min and the excitation and emission wavelengths for the fluorescence detector were 227 and 305 nm, respectively. The typical retention times for tNP, 4-*n*-NP and 4-*tert*-OP were 7.4, 9.6 and 5.8 min, respectively. It should be noted that on the chromatogram, tNP appeared as a series peaks ranged from about 6 min to about 9 min due to its composition of many isomers.

#### Extraction and Analysis of Low Concentrations of Technical Nonylphenol

After quenched by 0.5 mL 50mg/mL L-ascorbic acid, 50 μL of 10 mg/L 4-*n*-NP was added to the reaction suspension as the recovery surrogate. The suspension was then extracted by shaking with 15 mL hexane for 1 h twice. The hexane was combined and

condensed to about 1 mL under gentle nitrogen flow. An addition of 25  $\mu\text{L}$  1 mg/L 4-*tert*-Octylphenol-3,5- $\text{d}_2$  in acetone was the internal standard. This liquid-liquid extract achieved high efficacy with the recovery  $98 \pm 3\%$ . To further validate the method when extracting soil suspension, the filtered soil was freezing dried and extracted by Dionex ASE 350 at 50  $^\circ\text{C}$  and 1500 psi with 50:50 acetone and hexane, 2 cycles, static time 5 min, flush volume 60% and finally purged with nitrogen for 100 s. The extract contained no significant level of tNP.

The samples were analyzed on Agilent 6890 GC coupled with 5973 MSD (Agilent Technologies, Wilmington, DE). . Samples (2  $\mu\text{L}$ ) were introduced into the inlet at 250  $^\circ\text{C}$  and the separation was achieved on a DB-5MS Ultra Inert capillary column (60m  $\times$  0.25 mm  $\times$  0.25  $\mu\text{m}$ , Agilent, Wilmington, DE). The carrier gas was helium (99.999%) and the flow rate was set at 1.0 mL/min. The column temperature was initially programmed at 80  $^\circ\text{C}$  for 0 min, then ramped to 160  $^\circ\text{C}$  at 10  $^\circ\text{C}/\text{min}$  and held for 42 min, and then ramped to 300  $^\circ\text{C}$  at 30  $^\circ\text{C}/\text{min}$  for 3 min. The mass spectrometer was operated in EI SIM mode at 70 eV.  $m/z$  137 was used for quantification the internal standard and  $m/z$  107 was used for recovery surrogate and  $m/z$  121, 135, 149, 163, 177 and 191 were used for tNP. Totally, 19 peaks were separated from tNP.

#### Identification of Reaction Products by GC-MS/MS

Briefly, for the identification of products by GC-MS/MS, after 4 h of reaction, 50 mL of the reaction mixture (pH 5.5) with initially 20 mg/L 4-*n*-NP or 4-*tert*-OP and 100 mg/L  $\text{MnO}_2$  was extracted with 15 mL methylene chloride for three consecutive times. The

extract was condensed to near dryness, followed by dissolution in 1.0 mL hexane-acetone (1: 1, v: v). The samples were analyzed directly or after derivatization by adding 150  $\mu$ L of *N,O*-bis(trimethylsilyl)trifluoroacetamide (BSTFA) with 1% trimethylsilyl chloride (TMCS) on a GC-MS/MS.

A Varian 3800 GC (Varian Instruments, Sunnyvale, CA) coupled with a Varian 1200 triple-quadrupole mass spectrometer and a CombiPal autosampler (CTC Analytics, Zwingen, Switzerland) were used. Samples (1  $\mu$ L) were introduced into the inlet at 260  $^{\circ}$ C and the separation was achieved on a DB-5ms capillary column (30m  $\times$  0.25 mm  $\times$  0.25  $\mu$ m, Agilent, Wilmington, DE). The carrier gas was helium (99.999%) and the flow rate was set at 1.0 mL/min. The column temperature was initially programmed at 80  $^{\circ}$ C for 3.0 min, then ramped to 300  $^{\circ}$ C at 5  $^{\circ}$ C/min, and held at 300  $^{\circ}$ C for 20 min. The triple-quadrupole mass spectrometer was operated in EI daughter scan mode at 70 eV. The transfer line, ion source, and manifold temperatures were set at 300, 170, and 40  $^{\circ}$ C, respectively. Argon (99.999%) in 2.0-2.1 mTorr was used as the collision gas, and a 5 min solvent delay and extended dynamic range (EDR) were enabled for the detector.

#### Identification of Reaction Products by UPLC-MS/MS

For the identification by UPLC-MS/MS, after 4 h of reaction, 20 mL reaction solution with 250 mg/L 4-*n*-NP or 4-*tert*-OP and 500 mg/L MnO<sub>2</sub> was quenched and analyzed. An ACQUITY UPLC system (Waters, Milford, MA) consisting of binary solvent manager and sample manager was used. Chromatographic separation of compounds was performed at 40 $^{\circ}$ C, using ACQUITY UPLC BEH C18 column (2.1 $\times$ 100 mm, 1.7  $\mu$ m

particle size, Waters). Mobile phase A was water and mobile phase B was methanol. The following gradient was used: 0-3 min, 10% to 50% B; 3-8 min, 50% to 100% B; 8-15 min, 100% B; 15-17 min, and re-equilibrate with 10% B. The flow rate of mobile phase was 0.2 ml/min, and the sample volume injected was 5  $\mu$ l. Analytes were determined using a Waters Micromass triple quadrupole detector equipped with an electrospray ionization (ESI) source. Data acquisition was performed in negative ESI mode and the optimized MS parameters were as follows: source temperature, 120  $^{\circ}$ C; desolvation temperature, 350  $^{\circ}$ C; capillary voltage, 3.2 kV; cone voltage, 30 V; desolvation gas flow, 600 L/h and cone gas flow, 50 L/h. The collision gas (Argon, 99.999%) flow in the collision cell was kept at 0.2 ml/min. All data were acquired and processed using MassLynx 4.1 software.

#### Text S 5-4 Derivation of Kinetic Expression

The reaction rates of these compounds and  $\text{MnO}_2$  may be described as:

$$r = \frac{d[\text{substrate}]}{dt} = k[\text{substrate}]^a [\text{MnO}_2]^b [\text{H}^+]^c \quad (1)$$

where  $r$  is the reaction rate, (substrate) is the concentration of tNP, 4-*n*-NP or 4-*tert*-OP,  $k$  is the rate constant, ( $\text{MnO}_2$ ) and ( $\text{H}^+$ ) are the concentrations of  $\text{MnO}_2$  and  $\text{H}^+$ , respectively and  $a$ ,  $b$  and  $c$  are the reaction orders with respect to substrate,  $\text{MnO}_2$  and  $\text{H}^+$ , respectively. In this study, pH was kept constant during the reaction using different pH buffers and the initial concentrations of  $\text{MnO}_2$  (usually 100 mg/L) were much higher than

the initial substrate concentration (i.e., 1 mg/L). Therefore, the concentrations of MnO<sub>2</sub> and H<sup>+</sup> were almost constant during the reaction, and Equation 1 may be written as:

$$r = \frac{d[\text{substrate}]}{dt} = k[\text{substrate}]^a [\text{MnO}_2]_0^b [\text{H}^+]_0^c \quad (2)$$

where [MnO<sub>2</sub>] and [H<sup>+</sup>] are the initial concentrations of MnO<sub>2</sub> and H<sup>+</sup>, respectively. Under the conditions with fixed pH and initial MnO<sub>2</sub> concentration, Equation 2 can be simplified as:

$$r = \frac{d[\text{substrate}]}{dt} = k_{\text{observ}}[\text{substrate}]^a \quad (3)$$

$$k_{\text{observ}} = k[\text{MnO}_2]_0^b [\text{H}^+]_0^c \quad (4)$$

where  $k_{\text{observ}}$  is the observed rate constant. If the reaction order for substrate is 1 (i.e.,  $a = 1$ ), the reaction is a pseudo-first-order reaction. Equation 3 can be written in a linear form:

$$\ln[\text{substrate}] = -k_{\text{observ}}t + \ln[\text{substrate}]_0 \quad (5)$$

where [substrate] is the initial concentration of tNP, 4-*n*-NP or 4-*tert*-OP.

When logarithmic concentrations of tNP, 4-*n*-NP or 4-*tert*-OP were plotted against the reaction time, all curves became linear with  $R^2 \geq 0.93$  ( $P < 0.05$ ). Therefore, the reaction orders with respect to the three substrates were clearly 1.0, with the slopes of the linearized curves representing the pseudo-first-order rate constant  $k_{\text{observ}}$  (min<sup>-1</sup>). The logarithmic form of Equation 4 is:



$$\log_{10} k_{\text{observ}} = b \log_{10} [\text{MnO}_2]_0 + \log_{10} k [\text{H}^+]_0^c \quad (6)$$

Or

$$\log_{10} k_{\text{observ}} = c \cdot \log_{10} [\text{H}^+]_0 + \log_{10} k [\text{MnO}_2]_0^b = -c \cdot \text{pH} + \log_{10} k [\text{MnO}_2]_0^b \quad (7)$$

In Equations 6 and 7, logarithm based on 10 is used instead of natural logarithm to be consistent with pH. Therefore, when plotting the  $\log_{10} k_{\text{observ}}$  against the  $\log_{10} [\text{MnO}_2]$  or pH, the slope of the linearized curve would be the order of  $\text{MnO}_2$  or pH.

**Table S 5–1** Properties of high Mn content soil

Depth (cm)	Texture	Particle Size (%)				pH		TOC (g/kg)	CEC (me/100g soil)	pH 7*
		Sand	Silt	Clay	1:1 H <sub>2</sub> O	1 mol/L KCl				
232-256	Silty clay	11.3	45.5	43.2	6.2	7.0	2.3	0.45		

\*This soil has a high content of goethite, so the CEC value is obtained by the sum of by sum of exchangeable cations plus exchangeable acidity.

**Table S 5–2** Concentrations of 4-n-NP, tNP and 4-tert-OP in the MnO<sub>2</sub>-free controls at pH 5.5 compare to their initial concentrations

Time/min	tNP (%)	4-n-NP (%)	4-tert-OP (%)
5	100.3±0.8	100.3±0.2	99.6±0.6
10	100.4±0.8	100.7±0.1	100.1±0.4
20	99.7±0.7	100.7±0.1	100.0±0.3
40	100.2±0.6	100.7±0.2	100.0±0.1
60	100.1±0.9	99.1±2.3	99.3±0.8
90	100.3±0.8	100.3±0.6	99.9±0.8

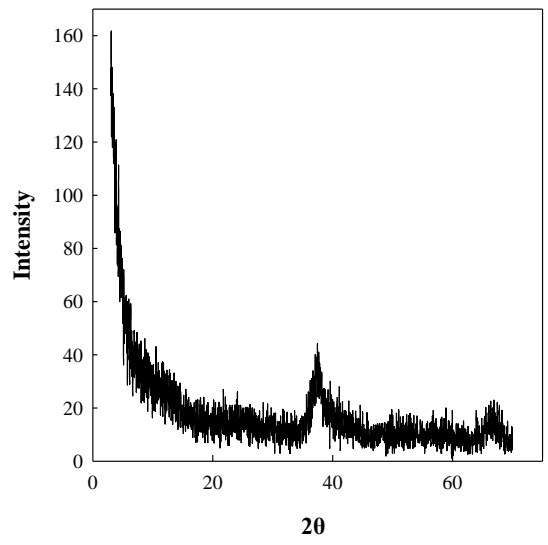


**Figure S 5–1** X-ray diffractogram of MnO<sub>2</sub>

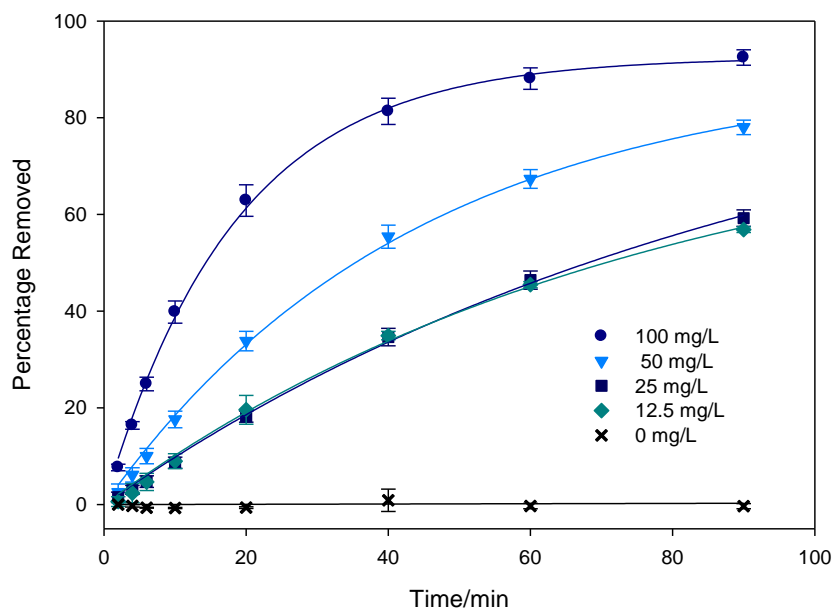


**Figure S 5–2** Removal of 1.0 mg/L 4-n-NP with different initial MnO<sub>2</sub> loadings (100 mg/L, 50 mg/L, 25 mg/L and 12.5 mg/L) at pH 5.5

Data points are given as mean  $\pm$  standard deviation (n = 3).

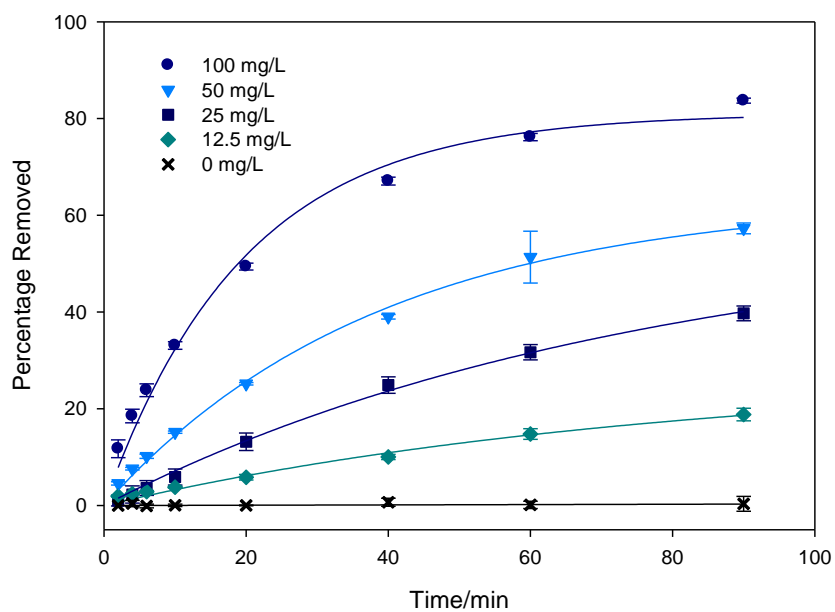


**Figure S 5–3** Removal of 1.0 mg/L OP with different initial MnO<sub>2</sub> loadings (100 mg/L, 50 mg/L, 25 mg/L and 12.5 mg/L) at pH 5.5

Data points are given as mean  $\pm$  standard deviation (n = 3).

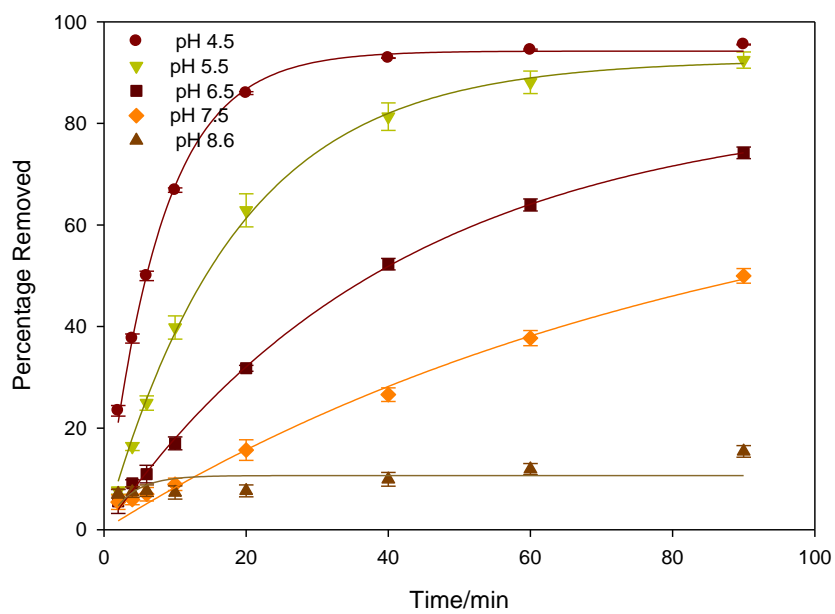


**Figure S 5–4** Removal of 1.0 mg/L 4-n-NP by 100 mg/L MnO<sub>2</sub> at different pH

Data points are given as mean  $\pm$  standard deviation (n = 3).

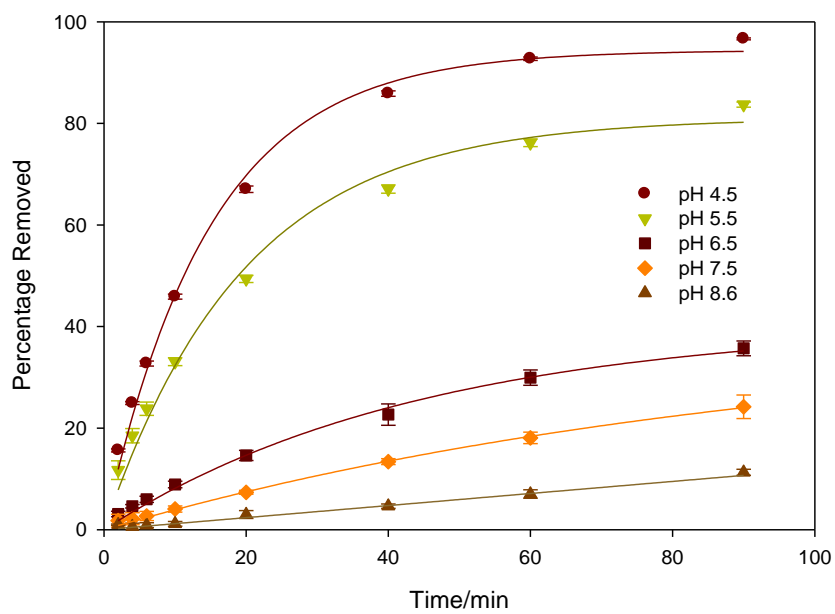


**Figure S 5–5** Removal of 1.0 mg/L OP by 100 mg/L MnO<sub>2</sub> at different pH

Data points are given as mean  $\pm$  standard deviation (n = 3).



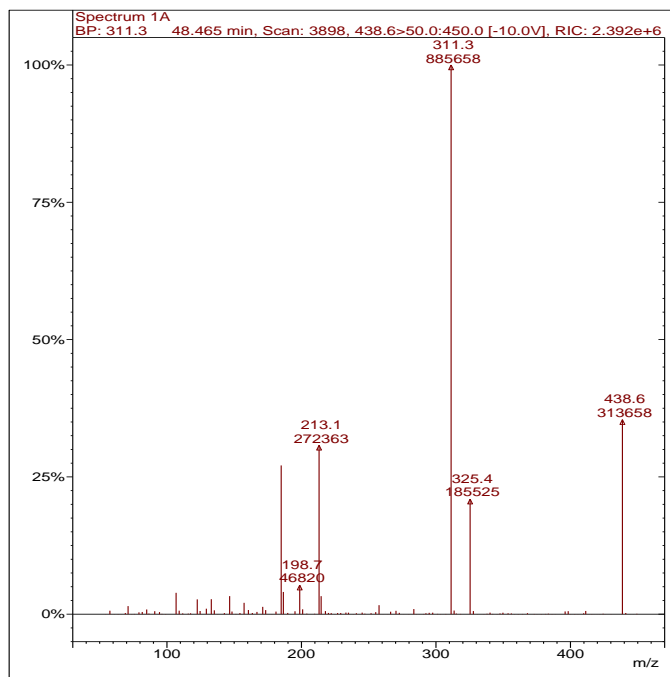


**Figure S 5–6** GC-MS-MS spectra of NP-1-1-A at retention time 48.46 min, a dimer of nonylphenol

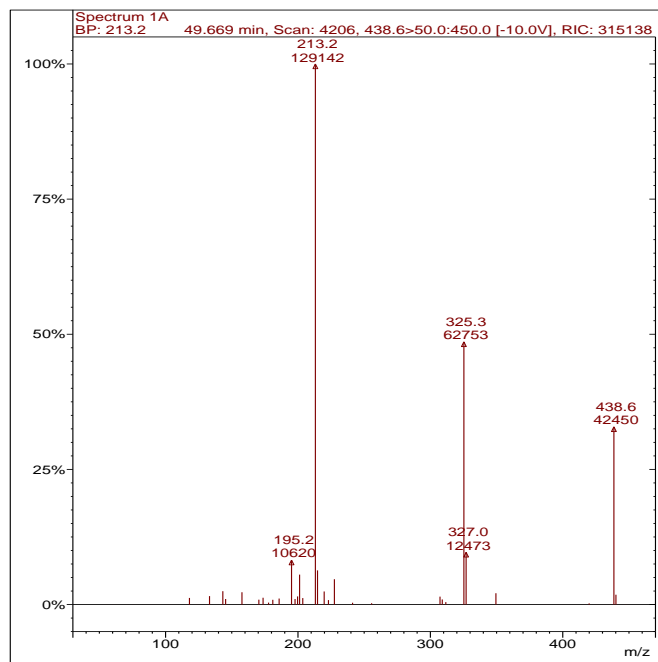
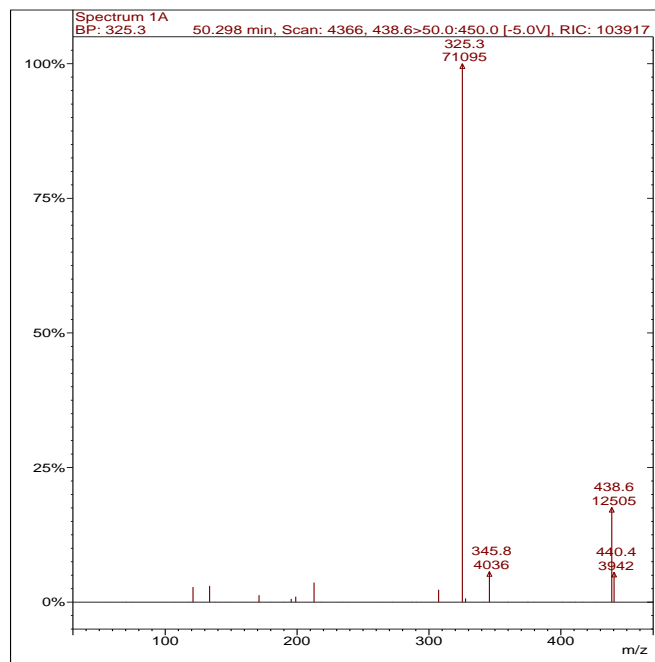
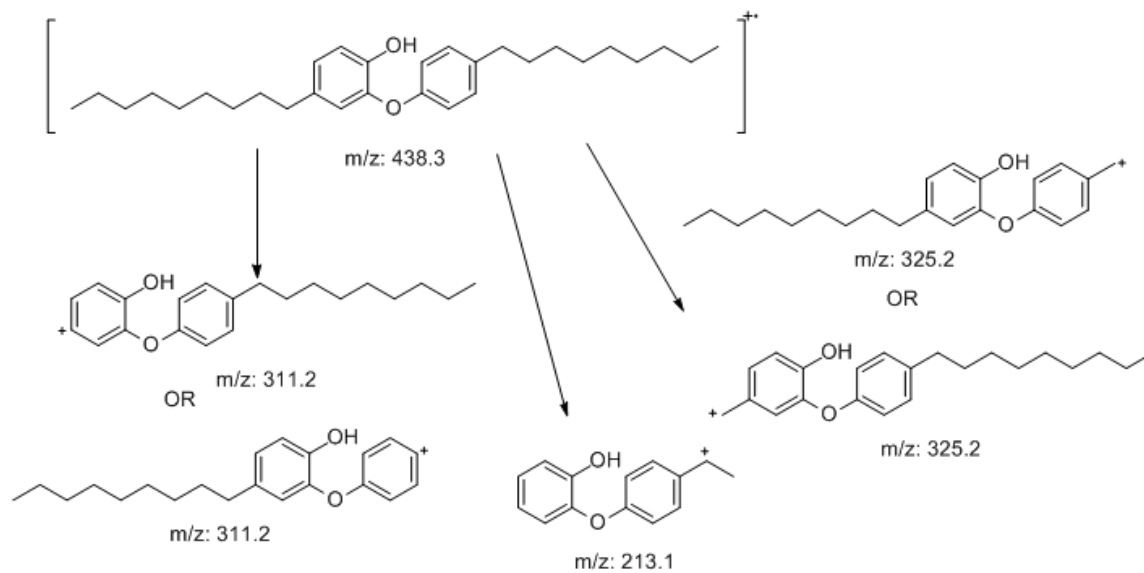


Figure S 5-7 GC-MS-MS spectra of NP-1-1-B at retention time 49.67 min, a dimer of nonylphenol



**Figure S 5-8** GC-MS-MS spectra of NP-1-1-C at retention time 50.30, a dimer of nonylphenol.



**Figure S 5–9** Possible ion fragment assignments of products NP-1-1-A, B, C, dimmers of nonylphenol

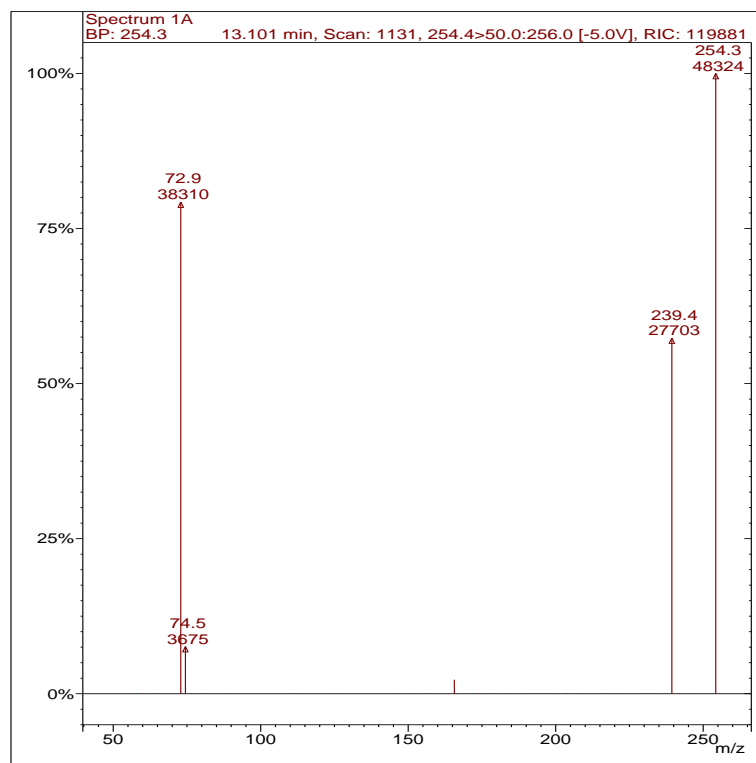


**Figure S 5–10** GC-MS-MS spectra of NP-2-1 at retention time 13.1 min, hydroquinone silylated

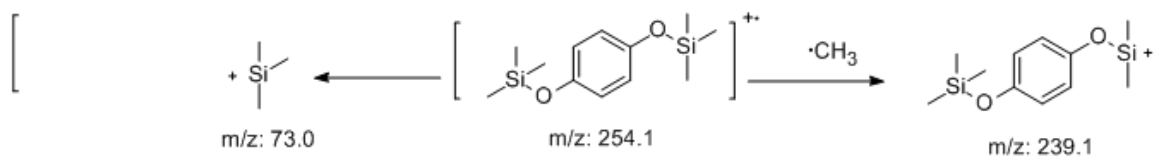


**Figure S 5-11** Possible ion fragment assignments of products NP-2-1, hydroquinone silylated

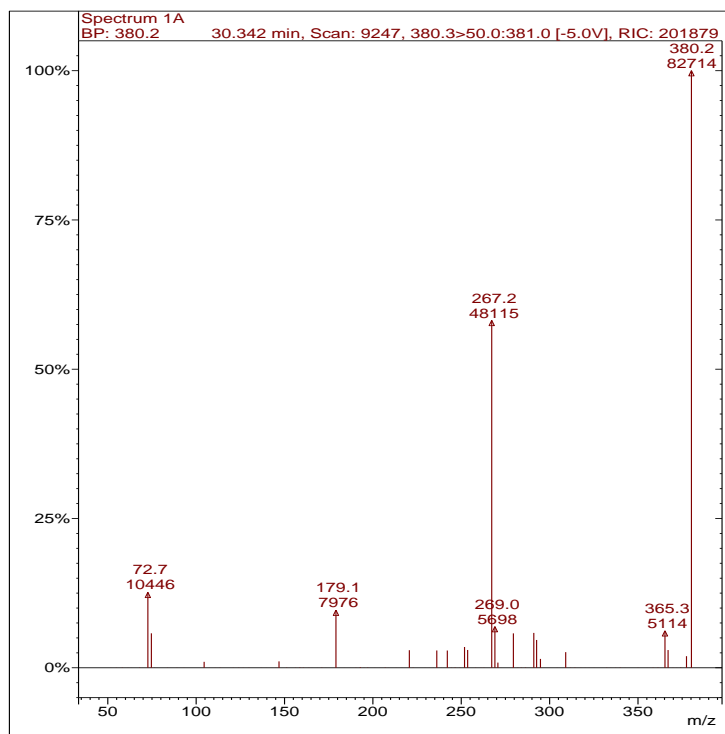


**Figure S 5–12** GC-MS-MS spectra of NP-2-2 at retention time 30.3 min, hydroxylated nonylphenol, silylated

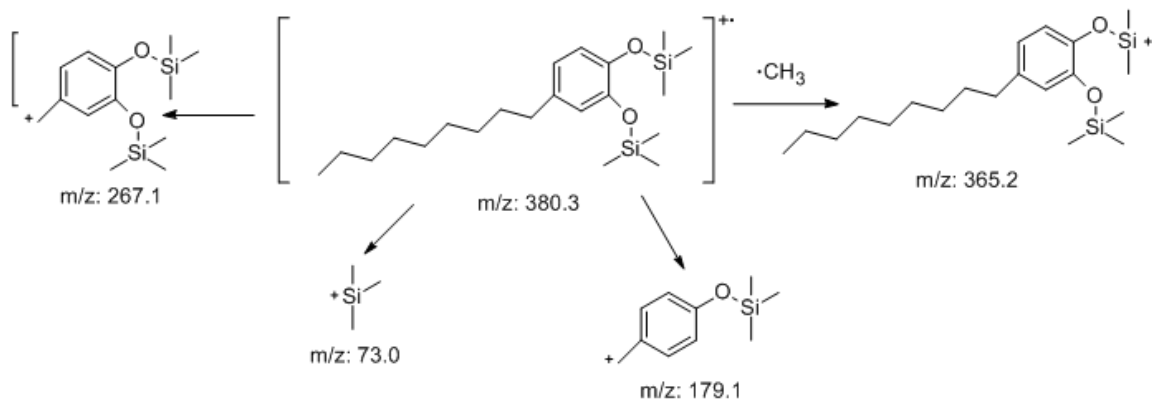


**Figure S 5–13** Possible ion fragment assignments of products NP-2-2



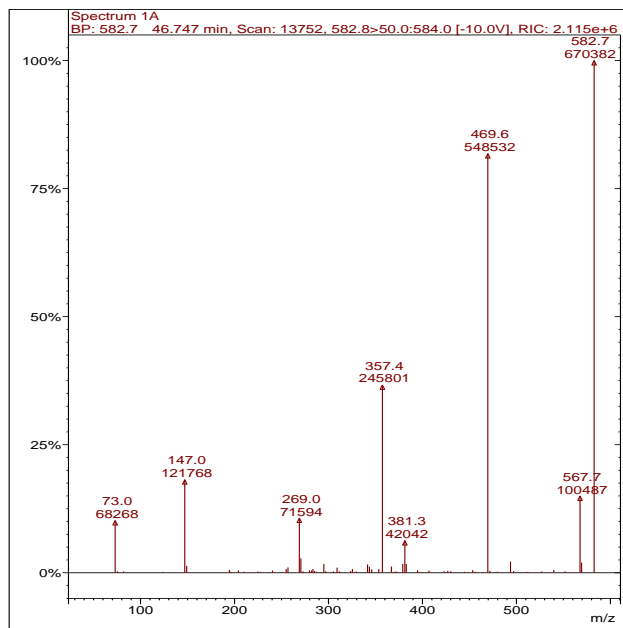
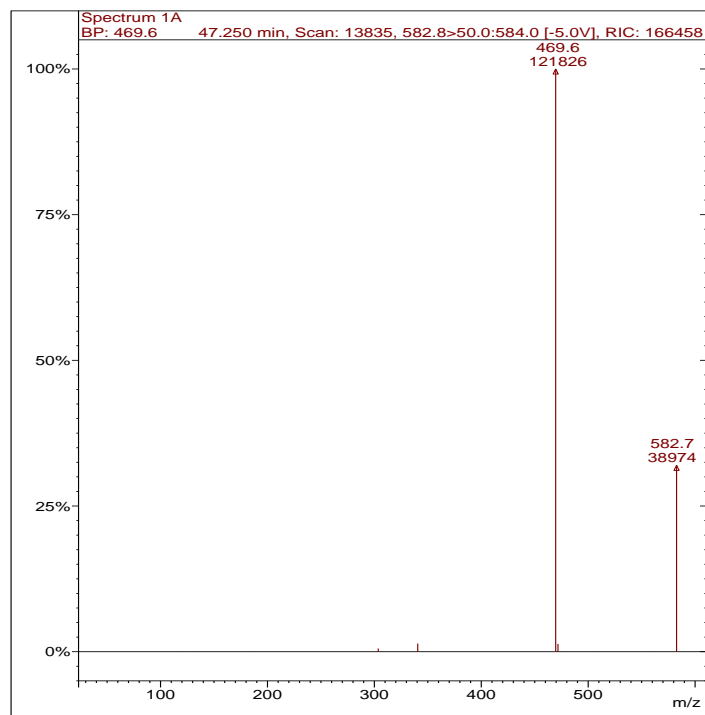
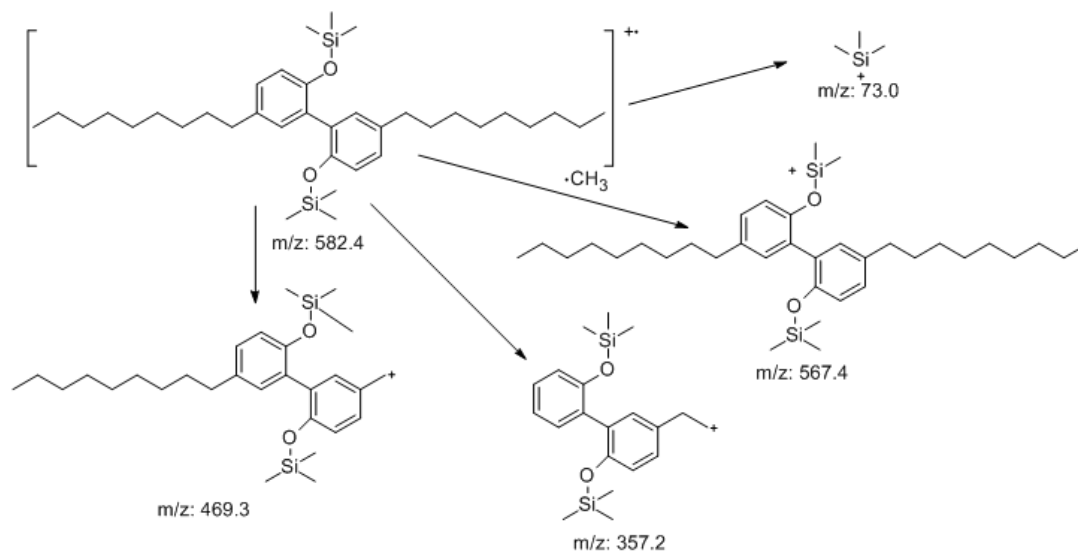


Figure S 5-14 GC-MS-MS spectra of NP-2-3A at retention time 46.7 min, dimer of nonylphenol, silylated



**Figure S 5–15** GC-MS-MS spectra of NP-2-3B at retention time 47.3 min, dimer of nonylphenol, silylated



**Figure S 5-16** Possible ion fragment assignments of products NP-2-3A/B

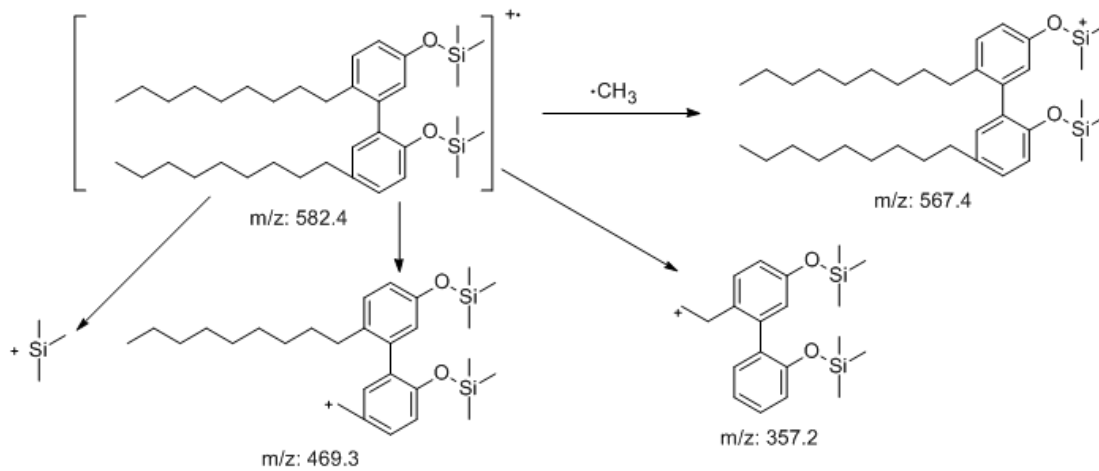


**Figure S 5-17** Another Possible ion fragment assignments of products NP-2-3A/B

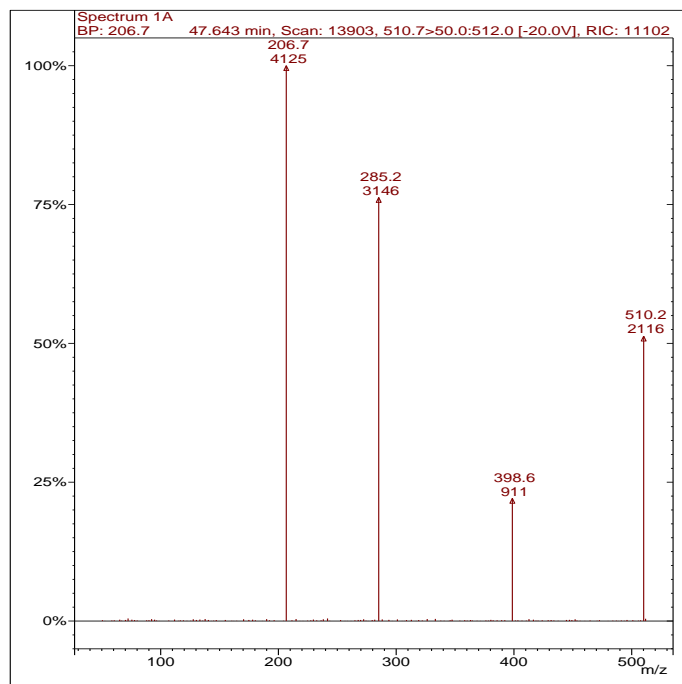


**Figure S 5–18** GC-MS-MS spectra of NP-2-4A at retention time 47.6 min, dimer of nonylphenol, silylated.

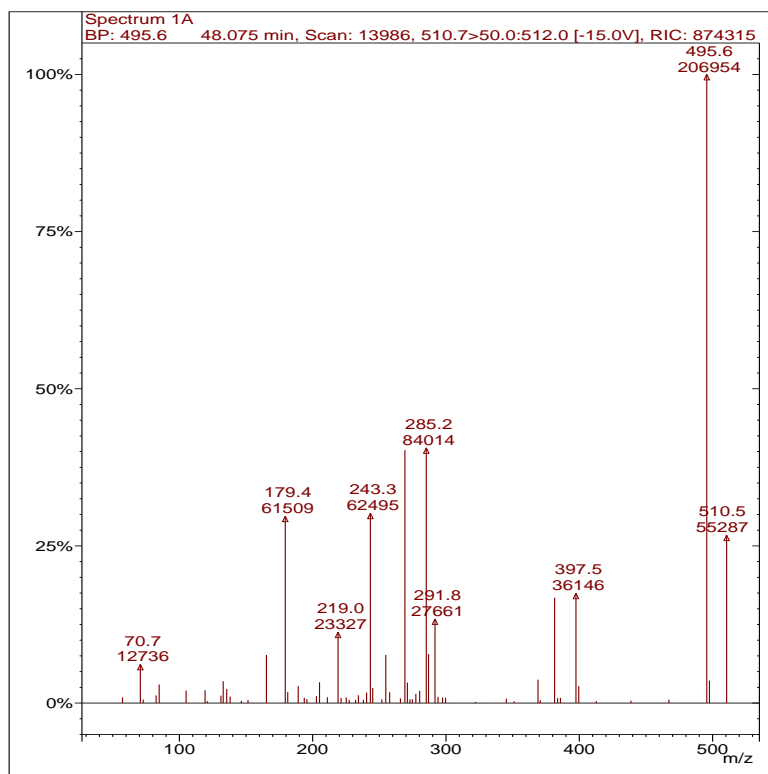
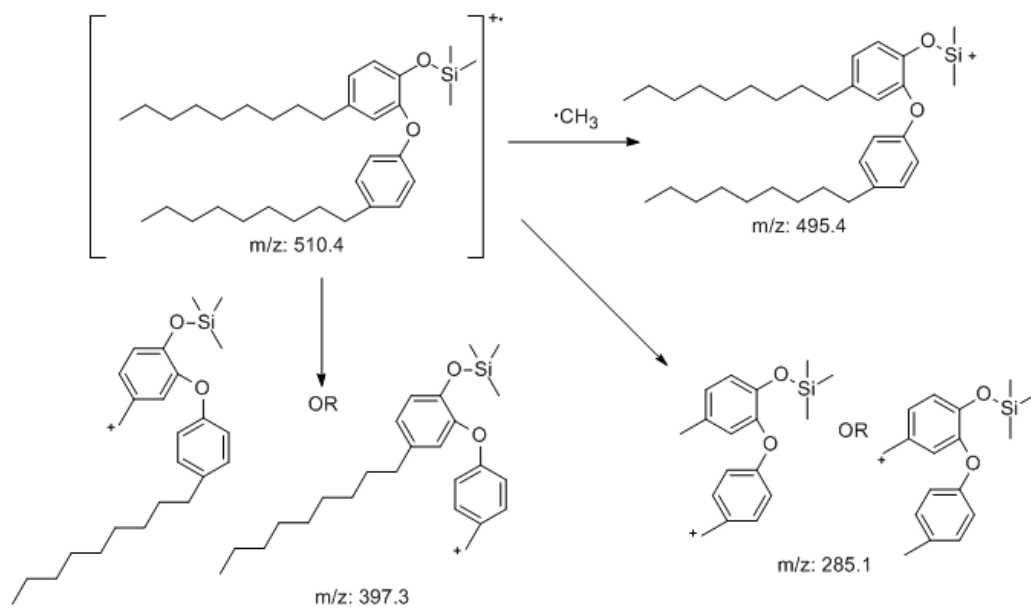
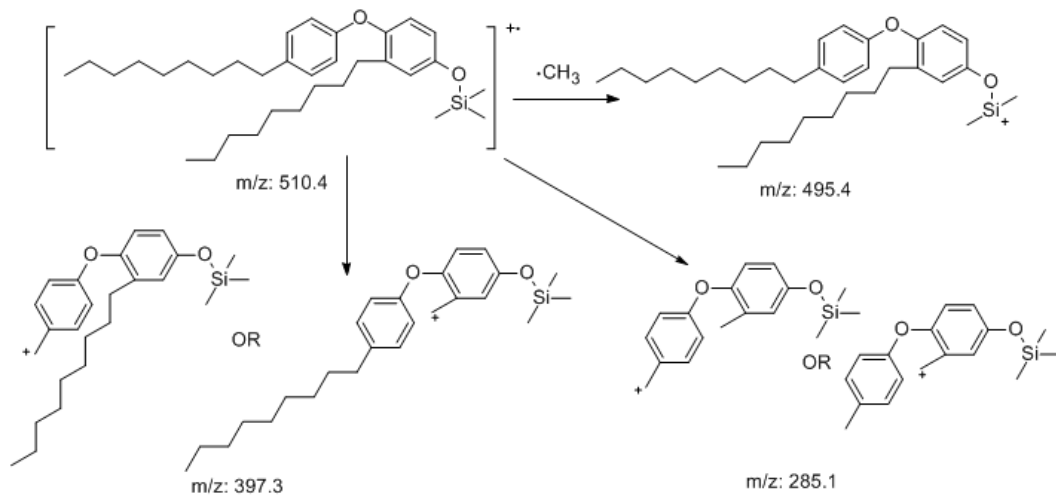


Figure S 5–19 GC-MS-MS spectra of NP-2-4B at retention time 48.1 min, dimer of nonylphenol, silylated



**Figure S 5–20** Possible ion fragment assignments of products NP-2-4A/B



**Figure S 5–21** Another Possible ion fragment assignments of products NP-2-4A/B



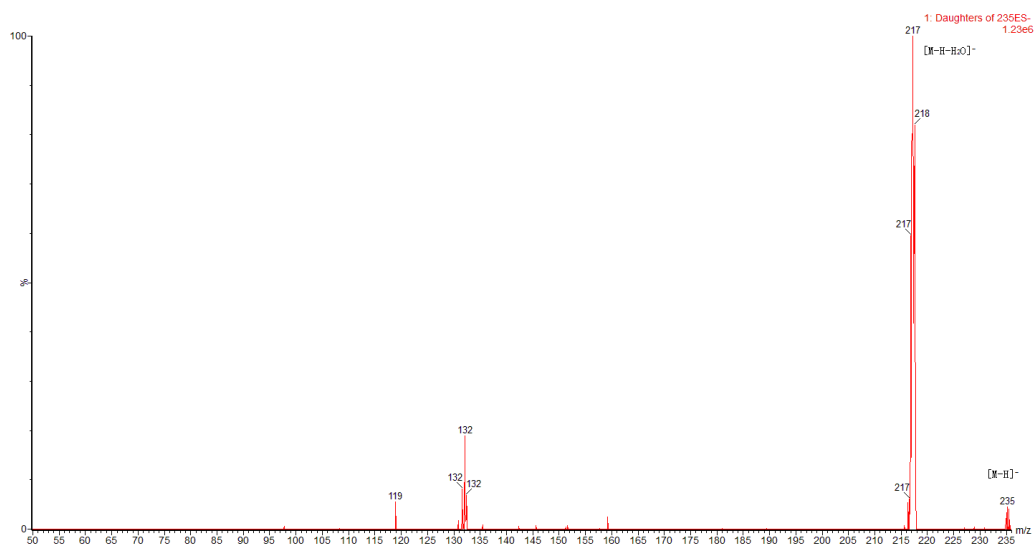


**Figure S 5-22** UPLC-MS-MS spectra of NP-3-1 at retention time 6.67 min, hydroxylated nonylphenol

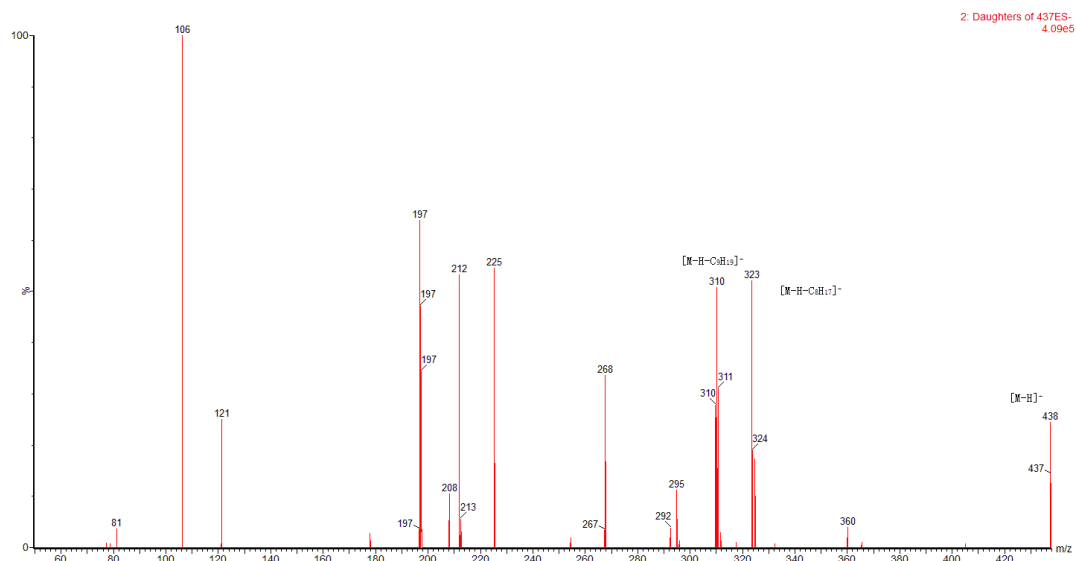


**Figure S 5–23** UPLC-MS-MS spectra of NP-3-2 at retention time 8.94 min, dimer of nonylphenol

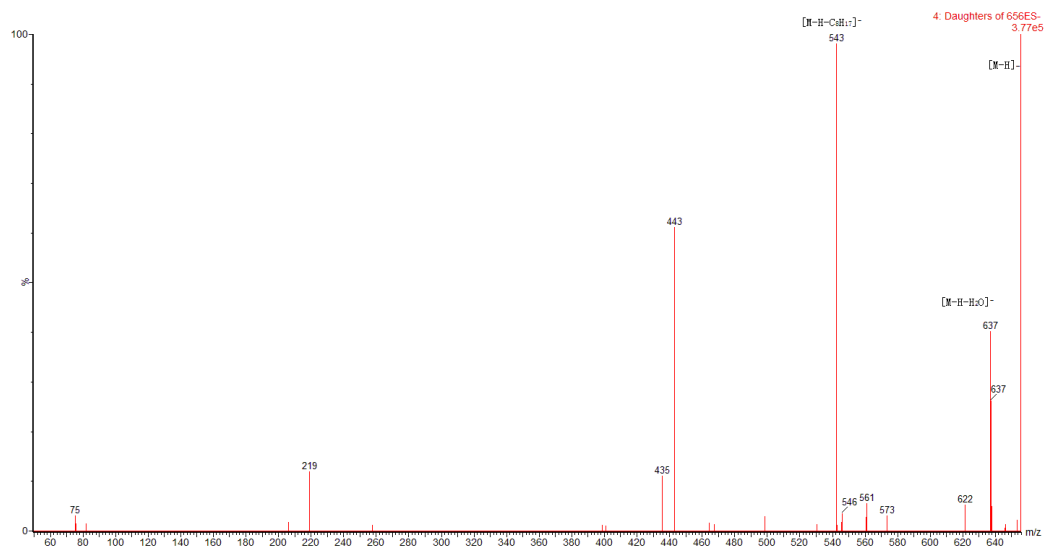


**Figure S 5–24** UPLC-MS-MS spectra of NP-3-3 at retention time 8.91 min, trimer of nonylphenol

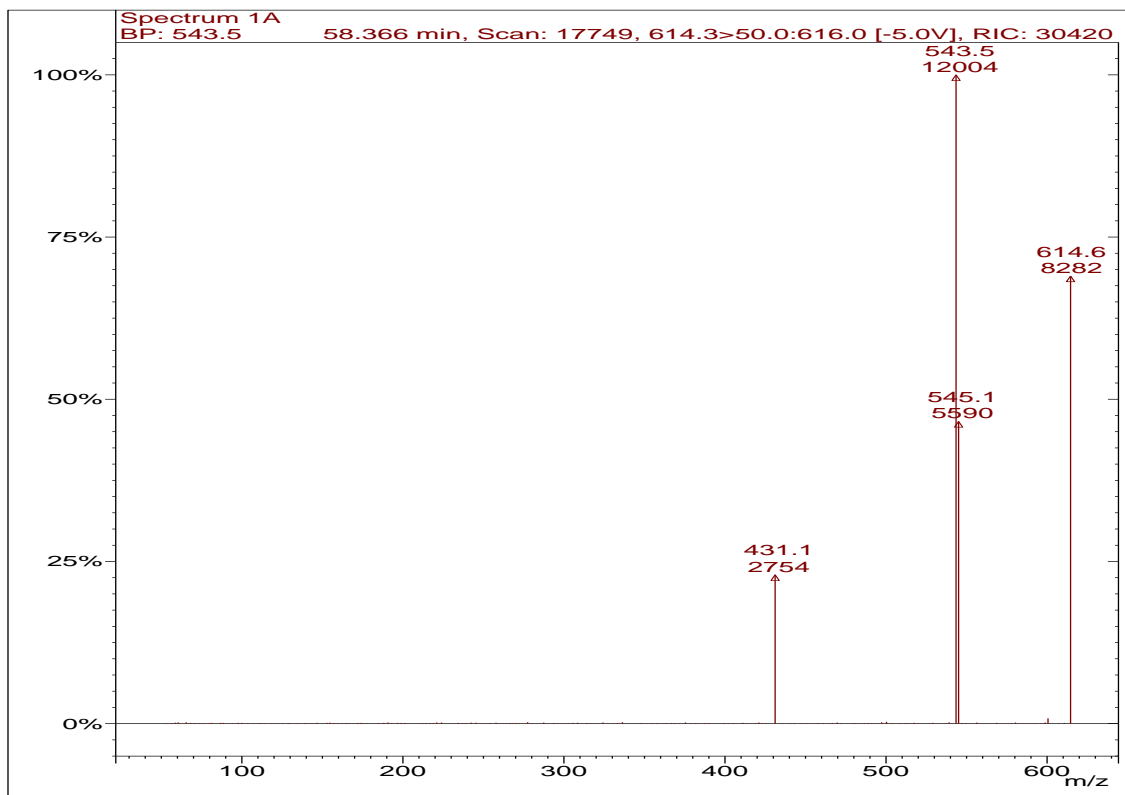


Figure S 5–25 GC-MS-MS spectra of OP-1-1A at retention time 58.3 min, trimmer of octylphenol

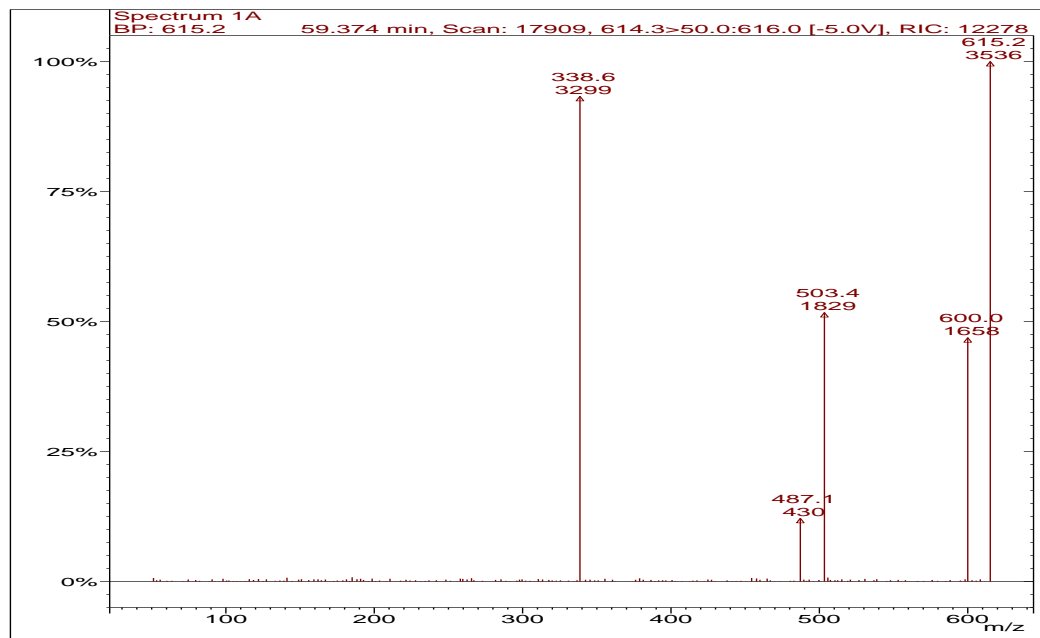
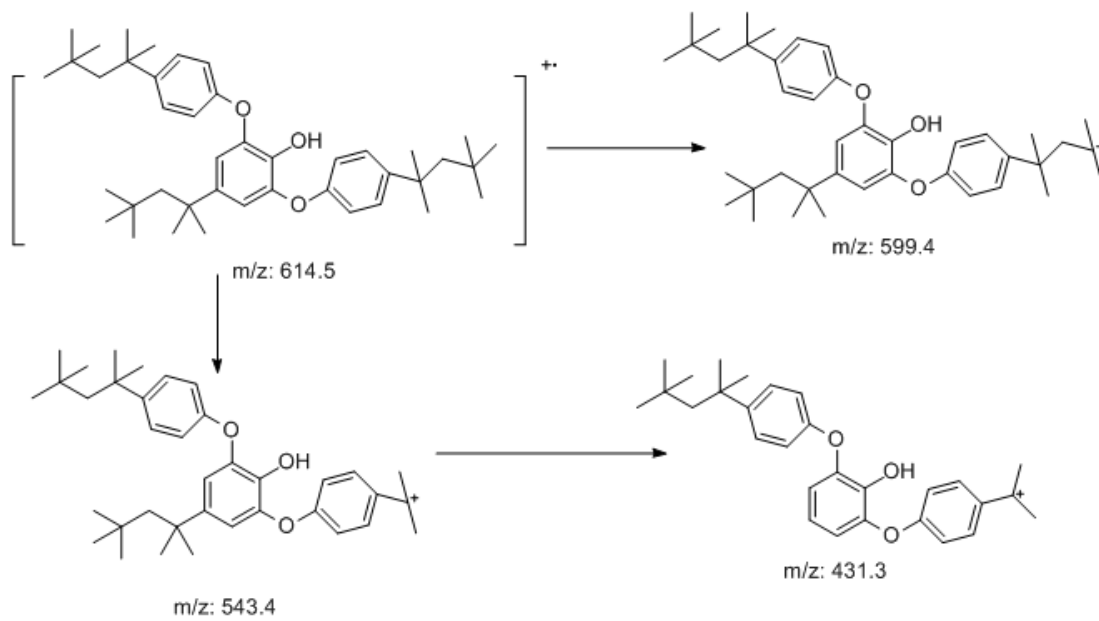
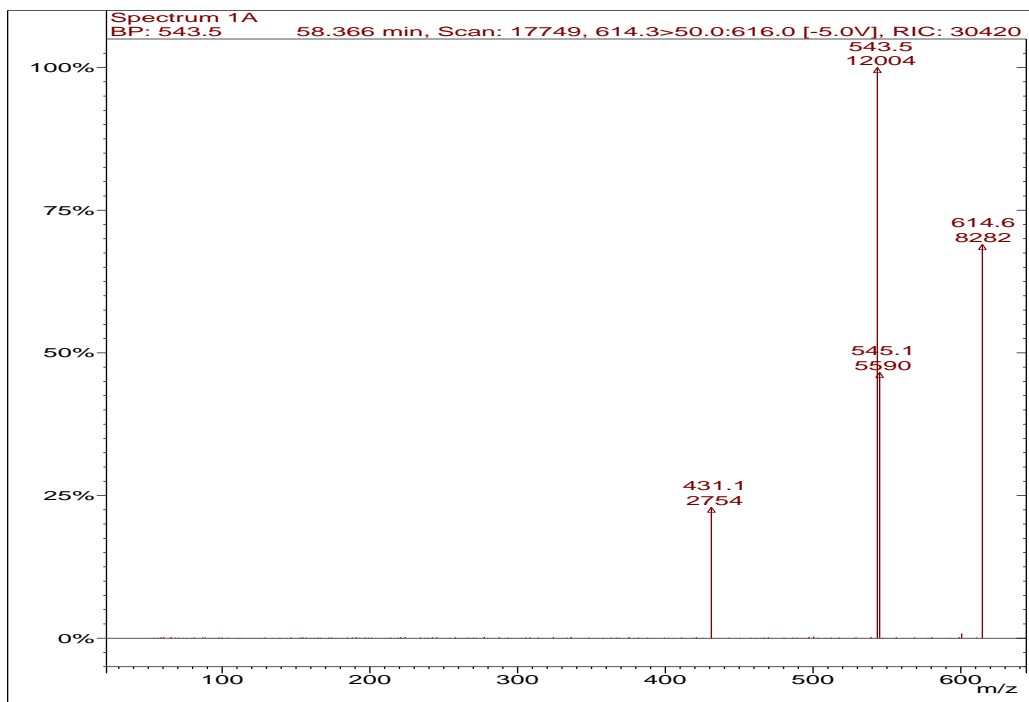


Figure S 5-26 GC-MS-MS spectra of OP-1-1B at retention time 59.4 min, trimmer of octylphenol



**Figure S 5–27** One possible ion fragmentation of Product OP-1-1A/B



**Figure S 5–28** GC-MS-MS spectra of OP-2-1 at retention time 24.5 min, hydroxylated octylphenol, silylated

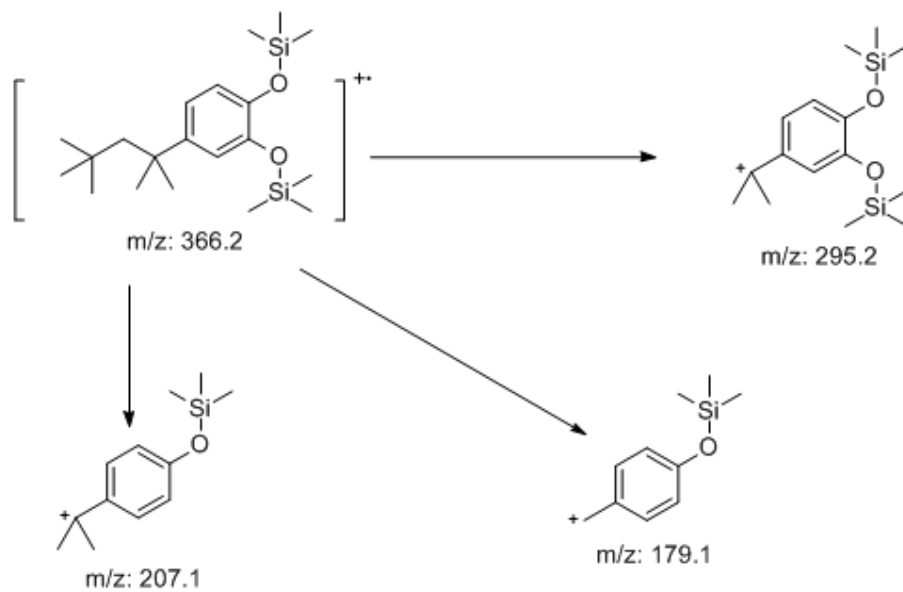


**Figure S 5–29** Possible ion fragmentation of Product OP-2-1



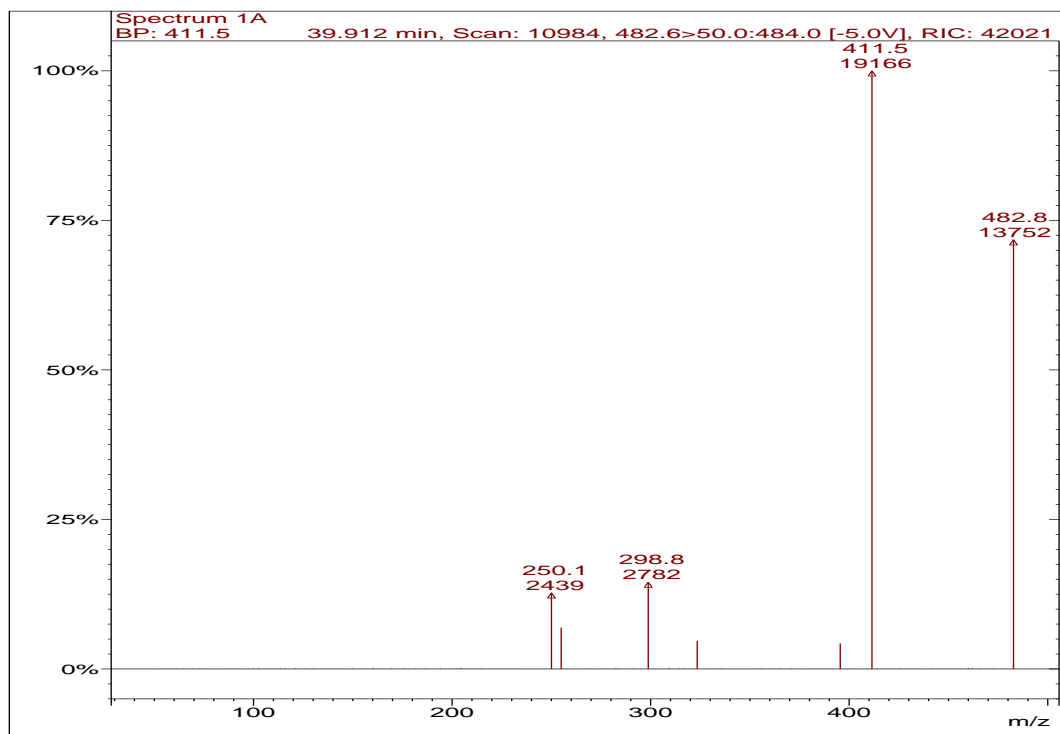


**Figure S 5-30** GC-MS-MS spectra of OP-2-2A at retention time 39.9 min, dimer of octylphenol, silylated

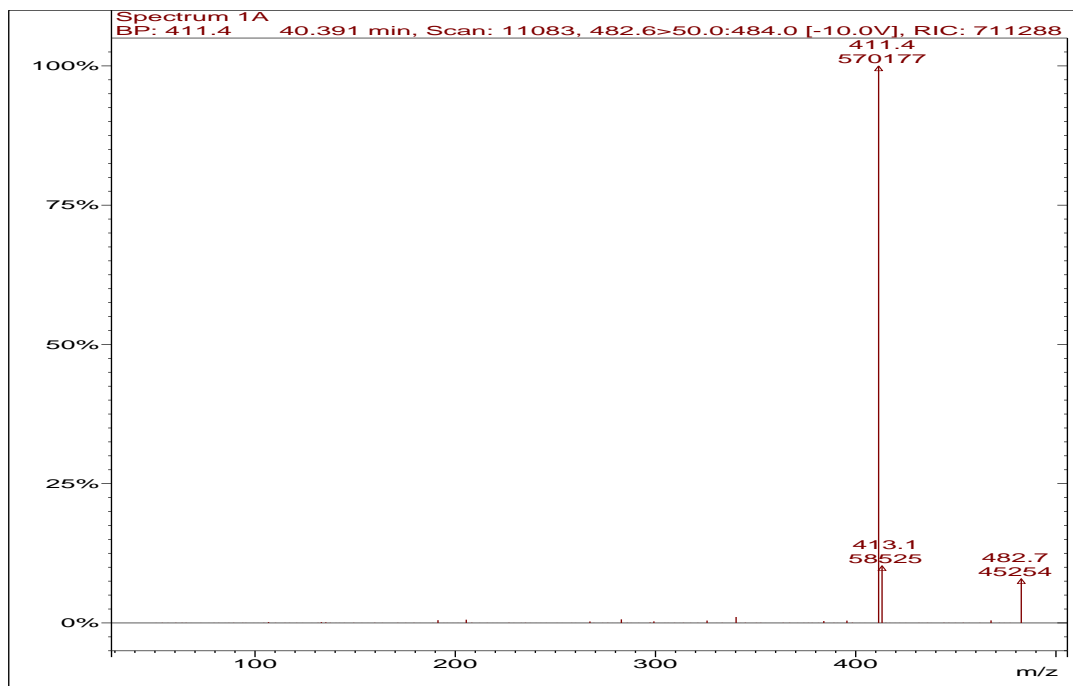


**Figure S 5-31** GC-MS-MS spectra of OP-2-2B at retention time 40.4 min, dimer of octylphenol, silylated

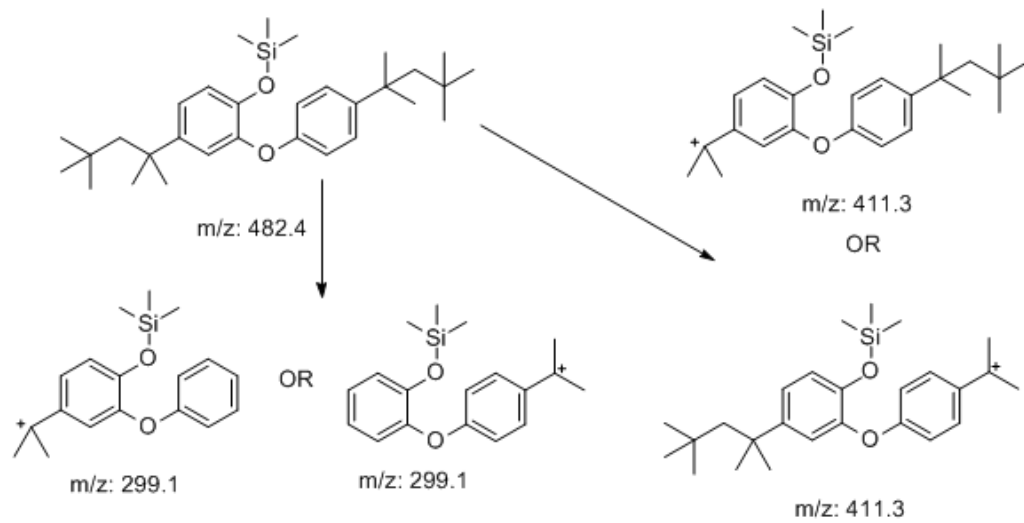


**Figure S 5–32** Possible ion fragmentation of Product OP-2-2A/B

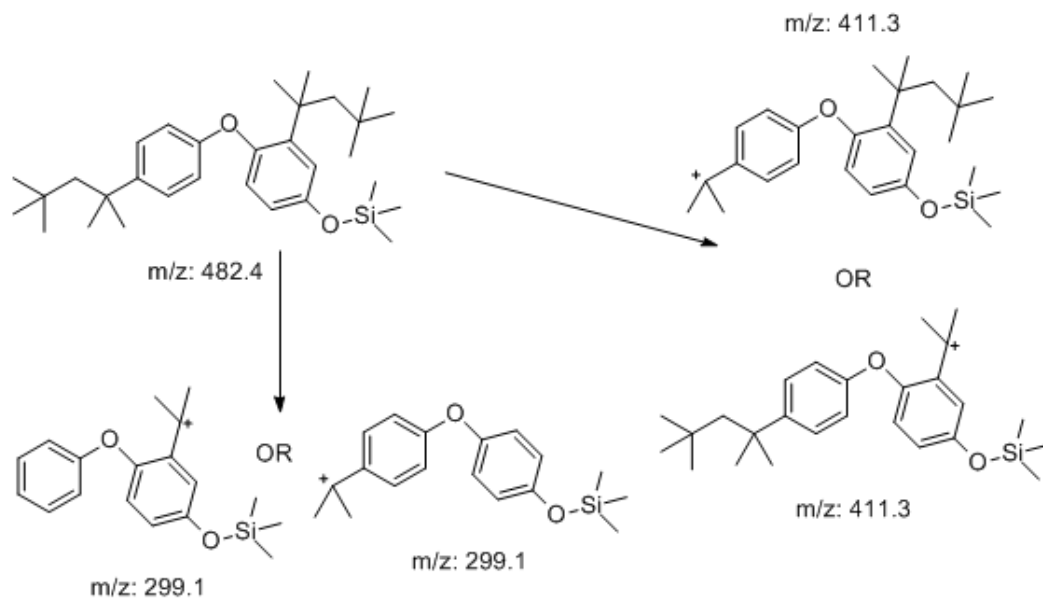


**Figure S 5-33** Another possible ion fragmentation of Product OP-2-2A/B

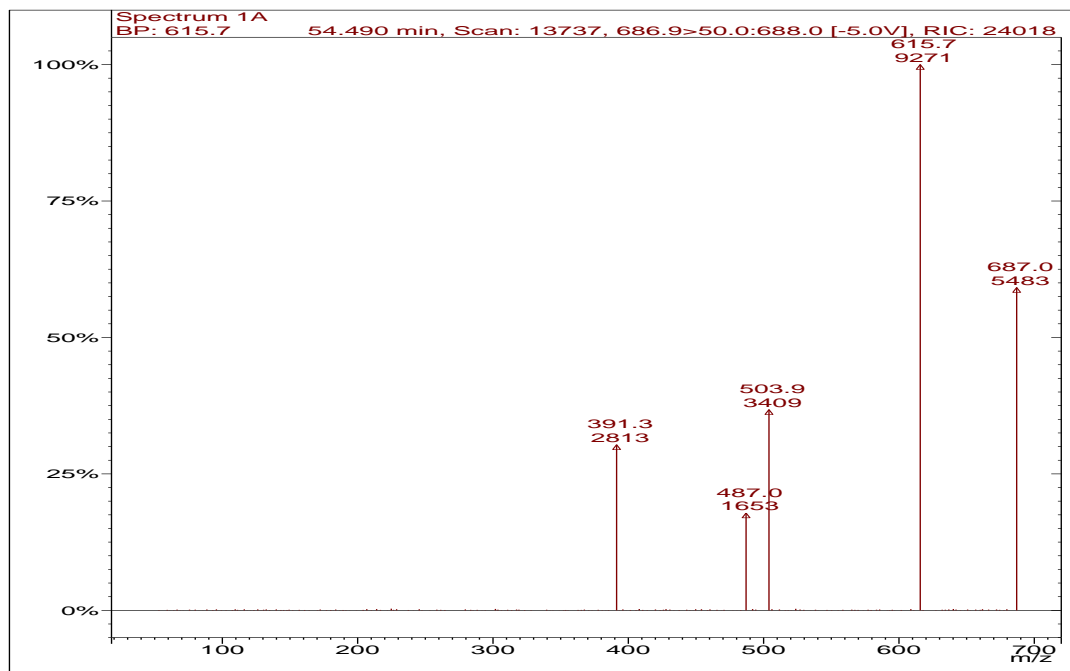


**Figure S 5-34** GC-MS-MS spectra of OP-2-3A at retention time 54.5 min, trimmer of octylphenol, silylated

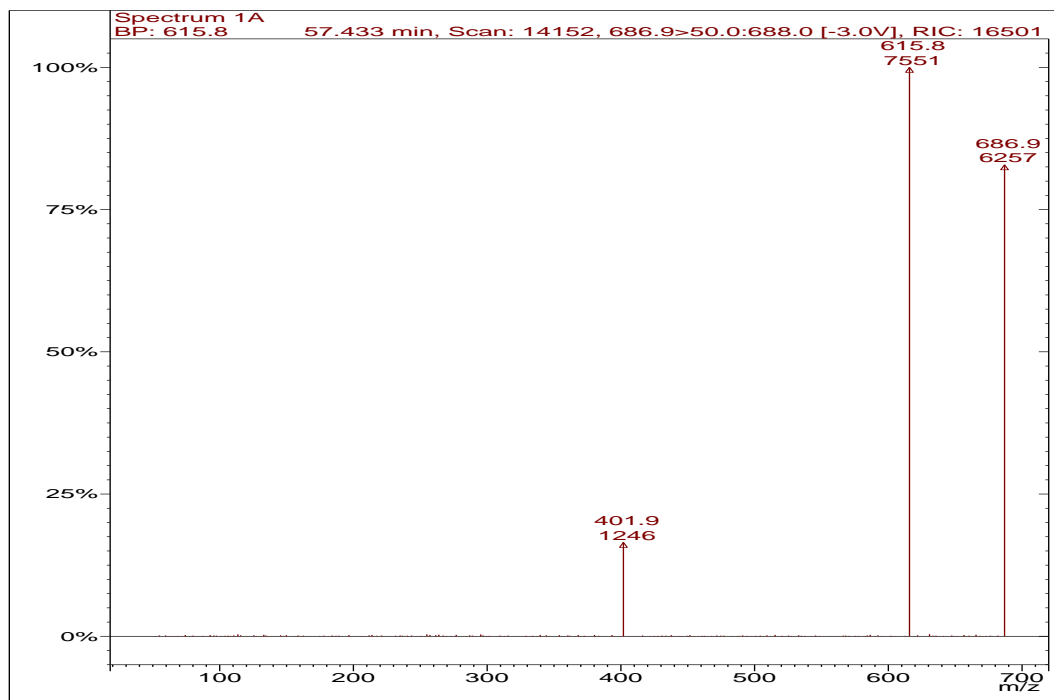
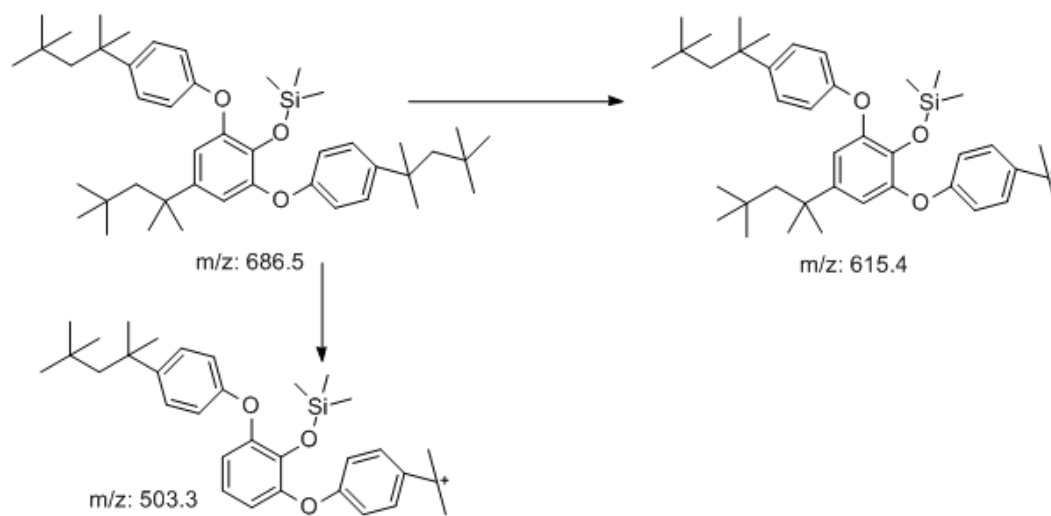


Figure S 5-35 GC-MS-MS spectra of OP-2-3B at retention time 57.4 min, trimmer of octylphenol, silylated



**Figure S 5–36** Figure S36. Possible ion fragmentation of Product OP-2-3A/B

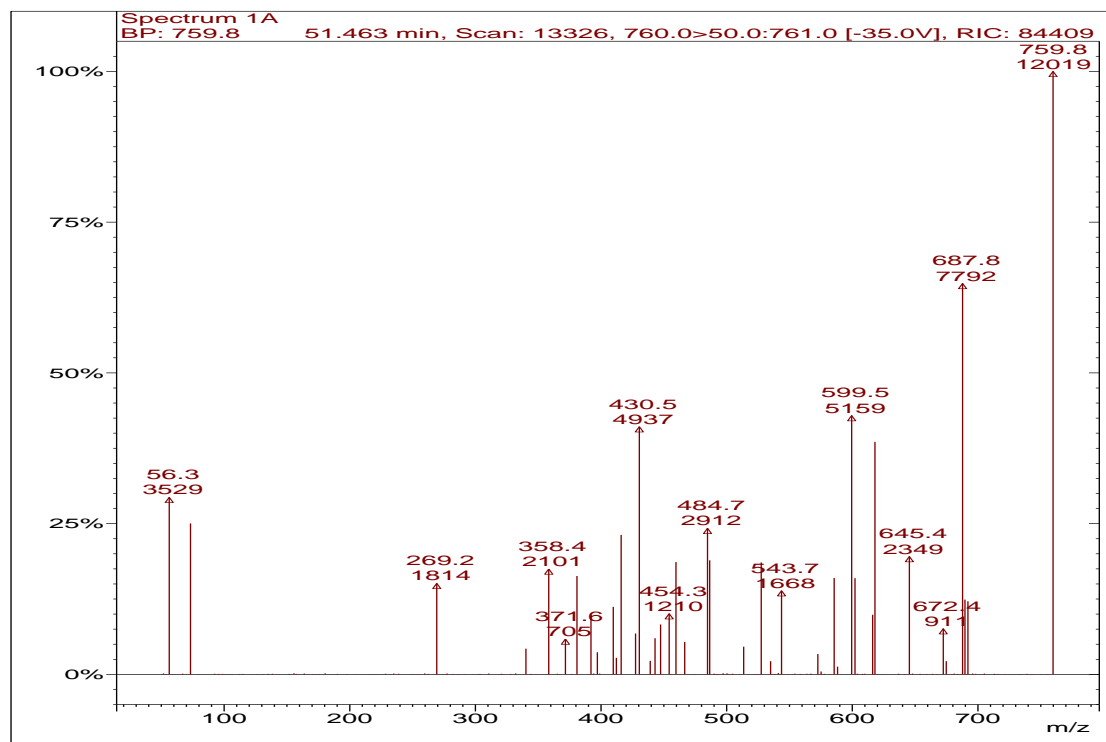


Figure S 5-37 GC-MS-MS spectra of OP-2-4A at retention time 51.5 min, trimmer of octylphenol, silylated



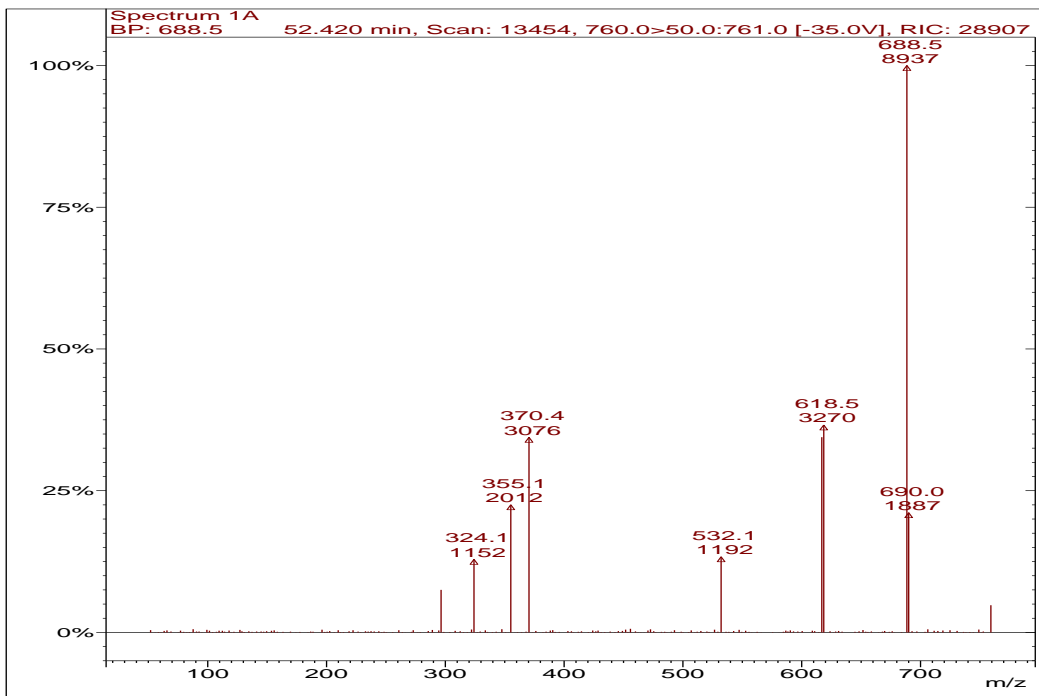
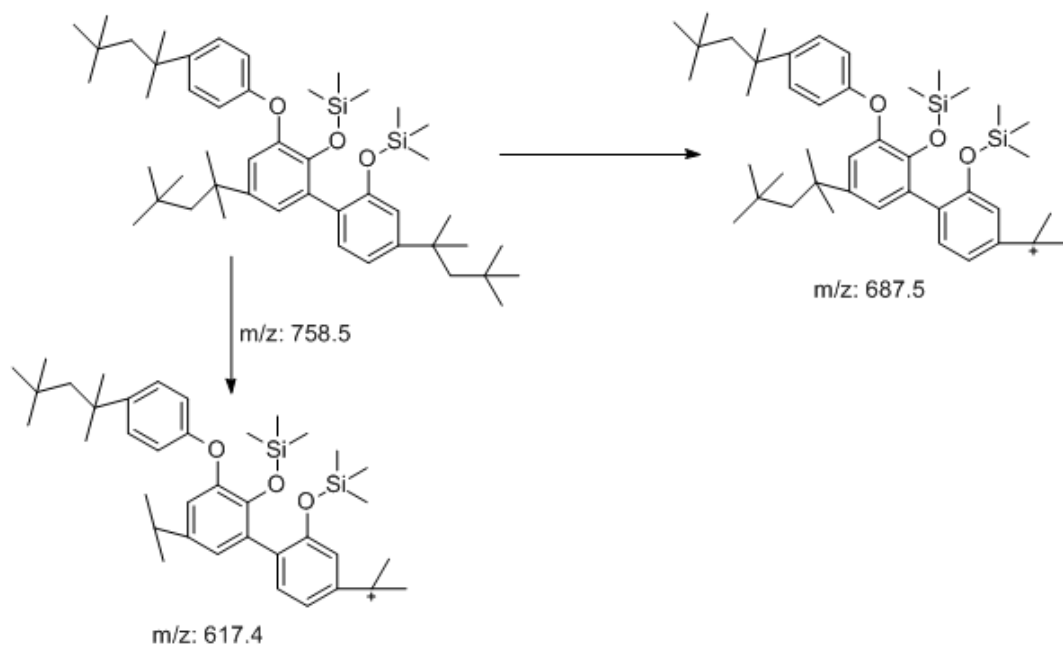
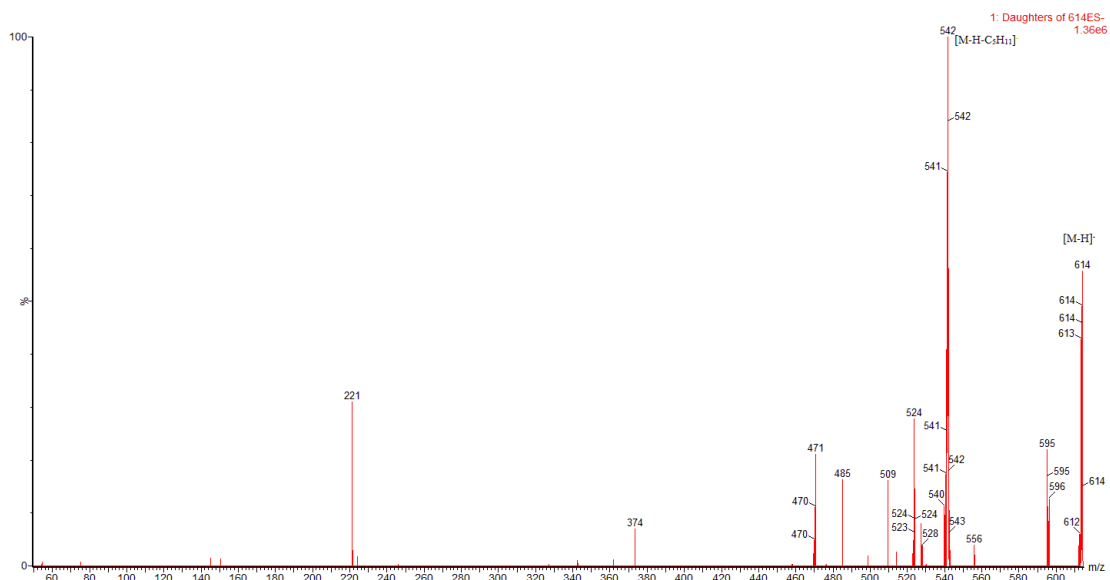


Figure S 5-38 GC-MS-MS spectra of OP-2-4B at retention time 52.4 min, trimmer of octylphenol, silylated



**Figure S 5–39** Possible ion fragmentation of Product OP-2-4A/B



**Figure S 5-40** UPLC-MS-MS spectra of OP-3-1A at retention time 8.71 min, trimmer of octylphenol

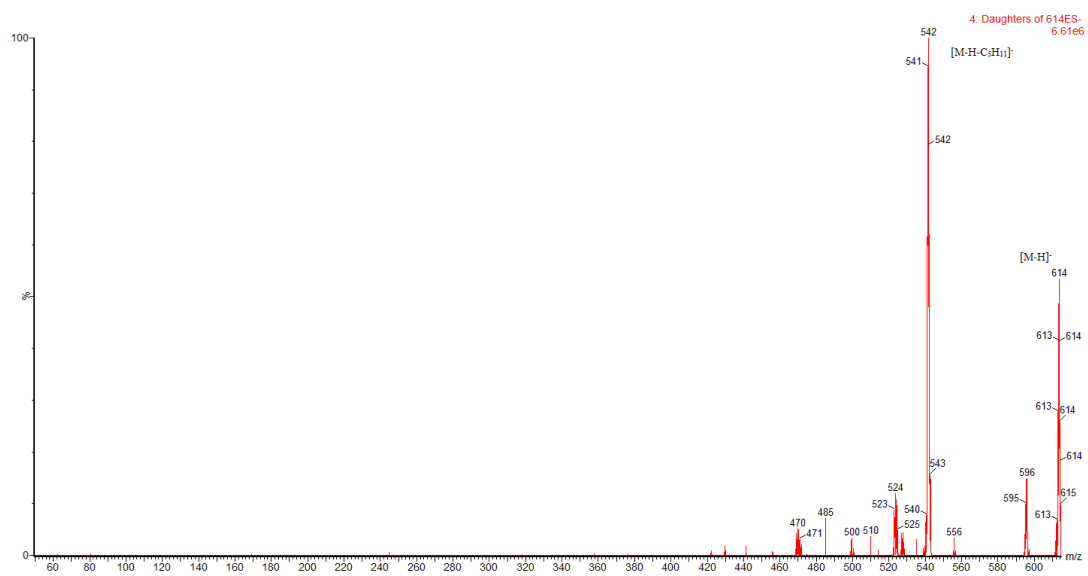


**Figure S 5-41** UPLC-MS-MS spectra of OP-3-1B at retention time 9.59 min, trimmer of octylphenol



**Figure S 5-42** UPLC-MS-MS spectra of OP-3-1C at retention time 10.65 min, trimmer of octylphenol

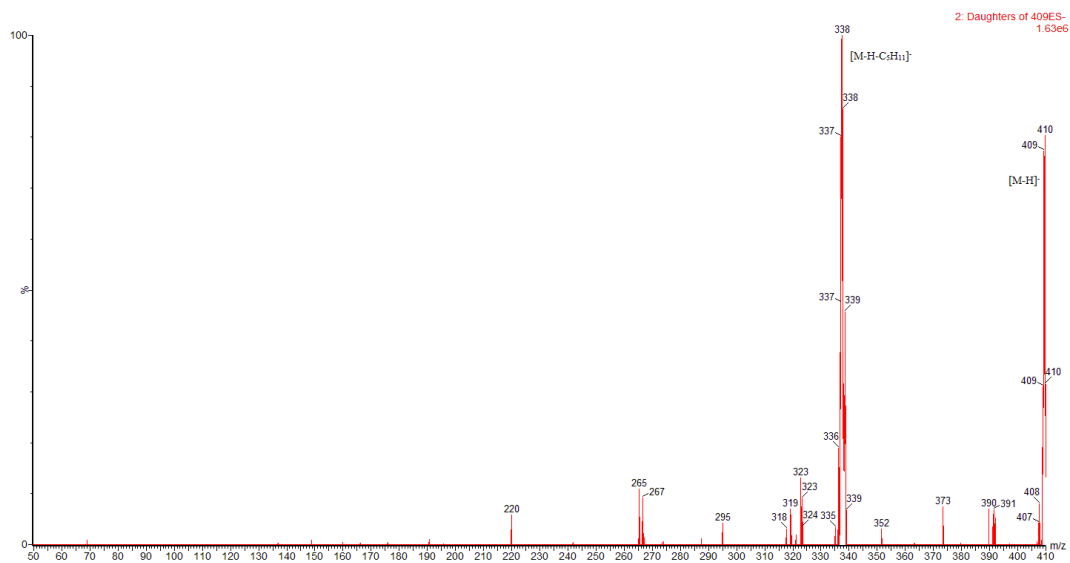


**Figure S 5-43** UPLC-MS-MS spectra of OP-3-2A at retention time 9.69 min, dimer of octylphenol.



**Figure S 5-44** UPLC-MS-MS spectra of OP-3-2B at retention time 9.79 min, dimer of octylphenol

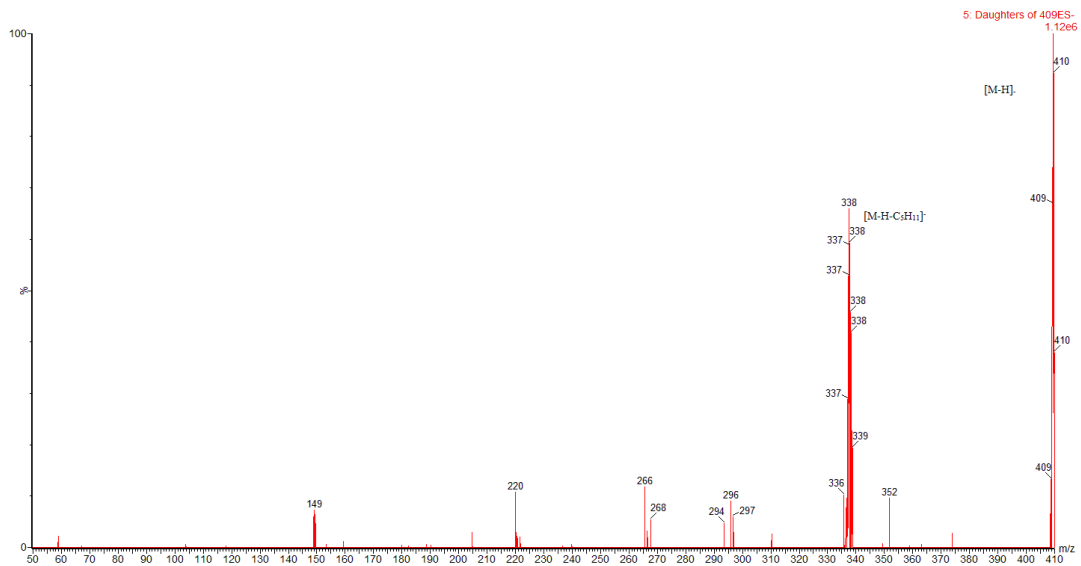


**Figure S 5–45** UPLC-MS-MS spectra of OP-3-2A at retention time 10.32 min, dimer of octylphenol



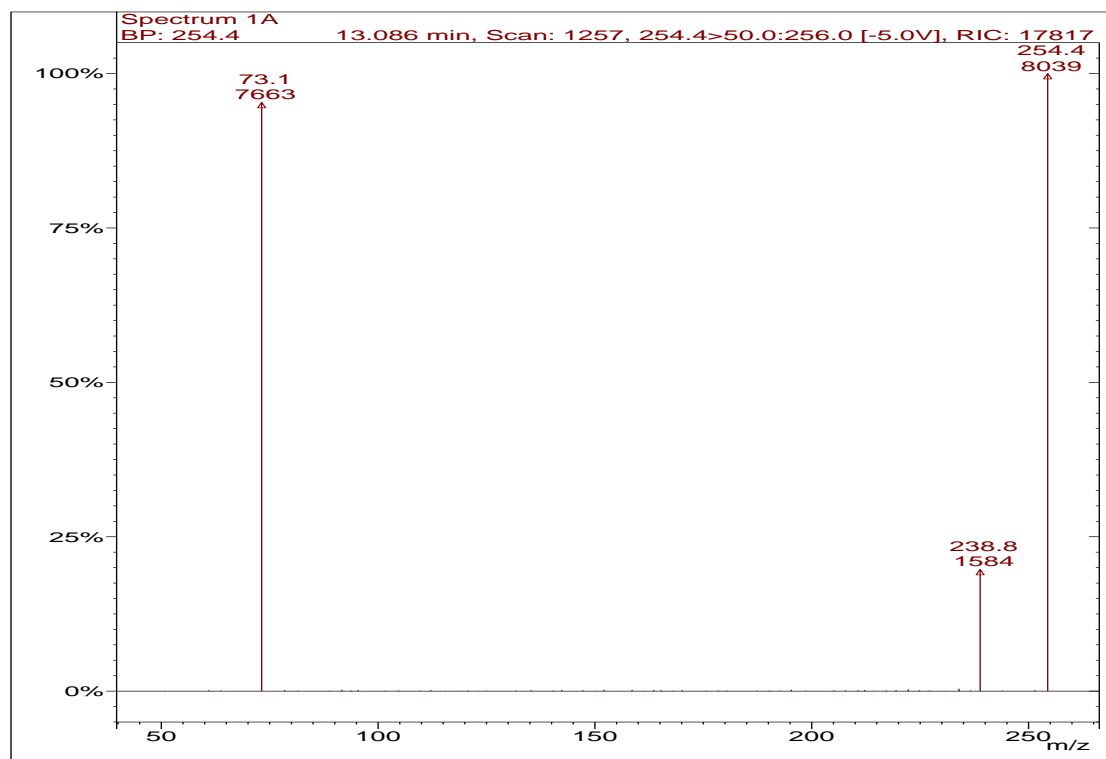


Figure S 5-46 GC-MS-MS spectra of the hydroquinone standard

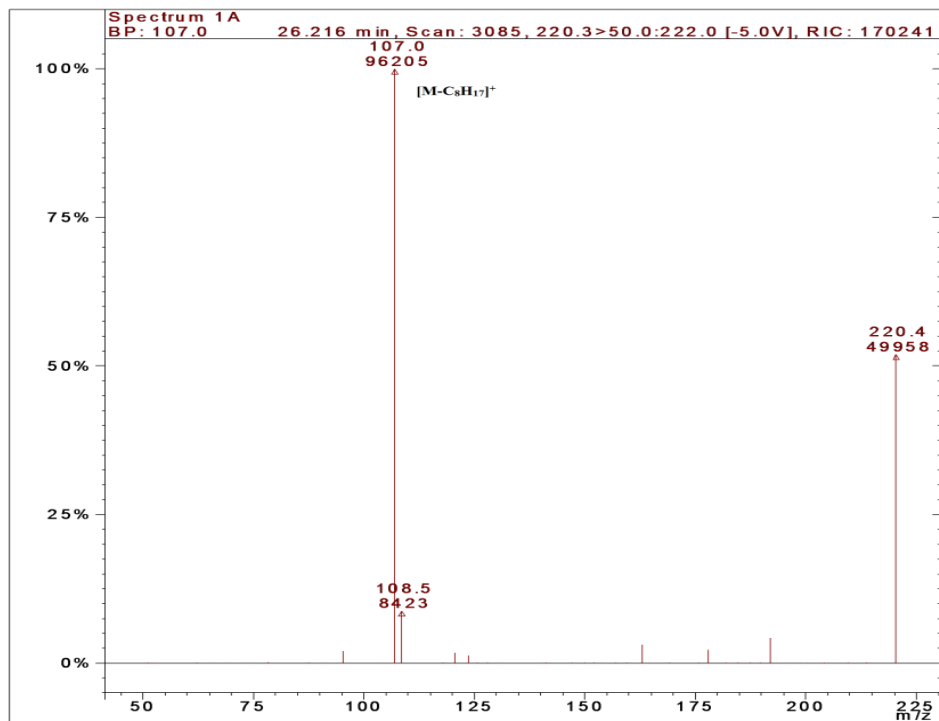


Figure S 5-47 GC-MS-MS spectra of 4-n-NP

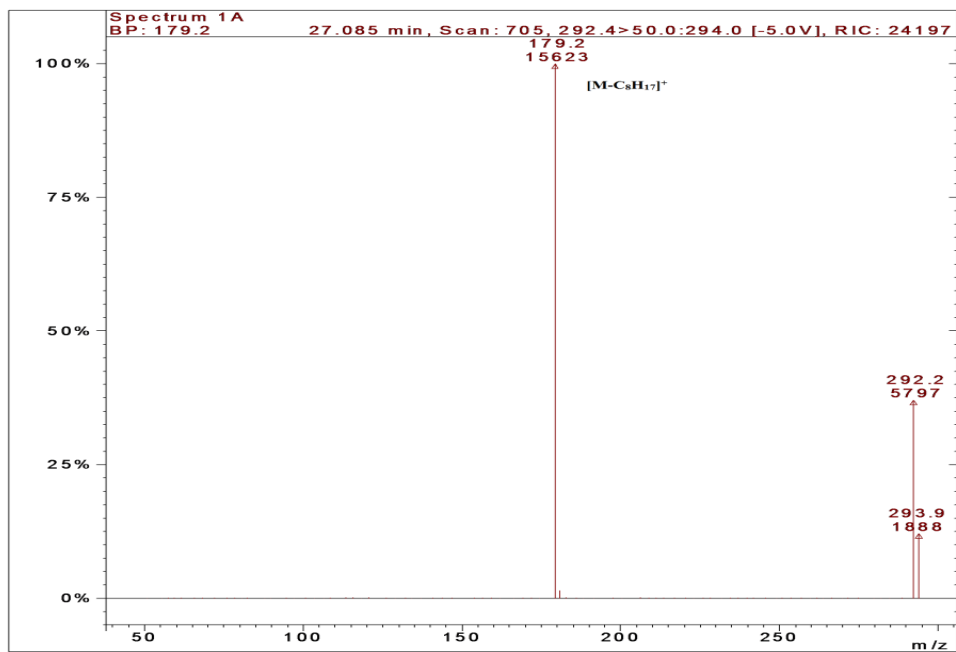


Figure S 5-48 GC-MS-MS spectra of 4-n-NP silylated

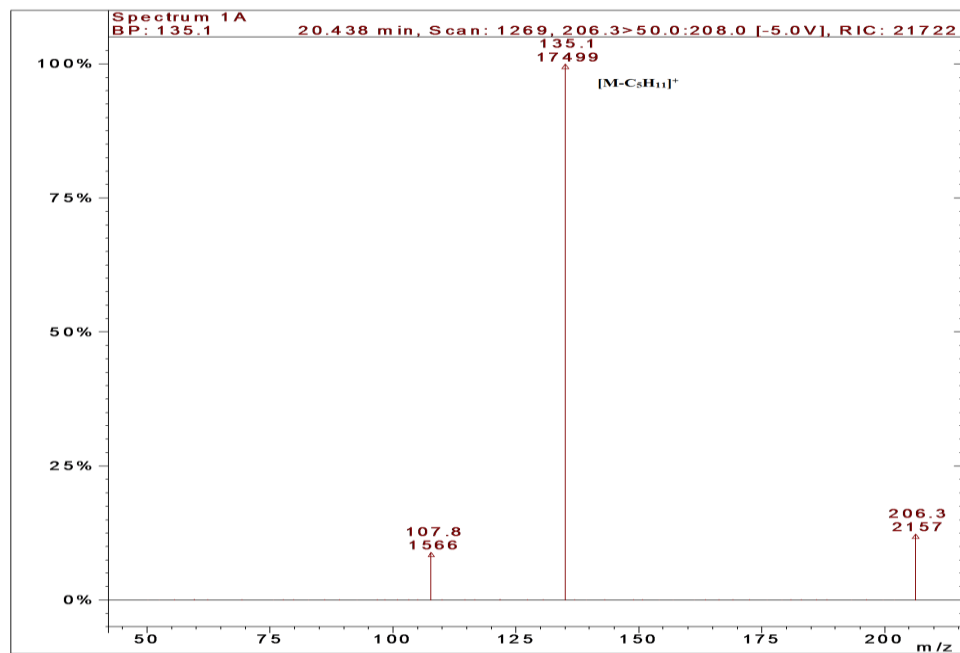


Figure S 5-49 GC-MS-MS spectra of 4-tert-OP

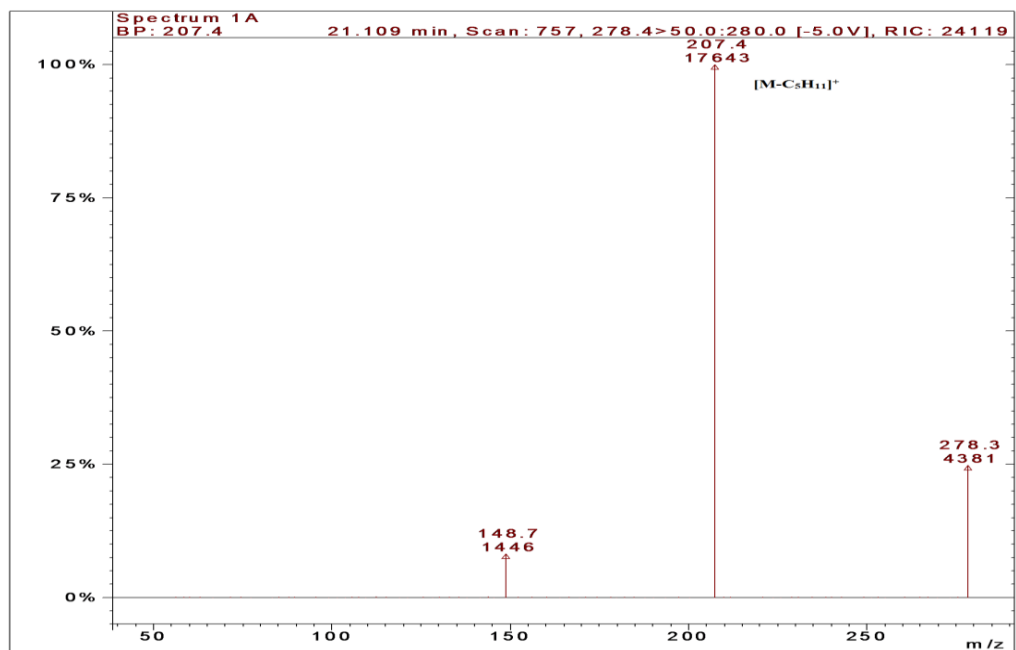


Figure S 5-50 GC-MS-MS spectra of 4-tert-OP silylated

## Chapter 6 General Conclusions and Future Work

### 6.1 Isomer-Specific Biodegradation in River Sediments and Bioreactor

Biodegradation of tNP in the river sediments and the conventional activated sludge bioreactor was found to be isomer specific. NP biodegradation in bed sediments was affected greatly by the redox potential. While most NP isomers were recalcitrant to degradation in reduced sediments, under true oxic conditions, the half-lives of NP isomers ranged from 0.9 to 13.2 d. The overall removal of tNP was much more efficient during the wastewater treatment processes simulated in a laboratory-scale CAS bioreactor, ranging 90 to 99%, depending on the operational conditions. In the bioreactor and river sediments, the biodegradability of NP isomers was closely dependent on the structures of NP isomers. Isomers with short side chain and bulky  $\alpha$ -substituents were generally more persistent, following the order of dimethyl  $\geq$  ethylmethyl  $>$  methylpropyl  $\geq$  *iso*-propylmethyl. Regression analysis validated that steric effect index and degree of branching as quantified by  $I_{DWbar}$  may be used to predict the relative biodegradability of NP isomers.

### 6.2 Isomer-Specific Oxidation of Nonylphenol by Potassium Permanganate

Some isomeric selectivity was apparent in the oxidation of NP by  $KMnO_4$ , although the selectivity appeared to be more limited as compared to that in biodegradation. At pH 7 with 10 mg/L of  $KMnO_4$  and 50  $\mu$ g/L tNP, the half-lives of 19 isomers varied from 4.8 to 6.3 min. In general, NP isomers with less bulky  $\alpha$  substituents had higher reactivity and

followed the same trend as in the biodegradation: dimethyl > ethylmethyl  $\approx$  methylpropyl  $\approx$  *iso*-propylmethyl. However, the substituent effects during potassium permanganate oxidation may originate from inductive effects rather than the steric hindrance of *ipso*-hydroxylation as observed in biodegradation.

### 6.3 Oxidation by Soil Manganese Dioxide

Naturally occurring MnO<sub>2</sub> has the capability to oxidize tNP and its structural analogues 4-*n*-NP, 4-*tert*-OP and bisphenol F in soil, water and sediment. At pH 5.5 and 100 mg/L synthetic  $\delta$ -MnO<sub>2</sub>, 92, 84 and 76% of 4-*n*-NP, 4-*tert*-OP and tNP was transformed in 90 min, respectively. A further experiment using a Mn-containing soil and Mn-removed soil confirmed that soil MnO<sub>2</sub> caused NP removal, although at a rate substantially slower than that by synthetic MnO<sub>2</sub>. Multiple reaction products, including hydroquinone, hydroxylated products, dimers and trimers were identified through fragmentation analysis by GC-MS/MS and UPLC-MS/MS. Based on these reaction products, tentative pathways were constructed: NP, OP and bisphenol F are first adsorbed on the surface of MnO<sub>2</sub> and then one electron is transferred from these phenolic compounds yielding phenoxy radicals. These radicals further couple with each other, forming dimers. These dimers may be further attacked by the phenoxy radicals to form trimers. The phenoxy radicals may be also further oxidized to form hydroxylated products and hydroquinone.

## 6.4 Environmental Implications

Since WWTPs are the primary source for NP entering the environment, the isomer preferential enrichment implies that some NP isomers are introduced into the environment at levels higher than that indicated by non-discriminatory analysis of NP. Surface aquatic systems are often the primary sink of NP contamination due to the often-practiced discharge of NP-containing WWTP effluents. The isomer-specificity in NP attenuation in river sediments may result in selective accumulation of recalcitrant NP isomers in the bed sediment and other environmental matrices such as the overlaying water due to sediment resuspension and desorption of NP. The preferential attenuation of NP isomers in the surface aquatic systems will further impact other closely related environment compartments, for example, source drinking water and ground water. Isomeric selectivity in  $\text{KMnO}_4$  oxidation may result in accumulation of recalcitrant isomers in tertiary treated effluent, drinking water and ground water. Soils are also an important sinks of NP due to land application of NP-containing sludge. Abiotic oxidation by manganese dioxide in soil may contribute to the natural dissipation NP and their analogues.

## 6.5 Future Work

This dissertation project has comprehensively considered biodegradation of NP isomers in two environmentally important processes; however, more processes need to be evaluated to gain a full knowledge on the fate and transport of NP isomers. For example, sludge treatment, including anaerobic and aerobic digestion and composting, is an



important step before disposal of primary and secondary sludge. The nonylphenol profile shifts during the sludge treatment will directly change NP isomer profiles released into the environment via land application. When sludge is land applied, soil biodegradation and plant uptake of NP isomers can have direct implications for food safety and human health risks. It is likely that isomer selectivity may also occur during NP bioaccumulation by aquatic species or biomagnification through food webs.

In this project, a total of 19 4- $\alpha$ -quaternary NP isomers, which comprise the majority parts of tNP, were considered. However, the minor components, such as 4- $\alpha$ -tertiary NP and 2-NP isomers, may contribute estrogenic activity higher than that indicated by their content in the tNP. Moreover, these isomers may have lower biodegradability and thus become relatively enriched in the environment. More research is needed to understand the biodegradation kinetics, mechanisms and pathways of these 4- $\alpha$ -tertiary NP and 2-NP isomers under natural and artificial conditions.

Isomer-specific occurrences of NP have been mostly observed in water samples. However, due to its high log  $K_{OC}$  value, NP is highly enriched in the sludge, sediment and likely aquatic biota. Therefore, future research on isomer selectivity in these environmental compartments is of scientific merit. Moreover, biodegradation of NP isomers may form various metabolites, such as 2-nonyl-*p*-benzoquinones and nitro-nonylphenol. Furthermore, disinfection of secondary effluent and drinking water may form chlorinated NP. These metabolites and disinfect byproducts may have higher

toxicity. Future research on their formation, elimination, toxicity and structure-toxicity relationship is also meritorious.

## **Appendix Oxidation of Bisphenol F (BPF) by Manganese Dioxide**

### A.1 Introduction

Bisphenol F (4,4'-dihydroxydiphenyl-methane, BPF) is a member of bisphenols, which are a group of compounds with two hydroxyphenyl functionalities. Bisphenol F is structurally similar to bisphenol A (4,4'-dihydroxydiphenyl-propane, BPA) – the most widely used bisphenol (Figure A-1). Like BPA, BPF is used as the starting monomer for polycarbonate plastics and epoxy resins that are commonly found in household items, such as plastic bottles and cups, bicycle and motorcycle helmets, dental materials, protective coatings on food, soft drink cans and water pipes (Cabaton et al., 2009; Danzl et al., 2009). Bisphenol F epoxy resin has lower viscosity and better resistance against solvents than BPA epoxy resin, and hence the production of BPF has increased over the years (Danzl et al., 2009).

Like BPA, BPF is increasingly detected in environmental media due to its widespread use. For instance, Fromme et al. (Fromme et al., 2002) found BPF in 77% of the surface water samples, 72% of the sewage water samples, and 58% of the sediment samples in Germany. Stachel et al. (Stachel et al., 2003) also detected BPF in surface water and freshly deposited sediments in River Elbe and its tributaries in Germany. Bisphenol F is a xenoestrogen as shown in vivo in the uterotrophic assay of BPF-exposed rats (Yamasaki et al., 2002). In vitro, BPF showed higher estrogenicity than BPA in a yeast two-hybrid system, human MCF-7 cells and human HepG2 cells (Cabaton et al., 2009; Stroheker et

al., 2004). For example, in the human MCF-7 cell proliferation assay (E-Screen assay), estrogenicity of BPF was about 5 times higher than BPA (Stroheker et al., 2004).

Elucidation of transformations of BPF is important for understanding its natural attenuation in the environment as well as for exploring possibilities for decontamination. Inoue et al. (Inoue et al., 2008) reported that BPF was completely degraded in 9 h by *Sphingobium yanoikuyae* isolated from river water. Suzuki et al. (Suzuki et al., 2010) and Yamada et al. (2010) found that peroxidase and tyrosinase effectively oxidized BPA, BPF and other bisphenol derivatives, especially in the presence of H<sub>2</sub>O<sub>2</sub>. Xiao et al. (Xiao et al., 2007) further observed that  $\beta$ -cyclodextrin ( $\beta$ -CD) was able to enhance photodegradation of BPF by TiO<sub>2</sub>.

Manganese oxides/hydroxides are important components in most soils, water and sediments. Owing to their high negative surface charge, low point of zero charge, large surface area, low crystallinity and dynamic redox behavior, they are geochemically more active than that indicated by their abundance (Negra et al., 2005). Many studies show that manganese oxides/ hydroxides are efficient in degrading different organic pollutants, including phenolic compounds (Lin et al., 2009), amines (Chen et al., 2010), azo compounds (Clarke et al., 2010), and steroid hormones (Xu et al., 2008).

In this study, we examined degradation of BPF by synthesized manganese dioxide ( $\delta$ -MnO<sub>2</sub>) that was similar to the naturally abundant birnessite. The kinetics of the reaction and the reaction pathways were explored, and the influences of pH and common

cosolutes, including humic acid, common cations and anions, on the reaction were considered.

## A.2 Materials and Methods

### A.2.1 Chemicals

Hydroquinone (99%), and bisphenol F (98%), bisphenol A (98%), bis(2-hydroxyphenyl) methane (98%) and 2, 2'-diphenol (97%) and analytical grade chemicals of manganese chloride (> 98%), sodium permanganate (> 97%), humic acid (sodium saturated), 4-morpholinepropanesulfonic acid (MOPS), 2-(cyclohexylamino) ethanesulfonic acid (CHES), and L-ascorbic acid were purchased from Sigma-Aldrich (St. Louis, MO). Silylation reagent *N*, *O*-bis(trimethylsilyl)trifluoroacetamide with trimethylchlorosilane (BSTFA+TMCS, 99:1) was purchased from Supelco (Bellefonte, PA). 4-Hydroxybenzaldehyde (98%) was purchased from VWR (West Chester, PA). 4-Hydroxybenzyl alcohol (97%) and other chemicals and solvents were all purchased from Fisher Scientific (Fair Lawn, NJ). Reagent water (18.3 M-cm resistivity) was prepared using a Barnstead Nanopure water system (Barnstead/Thermolyne, Dubuque, IA). Stock solution of 4.40 mM BPF was prepared in methanol and stored at 4 °C prior to use.

Manganese dioxide ( $\delta$ -MnO<sub>2</sub>) was synthesized according to Murray's method (Murray, 1974). Briefly, 320 mL of 0.1 M NaMnO<sub>4</sub> and 640 mL of 0.1 M NaOH were added to 6.56 L of nitrogen-purged reagent water, followed by a dropwise addition of 480 mL of 0.1 M MnCl<sub>2</sub> while keeping the solution constantly sparged with nitrogen. The formed

MnO<sub>2</sub> particles were allowed to settle, and the supernatant was decanted and replaced with fresh reagent water several times until the conductivity of supernatant was below 2 μS/cm. The MnO<sub>2</sub> suspensions were stored at 4 °C and were diluted to appropriate concentrations prior to use. The surface area was measured to be 269.1 m<sup>2</sup>/g on a Micromeritics 2100 system (Micromeritics, Norcross, GA). Powder X-ray diffraction analysis carried out on a Bruker D8 Advance Diffractometer (Bruker AXS, WI) with Cu Kα radiation showed that the synthetic MnO<sub>2</sub> was amorphous, as shown in the X-ray diffractogram in the Supporting Information (SI).

#### A.2.2 Reaction Setup

Batch experiments were conducted in 125-mL wide-mouth amber borosilicate glass bottles with Teflon-faced caps at room temperature with the reaction solution temperature measured to be 25 ± 2 °C. Reaction mixtures were constantly stirred with Teflon-coated magnetic stir bars at 480 rpm on a Variomag® Poly 15 plate (Fisher Scientific, Fair Lawn, NJ). Reaction solutions were maintained at a constant ionic strength of 0.01M (by adding suitable amount of sodium chloride) and different pH with 10 mM of these following buffers: pH 4.5 and pH 5.5, acetic acid/sodium acetate; pH 6.5 and pH 7.5, MOPS and its sodium salt; pH 8.6 and pH 9.6, CHES and its sodium salt.

Prior to the initiation of reactions, MnO<sub>2</sub> suspensions in buffer solutions (40 mL) with or without cosolutes (e.g., CaCl<sub>2</sub>, MnCl<sub>2</sub>, MgCl<sub>2</sub>, FeCl<sub>3</sub>, humic acid) were constantly stirred at 480 rpm for about 16 h. Reactions were initiated by adding 40 μL of 4.4 mM BPF in methanol to the continuously stirred MnO<sub>2</sub> suspensions. Aliquots of 1.0 mL of reaction

mixture were periodically withdrawn with a pipette, transferred to 2-mL HPLC vials containing 5  $\mu$ L L-ascorbic acid solutions (50 mg/mL) and immediately vortexed for 10 s. Dissolution of the  $\text{MnO}_2$  by L-ascorbic acid released the adsorbed BPF and reaction products and quickly quenched the reaction. All samples were stored at 4  $^{\circ}\text{C}$  and analyzed within 24 h. Preliminary experiments showed that there was no change in concentration during the storage.

The effect of initial  $\text{MnO}_2$  loadings on BPF removal was studied by considering different  $\text{MnO}_2$  concentrations (0, 12.5, 25, 50, 100 and 200  $\mu\text{M}$ ) under the fixed conditions of pH 5.5, 4.4  $\mu\text{M}$  BPF, and 0.01 M ionic strength. The effect of pH was evaluated in solutions with different pH values (4.5, 5.5, 6.5, 8.6, and 9.6), under the fixed conditions of 100  $\mu\text{M}$   $\text{MnO}_2$ , 4.4  $\mu\text{M}$  BPF, and 0.01 M ionic strength. The cosolute effects of cations and anions were investigated by fortifying two different concentrations (e.g., 0.01 and 0.05 M) of the cosolutes including  $\text{CaCl}_2$ ,  $\text{MgCl}_2$ ,  $\text{MnCl}_2$ ,  $\text{Na}_2\text{SO}_4$ ,  $\text{Na}_2\text{HPO}_4$  and  $\text{NaNO}_3$  under the fixed conditions of 100  $\mu\text{M}$   $\text{MnO}_2$ , 4.4  $\mu\text{M}$  BPF, and pH 5.5. The effect of humic acid was determined at pH 5.5 and 8.6 by amending the reaction solution with humic acid (Sigma-Aldrich St. Louis, MO) at 0.1 or 10 mg/L under the fixed conditions of 100  $\mu\text{M}$   $\text{MnO}_2$ , 4.4  $\mu\text{M}$  BPF, and 0.01 M ionic strength. As analogs to BPF, BPA and bis(2-hydroxyphenyl) methane were also reacted with 100  $\mu\text{M}$   $\text{MnO}_2$  at pH 5.5 and 0.01 M ionic strength for the purpose of structure-activity relationship evaluation.

### A.2.3 Chemical Analysis

Analysis of BPF, BPA and bis(2-hydroxyphenyl) methane was carried out on an Agilent 1100 HPLC (Agilent Technologies, Wilmington, DE) coupled with a multi-wavelength UV detector and a Dionex Acclaim® 120 C18 column (4.6 × 250 mm, 5µm). For BPF, the isocratic mobile phase was acetonitrile (50%)-water (50%) at 1.0 mL/min and the UV wavelength was 200 nm. The injection volume was 25 µL. Under these conditions, the typical retention time for BPF was 5.4 min. For BPA and bis(2-hydroxyphenyl) methane, all the HPLC conditions were the same except the mobile phase was acetonitrile (75%)–water (25%). Identification of reaction products followed a similar procedure described in Lin et al. (2009) and detailed information can be found in the Supporting Information (SI).

### A.2.4 Molecular Modeling

Molecular modeling was performed using a Hyperchem 8.0 program (Hypercube, Gainesville, FL). Semiempirical quantum mechanical Austin model 1 (AM1) molecular orbital method was used for geometry optimization with Polak-Ribiere algorithm until RMS gradient (total energy gradient calculated as a root mean square) less than 0.01 kcal/mol. The highest occupied molecular orbitals (HOMO) for gas and aqueous phases were calculated.



### A.3 Results and Discussion

#### A.3.1 Removal Efficiency and Orders of Reaction

In the presence of MnO<sub>2</sub>, BPF rapidly dissipated from the reaction mixture at pH 5.5 (Figure A-2). For example, about 90% of the initial BPF was reacted in 20 min in the solution containing 100 μM MnO<sub>2</sub>, while the level of BPF was essentially unchanged in the MnO<sub>2</sub>-free control. When logarithmic BPF concentrations were plotted against time, all the curves were linear with  $R^2 \geq 0.93$  for the linear regression. Therefore, the reaction order with respect to BPF was clearly 1.0, with the slopes of the linearized curves representing the pseudo-first-order rate constant  $k_1$  (min<sup>-1</sup>).

As the reaction order for BPF was unity, the rate of reaction of BPF and MnO<sub>2</sub> may be described as:

$$r = -\frac{d[\text{BPF}]}{dt} = k[\text{MnO}_2]^a[\text{BPF}]^b = k_1[\text{BPF}] \quad (1)$$

$$k_1 = k[\text{MnO}_2]^a \quad (2)$$

where  $k$  is the rate constant,  $k_1$  is the pseudo-first-order rate constant, and  $a$ ,  $b$  are the reaction orders with respect to MnO<sub>2</sub> and BPF, respectively. The logarithmic form of Equation 2 is:

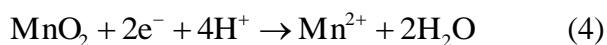
$$\ln k_1 = \ln k[\text{MnO}_2]^a = \ln k + a \ln[\text{MnO}_2] \quad (3)$$

Therefore, when plotting  $\ln k_1$  against  $\ln[\text{MnO}_2]$ , the slope of the linearized curve would reflect the reaction order for  $\text{MnO}_2$ . The slope of the regression lines was found to be 1.25 ( $R^2 = 0.99$ ), suggesting that the reaction order with respect to  $\text{MnO}_2$  for the oxidation reaction was 1.25.

### A.3.2 Effect of pH

The rate of oxidation of BPF by  $\text{MnO}_2$  was greatly affected by pH and the reaction followed an order of  $\text{pH } 4.5 > \text{pH } 5.5 > \text{pH } 8.6 > \text{pH } 7.5 > \text{pH } 6.5 > \text{pH } 9.6$  (Figure A-3). The oxidation of organic pollutants by  $\text{MnO}_2$  was usually pH-dependent (Chen et al., 2010; Lin et al., 2009), because of the pH-dependent redox potential of  $\text{MnO}_2/\text{Mn}^{2+}$  and the speciation of organic pollutants. In a previous study, a similar pH effect was observed for BPA (Lin et al., 2009). For the same reason, pH may also be expected to influence the oxidation of other bisphenol derivatives.

The pH dependence may be explained both macroscopically and microscopically. Macroscopically, the redox potential of the solution is dependent on pH. For example, the oxidation of BPF to 3, 4-hydroxybenzyl alcohol (product 3) and hydroquinone (product 4), two of the structurally identified reaction products (see *Reaction Pathway* below), may be expressed as:





As pH was increased from 4.5 to 6.5, the concentration of proton would decrease, which would result in a decrease in the reaction rate. Microscopically, the reaction may be separated into three steps: BPF forms complexes with  $\text{MnO}_2$ , one electron is transferred to  $\text{MnO}_2$ , and finally, the products dissociate from  $\text{MnO}_2$  (Lin et al., 2009; Stone, 1987). The first two steps are usually rate limiting. The first step may be described as:



where  $\equiv\text{SOH}$  is the neutral surface hydroxyl group of  $\text{MnO}_2$  and  $\text{RO}^-$  is the monobasic BPF and  $\equiv\text{SOR}$  is the complex formed. According to Eq. 7, the speciation of  $\text{MnO}_2$  surface hydroxyl groups and BPF (Figure A-4) may significantly affect the formation of complex and at higher pH, the second step of the reaction may be inhibited. Moreover, in the second step, deprotonated phenol should be able to give an electron more readily than the protonated phenol (Stone, 1987), thus facilitating electron transfer at higher pH. The overlapping and interactions of the above processes may have contributed to the observed unique trend in pH influences.

### A.3.3 Effect of Cosolutes

Humic acids are a ubiquitous environmental sorbent that may inhibit the  $\text{MnO}_2$ -mediated oxidation of BPF by competitive sorption to the active surface hydroxyl groups and dissolution of  $\text{MnO}_2$  (Klausen et al., 1997). On the other hand, humic acids may also

enhance the reaction by binding  $\text{Mn}^{2+}$  (Xu et al., 2008). The sorption of humic acids on manganese oxides decrease with increasing pH (Tipping and Heaton, 1983)

The binding of  $\text{Mn}^{2+}$  by humic acid should also decrease with increasing pH (McBride, 1978). In this study, at pH 5.5, the inhibition of humic acid at both 10 and 0.1 mg/L was significant (with 79.8 and 37.9% reduction, respectively), while at pH 8.6, the inhibition was found to be insignificant when the humic acid amendment level was 0.1 mg/L. (Table A-1) Therefore, at higher pH and lower humic acid concentrations, the inhibition and enhancement effects of humic acids were similar and likely offset each other. This was in agreement with Klausen et al. (Klausen et al., 1997) who showed the inhibitory effect of humic acids to substituted anilines was more significant with increasing humic acid concentrations. Under the other conditions examined in this study, however, the effect of humic acids was dominated by inhibition.

The effect of cations as cosolutes was evaluated and the results show that  $\text{Mn}^{2+}$  displayed the greatest inhibition (Table A-2). The overall inhibitory effect followed an order of  $\text{Mn}^{2+} > \text{Ca}^{2+} > \text{Mg}^{2+} > \text{Na}^+$ . This pattern was in good agreement with those observed in other studies showing a general order of  $\text{Mn}^{2+} > \text{Ca}^{2+} > \text{Mg}^{2+}$  in similar oxidation reactions (Chen et al., 2010; Lin et al., 2009). The inhibitory effects of cations may be attributed to their binding to reactive sites on  $\text{MnO}_2$ :



where M is the cation and z is the valence of cation. The inhibitory capacities observed in this study followed the binding capacity of cations, which decrease in the order  $\text{Co} > \text{Mn} > \text{Zn} > \text{Ni} > \text{Ba} > \text{Sr} > \text{Ca} > \text{Mg} > \text{Na} = \text{K}$  (Murray, 1975). The strong inhibition of  $\text{Mn}^{2+}$  may be partly due to its reduction of redox potential of  $\text{MnO}_2/\text{Mn}^{2+}$  (Lin et al., 2009; Zhang and Huang, 2003). However, a previous study suggested that cosolutes like  $\text{Ca}^{2+}$  and  $\text{Mg}^{2+}$  did not compete for the same surface sites with organic compounds. Rather, cations were adsorbed to the surface and inhibited the transfer of electron, thus decreasing the oxidation state of  $\text{MnO}_2$  (Zhang et al., 2008). The same authors also suggested that only  $\text{Mn}^{2+}$  may compete for the same surface sites and thus had a stronger inhibitory effect as compared to the other cations (Zhang et al., 2008). Another potential cause may be  $\text{MnO}_2$  aggregation caused by metal ion adsorption. Metal ion adsorption increases the  $\zeta$  potential and can cause particle aggregation and decrease surface areas. Liu et al. (2009) reported that 1 mM  $\text{Ca}^{2+}$  increased the diameter of  $\text{MnO}_2$  aggregates from less than 0.5  $\mu\text{m}$  to larger than 3.6  $\mu\text{m}$  and decreased the surface area from 117.4 to 80.5  $\text{m}^2/\text{g}$ .

The effect of anions was also investigated in this study (Table A-3). The anions showed inhibitory effects in the order  $\text{HPO}_4^{2-} > \text{Cl}^- > \text{NO}_3^- \approx \text{SO}_4^{2-}$ . The inhibitory effect of  $\text{HPO}_4^{2-}$  may be due to its formation of complexes with surface hydroxyl groups of  $\text{MnO}_2$ , because  $\text{HPO}_4^{2-}$  was shown to be strongly adsorbed to  $\text{MnO}_2$  (Yao and Millero, 1996). However,  $\text{Cl}^-$  and  $\text{SO}_4^{2-}$  are not adsorbed onto  $\text{MnO}_2$  between pH 2-9 (Balistrieri and Murray, 1982). Wang and Stone (Wang and Stone, 2006) suggested that during the oxidation of citric acid by  $\text{MnO}_2$  (birnessite), the main mechanism was citrate and Mn

(III) forming complexes and transferring electron intramolecularly. Ligand, such as pyrophosphate and EDTA, may form stable or metastable complexes with Mn (III) in solution (Klewicki and Morgan, 1998). Nico and Zasoski (Nico and Zasoski, 2001) reported that oxidation of phenols and sulfides by MnO<sub>2</sub> was dependent on the Mn (III) center surface availability. In this study, the anions (ligands) may also complex with Mn(III) and thus decrease the reactivity of MnO<sub>2</sub>.

#### A.3.4 Reactivity Relative to Analogs

Two structurally similar compounds (Figure. A-1) were selected to react with MnO<sub>2</sub> under the same conditions as BPF. The reaction rate followed the order BPA > BPF > bis(2-hydroxyphenyl) methane (Table A-4). Stone (1987) showed that the reaction rate of substituted phenols with MnO<sub>2</sub> decreased as Hammett constant increased and that the reaction rates were linearly correlated with half-wave potentials. Winget et al. (2000) showed that one-electron oxidation potentials for anilines as predicted by semiempirical molecular orbital theory and density functional theory agreed with experimental oxidation potentials. The oxidation potentials were strongly correlated with highest energy-occupied molecular orbital (HOMO), pK<sub>a</sub>, Hammett constant and Brown constant. For example, the R value of simple linear regression for experimental oxidation potentials of 13 anilines and their HOMO values was 0.901 (Winget et al., 2001). In this study, the rate constants of the three compounds were not correlated with pK<sub>a</sub> values (Table A-4) calculated using Marvin Sketch 5.37 (ChemAxon, Budapest, Hungary). However, the reactivity followed the same order of the estimated HOMO energies (Table

A-4). Since HOMO provide a good estimate of the first ionization potential (Koopmans' theorem), the structural differences of these three analogs may have resulted in different electron transfer ability, and thus the different reaction rates.

### A.3.5 Reaction Pathways

A total of 5 products were tentatively identified and their mass spectra and possible fragmentation mechanisms are shown in SI. Based on the structures of these products, a tentative pathway was proposed (Figure A-5). To confirm the products outlined in Fig. 5, authentic standards were purchased and the mass spectra of their silylated products are also given in SI. The identified products include 2,2'-bisphenol (product 2), 3, 4-hydroxybenzyl alcohol (product 3), hydroquinone (product 4), and 4-hydroxybenzaldehyde (product 5). Due to the detection and/or extraction limitations, some products were probably not detected in this study. For example, it is possible that benzoquinone was one of the products of BPF (as the further oxidation product of product 4, see Figure A-5), but was not detected likely due to limitations of the analytical method. In addition, some products from ring cleavage, such as oxalic acid and malonic acid, were likely not detected because of their polarity and the use of a nonpolar solvent (methylene chloride) for extraction.

In the proposed pathway, BPF transfers electrons to  $\text{MnO}_2$  and forms two types of radicals (radical 1 and radical 2 in Figure A-5), and these two radicals are then coupled to form product 1 and product 2, which are further oxidized to form product 3 and product 4,

respectively. Further oxidation results in the formation of product 5 and benzoquinone. Product 4 may be further oxidized to yield 4-hydroxybenzoic acid.

#### A.4 Conclusions

This study showed that natural occurring  $\text{MnO}_2$  has the capability to oxidize BPF. However,  $\text{MnO}_2$ -mediated oxidation of BPF was found to depend closely on pH and to be inhibited by cosolutes including organic matter, cations and anions. These interactions with other environmental variables preclude a simple prediction of the actual role of  $\text{MnO}_2$  in the attenuation of BPF in the natural environment. The effective reaction of BPF by  $\text{MnO}_2$  also suggested that  $\text{MnO}_2$  may be potentially used as a treatment method to remove BPF in wastes before their release into the environment.



## References

- Balistrieri, L. S. and Murray, J. W. (1982). The surface-chemistry of delta-MnO<sub>2</sub> in major ion sea-water. *Geochim. Cosmochim. Acta* **46**(6): 1041-1052.
- Cabaton, N., Dumont, C., Severin, I., Perdu, E., Zalko, D., Cherkaoui-Malki, M. and Chagnon, M. C. (2009). Genotoxic and endocrine activities of bis(hydroxyphenyl)methane (bisphenol F) and its derivatives in the HepG2 cell line. *Toxicology* **255**(1-2): 15-24.
- Chen, W. R., Ding, Y. J., Johnston, C. T., Teppen, B. J., Boyd, S. A. and Li, H. (2010). Reaction of lincosamide antibiotics with manganese oxide in aqueous solution. *Environ. Sci. Technol.* **44**(12): 4486-4492.
- Clarke, C. E., Kielar, F., Talbot, H. M. and Johnson, K. L. (2010). Oxidative decolorization of acid azo dyes by a Mn oxide containing waste. *Environ. Sci. Technol.* **44**(3): 1116-1122.
- Danzl, E., Sei, K., Soda, S., Ike, M. and Fujita, M. (2009). Biodegradation of Bisphenol A, Bisphenol F and Bisphenol S in Seawater. *Int. J. Environ. Res. Public. Health* **6**(4): 1472-1484.
- Fromme, H., Kuchler, T., Otto, T., Pilz, K., Muller, J. and Wenzel, A. (2002). Occurrence of phthalates and bisphenol A and F in the environment. *Water Res.* **36**(6): 1429-1438.
- Inoue, D., Hara, S., Kashihara, M., Murai, Y., Danzl, E., Sei, K., Tsunoi, S., Fujita, M. and Ike, M. (2008). Degradation of bis(4-hydroxyphenyl) methane (bisphenol F)

- by *Sphingobium yanoikuyae* strain FM-2 isolated from river water. *Appl. Environ. Microbiol.* **74**(2): 352-358.
- Klausen, J., Haderlein, S. B. and Schwarzenbach, R. P. (1997). Oxidation of substituted anilines by aqueous  $MnO_2$ : Effect of co-solutes on initial and quasi-steady-state kinetics. *Environ. Sci. Technol.* **31**(9): 2642-2649.
- Klewicki, J. K. and Morgan, J. J. (1998). Kinetic behavior of Mn(III) complexes of pyrophosphate, EDTA, and citrate. *Environ. Sci. Technol.* **32**(19): 2916-2922.
- Lin, K., Liu, W. and Gan, J. (2009). Oxidative removal of bisphenol A by manganese dioxide: Efficacy, products, and pathways. *Environ. Sci. Technol.* **43**(10): 3860-3864.
- Liu, R. P., Liu, H. J., Qiang, Z. M., Qu, J. H., Li, G. B. and Wang, D. S. (2009). Effects of calcium ions on surface characteristics and adsorptive properties of hydrous manganese dioxide. *J. Colloid Interface Sci.* **331**(2): 275-280.
- McBride, M. B. (1978). Transition-metal bonding in humic-acid - ESR study. *Soil Sci.* **126**(4): 200-209.
- Murray, J. W. (1974). Surface chemistry of hydrous manganese dioxide. *J. Colloid Interface Sci.* **46**(3): 357-371.
- Murray, J. W. (1975). Interaction of metal -ions at manganese dioxide solution interface. *Geochim. Cosmochim. Acta* **39**(4): 505-519.
- Negra, C., Ross, D. S. and Lanzirrotti, A. (2005). Oxidizing behavior of soil manganese: Interactions among abundance, oxidation state, and pH. *Soil Sci. Soc. Am. J.* **69**(1): 87-95.

- Nico, P. S. and Zasoski, R. J. (2001). Mn (III) center availability as a rate controlling factor in the oxidation of phenol and sulfide on delta-MnO<sub>2</sub>. *Environ. Sci. Technol.* **35**(16): 3338-3343.
- Stachel, B., Ehrhorn, U., Heemken, O. P., Lepom, P., Reincke, H., Sawal, G. and Theobald, N. (2003). Xenoestrogens in the River Elbe and its tributaries. *Environ. Pollut.* **124**(3): 497-507.
- Stone, A. T. (1987). Reductive dissolution of manganese(III/IV) oxides by substituted phenols. *Environ. Sci. Technol.* **21**(10): 979-988.
- Stroheker, T., Picard, K., Lhuguenot, J. C., Canivenc-Lavier, M. C. and Chagnon, M. C. (2004). Steroid activities comparison of natural and food wrap compounds in human breast cancer cell lines. *Food Chem. Toxicol.* **42**(6): 887-897.
- Suzuki, M., Sugiyama, T., Musashi, E., Kobiyama, Y., Kashiwada, A., Matsuda, K. and Yamada, K. (2010). Use of chitosan for removal of bisphenol A and bisphenol derivatives through tyrosinase-catalyzed quinone oxidation. *J. Appl. Polym. Sci.* **118**(2): 721-732.
- Tipping, E. and Heaton, M. J. (1983). The adsorption of aquatic humic substances by two oxides of manganese. *Geochim. Cosmochim. Acta* **47**(8): 1393-1397.
- Wang, Y. and Stone, A. T. (2006). The citric acid-(MnO<sub>2</sub>)-O-III,IV(birnessite) reaction. Electron transfer, complex formation, and autocatalytic feedback. *Geochim. Cosmochim. Acta* **70**(17): 4463-4476.

- Winget, P., Weber, E. J., Cramer, C. J. and Truhlar, D. G. (2000). Computational electrochemistry: aqueous one-electron oxidation potentials for substituted anilines. *Phys. Chem. Chem. Phys.* **2**(6): 1231-1239.
- Xiao, J. Q., Wang, G. H., Xue, X. F., Wu, F., Luan, H. and Deng, N. S. (2007). Enhanced photodegradation behavior of bisphenol F in the presence of beta-cyclodextrin under UV light. *Environ. Eng. Sci.* **24**(6): 812-820.
- Xu, L., Xu, C., Zhao, M. R., Qiu, Y. P. and Sheng, G. D. (2008). Oxidative removal of aqueous steroid estrogens by manganese oxides. *Water Res.* **42**(20): 5038-5044.
- Yamada, K., Ikeda, N., Takano, Y., Kashiwada, A., Matsuda, K. and Hirata, M. (2010). Determination of optimum process parameters for peroxidase-catalysed treatment of bisphenol A and application to the removal of bisphenol derivatives. *Environ. Technol.* **31**(3): 243-256.
- Yamasaki, K., Takeyoshi, M., Yakabe, Y., Sawaki, M., Imatanaka, N. and Takatsuki, M. (2002). Comparison of reporter gene assay and immature rat uterotrophic assay of twenty-three chemicals. *Toxicology* **170**(1-2): 21-30.
- Yao, W. S. and Millero, F. J. (1996). Adsorption of phosphate on manganese dioxide in seawater. *Environ. Sci. Technol.* **30**(2): 536-541.
- Zhang, H. C., Chen, W. R. and Huang, C. H. (2008). Kinetic modeling of oxidation of antibacterial agents by manganese oxide. *Environ. Sci. Technol.* **42**(15): 5548-5554.
- Zhang, H. C. and Huang, C. H. (2003). Oxidative transformation of triclosan and chlorophene by manganese oxides. *Environ. Sci. Technol.* **37**(11): 2421-2430.

Tables

**Table A-1** Effects of humic acid on degradation of BPF in the reaction mixture containing 4.4  $\mu\text{M}$  BPF and 100  $\mu\text{M}$   $\text{MnO}_2$  (n = 3)

Humic acid (mg/L)	$k_1$ ( $\text{min}^{-1}$ )	
	pH 5.5	pH 8.6
0	$0.0791 \pm 0.0026$	$0.0111 \pm 0.00016$
0.1	$0.0494 \pm 0.0063$	$0.0097 \pm 0.0011$
10	$0.0166 \pm 0.0010$	$0.0057 \pm 0.000060$

**Table A-2** Effects of cations (n = 3) on the reaction rate of bisphenol F (BPF) by MnO<sub>2</sub> under the initial conditions of 4.4 μM BPF, 100 μM MnO<sub>2</sub> and pH 5.5

Cation	Concentration(M)	$k_1$ (min <sup>-1</sup> )	Decrease (%)
Control	No cation	0.0791 ± 0.0026	0.0
Na <sup>+</sup>	0.15	0.0463 ± 0.0039	41.5
Na <sup>+</sup>	0.03	0.0558 ± 0.0040	29.5
Ca <sup>2+</sup>	0.05	0.0118 ± 0.00061	85.1
Ca <sup>2+</sup>	0.01	0.0188 ± 0.00032	76.2
Mg <sup>2+</sup>	0.05	0.0313 ± 0.0022	60.4
Mg <sup>2+</sup>	0.01	0.0352 ± 0.0032	55.5
Mn <sup>2+</sup>	1×10 <sup>-4</sup>	0.0010 ± 0.000095	98.8
Mn <sup>2+</sup>	1×10 <sup>-5</sup>	0.0270 ± 0.00069	65.9

**Table A-3** Effects of anions (n = 3) on the reaction rate of bisphenol F (BPF) and MnO<sub>2</sub> under the initial conditions of 4.4 μM BPF, 100 μM MnO<sub>2</sub> and pH 5.5

Anion	Concentration(M)	$k_1$ (min <sup>-1</sup> )	Decrease (%)
Control	No anion	0.0791 ± 0.0026	0.0
Cl <sup>-</sup>	0.15	0.0463 ± 0.0039	41.5
Cl <sup>-</sup>	0.03	0.0558 ± 0.0040	29.5
SO <sub>4</sub> <sup>2-</sup>	0.05	0.0572 ± 0.0047	27.7
SO <sub>4</sub> <sup>2-</sup>	0.01	0.0747 ± 0.0063	5.6
NO <sub>3</sub> <sup>-</sup>	0.15	0.0567 ± 0.0011	28.3
NO <sub>3</sub> <sup>-</sup>	0.03	0.0711 ± 0.0024	10.1
HPO <sub>4</sub> <sup>2-</sup>	0.05	0.0097 ± 0.00034	87.7
HPO <sub>4</sub> <sup>2-</sup>	0.01	0.0214 ± 0.0012	72.9

Figures

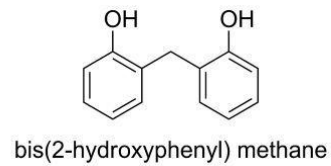
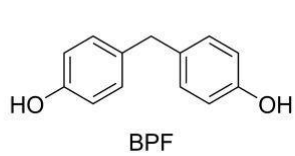
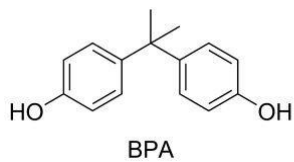


**Figure A-1** Chemical structures of bisphenol A (BPA), bisphenol F (BPF) and bis(2-hydroxyphenyl) methane



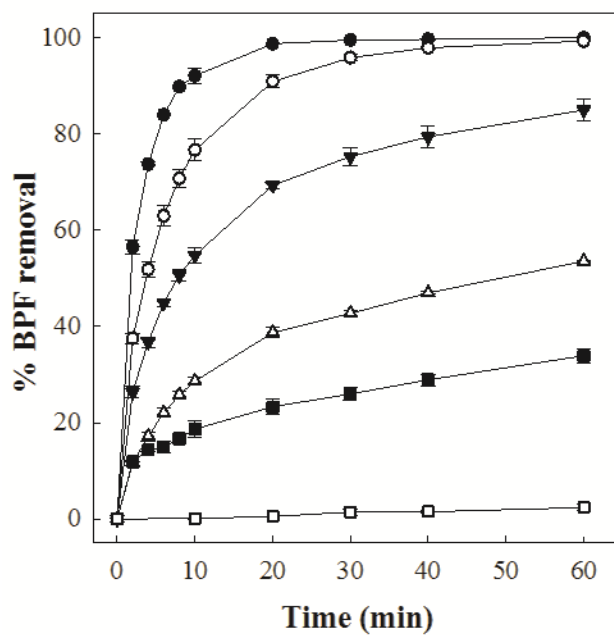


**Figure A-2** Removal efficiency of bisphenol F (BPF) at different initial MnO<sub>2</sub> concentrations

Data points are given as mean  $\pm$  standard deviation ( $n = 3$ ). The other initial conditions are pH 5.5, ionic strength 10 mM, and BPF concentration 4.4  $\mu$ M.

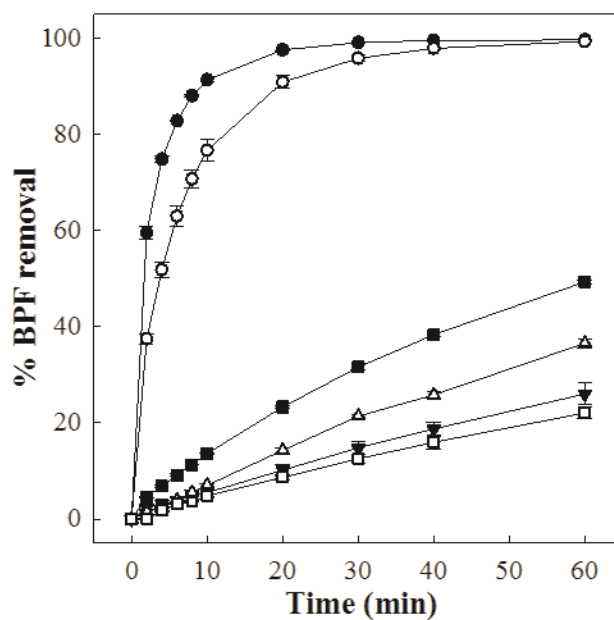


**Figure A-3** Removal efficiency of bisphenol F (BPF) under different pH conditions

Data points are given as mean  $\pm$  standard deviation ( $n = 3$ ). The other initial conditions are ionic strength 10 mM, BPF concentration 4.4  $\mu$ M and MnO<sub>2</sub> concentration 100  $\mu$ M.

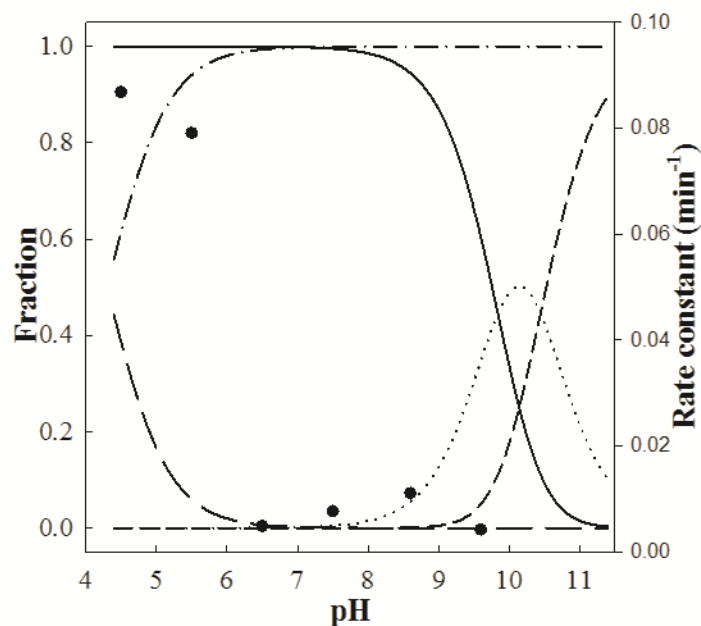


**Figure A-4** Speciation of bisphenol F (BPF) and MnO<sub>2</sub> surface hydroxyl groups and the pseudo first order rate constants at different pH

The  $pK_{a1}$  and  $pK_{a2}$  values for BPF are 9.840 and 10.447, respectively. For MnO<sub>2</sub>, the intrinsic  $pK_{a1}$  is -0.7, and the intrinsic  $pK_{a2}$  is 4.3. H<sub>2</sub>A, undissociated BPF; HA<sup>-</sup>, monobasic BPF; A<sup>2-</sup>, dibasic BPF. SOH<sub>2</sub><sup>+</sup>, protonated surface group; SOH, neutral surface group; SO<sup>-</sup>, deprotonated surface group. The fraction for SOH<sub>2</sub><sup>+</sup> (protonated surface group) is always less than 0.00045% and not shown.

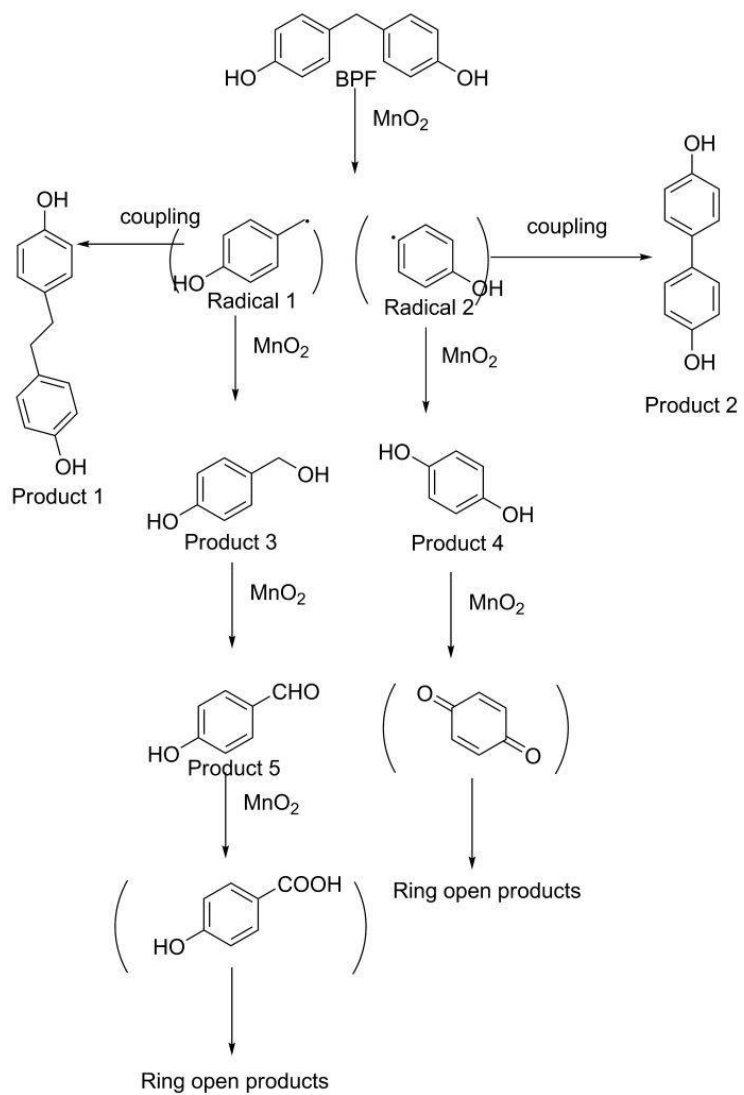


**Figure A-5** A possible reaction pathway describing the oxidation of bisphenol F (BPF) by  $MnO_2$

Compounds in brackets were possible products or intermediates but were not identified in this study due to analytical limitations.

## Supporting Information

### Text S A-1. Chemical Analysis

Reaction solution (100 mL) containing 44  $\mu\text{M}$  BPF and 800  $\mu\text{M}$   $\text{MnO}_2$  were reacted in 10 mM sodium acetate solutions (pH 5.5), and the reaction was quenched after 4 h by adding an excess amount of L-ascorbic acid. The products in the reaction solution were extracted, derivatized, and subjected to analysis using a gas chromatography (GC) coupled with mass spectrometer (MS) (Agilent Technologies, Wilmington, DE). The solution was extracted twice with 50 mL methylene chloride. The combined organic phases were dehydrated by passing through a filter paper filled with anhydrous sodium sulfate, and concentrated to near dryness on a vacuum rotary evaporator. The residue was redissolved in 1.0 mL benzene and transferred to a 1.5 mL vial, from which 100  $\mu\text{L}$  was analyzed directly and the remaining sample was derivatized before analysis. For derivatization, the extract was evaporated to dryness under a gentle nitrogen stream, and 150  $\mu\text{L}$  of BSTFA+TMCS was added to silylate polar products. Immediately after the addition of the silylation reagent, the vial was crimped with a cap with Teflon-lined septum and the silylation reaction was held for 2 h at 60  $^\circ\text{C}$ . Benzene (350  $\mu\text{L}$ ) was added into the vial to dissolve the silylated products. Aliquots (2- $\mu\text{L}$ ) of silylated and non-silylated extract were analyzed on an Agilent 6890 gas chromatograph (GC) coupled with an Agilent 5975 mass spectrometer (MS) (Agilent Technologies, Wilmington, DE) for chemical structural analysis. A HP-5MS column (30 m  $\times$  0.25 mm  $\times$  0.25  $\mu\text{m}$ ; Agilent

95 Technologies) was employed for separation and analysis of reaction products. The inlet temperature was 260 °C, and the detector temperature was 320 °C. The oven temperature was initiated at 80 °C and held for 3 min, then increased to 300 °C at 3 °C/min and held for 30 min. The flow rate of the carrier gas helium was 1.0 mL/min. The injection of 2- $\mu$ L sample was conducted by an Agilent 7683 autosampler (Agilent Technologies) in the pulsed splitless mode and the split mode was turned on after 1.0 min. The temperatures of transfer line, ion source, and MS detector were 280, 230, and 150 °C, respectively. The MS detector was operated in the electron impact mode with 70 eV of ionization energy and the mass spectra were acquired in the full scan mode with m/z ranging from 40 to 800.

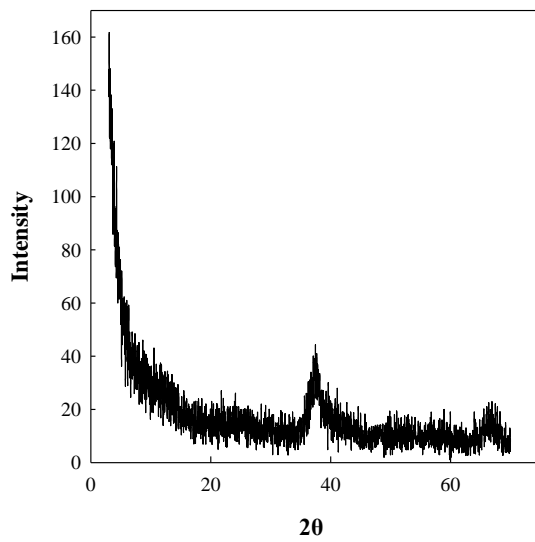


**Figure S A-1** X-ray diffractogram of  $\text{MnO}_2$

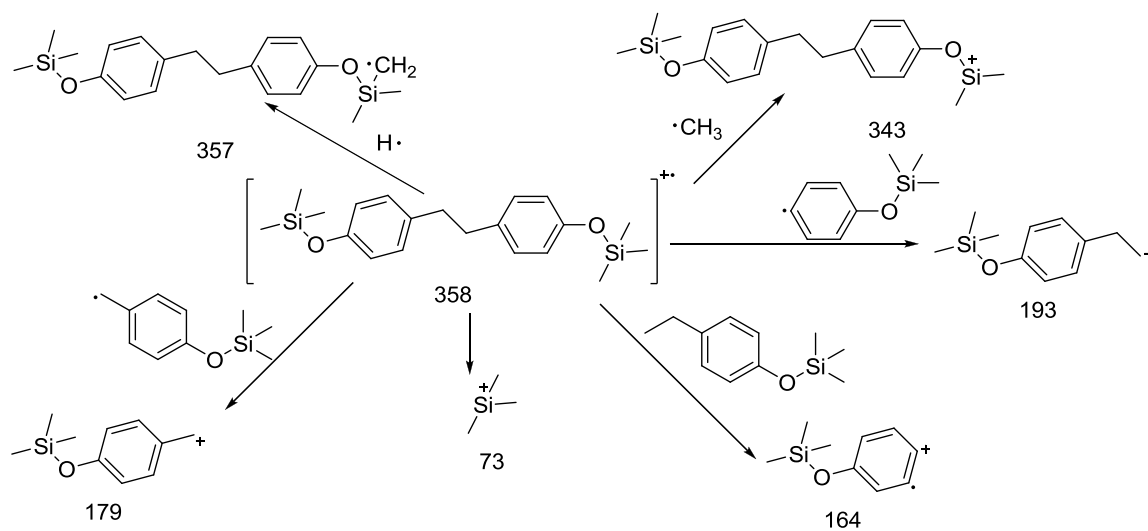
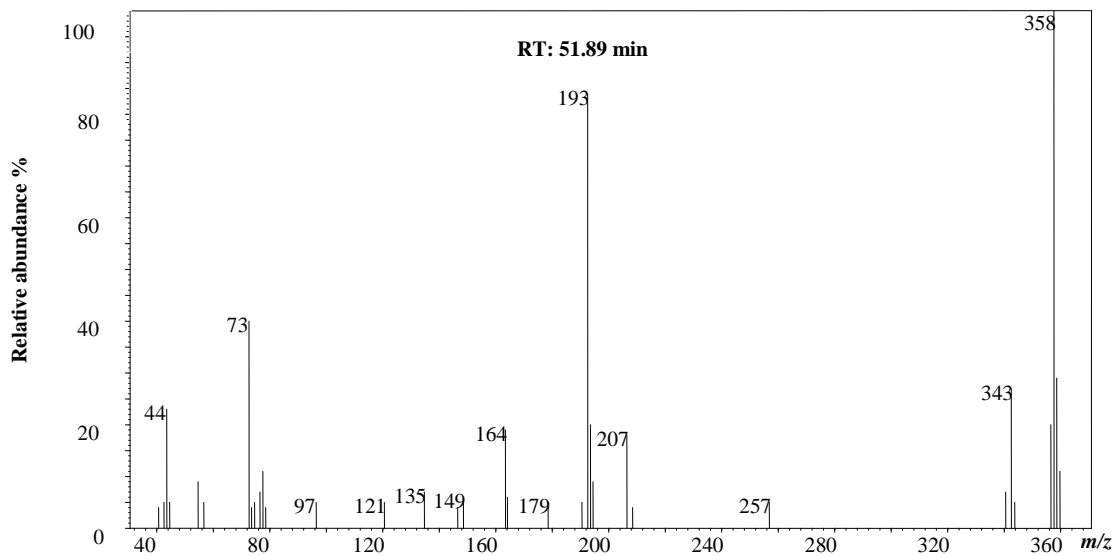


**Figure S A-2** Mass spectrums and possible ion fragment assignments of 4,4'-(ethane-1,2-diyl)diphenol



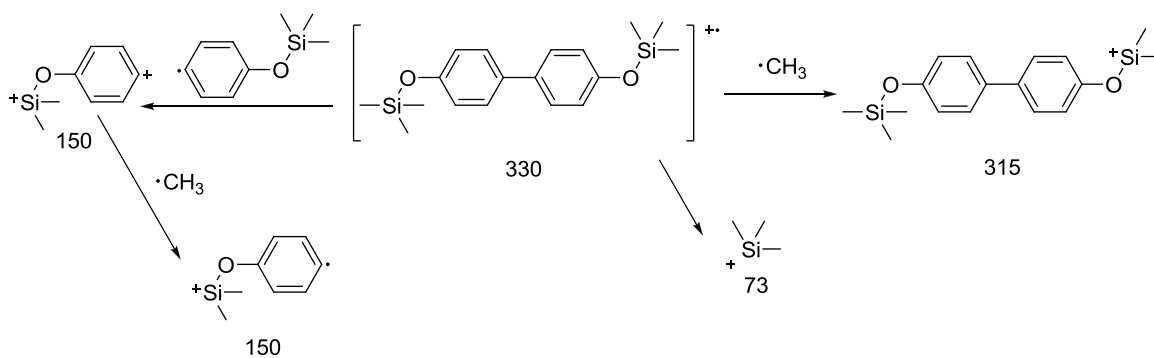
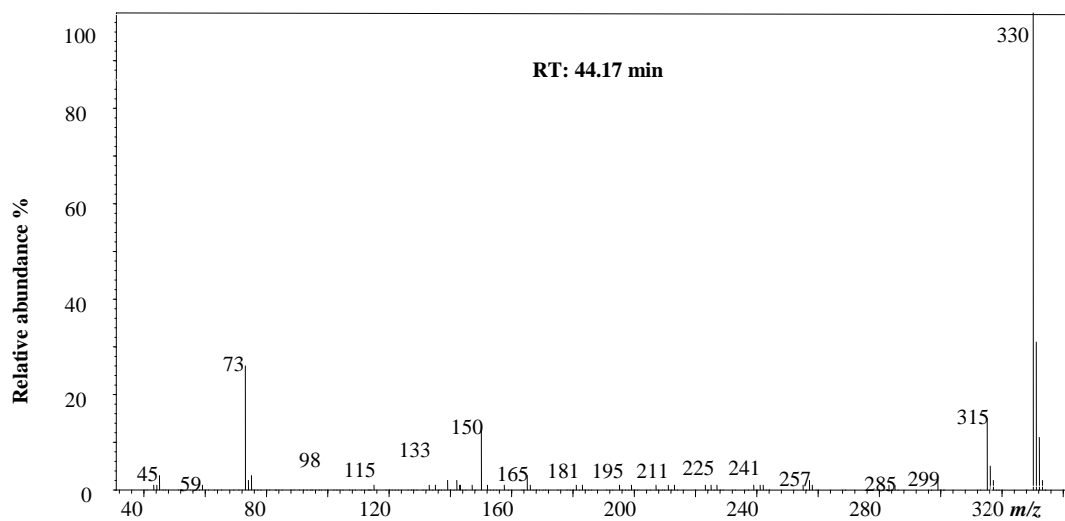


**Figure S A-3** Mass spectrums and possible ion fragment assignments of 2,2'-bisphenol

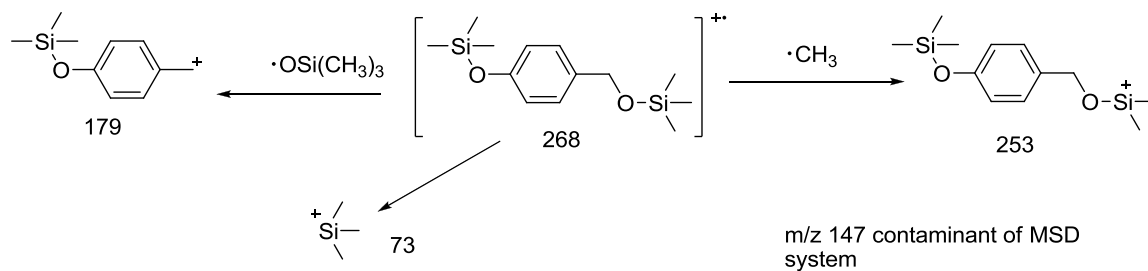
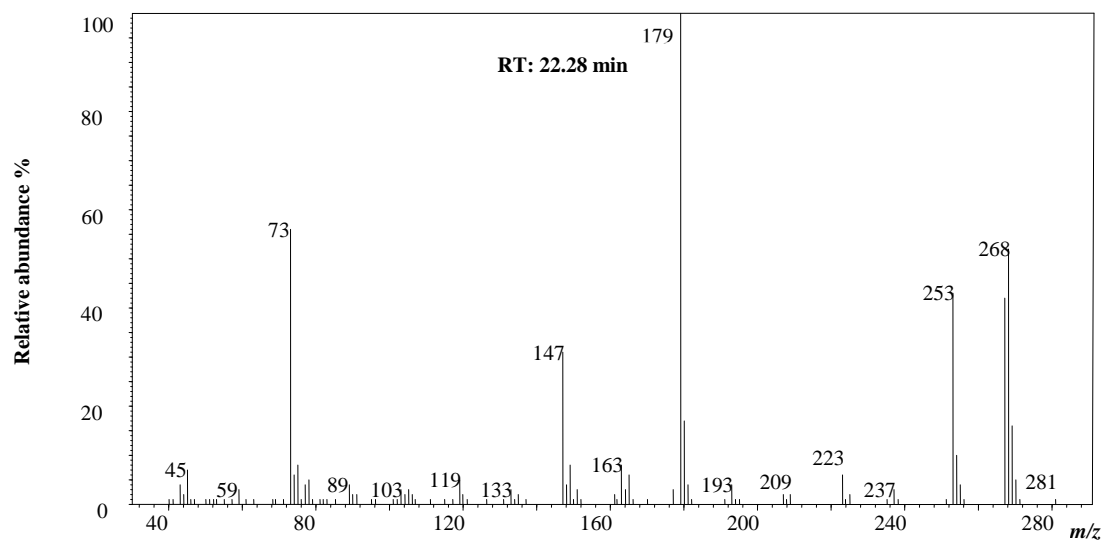


**Figure S A-4** Mass spectrums and possible ion fragment assignments of 4-hydroxybenzyl alcohol

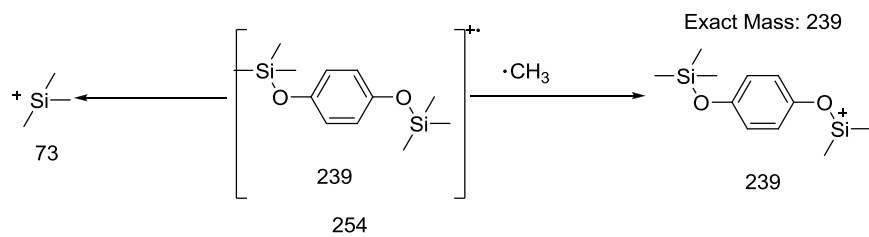
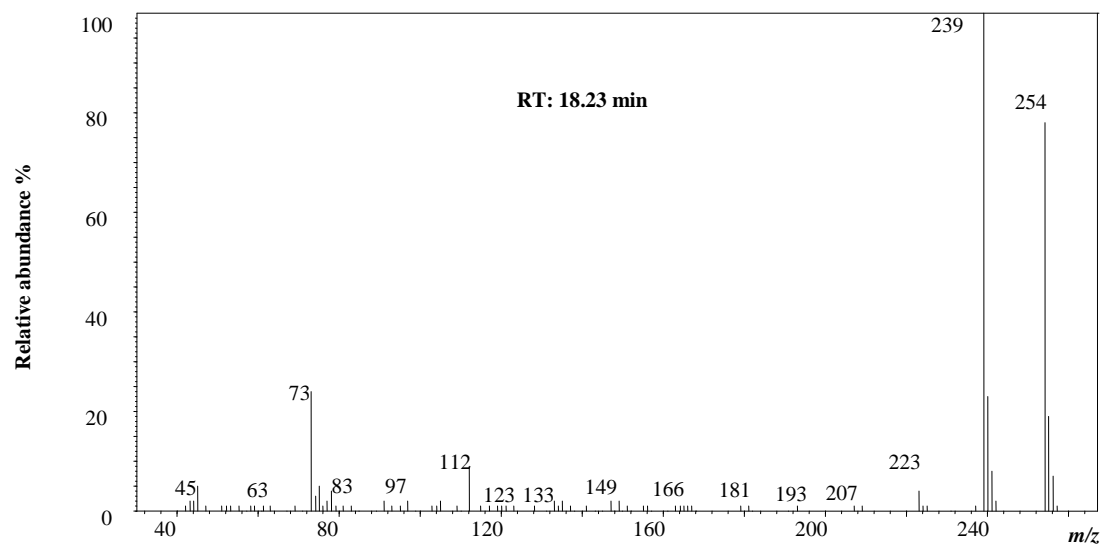
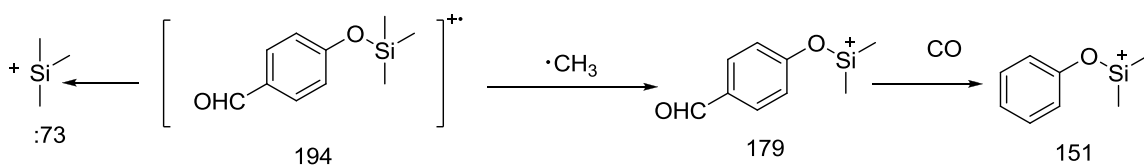
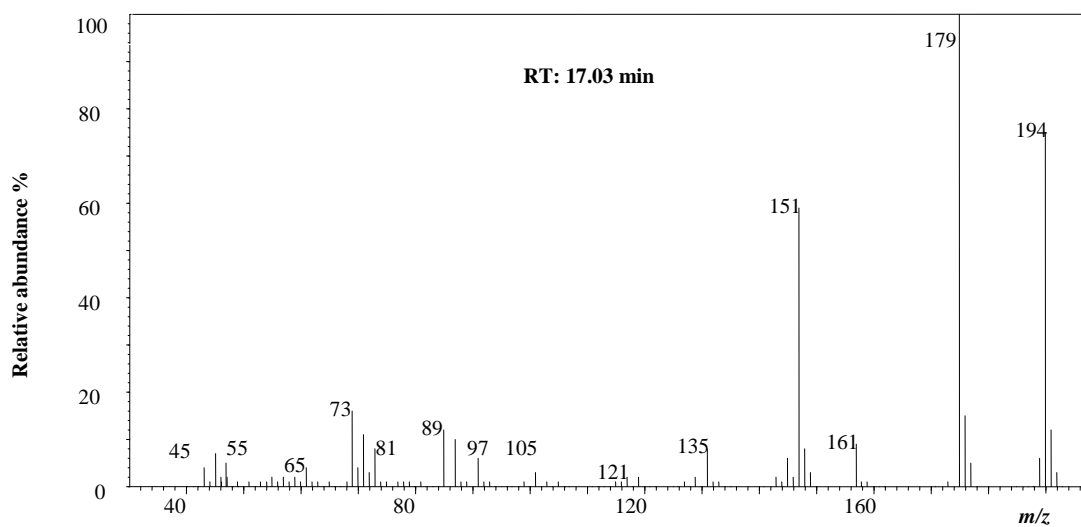
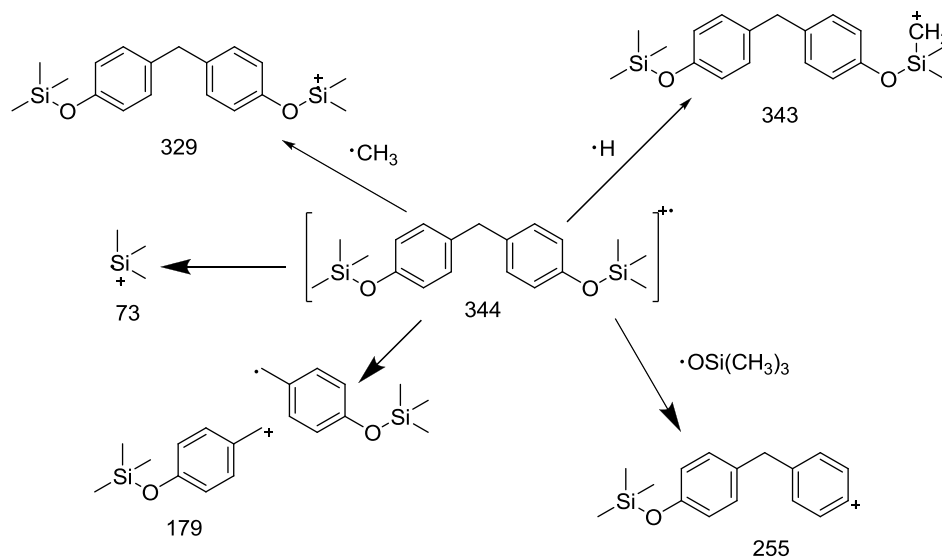
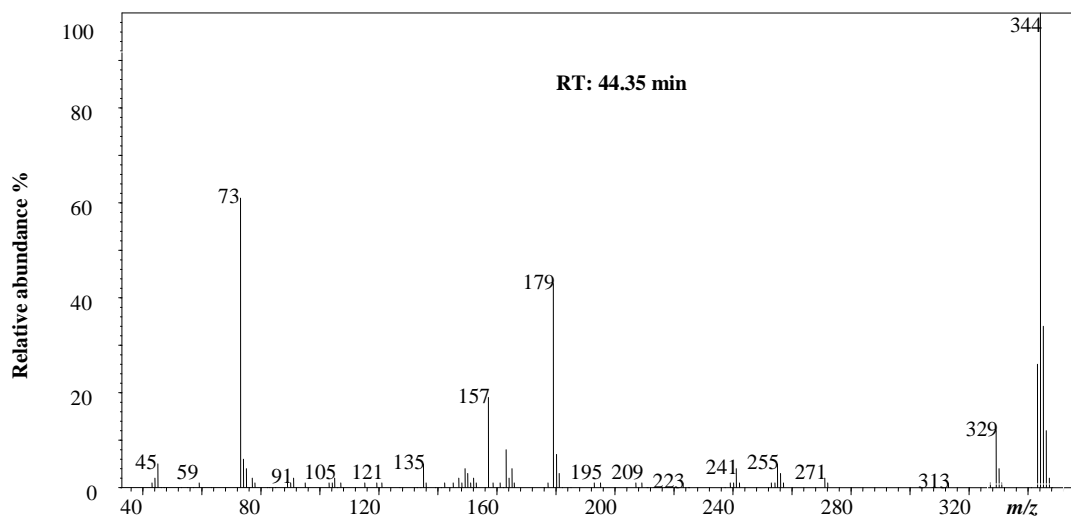


Figure S A-5 Mass spectrums and possible ion fragment assignments of hydroquinone



**Figure S A-6** Mass spectrums and possible ion fragment assignments of 4-hydroxybenzaldehyde



**Figure S A-7** Mass spectrums and possible ion fragment assignments of authentic standards bisphenol F

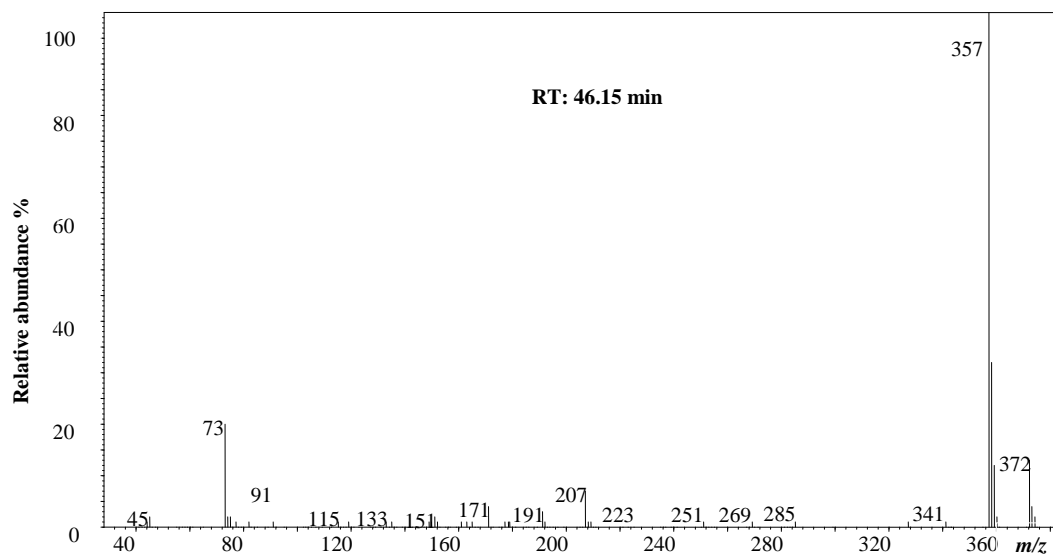


**Figure S A-8** Mass spectrums of authentic standards bisphenol A

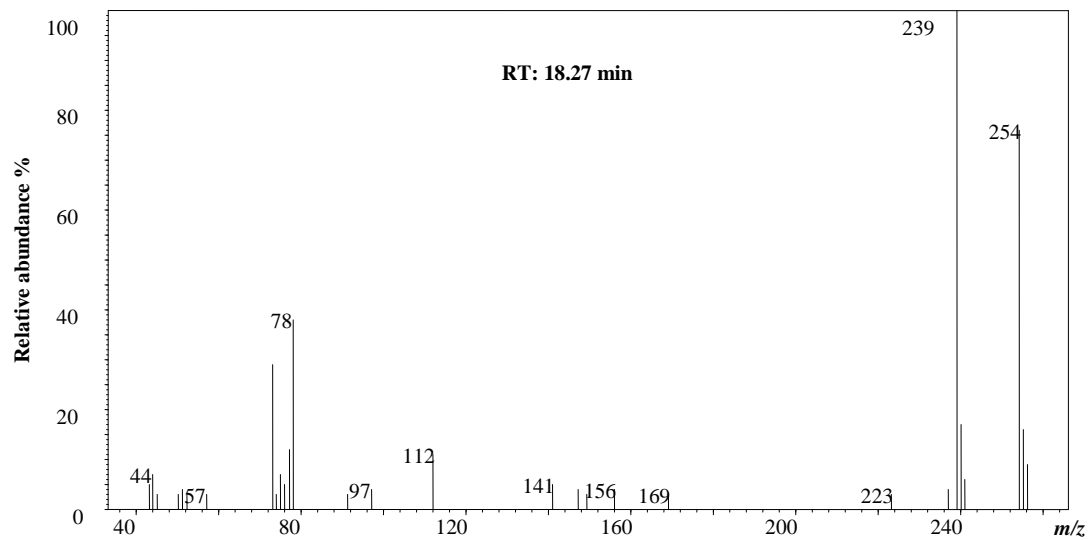


**Figure S A-9** Mass spectrums of authentic standards hydroquinone

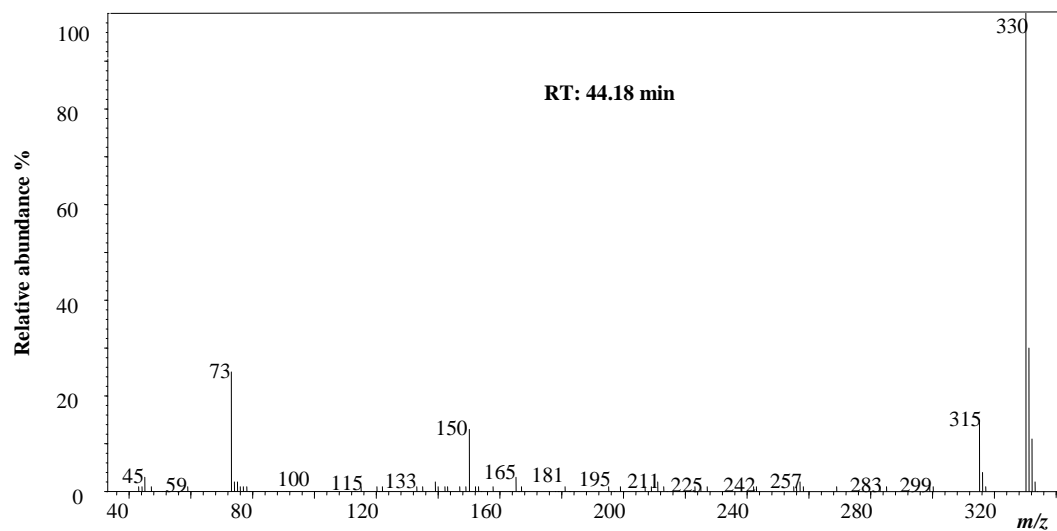


**Figure S A-10** Mass spectrums of authentic standards 2,2'-bisphenol



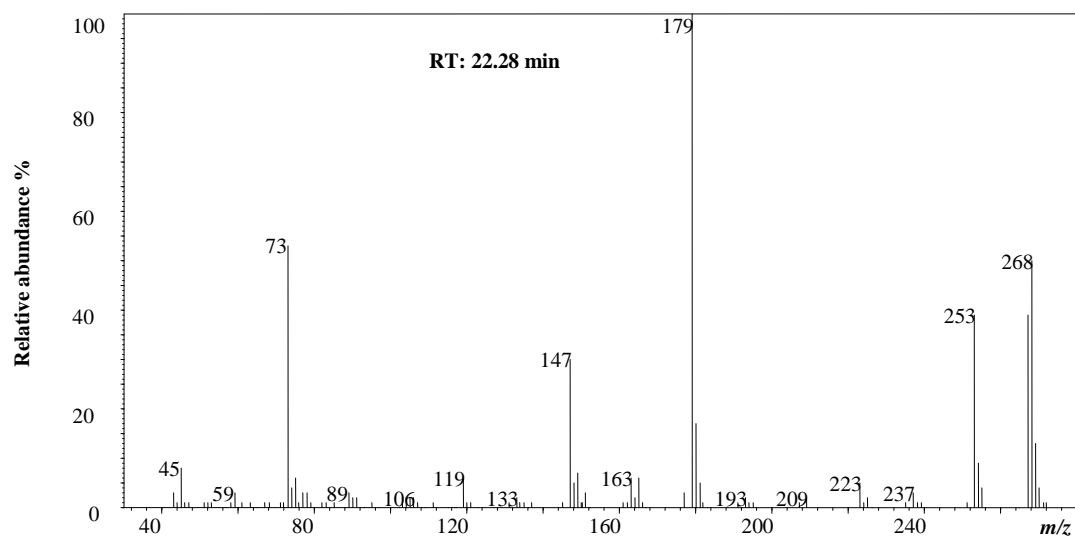


**Figure S A-11** Mass spectrums of authentic standards 4-hydroxybenzyl alcohol

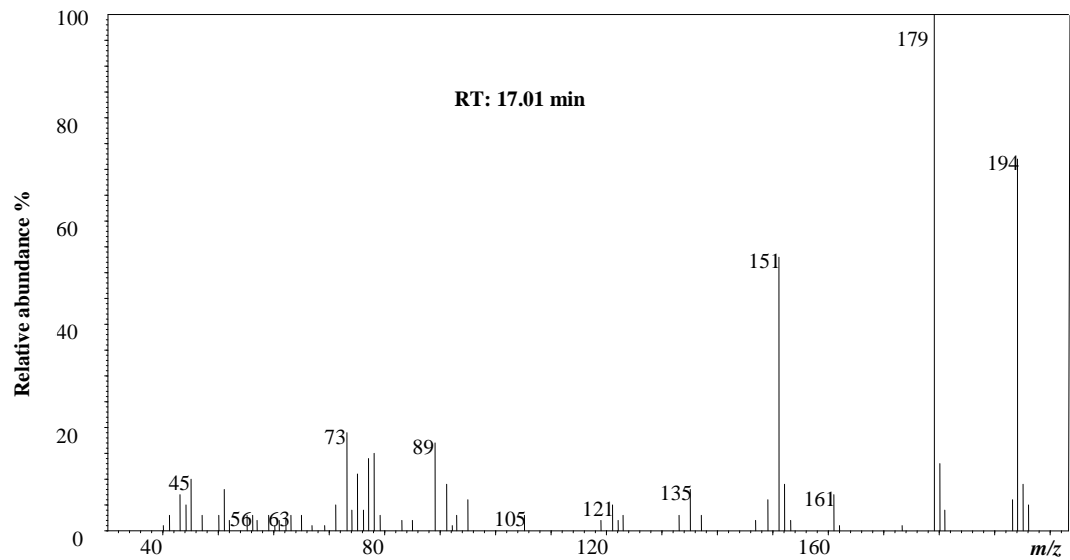


**Figure S A-12** Mass spectrums of authentic standards 4-hydroxybenzaldehyde